Atlasing white matter pathways using diffusion magnetic resonance imaging (dMRI) : With a focus on human association tracts in the external and extreme capsules

Janice Hau

université de BORDEAUX

THÈSE PRÉSENTÉE

POUR OBTENIR LE GRADE DE

DOCTEUR DE

L'UNIVERSITÉ DE BORDEAUX

ÉCOLE DOCTORALE DES SCIENCES DE LA VIE ET DE LA SANTÉ

SPÉCIALITÉ NEUROSCIENCES

Par Janice HAU

ATLASING WHITE MATTER PATHWAYS

USING DIFFUSION MAGNETIC RESONANCE IMAGING (dMRI)

With a focus on human association tracts in the external and extreme capsules

Sous la direction de : Laurent PETIT

Soutenue le 16 décembre 2015

Membres du jury :

M. DESCOTEAUX, Maxime	Professor, Université de Sherbrooke	Président
M. THIEBAUT DE SCHOTTEN, Michel	CR, King's College London	Rapporteur
M. MANDONNET, Emmanuel	PUPH, Hôpital Lariboisière	Rapporteur
M. LEEMANS, Alexander	Professor, University Medical Center Utrecht	Examinateur
M. PETIT, Laurent	CR, Université de Bordeaux	Directeur de thèse

It is intolerable that we do not have [a connectional map] for the human brain. Without it there is little hope of understanding how our brains work except in the crudest way.

Francis Crick and Edward Jones, "Backwardness of Human Neuroanatomy", Nature (Issue 361, p.110), 1993

I am told there are people who do not care for maps, and I find it hard to believe.

Robert Louis Stevenson, "My first book: Treasure Island", Essays in the Art of Writing, 1905. (On his drawing of an island map that would be his inspiration for Treasure Island)

Atlasing white matter pathways with diffusion-weighted imaging with a focus on the human association pathways of the external and extreme capsules

Abstract

The importance of the brain's connections for cerebral function is increasingly emphasized especially for higher cognitive functions like language. But the imperfection of the techniques used to address the human macroscopic connections has prevented the advancement of our knowledge on the anatomy of fibre pathways. Thus we rely heavily on XIXth century literature. Controversy surrounding the anatomical course and connections of many fibre pathways persists. Using diffusion imaging, we re-evaluate the anatomies of key pathways in a large healthy cohort. We use a novel tract segmentation approach that aims to reproduce the method introduced by dissectionists – defining a tract as all fibers passing through a stem, thus minimizing *a priori* on their terminations. We focus on the association pathways of the external and extreme capsules, namely the inferior fronto-occipital (IFOF) and uncinate fasciculi (UF), implicated in the ventral language circuitry. We review the literature on these tracts, provide detailed descriptions of their connectional anatomies and present new insights regarding their asymmetry and internal organization. In a first study, we confirm that both tracts have more extensive projections within the cortex than previously thought and present new results regarding asymmetrical tract branches. In a second study we further investigate the UF including its subcomponents. We resolve a century old debate by clarifying its elusive boundary with the IFOF and reveal the distinctive anatomical features including asymmetry patterns of each subcomponent. These results shed new light on the IFOF and UF and will be crucial for disentangling their multifunctional roles.

Keywords**:** White matter, neuroanatomy, diffusion imaging, tractography, fibre pathways, inferior fronto-occipital fasciculus, uncinate fasciculus, subcomponents, external capsule, extreme capsule.

Création d'un atlas des faisceaux de la matière blanche par imagerie de diffusion axé sur les faisceaux d'association humains des capsules externe et extrême

Résumé

Il est de plus en plus reconnu que les connexions du cerveau jouent un rôle important sur la fonction cérébrale, en particulier les fonctions cognitives supérieures comme le langage. Cependant l'imperfection des techniques traitant les connexions macroscopiques humaines a empêché l'avancement de nos connaissances sur l'anatomie des faisceaux. Nous nous appuyons ainsi aujourd'hui essentiellement sur la littérature du XIXème siècle. Les définitions des trajets et des connexions anatomiques de nombreux faisceaux sont constament redébattut. En utilisant l'imagerie de diffusion, nous réévaluons les anatomies des faisceaux clés dans une grande cohorte saine. Nous utilisons une nouvelle approche de segmentation des faisceaux qui vise à reproduire la méthode introduite par les dissectionistes. Celle-ci définit un tract comme l'ensemble des fibres passant par une même tige, minimisant ainsi l'*a priori* sur leurs terminaisons. Nous nous concentrons sur les faisceaux d'association des capsules externe et extrême, notamment les faisceaux occipito-frontal inférieur (FOFI) et unciné (FU) impliqués dans le circuit du language ventral. Nous passons en revue la littérature sur ces tracts, fournissons des descriptions détaillées de leurs connectivités anatomiques et donnons un nouvel éclairage sur leur asymétrie et organisation interne. Dans une première étude, nous confirmons que les deux faisceaux ont de plus vastes projections dans le cortex qu'on ne le pensait, et nous présentons de nouveaux résultats concernant les branches asymétriques des faisceaux. Dans une deuxième étude, nous étudions en profondeur le FU et ses sous-composantes. Nous résolvons un débat d'un siècle en exhibtant clairement sa frontière avec le FOFI et nous identifions pour chaque sous-composante des caractéristiques anatomiques distinctives y compris des asymétries. Ces résultats apportent un éclairage nouveau sur le FOFI et le FU qui sera crucial pour démêler leurs rôles multifonctionnels.

Mots clés : Matière blanche, neuroanatomie, imagerie de diffusion, tractographie, voies de fibres, faisceau occipito-frontale inférieure, faisceau unciné, sous-composants, capsule externe , capsule extrême.

Unité de recherche

Groupe d'Imagerie Neurofonctionnelle (GIN UMR 5296)

146 rue Léo-Saignat, Case 71, CS 61292

33076 Bordeaux Cedex

ACKNOWLEDGEMENTS

First, I would like to thank my jury for spending the time and effort to review my thesis and for being a lively panel at my thesis defense. Thanks to my supervisor Laurent for believing in me and providing me with unwavering support throughout these 3 years. It wasn't always easy but we made it to the end and I can say that I am proud of what we have accomplished together.

Thanks Silvio for teaching me about anatomy and giving me a perspective from a neurosurgical point of view. Thanks Maxime for welcoming me in Sherbrooke and teaching me a lot about tractography especially its pitfalls.

Thanks to Emmanuel, Bernard, Nathalie, Gaël, Laure, Marc, Fabrice, Anita, Guy, Jean-Philippe, Kristelle and everyone at the GIN for welcoming me in Bordeaux. Thank you to my fellow grad students in the lab Sophie, Quentin and Damien for accompanying me on this grad school journey.

Thank you PY for the evening company at the lab when it was crunch time and for providing random musings in the open space. Thanks to Gaelle for the daily encouragement. Thank you Sanja, Nicolas and Haemi for being other English speakers in our lab and bringing your international culture and cuisine. Thanks Johann for the interesting talks and proofreading my French and Solveig for board game afternoons.

Thanks to the SCIL and everyone I met at the U de S, Eleftherios, Chantal, Mic and Mathieu for making me feel at home in Francophone Canada. It was a memorable summer of 5-à-8's, poutine, camping and downtown Sherbrooke.

Thank you mom for making the long trips to Bordeaux all the way from Toronto to visit me, for sending me your lovely care packages every year at Christmas time and for just being my mom. Thanks dad for your loving support and Jeff and Diana for always being there and for fun Jays/Raps outings, and a big hello to little Kiara who was born this month. Thanks to Sylvie and Bruno for supporting me and seeing me defend. Thanks to all my friends in Canada whom i've kept in contact with and my friends in Paris. Finally, thank you Charles for the proofreading even though it is not your domain, for providing me with amazing food during my thesis writing and for always being supportive.

Project funding

This thesis, carried out in the frame of LabEx TRAIL bearing the reference ANR-10-LABX-57, has received financial support from the French State, managed by the French National Research Agency (ANR) in the frame of the "Investments for the future" programme IdEx Bordeaux, reference ANR-10-IDEX-03-02.

The Initiative d'Excellence (IdEx) International Mobility program financially supported a three-month academic visit at the Sherbrooke Connectivity Imaging Lab (SCIL) with Maxime Descoteaux.

RESUME (EN FRANCAIS)

Si le cortex cérébral était organisé sous la forme d'une « *chaîne de montage* », comme Marsel Mesulam (2006) le souligne, « *où chaque station ajoute un nouvel élément puis transmet sa production à la suivante* », alors il n'y aurait pas de réel besoin d'avoir une carte détaillée puisque les connexions pourraient être déduites directement à partir d'expériences dédiées. Ceci n'est cependant pas le cas car la matière blanche est complexe, constituée de fibres innombrables qui fonctionnent en parallèle, permettant des connexions variées et distribuées. Néanmoins, ces fibres sont soumises à des contraintes établies phylogénétiquement et suivent une certaine organisation, ainsi elles ont des structures reconnaissables qui peuvent être identifiées. La structure principale de la matière blanche est le faisceau ou tract composé d'une vaste collection groupée de fibres. Ces faisceaux constituent l'essentiel des connexions à longue portée dans le cerveau humain qui sont nécessaires pour la fonction intégrative entre les aires fonctionnellement distinctes. Il devient de plus en plus évident qu'ils jouent un rôle important comme intermédiaire de l'activité fonctionnelle. La cartographie détaillée de ces faisceaux est donc essentielle pour comprendre les processus cognitifs de niveau supérieur, y compris le langage, la mémoire et l'attention.

Dans le Chapitre 2, nous discutons des fondements des connexions du cerveau, y compris au niveau biologique (cellulaire) (i.e., l'axone, synapse et potentiel d'action). Nous présentons les concepts clés de leur organisation, en particulier la notion de fasciculation, un processus biologique que les axones subissent au cours de leur formation à l'origine du regroupement des fibres qui présentent une tige ou un point de convergence. Enfin, nous discutons pourquoi l'étude de l'anatomie des faisceaux est importante et comment la connaissance de la façon dont le cerveau est structurellement relié peut contribuer à notre quête pour comprendre le fonctionnement du cerveau.

Le débat sur l'anatomie des faisceaux

Le problème est un manque de compréhension claire concernant plusieurs faisceaux ainsi qu'une littérature encore trop confuse et sujette au débat. Par exemple, l'existence et l'inexistence de certains tracts sont débattues, ainsi que leurs noms et de leurs définitions (pour plus de détails voir le Chapitre 3). Une grande partie de la controverse date du 19ème siècle sur des études de dissection et d'histologie. Celle-ci résulte à la fois des limitations des techniques et de la difficulté d'étudier des faisceaux ayant des relations spatiales complexes les unes avec les autres.

Il existe essentiellement deux œuvres fournissant une description détaillée des faisceaux. La description la plus complète des faisceaux dans le cerveau humain est le travail séminal de Dejerine sur des sections de la myéline du cerveau teinté (Dejerine & Dejerine-Klumpe, 1895). Cependant, il semble que certaines de leurs descriptions soient erronées (ce qui inclut le faisceau occipito-frontal qu'ils ont décrit comme étant situé au-dessus du noyau caudé, figurant sur p.762 dans Dejerine & Dejerine-Klumpke, 1895). De plus, les descriptions des faisceaux sont davantage axées sur leurs chemins et sur leurs relations spatiales que sur leurs terminaisons détaillées. Plus récemment, Schmahmann et Pandya (2006) ont fourni des descriptions détaillées et complètes de plusieurs faisceaux basées sur le traçage axonal de 36 études de cas dans le macaque. Cependant, il y a des limites quant à leur généralisation au cerveau humain à cause de la présence de certaines régions plus vastes et plus complexes. De plus, d'importantes différences au niveau des fibres ont été récemment révélées entre singes et humains (tels que les faisceaux fronto-occipitaux supérieur et inférieur). Sans aucun doute ces deux œuvres ont significativement contribuées dans le domaine de la neuroanatomie connexionnelle. Tous deux ont également reconnu la controverse et ont tenté de clarifier une partie du débat particulièrement au sujet de l'anatomie des faisceaux. Néanmoins, le débat et la controverse entourant un grand nombre de tracts se poursuit aujourd'hui et il ne reste aucun compte rendu complet et détaillé des faisceaux chez l'homme.

L'absence d'un consensus sur la définition des voies est problématique (que les scientifiques peuvent ou ne peuvent pas se référer à la même structure de fibres), associée à un manque de prise de conscience des incohérences dans les définitions des faisceaux en raison des textes de référence « définitifs », qui conduit à la propagation des erreurs et de la confusion. Un premier objectif de cette thèse est de mettre au courant la communauté scientifique des incohérences et des débats concernant un certain nombre de faisceaux. Dans le Chapitre 3, nous faisons un historique des études concernant l'anatomie des faisceaux de l'Antiquité grecque à nos jours, nous mettons en évidence certains des débats sur les faisceaux (par exemple, les descriptions incompatibles, l'existence ou la non-existence, les problèmes de classification) et leur causes (par exemple, la nomenclature, les erreurs/omissions, extrapolation de l'animal à l'homme, de multiples représentations des données et variabilité interindividuelle). Enfin, nous discutons de la façon dont les travaux récents redéfinissent l'anatomie des faisceaux.

Une nouvelle technique pour étudier la matière blanche

Cela fait plus de 20 ans que Crick et Jones (1993) ont écrit leur fameux commentaire sur l'état de nos connaissances en neuroanatomie humaine (ou son absence) et la nécessité de nouveaux développements méthodologiques. En termes d'étude de l'anatomie de la matière blanche, les techniques disponibles à l'époque étaient invasives, demandaient beaucoup de temps et certaines ne pouvaient être effectuées que sur des animaux expérimentaux. L'imagerie par résonance magnétique de diffusion (IRMd) a été développée pour combler ce manque, offrant la possibilité d'effectuer des études de manière non invasive et *in vivo* sur l'architecture des fibres chez l'homme. Ce type d'imagerie est basé sur la mesure des collisions de molécules d'eau avec leur environnement et ainsi réalise des inférences sur la structure sous-jacente. En particulier, elle tire parti de la nature anisotrope de la diffusion dans la substance blanche. Une deuxième étape de traitement d'images, appelée la tractographie, permet de reconstruire approximativement l'architecture des fibres à partir de ces images. Cela a élargi les possibilités pour étudier les faisceaux chez les humains permettant des dissections virtuelles de la substance blanche et l'application d'une suite d'outils de neuro-imagerie (par exemple, l'enregistrement de l'image, des modèles anatomiques) ainsi permettant l'analyse et le traitement systématique et automatique des faisceaux, ainsi que des informations quantitatives sur les propriétés de la microstructure de la matière blanche dans le cerveau humain vivant. Plusieurs initiatives de grande envergure ont été lancées pour étudier le connectome macroscopique du cerveau humain, le plus connu est le Human Connectome Project (Van Essen et al., 2013).

On présente dans le Chapitre 4 une vue d'ensemble des techniques qui sont actuellement utilisées pour étudier l'anatomie de la matière blanche avec un accent particulier sur l'IRMd, y compris une discussion sur chacun de leurs avantages et inconvénients respectifs.

Mise au point de la thèse: Les faisceaux d'associations de la C2E2

L'objectif de cette thèse est de fournir une cartographie complète et détaillée des faisceaux du cerveau humain en utilisant l'imagerie de diffusion pondérée, et d'aller au-delà de ce que la dissection et d'autres techniques peuvent nous dire (e.g., sur l'asymétrie hémispherique des faisceaux). Nous nous concentrons sur les capsules externes et extrêmes, qui sont des zones topographiques de la substance blanche située entre l'insula et le putamen et qui sont séparées par une mince bande de matière grise appelée le claustrum (voir Figure I), que nous appelons collectivement sous le nom de complexe des capsules externe et extrême (C2E2). Le C2E2 constitue une zone de passage de multiples faisceaux de la matière blanche dont la commissure antérieure, la boucle de Meyer et les fibres de projection. Sa partie ventrale est constituée de deux voies qui relient les zones corticales intra- hémisphérique (connues comme faisceaux d'associations) : le faisceau occipito-frontal inférieur (FOFI) et le faisceau unciné (FU) (voir la figure I).

L'étude des faisceaux d'association du C2E2 est récemment devenu un sujet brullant étant donné l'intérêt croissant concernant le FOFI alors jusque là peu étudié, et les nombreux travaux

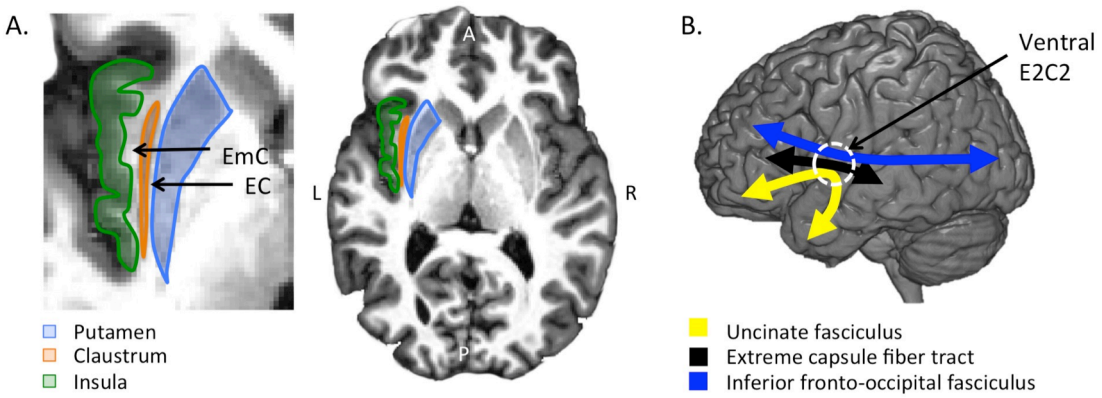

Figure I. Le C2E2 subtil et complexe. A) Les capsules externe (EC) et extrême (EmC) sont indiquées sur la coupe axiale d'une image T1 anatomique dans un seul sujet, indiqué par les flèches. B) Représentation schématique des faisceaux d'association qui traversent le C2E2 (cercle blanc en tirés), comprenant le faisceau récemment nommé « faisceau de la capsule extrême » (Petrides & Pandya, 1988; Schmahmann & Pandya, 2006). Le faisceau unciné (jaune) relie la partie frontale à l'antérieure du lobe temporal et a une forme caractéristique en crochet. Le faisceau occipito-frontal inférieur (bleu) se trouve en position médiale et dorsale par rapport au FU et relie le lobe frontal aux lobes occipital, pariétal et temporal. Le faisceau de la capsule extrême (noir) se trouve en position dorsale et latérale par rapport au FU et relie la partie médiale et frontale des lobes temporaux.

portant sur le FU et son lien possible avec divers troubles cliniques. Par ailleurs, il a été récemment montré que ces deux faisceaux sont impliqués dans le circuit du langage (Saur et al., 2008; Bajada et al., 2015). Cela a changé notre compréhension de la connectivité du langage, et attiré ainsi de plus en plus d'attention à ces deux faisceaux pour déterminer leurs rôles spécifiques sur le langage. Le C2E2 constitue aussi une région très complexe et subtile. Tandis que la séparation entre les capsules est claire, la frontière entre les deux faisceaux est bien moins évidente car il n'y a pas d'assignement exact des faisceaux aux capsules (le FOFI et le FU traversent tous deux à la fois la capsule externe et la capsule extrême) (Ebeling & Cramon, 1992; Kier et al., 2004). Un élément rend d'autant plus confuse l'étude de cette région : il s'agit de la récente description d'un groupe de fibres chez le singe (et a depuis été appliquée à l'anatomie humaine), dénommé « faisceau de la capsule extrême » (Figure I), reliant la partie intermédiaire du gyrus temporal supérieur et moyen avec le lobe frontal (Schmahmann & Pandya, 2006; Saur et al., 2008; Mars et al., 2015). En effet, l'identité anatomique de ce groupe de fibres est difficile à cerner car, compte tenu de son emplacement, il pourrait appartenir au FOFI et/ou au FU.

Dans cette thèse, nous utilisons l'imagerie de diffusion pour analyser et tenter de clarifier la frontière anatomique entre ces deux faisceaux et pour fournir une description complète de leur connectivité anatomique fondée sur une large cohorte saine.

Dissection virtuelle anatomique : Segmentation par tiges appliquée à une tractographie IRMd (inspirée de la dissection post-mortem)

L'application récente de l'imagerie de diffusion à l'étude de la matière blanche a principalement mis l'accent sur l'identification et la localisation des faisceaux connus d'après la littérature classique du 19ème siècle. Cela a conduit à la publication d'atlas de références sur la substance blanche, utilisés à des fins éducatives, et montrant les emplacements généraux des faisceaux les uns par rapport aux autres (Oishi et al., 2005; Catani & Thiebaut de Schotten, 2008). Cependant, ces études ne visaient pas à affiner notre connaissance sur l'anatomie des faisceaux mais plutôt à créer des atlas à partir de la connaissance *a priori* provenant d'études de dissections. Ces atlas restent donc souvent limités à des définitions anatomiques pré-existantes et ne tirent pas parti de la quantité d'informations disponibles sur les données IRMd.

Nous avons développé une approche originale pour segmenter les faisceaux d'association du C2E2 avec un minimum d'*a priori* sur un jeu de données de tractographie. Elle est basée sur le procédé d'extraction qui a été introduit (et qui continue à être utilisé) par les neuroanatomistes,

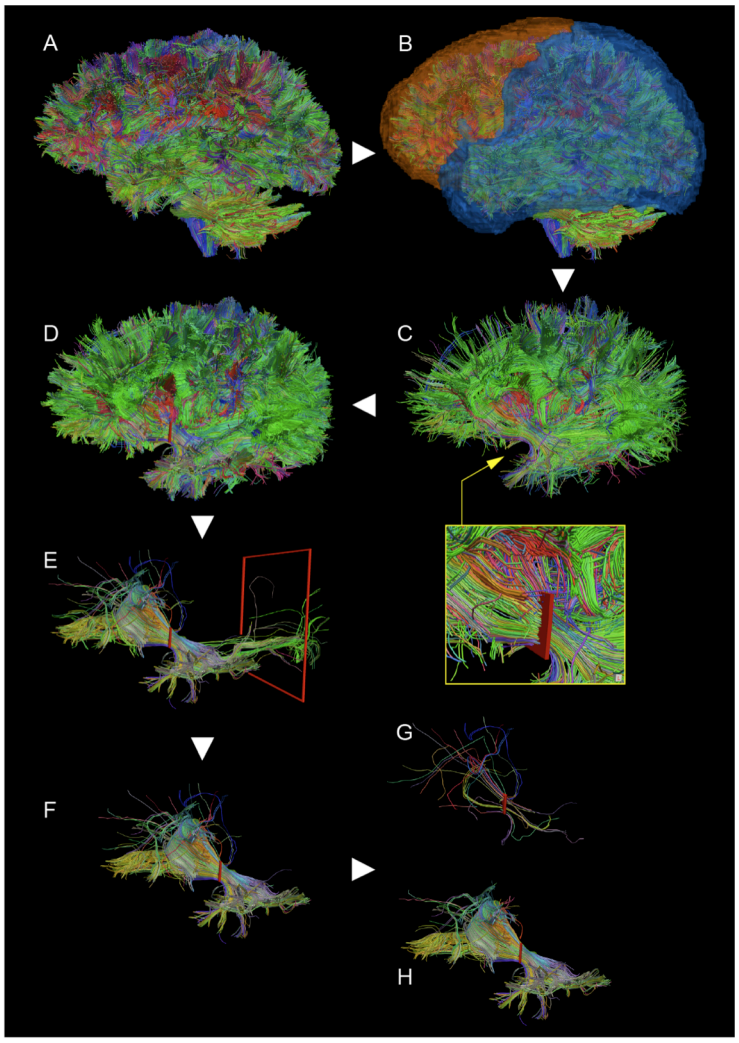

Figure II. Dissection virtuelle anatomique basée sur la tige du FU. **A**. Vue de 10 % des streamlines intra-hémisphériques gauches d'un seul tractogram du cerveau entier ; **B** à **C**. Vue de 10% des streamlines avec une terminaison dans le lobe frontal (en orange) et l'autre soit dans le lobe temporel, cingulaire, pariétal ou occipital (en bleu) ; **C** (zoom). ROI rectangulaire initiale (en rouge), établie au niveau des streamlines en forme de crochet (flèche jaune); **D**. Vue de 100 % des streamlines une fois la taille de la tige FU ajustée (en rouge); **E**. Tous les streamlines passant à travers la tige FU sont affichés. Un filtre sur la coupe coronale supplémentaire (cadre rouge) a été utilisé pour enlever les streamlines restant du FOFI. **F**. Application de l'algorithme d'élimination des valeurs aberrantes pour tailler les streamlines aberrants (**G**) et pour fournir le FU final (**H**).

qui définit un faisceau par sa tige (sa partie la plus compacte) et considère toutes les fibres inclues dans la tige comme appartenant au faisceau. Notre approche imite ce procédé de dissection post-mortem en effectuant des dissections virtuelles interactives sur les tractograms (reconstructions 3D de la structure de matière blanche produit par la tractographie) du cerveau entier. En s'appuyant sur les emplacements du FOFI et FU bien documentés des dissectionistes et en utilisant un modèle anatomique (atlas « Eve » de Johns Hopkins University, Oishi et al., 2009), nous avons supprimé de manière sélective des « streamlines » (i.e., « fibres virtuelles ») dans certaines zones superficielles du cerveau afin de localiser et d'identifier les tiges, qui se trouvent au plus profond de la matière blanche du cerveau. Une fois identifiées, on délimite manuellement une région d'intérêt (ROI) autour de la tige d'intérêt qui sera utilisée pour extraire le faisceau. Un exemple de l'approche de dissection virtuelle basée sur la tige pour le FU est illustré dans la Figure II.

Étude 1 : Terminaisons corticales du FOFI et FU étudiés avec une approche de dissection virtuelle anatomique basé sur la tige

Dans une première étude, nous avons étudié les régions de terminaisons du FOFI et FU, qui ont été rapportés dans la littérature d'une manière incompatible. On a aussi inclus pour la première fois une description de leurs asymétries en utilisant l'imagerie de diffusion. Nous avons appliqué notre approche de segmentation par tige pour extraire ces deux faisceaux dans un groupe de 60 sujets sains de la base de données BIL&GIN (un ensemble de données précédemment acquises par notre laboratoire contenant des données d'imagerie de diffusion

sur > 400 sujets, Mazoyer et al., 2015). Les ensembles de données de diffusion ont été traité avec un pipeline de tractographie standard en utilisant le modèle de tenseur (DTI, Basser et al., 1994).

Nous avons délimité le FOFI et FU chez tous les sujets, en observant deux tiges distinctes dans le C2E2. En utilisant l'atlas Eve de Johns Hopkins pour définir des régions anatomiques macroscopiques, nous avons cartographié la fréquence et la distribution des terminaisons de ces deux faisceaux dans les différentes régions corticales et évalué les asymétries hémisphériques au sein de leurs branches individuelles. Dans les deux faisceaux, nous avons constamment observé de plus vastes territoires de terminaison que leurs définitions conventionnelles : dans les gyris frontal moyen et supérieur, pariétal supérieur et angulaire pour le FOFI et les gyri frontal moyen et temporal supérieur, moyen et inférieur au-delà du pôle temporal pour le FU (Figure III). Ces résultats convergent avec récentes études de dissection sur le FOFI. Nous avons révélé de nouvelles idées concernant l'organisation interne de ces tracts. De façon intéressante, nous avons observé une dissociation au sein du FOFI entre les branches médiale et latérale occipito-frontal qui ont été asymétriques gauche et droite, respectivement (Figure III, Aii). Dans le FU, nous avons observé une latéralisation droite de certaines branches orbito-frontales et temporales (Figure III, Bii). Ces nouvelles découvertes anatomiques concernant ces faisceaux permettront une plus grande spécificité pour les corréler avec les populations cliniques et d'autres mesures comportementales. Dans cette première étude, nous avons aussi démontré l'avantage de l'approche de dissection virtuelle basée sur la tige par rapport aux approches basées sur les atlas standards, pour étudier l'anatomie des faisceaux de la matière blanche.

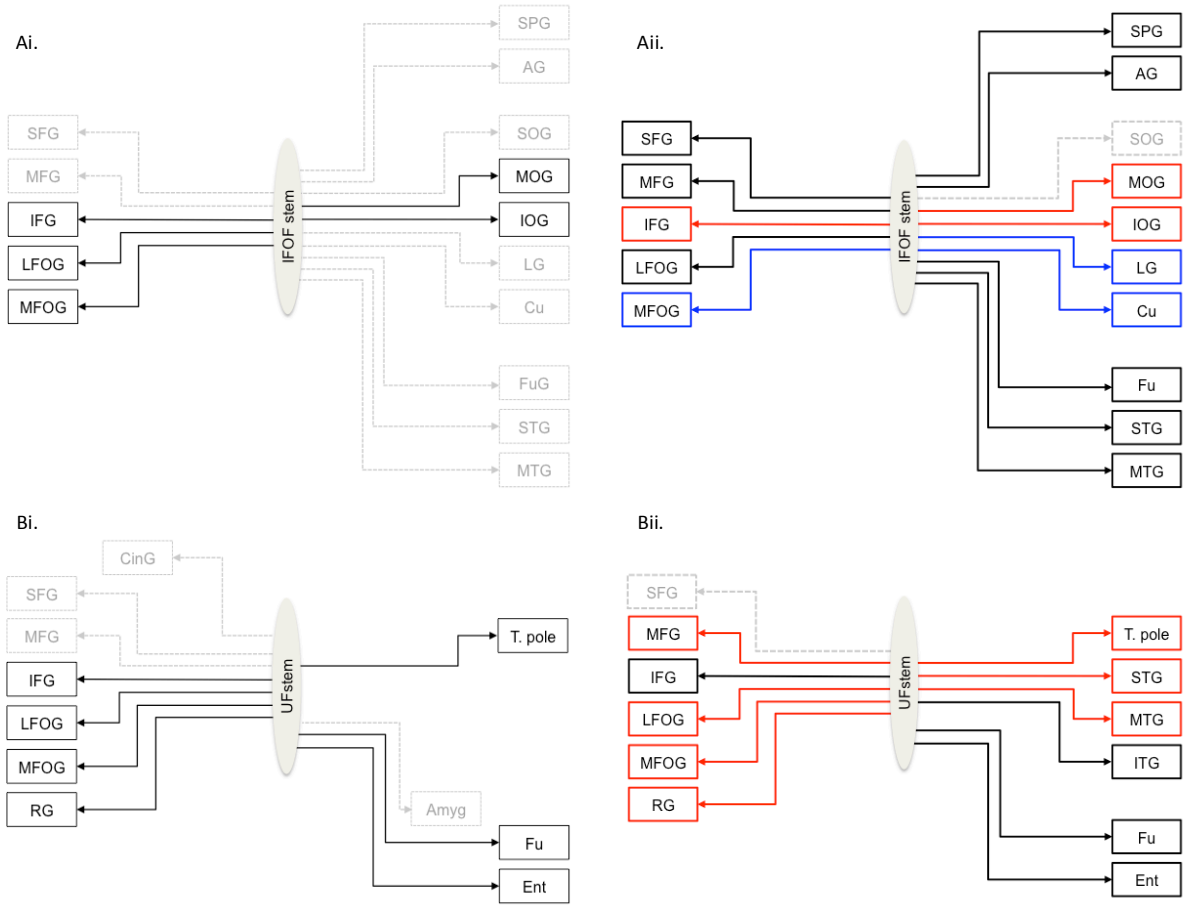

Figure III. Schémas résumant les territoires de terminaison corticales du IFOF (A) et UF (B) dans la littérature (A-B, i) et à la lumière de notre étude de tractographie base de tige (A-B, ii). Le consensus / territoires corticaux confirmés sont représentés par des traits pleins et les régions qui demeurent (ou ont demeuré) douteuses sont représentés par des lignes en pointillés. Les projections latéralisées gauche et droites sont indiquées en bleu et en rouge, respectivement. Abréviations: SFG, MFG, IFG : gyus frontal supérieur, moyen et inférieur; LFOG, MFOG : gyrus fronto-orbitaire latéral et médial; RG : gyrus rectus; SOG, MOG, IOG : gyrus occipital supérieur, moyen et inférieur; Cu : cuneus ; LG; gyrus lingual ; T. pole : pole temporal; STG, MTG, ITG : gyrus temporal supérieur, moyen et inférieur; Fu : gyrus fusiforme; SPG : gyrus pariétal supérieur; AG : gyrus angulaire; Ent : gyrus entorhinal.

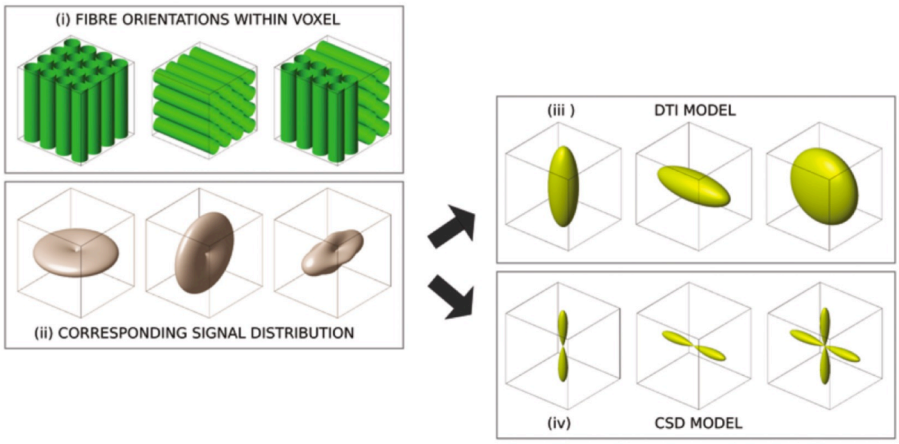

Figure IV. DTI modèle l'orientation des fibres avec un ellipsoïde qui réussit à capturer les orientations simples des fibres dans un voxel (deux premiers cas, à gauche et au centre), mais pas quand il y a deux orientations de fibres de passage (troisième cas, à droite), alors que les modèles avancés tels que la CSD est capable de capturer correctement les trois cas (figure repris de Farquharson et al., 2013).

Considérations méthodologiques : L'application des méthodes de tractographie avancés

Cette thèse apporte également des contributions concernant les techniques de traitement et d'analyse de données d'imagerie de diffusion. La première étude a mis en lumière les limites des méthodes de tractographie utilisés dans notre pipeline standard, en particulier le modèle de tenseur (DTI). Ceux-ci comprennent la perte de données en raison de streamlines qui se terminent prématurément dans la substance blanche et le problème bien connu de l'incapacité du DTI à résoudre des configurations complexes de fibres (par exemple, deux populations de fibres qui traversent perpendiculairement dans un voxel, voir le Figure IV). Nous avons fait des améliorations significatives à nos données de tractographie en appliquant des méthodes de pointe par une collaboration internationale avec Maxime Descoteaux (Université de Sherbrooke, Canada). J'ai reçu la bourse d'IdEx pour la mobilité internationale des doctorants et j'ai fait une visite de trois mois au sein du laboratoire Descoteaux où j'ai appris des méthodes de tractographie avancées comme la déconvolution sphérique sous contrainte (CSD) (Tournier et al., 2007; Descoteaux et al., 2009) et des méthodes de tracking qui optimisent l'analyse de la connectivité anatomique (Girard et al., 2014). Nous avons implémenté un nouveau pipeline de tractographie pour nos données BIL&GIN qui utilise crucialement le CSD au lieu de DTI qui est robuste au problème du croisement de fibres (Figure IV) ainsi que les méthodes de tracking optimisés. En lien avec cette collaboration, deux expériences informelles ont été menées : 1) une analyse complémentaire sur les tiges à partir des données d'imagerie de diffusion (et une étude sur la possibilité d'automatiser la méthode basée sur tige) et 2) l'influence du pipeline de tractographie sur la connectivité anatomique (pour plus de détails voir le Chapitre 6). Une revue des méthodes de tractographie ainsi que les méthodes de tractographie avancées de pointe utilisées dans cette thèse sont présentés au Chapitre 4.

Étude 2 : Revisiter le FU, ses sous-composants et les asymétries avec tractographie base de tige et la validation de microdissection

Dans une deuxième étude, nous nous sommes concentrés sur la description de l'anatomie connexionnelle détaillée du faisceau unciné (FU) et de ses sous-composants. Nous avons segmenté le FU en utilisant l'approche basée sur la tige sur le pipeline amélioré de tractographie CSD (Figure II) dans un groupe de 30 sujets. De manière surprenante, nous avons obtenu des résultats remarquables en observant systématiquement un FU comprenant non seulement les fibres classiques en forme de crochet, mais également des fibres orientées horizontalement à droite (cela n'a pas été considéré dans l'Etude 1 et est devenu évident que lorsque nous avons

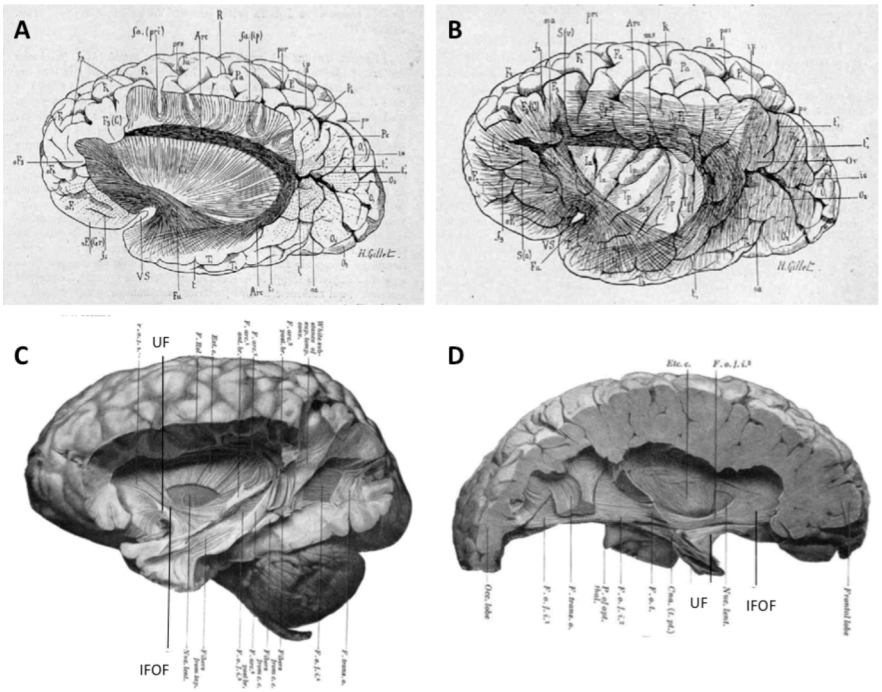

Figure IV. Représentation schématique du FU de Dejerine aux médiane (A) et latérale (B) étapes de dissection (figures 376-377, Dejerine & Dejerine-Klumpe, 1895). La dissection du FOFI gauche (C) et droite (D) de Curran où le sous-composant dorsale horizontale du FU peut être clairement vu (planche I, Curran, 1909).

utilisé le pipeline CSD). Cela a permis d'actualiser un débat vieux d'un siècle concernant la limite postérieure du FU et sa frontière avec le FOFI (Trolard, 1906). Le FU que nous avons observé, dont la forme en éventail fait une transition progressive d'une forme de crochet vers une trajectoire horizontale, correspond en fait exactement à la description originale de Dejerine (1895) (schémas dans le figure IV, A-B) et peut également être vu dans la dissection emblème du FOFI de Curran (1909), qui a démontré une frontière relativement claire entre le FOFI et FU au niveau de la tige (Figure IV, C-D). D'autres études de dissection classiques ont également décrit un FU qui dévie de la forme en crochet stricte (Gordinier, 1899; Testut, 1900; Wernicke, 1908), mais ces rapports ont été largement ignorés.

Compte tenu de la plus vaste FU, nous avons appliqué une méthode de classification automatique afin de subdiviser le faisceau en plus petits sous-composants, basée sur les emplacements et les orientations des points de terminaison des streamlines. Le regroupement de streamlines a identifié cinq sous-composants, dont chacun présentaient des profils de connectivité anatomiques distincts (Figure V): C1 relie les régions frontales dorso-latérales avec la partie médiane du lobe temporal, C2 relie les régions ventro-latérales et C3-C5 relie différentes régions ventro-médiale frontales avec le lobe temporal. En outre, une dissection post-mortem couche-par-couche du FU a été réalisée dans 4 hémisphères par Silvio Sarubbo (Hôpital Saint Chiara, Trento, Italie) a révélé également cinq couches de fibres au niveau de la tige du FU. En considérant les différent approches et les principes anatomique sur lesquels la clusterisation de streamlines (i.e., les cinq sous-composants) et les couches de dissection sont fondées, certaines divergences sont apparues dans la distribution des fibres. Néanmoins, les dissections ont systématiquement confirmé tous les territoires de terminaisons identifiés par sphérique déconvolution tractographie (Figure VI). Fait intéressant, le récemment décrit « faisceau de la capsule extrême » correspond exactement au sous-composant dorsal du FU et doit ainsi être considéré comme une partie du FU.

Nous avons également évalué, pour la première fois, l'asymétrie hémisphérique du FU à l'égard de ses sous-composants. Les études sur l'asymétrie de FU sont non-conclusives, certaines ayant trouvé une asymétrie à gauche (Kubicki et al., 2002; Hasan et al., 2009), d'autres à droite

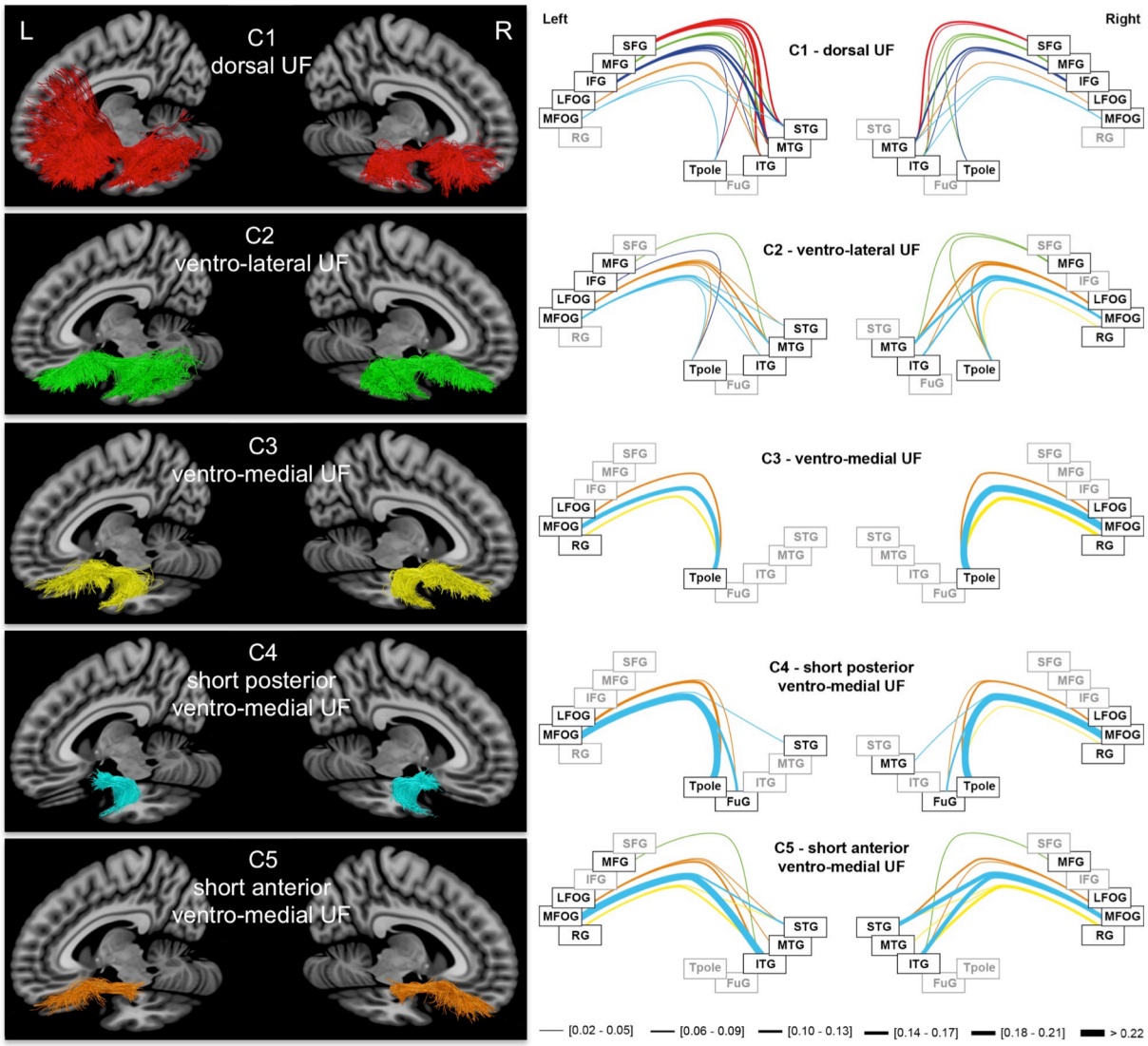

Figure V. Les cinq sous-composants du FU sur les données de groupe échantillonnées à 20 % du total des streamlines pour l'affichage visuel (à gauche) et de leurs anatomies connexionnelles moyennes (à droite). L'épaisseur des lignes est proportionnelle au nombre de streamlines normalisé moyen reliant une paire de régions. La couleur de la ligne permet de distinguer les lignes des différentes régions frontales. SFG (rouge), MFG (vert), IFG (bleu), LFOG (orange), MFOG (bleu clair), RG (jaune). Abréviations (voir Figure III).

(Highley et al., 2002; Rodrigo et al., 2007) et d'autres pas d'asymétrie (Thiebaut de Schotten et al., 2011). Nous avons observé un sous-composant du FU dorsal latéralisée à gauche et un sous-composant du FU ventro-médiale latéralisé à droite. Ces résultats concilient la récente controverse sur l'asymétrie UF et soulignent l'importance de la considérer comme un faisceau à plusieurs composants.

Conclusion and perspectives

Nous avons donc fourni quelques élucidation des faisceaux d'association de la E2C2 chez l'homme, avec un FOFI plus vaste, un FU beaucoup plus vaste qui comprend le faisceau précédemment connu sous le nom de faisceau de la capsule extrême (Figure VII), et fourni de nouvelles informations relatives à l'organisation interne (sous-composants et l'asymétrie) de ces faisceaux. En outre, nous avons réintroduit un paradigme classique, l'approche basée sur la

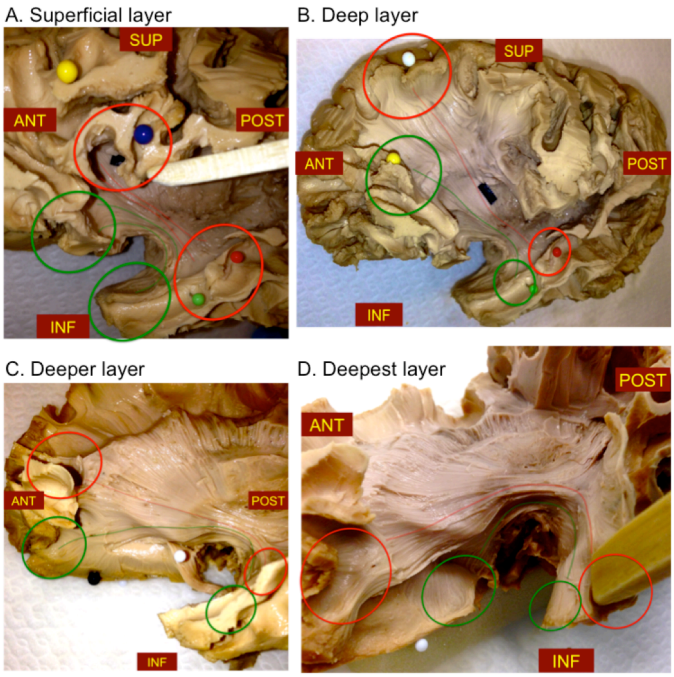

Figure VI. La dissection post-mortem couche-par-couche du FU a montré cinq couches de fibres au niveau de sa tige et a confirmé les connexions anatomiques observées de la tractographie CSD.

tige, et l'a appliqué à la tractographie IRMd qui se révèle être une façon fructueuse pour étudier l'anatomie des faisceaux.

Les travaux futurs avec la tractographie IRMd devraient se concentrer sur la cartographie d'autres faisceaux à l'aide de l'approche basée sur la tige (par exemple, MDLF, SLF, ILF), décrivant l'anatomie plus fine des faisceaux (c.f. les sous-composants) et de relier les variations de leurs structures avec la fonction, le comportement et la maladie. Cela nécessitera à décrire les faisceaux de la matière blanche dans des grandes populations afin de créer des cartes normatives. Le développement d'une méthode automatique de segmenter les faisceaux d'un jeu de donnée de tractographie à travers une approche basée sur sa tige sera la clé de la réalisation de ces cartes.

Nous concluons que l'imagerie de diffusion par tractographie est une technique complémentaire pour l'étude de l'anatomique des faisceaux de la substance blanche chez les humains. Il apporte la capacité unique de réaliser des dissections virtuelles de la substance blanche et d'obtenir des mesures quantitatives sur une population vivante. Néanmoins, il reste une mesure indirecte de la structure de la substance blanche et donc la validation des techniques primaires est essentielle. En combinant l'imagerie de diffusion avec les techniques

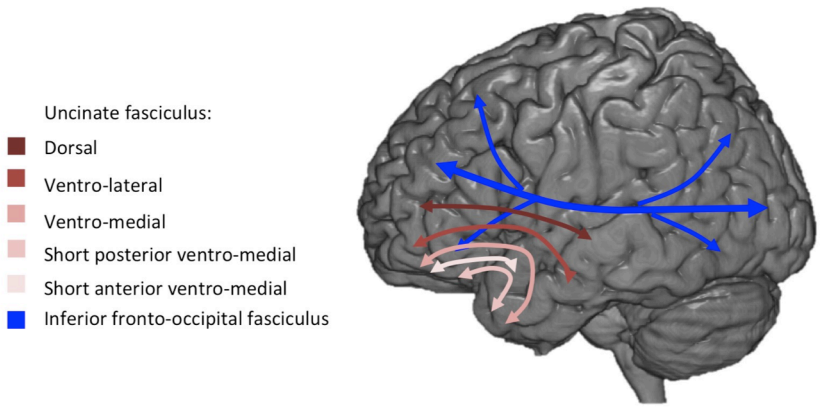

Figure VII. Schéma de l'anatomie connective des faisceaux d'association humains des capsules extrêmes et externes.

primaires de dissection et le traçage axonal pour valider et converger sur l'anatomie des faisceaux, nous serons en mesure de comprendre plus précisément les fonctions et les comportements qu'ils soutiennent ainsi que leur lien avec les différents troubles cliniques.

Références

Bajada et al. (2015). *Transport for Language South of the Sylvian Fissure: The routes and history of the main tracts and stations in the ventral language network*. *Cortex*, *69*, 141–151.

Basser et al. (1994). *Estimation of the effective self-diffusion tensor from the NMR spin echo. J. Magn. Reson. B*.

Catani, & Thiebaut de Schotten. (2008). *A diffusion tensor imaging tractography atlas for virtual in vivo dissections. Cortex*, *44*(8), 1105–32.

Crick, & Jones. (1993). *Backwardness of human neuroanatomy. Nature*, *361*(6408), 109–110.

Curran. (1909). *A new association fiber tract in the cerebrum*. *J. Comp. Neurol. Psychol.*, *19*(6), 645–656.

Dejerine, & Dejerine-Klumpe. (1901). Anatomie des Centres Nerveux. Paris: Rueff et Cie.

Descoteaux et al. (2009). *Deterministic and Probabilistic Tractography Based on Complex Fiber Orientation Distributions*. *IEEE Trans. Med. Imaging*, *28*(2), 269–286.

Ebeling, & Cramon. (1992). *Topography of the Uncinate Fascicle and Adjacent Temporal Fiber Tracts*. *Acta Neurochir. (Wien).*, *115*, 143–148.

Farquharson et al. (2013). *White matter fiber tractography: why we need to move beyond DTI. J. Neurosurg.*, *118*(6), 1367–77.

Girard et al. (2014). *Towards quantitative connectivity analysis: reducing tractography biases. Neuroimage*, *98*, 266–78.

Gordinier. (1899). *The gross and minute anatomy of the central nervous system*.

Hasan et al. (2009). *Development and aging of the healthy human brain uncinate fasciculus across the lifespan using diffusion tensor tractography. Brain Res.*, *1276*, 67–76.

Highley et al. (2002). *Asymmetry of the uncinate fasciculus: a post-mortem study of normal subjects and patients with schizophrenia. Cereb. Cortex*, *12*(11), 1218–1224.

Kier et al. (2004). *MR imaging of the temporal stem: Anatomic dissection tractography of the uncinate fasciculus, inferior occipitofrontal fasciculus, and Meyer's loop of the optic radiation*. *Am. J. Neuroradiol.*, *25*(5), 677–691.

Kubicki et al. (2002). *Uncinate fasciculus findingsin schizophrenia: a magnetic resonance diffusion tensor imaging study*. *Am. J. Psychiatry*, *159*(18), 813–820.

Mars et al. (2015). *The extreme capsule fiber complex in humans and macaque monkeys: a comparative diffusion MRI tractography study*. *Brain Struct. Funct.*, 1–13.

Mazoyer et al. (2016). *BIL&GIN: A neuroimaging, cognitive, behavioral, and genetic database for the study of human brain lateralization*. *Neuroimage*, *124*, 1225–1231.

Mesulam. (2006). *Foreword*. In *Fiber pathways of the brain, Schmahmann J D, Pandya, D N*. New York: Oxford University Press.

Oishi et al. (2005). MRI atlas of human white matter (2nd ed.). Amsterdam: Elsevier.

Oishi et al. (2009). *Atlas-based whole brain white matter analysis using large deformation diffeomorphic metric mapping: Application to normal elderly and Alzheimer's disease participants*. *Neuroimage*, *46*(2), 486–499.

Petrides, & Pandya. (1988). *Association fiber pathways to the frontal cortex from the superior temporal region in the rhesus monkey*. *J. Comp. Neurol.*

Rodrigo et al. (2007). *Uncinate fasciculus fiber tracking in mesial temporal lobe epilepsy. Initial findings*. *Eur. Radiol.*, *17*(7), 1663–1668.

Saur et al. (2008). *Ventral and dorsal pathways for language. Proc. Natl. Acad. Sci. U. S. A.*, *105*(46), 18035–40.

Schmahmann, & Pandya. (2006). Fiber pathways of the brain. New York: Oxford University Press.

Testut. (1900). Traité d'anatomie humaine: Tome 2 (4th ed.). Paris: Octave Doin.

Thiebaut de Schotten et al. (2011). *Atlasing location, asymmetry and inter-subject variability of white matter tracts in the human brain with MR diffusion tractography*. *Neuroimage*.

Tournier et al. (2007). *Robust determination of the fibre orientation distribution in diffusion MRI: Non-negativity constrained super-resolved spherical deconvolution*. *Neuroimage*, *35*(4), 1459–1472.

Trolard. (1906). *Le faisceau longitudinal inférieur du cerveau*. *Rev Neurol*.

Van Essen et al. (2013). *The WU-Minn Human Connectome Project: an overview. Neuroimage*, *80*, 62–79.

Wernicke. (1908). *Diseases of the nervous system*. *Mod. Clin. Med.*

Table Of Contents

1 GENERAL INTRODUCTION 1

2 THE BASICS OF BRAIN CONNECTIONS 3

2.1 Neurophysiological basis 3

2.1.1 Axon 4

2.1.2 Synapse 4

2.1.3 Action potential 4

2.2 General principles of white matter organization 5

2.2.1 Complex but ordered 5

2.2.2 Fasciculation 5

2.2.3 Other principles 6

2.3 Why study connections? 7

2.3.1 (Dis)connections and disorders 7

2.3.2 Thinking of the brain in terms of its circuitry 8

2.3.3 A brief note on scales 9

3 BACKGROUND ON THE ANATOMY OF FIBRE PATHWAYS 10

3.1 Historical perspective 10

3.1.1 The beginnings of the study of nerves and human dissection 10

3.1.2 Recognition of white matter as an organized structure 12

3.1.3 Beginnings of gross dissection 12

3.1.4 Gross dissection flourishes (19th century) 12

3.1.5 Gross histology (and the return to gross dissection) 13

3.2 Confusion and controversy in the literature 14

3.2.1 Causes of the confusion and controversy 15

3.3 Redefining the anatomy of fibre pathways 17

3.4 Discovering new tracts and resolving debates 17

3.4.1 More extensive connections and subcomponents 18

3.4.2 Describing tract properties and connectional anatomy 18

3.5 Background on the external and extreme capsule complex 19

3.5.1 A complex area of passage 20

4 TECHNIQUES FOR STUDYING THE ANATOMY OF FIBRE PATHWAYS 22

4.1 Gross dissection 23

4.2 Axonal tracing 24

4.3 Polarized light imaging 24

4.4 Diffusion MRI Tractography 25

4.4.1 Diffusion MRI 25

4.4.2 Tractography 28

4.4.3 Tract segmentation 33

4.4.4 Mapping the connectional anatomy of fibre pathways 34

4.4.5 Measuring microstructural properties 35

4.4.6 Limitations of diffusion tractography 36

4.5 Summary and concluding remarks 36

5 CORTICAL TERMINATIONS OF THE IFOF AND UF: ANATOMICAL STEM-BASED VIRTUAL DISSECTION 38

5.1 Introduction 39

5.2 Methods 41

5.3 Results 46

5.4 Discussion 51

5.5 Conclusion 56

6 METHODOLOGICAL CONSIDERATIONS 57
6.1 A FURTHER ANALYSIS ON STEMS 57
6.2 COMPARISON OF TRACTOGRAPHY PIPELINES 58
6.2.1 Technical improvements in our tractography data 60
6.2.2 Method 61
6.2.3 Results 62
6.2.4 Conclusion 64

7 REVISITING THE UNCINATE FASCICULUS, ITS SUBCOMPONENTS AND ASYMMETRIES WITH STEM-BASED TRACTOGRAPHY AND MICRODISSECTION VALIDATION 67
7.1 INTRODUCTION 68
7.2 METHODS 69
7.2.1 Results 74
7.2.2 Discussion 84

8 GENERAL DISCUSSION 89
8.1 CONTRIBUTIONS OF THE THESIS 89
8.2 PERSPECTIVES FOR THE BIL&GIN AND UF 91
8.1 FINAL REMARKS 92

List of Abbreviations and Acronyms

AF	Arcuate fasciculus
CMC	Continuous map criterion
CSD	Constrained spherical deconvolution
dMRI	Diffusion magnetic resonance imaging
DTI	Diffusion tensor imaging
E2C2	Extreme and external capsule complex
EC	External capsule
EmC	Extreme capsule
ECFT	Extreme capsule fibre tract
IFOF	Inferior fronto-occipital fasciculus
ILF	Inferior longitudinal fasciculus
MdLF	Middle longitudinal fasciculus
PFT	Particle filtering theory
ROI	Region of interest
SLF	Superior longitudinal fasciculus
UF	Uncinate fasciculus

1 General introduction

If the cerebral cortex was organized in the form of an "*assembly line*" as Marsel Mesulam (2006) points out, "*where each station adds a new ingredient and hands its product to the next*", then there would be no real need to have a detailed map as the connections could be inferred through well-designed experiments. This is however not the case as the white matter is complex, being made up of innumerous fibres that run in parallel, enabling varied and distributed connections. Nevertheless, these fibres are subject to phylogenetically established constraints and follow a certain organization, thus they have recognizable structures that can be identified (see Section 2.2.2 for more details). The primary white matter structure is the fibre tract or fibre pathway consisting of a vast bundled collection of fibres. These pathways provide the bulk of the long-range connections in the human brain that are needed for integrative function between functionally distinct areas. It is becoming increasingly apparent that they play an important role in mediating functional activity. The detailed mapping of these pathways is therefore essential for understanding higher-level cognitive processes including language, memory and attention.

The problem is that there is no clear understanding regarding several of the fibre pathways and the literature is mired in confusion and debate. For example there is debate over the existence and inexistence of tracts, their names and their definitions. Much of the controversy originated from the 19th century from dissection and gross histology studies. This is a reflection of both the limitations of the techniques and the difficulty in studying the fibre pathways that have complex spatial relationships with one another. There are essentially two definitive works that have provided detailed accounts of the fibre pathways. The most comprehensive description of the fibre pathways in the human brain is the Dejerines' seminal work on myelin-stained brain sections (Dejerine & Dejerine-Klumpe, 1895). However, it appears that some of their descriptions are erroneous (this includes the fronto-occipital fasciculus they described as being situated above the caudate nucleus, shown on p.762 in Dejerine & Dejerine-Klumpke, 1895). Moreover the descriptions of the fibre pathways are more focussed on their courses and spatial relationships than their detailed terminations. More recently, Schmahmann and Pandya (2006) have provided detailed and comprehensive descriptions of several fibre pathways based on axonal tracing of 36 case studies in the macaca mulatta. However, there are limitations when generalizing to the human brain due to some areas being more expansive and complex and, in fact, important interspecies differences regarding the fibre pathways between monkeys and humans have recently been revealed (these include the superior and inferior fronto-occipital fasciculi). No doubt both of these works have made important contributions to the field of connectional neuroanatomy. Both also acknowledged the controversy and attempted to clarify some of the earlier debate regarding the anatomy of the fibre pathways. Nevertheless, the debate and controversy surrounding many of the tracts continues into the present and there remains no complete and detailed account of the fibre pathways in humans.

It has been over 20 years since Crick and Jones (1993) wrote their famous commentary on the state of our knowledge on human neuroanatomy (or lack thereof) and the need for new methodological developments. In terms of studying white matter anatomy, the available techniques at the time were invasive and time consuming and some could only be performed in experimental animals. Diffusion magnetic resonance imaging (dMRI) was developed to fill the gap providing the possibility of performing non-invasive *in vivo* studies of the fibre architecture in humans. It is based on measuring the collisions of water molecules with their environment to make inferences about the underlying structure. In particular, it capitalizes on the anisotropic nature of diffusion in the white matter. A second image processing step, called tractography, can virtually reconstruct the fibre architecture based on the information obtained from these images. This has broadened the possibilities for studying the fibre pathways in humans enabling virtual dissections of the white matter and application of a suite of neuroimaging tools (e.g., image registration, anatomical templates) allowing for the systematic and automatic analysis and processing of tracts, as well as quantitative information on the microstructural properties of

the white matter in the living human brain. Several large-scale initiatives have been launched to study the macroscopic connectome of the human brain, the most well-known is the Human Connectome Project (Van Essen et al., 2013).

The aim of this thesis is to provide a detailed mapping of the fibre pathways within the human brain using diffusion MRI to complement and go beyond what dissection and other techniques can tell us. We focus on the external and extreme capsule complex (E2C2), an anatomical area of white matter passage that has remained elusive. It consists of two association pathways, the inferior fronto-occipital fasciculus (IFOF) and the uncinate fasciculus (UF) that lie adjacent to one another within the E2C2, whose boundaries are ambiguous (see Section 3.5 for more details). The E2C2 association pathways have recently been a hot topic with there being much interest in the previously understudied IFOF and many studies focusing on the UF and its possible link with various clinical disorders. Additionally, both pathways have been implicated in the language circuitry reflecting a changing concept in our understanding of language connectivity, thus drawing increasing attention to them to determine their specific roles in language. In this thesis, we use diffusion imaging to investigate and try to clarify the anatomical boundary between these two pathways and provide a comprehensive description of their anatomical connectivity based on a large healthy cohort.

The recent application of diffusion imaging for the study of white matter has mainly focussed on identifying and locating known fibre pathways according to the classic 19th century literature. This has led to the publication of educational white matter atlases that show the general locations of the tracts relative to one another (Oishi et al., 2005; Catani & Thiebaut De Schotten, 2012). However these atlases do not aim to elucidate the anatomy of the fibre pathways and instead rely on *a priori* knowledge derived from the dissection literature, often imposing constraints on their anatomy. We developed an original approach to segment the association pathways of the E2C2 with minimal *a priori* from tractography datasets. It is based on the extraction process that was first used (and continues to be used) by the neuroanatomists, which defines a fibre tract by its stem (or compact portion) and considers all fibres included within the stem to belong to the pathway. Such a method to segment and identify a pathway thus enables us to study its complete set of connections.

In a first study, we dissociated the association pathways of the complex E2C2 and described the detailed connectional anatomy of these tracts *vis-a-vis* the existing literature. We described their variability and identified asymmetries within the individual branches of the tracts. We noticed some shortcomings in our tractography data and worked to implement a new processing pipeline using advanced tractography methods for the next study. In the second study, with the improved tractography pipeline, we focussed on providing a detailed description of the UF's connectional anatomy. We developed this work further by applying a clustering technique to segment the UF into meaningful subcomponents enabling a more fine-grained description of the pathway. We identified distinctive connectivity patterns and asymmetries with respect to the subcomponents. The division of tracts into subcomponents has been demonstrated in a few dissection studies, but to our knowledge, this is the first time a tract has been segmented based on computational methods. Finally, we also provide anatomical validation of these tractography results with post-mortem dissection.

Chapter 2 will introduce what connections in the brain consist of and why they are important for understanding function and behaviour. Chapter 3 will review the anatomical study of fibre pathways from Renaissance up to the present and includes a literature review pertaining to the external and extreme capsules. Chapter 4 will be about the different techniques used to study the white matter fibre pathways with a special focus on diffusion imaging. Chapter 5 applies the stem-based approach to dissociate the IFOF and UF in DTI data and investigates their cortical terminations. Chapter 6 discusses methodological considerations on the stem-based method applied to dMRI and includes an informal study investigating the influence of tractograpy pipelines on tract anatomy. Chapter 7 is a detailed study of the UF based on a more advanced tractography pipeline and investigates its boundary with the IFOF and its connectional anatomy and asymmetry of its subcomponents. Finally, Chapter 8 discusses the findings presented in this thesis and future perspectives.

2 The basics of brain connections

The brain is made up of fundamental units that work in concert to deliver behaviour, emotions, thoughts, memories, future plans, and the entire spectrum of human sensations. The ancient Egyptians pondered upon the brain, identifying it for the first time as an organ that, when damaged, caused peculiarities in a person (Edwin Smith papyrus, circa 2500 BC). The curious fibrous mass lying below the mantle of the brain was eventually observed and perhaps by virtue of its form, its function as a transport system was inferred early on. Theories of brain function began with the Greek's conception of a psyche or animal spirit that runs through the brain via the fibres, and although this idea was far-fetched, terms such as: electrical impulses, neurotransmitters, oxyhemoglobin have now replaced it. Increasingly, models or theories of brain function have incorporated connections leading to more complex representations of function and dysfunction. Today we have converged on how function emerges from the brain, as fundamental units connected in a network of interconnected circuits.

While the study of cortical activity has been at the heart of neuroscience and has led to many advancements in understanding and localizing specialized functions, it is only through their connections that it exceeds the sum of its parts, resulting in "*almost infinite richness and flexibility*" of mental activity (Mesulam, 1990). Understanding exactly how the fundamental units are connected is necessary to elucidate these functional networks and understand how its specific functions emerge.

Below we discuss why connections are important at both a biological (cellular) level and at the circuit level. We introduce how connections are made, highlight the anatomical organization of the connections (the brain's pathways), and we review key developments that have contributed to our modern understanding of the brain and why it is important to study its wiring.

2.1 Neurophysiological basis

The fundamental unit of the brain is the neuron. Neurons do not function in isolation. In fact they thrive when connected with many other neurons and wither away and eventually die when deprived of connections (Gudden's law). These connections allow the transfer of information from one neuron to the other communicating through synapses (see Figure 1). While the neuron itself is highly specialized and differs according to its morphological aspect, its connections, collectively called the white matter, are not distinguishable (although they can be locally differentiated based on their thickness and compactness). Nevertheless, what determines the function of a neuron may have more to do with the neurons they communicate with. Cytoarchitectonics, the study of the arrangement of the neuron types has received extensive study and is widely used for cortical parcellation, however myeloarchitectonics, the study of the local arrangement of the white matter has received relatively little attention. Both are likely needed to understand the full diversity of the cortex. Thus at the most basic level of cellular function, not only are connections crucial for the survival of the soma, but these connections may prove to be important for defining the function of a neuron (Mesulam, 2006).

White matter refers to the nerve fibres in the brain. Its white-ish appearance is given by the myelin sheath covering the axons acting as an insulator for the electrical impulses. Although the macroscopic structure of the white matter was already being studied centuries ago by the early dissectionists (see Chapter 3), our modern understanding of the white matter as composed of axons did not occur until around the 1840s after the invention of the compound achromatic microscope (see Chapter 3 for more details). The axon's essential role in conducting electro-chemical signals between nerve cells forms the basis of brain connections and underlies the functional importance of white matter as a transport system.

2.1.1 Axon

The most basic unit of the white matter is the axon. It is a long branched filament-like component of the neuron (along with the cell body or soma, dendrites and terminal boutons, Figure 1) that carries electrical signals over distances that can range from 0.1mm to 2m (Kandel et al., 2014). Electrical impulses travel in a single direction starting from the dendrites or soma, down through the axon to the terminal boutons (called dynamic polarization). At the axon hillock (the part of the axon nearest to the soma), the summation of impulses from transmitting neurons to a given neuron determines whether an action potential (see below) will be initiated and propagate along an axon.

In the brain, the large majority of axons are myelinated (Figure 1) meaning that they are wrapped in a flat fatty tissue called the myelin sheath provided by the oligodendrocytes. This increases the rate of signal transmission by insulating the conducting axon and preventing the electricity from dissipating to outside sources. However, the myelin sheath is not continuous along the axon, separated by ~1μm gaps, called the nodes of Ranvier (Figure 1). This allows the electrical signal to jump from node to node, regenerating at each node and speeding up the rate of transmission, a process called saltatory conduction. As the electrical impulse reaches the terminal boutons it undergoes a synapse, transmitting information to a nearby neuron, which receives it through its dendrites or soma.

2.1.2 Synapse

The synapse is the fundamental computational unit of the brain. It is the process of transmitting information from a pre-synaptic neuron to a post-synaptic neuron across a small junction, called the synaptic cleft (Figure 1). As an electrical impulse from the soma travels to the terminal boutons of the pre-synaptic cell, it will trigger small sacs called vesicles within the terminal boutons to migrate towards the membrane of the pre-synaptic cell. These vesicles, containing neurotransmitters, will eventually fuse with the membrane and release the neurotransmitters into the synaptic cleft. The post-synaptic cell, in close proximity with its tentacle-like dendrites, contains receptors that can selectively bind with only certain neurotransmitters. When neurotransmitters successfully bind with the receptors of the post-synaptic cell they change the excitation in the post-synaptic cell and can be either inhibitory or excitatory. If the net excitatory change is sufficiently large it causes an action potential in the post-synaptic cell propagating the message.

2.1.3 Action potential

Electrical potential is determined by the relative quantity of ions inside and outside of the cell membrane that move across the membrane through ion channels. A neuron is at resting equilibrium when the potential charge across the cell membrane is approximately -70mV, with relatively more sodium ions outside and more potassium inside the neuron. When the neuron receives a depolarizing current across the membrane (caused by the opening of specific ion channels), it moves towards 0. If it reaches the threshold of -55mV an action potential will occur causing an explosion or “spike” in electrical activity of a fixed charge. An action potential does not occur if the neuron does not reach the critical threshold.

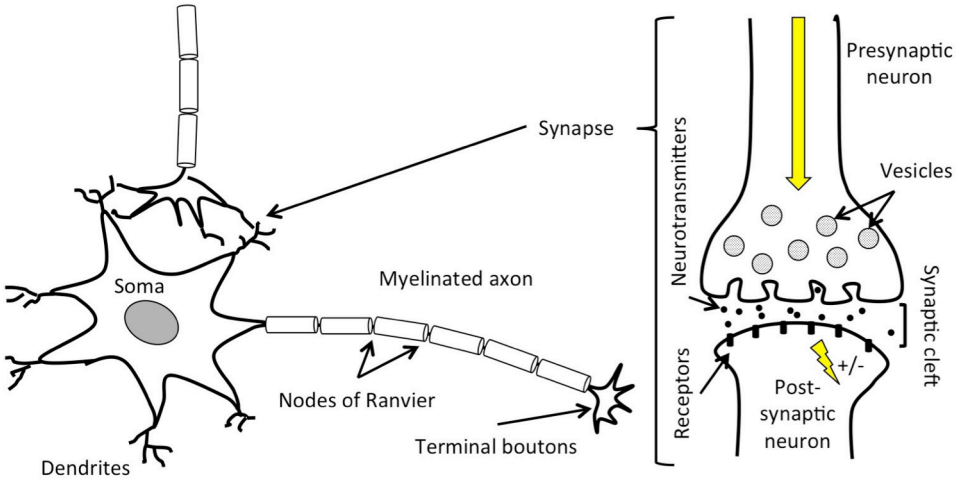

Figure 1. Signal transmission between neurons in the brain. Left: The structure of a typical neuron including its soma, dendrites, myelinated axon and terminal boutons, shown having a synapse with another neuron (depicted in detail on the right). Right: A synapse, triggered by an action potential in the pre-synaptic cell (yellow arrow), causing the vesicles to migrate and showing the diffusion of neurotransmitters crossing the synaptic cleft to bind with the selective receptors and elicit a change in excitation in the post-synaptic neuron (yellow charge).

2.2 General principles of white matter organization

2.2.1 Complex but ordered

The white matter is not arbitrarily arranged but organized following some general principles. This was captured in some of its earliest descriptions. The first anatomists who performed gross dissections to study the white matter were struck by both the orderliness and complexity of the fibre structure. Thomas Willis, in 1672, stated that he was "*astonished at the innumerable arrangements of nerve fibres distributed in wonderful order into the different parts of the entire body*" (p. 584, Clarke & O'Malley, 1996). Nicolas Steno, an eminent scholar of the time, regarded the white matter as "*nature's finest masterpiece*". Upon viewing gross dissections of the white matter, he wrote an essay concluding the following:

> *We are assured that wherever in the body there are fibres, they everywhere adopt a certain arrangement among themselves, created more or less according to the functions for which they are intended. If the substance is everywhere of fibres, as, in fact, it appears to be in several places, you must admit that these fibres have been arranged with great skill, since all the diversity of our sensation and our movements depends upon this. We admire the skilful construction of the fibres in each muscle; how much more then ought we to admire it in the brain, where each of these fibres, confined in a small space, functions without confusion and without disorder.* (Steno, 1665 from Clarke and O'Malley, 1996).

Thus although the white matter is highly intricate and complex, it has a general organization, and there lies the challenge in describing it.

2.2.2 Fasciculation

One of the predominant characteristics of white matter is that fibres bundle together to form fascicles or tracts. This reflects a biological process called fasciculation that occurs during the formation of axons. When axons develop, they migrate to their pre-determined targets (Sperry, 1943) guided by growth cones, during which they undergo a process of bundling

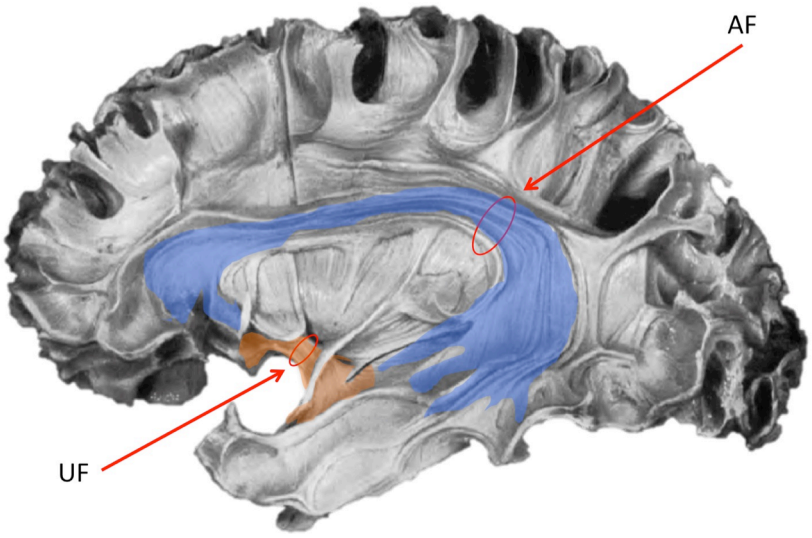

Figure 2. Photograph from gross dissection, lateral view of left hemisphere revealing the complex but ordered structure of the white matter forming fasciculi. The stems or core areas of the uncinate fasciculus (UF) and arcuate fasciculus (AF) are circled. Plate 6, modified from Ludwig & Klingler, 1956.

(coming together with other axons) and upon reaching their targets, debundling (they diverge to innervate their targets) (Nornes & Das, 1972; Kandel et al., 2014). The mechanisms and factors that contribute to fasciculation include chemoattractors and chemorepellents, though exactly how these and other factors (e.g., their random movement) cause axons to fasciculate is not known (Hentschel & Ooyen, 1999). Fasciculation has been reported at the microscopic level (Schmahmann & Pandya, 2006; Mikula et al., 2012). Fasciculation can also be seen at the macroscopic level with fibres visibly coming together and forming identifiable fibre pathways. The pioneers of white matter anatomy identified these fascicles that were observable with the naked eye through dissection (see Figure 2). Raymond de Vieussens, a contemporary of Willis and Steno, described the white matter as "*composed of innumerable fibrils connected together and arranged into various fasciculi*" (1684, as cited in Schmahmann & Pandya, 2006). While this rule may not apply to all fibre tracts (some are diffuse and sheet-like, e.g., the claustro-cortical tract, thalamo-cortical tract), many are identifiable based on their unique bundle form and thus have a point of convergence where all of their fibres come together into a compact bundle. For example, the cortico-spinal tract while it has a fanning configuration and disperses across a large cortical area, all of its fibres join together at the cerebellar peduncles before entering the spinal cord. Other bundle stems are visibly apparent, for example the arcuate fasciculus and uncinate fasciculus in Figure 2. Not surprisingly, the approach that dissectionists introduced and continue to use involves locating the compact portions of bundles in order to identify them as tracts and describe them. In Chapter 4, we present our novel method applying this concept of a compact stem or bottleneck to segment tracts in tractography datasets. Although only a general rule (that has exceptions), the concept of fasciculation or bundling remains a central assumption in the definition of many tracts. This applies to both long-range and short U-shaped fibres. Aside from an organizational advantage, with fibre groupings having generally homologous trajectories, origins and terminations, the reason why tracts fasciculate together is not known.

2.2.3 Other principles

Other general principles of organization have been identified. Schmahmann and Pandya observed, in macaques, a typical arrangement in how efferent connections from the cortex

emanate from the gyri to reach their terminations (Fig. 5-2 in Schmahmann & Pandya, 2006; see also Lehman et al., 2011). A few tract tracing studies have made general observations about the white matter regarding the distribution of the connections, the proportion of cortico-cortical connections and range of connection strengths (Markov et al., 2011, 2014). Such information will be useful for improving and validating DWI tractography. One study based on tractography has proposed that the white matter may be organized in a grid-like sheet structure (Wedeen et al., 2012b), with many orthogonal configurations. This theory, however, remains controversial (Catani et al., 2012; Wedeen et al., 2012a) as it relies on imaging data that is susceptible to biases and inaccuracies, and it may not be compatible with our current observations of white matter. As such, at the moment little is known about the organization of white matter (Johansen-Berg & Behrens, 2014).

2.3 Why study connections?

Just as neurons do not function in isolation, neither do brain regions each of which has a distinct pattern of inputs and/or outputs to other brain regions. The connections between brain areas enable their coordinated activity and the interruption of such connections leads to unique symptoms that arise from the severed connection between the two intact areas, known as disconnection syndromes. Below we briefly review how our understanding of brain function has reached its present form first derived from the study of clinical disorders and moving to more complex circuitry and wiring diagrams.

2.3.1 (Dis)connections and disorders

The study of the brain from a hodological perspective has its origins in clinical neuropsychology. Investigations of various forms of aphasia caused by brain lesions led to the observation of localized areas that support language production (known as Broca's area) and language comprehension (known as Wernicke's area). In 1874, Carl Wernicke proposed a clinico-anatomical model of aphasias (Figure 3a). His model indicated that not only do specific language deficits arise from damage to the specialized language areas (a1 or b, referring to Wernicke and Broca's aphasias respectively), but a unique pattern of deficits could arise from disconnections between these areas (a1-b connection), which he called *Leitungsaphasie*, translated as 'conduction aphasia' (Wernicke, 1874). Although not the present definition of the disorder, he described a situation in which patients had paraphasias accompanied with *conduite d'approche*, or attempts to correct them, because they would be able to hear and understand their own errors. Today, conduction aphasia refers to the condition of having conserved language production (fluent speech) and comprehension but an inability to repeat speech that is spoken to you. Wernicke was the first to propose a disconnection syndrome introducing the idea that brain dysfunction could arise not only from damage to the grey matter of the brain, but also in the white matter causing functional disconnections.

This led to more complex representations of function and more elaborate models including Lichtheim's model of aphasic disorders (Figure 3b) (Lichtheim, 1885). The neuroanatomical work on white matter pathways began to make its way into neuropsychological models to explain the observed clinical disorders. Dejerine worked on linking the different aphasia symptoms to different white matter pathways including the inferior longitudinal fasciculus (ILF), IFOF and arcuate fasciculus (AF) (Dejerine & Dejerine-Klumpe, 1895; Krestel et al., 2013). Although it is only starting to resurface in the language literature now, Wernicke was the first to propose a ventral pathway for language in the brain (Wernicke, 1874; Weiller et al., 2011). Wernicke was a pioneer of the associationist school that emphasized the importance of the cortical centres as well as the connections between them, opposing the localizationist school of thinking that he considered too limiting:

> *Any higher psychic process… could not be localized, but rested on the mutual interaction of fundamental psychic elements [e.g., sensory and motor activities as occurring in primary cortical areas] mediated by means of their manifold connections via the association fibres.* (Wernicke, 1885 as cited in Catani, 2007).

This concept was lost in the following years as holistic and localizationist theories prevailed, but advances in tract tracing in the 1970s brought new interest in brain connections and a shift to the associationist approach.

2.3.2 Thinking of the brain in terms of its circuitry

Over the last 30 years, models of sensory and cognitive function have developed starting initially with the visual system. This was the result of a combination of electrophysiology, behavioural and tract tracing studies. Ungerleider and Mishkin's (1983) iconic experiment in monkeys showed a double dissociation between tasks requiring spatial processing and object recognition. Based on the existing evidence of the visual circuitry, it led them to propose a theoretical framework that involved dual streams for visual processing: a ventral "*what*" pathway, responsible for the visual identification of objects and a dorsal "*where*" pathway, responsible for the visual location of objects. A similar theory was applied to the human visual system, though slightly revised, the ventral pathway became "*vision for perception*" and dorsal pathway "*vision for action*" (Goodale & Milner, 1992). Although they may no longer be understood strictly as dissociated pathways, this dual-stream model lay the groundwork for many experiments and was important in advancing our understanding of visual processing (Milner & Goodale, 2008). It has also extended to other domains including auditory processing (Rauschecker & Tian, 2000). Without the work on connections such theories would not have been possible.

During this period, using electrophysiology and tract tracing, the circuitry of the visual system in the monkey was revealed in unprecedented detail (Felleman & Van Essen, 1991). Such detailed mapping enabled more sophisticated models of function. Based on this work a theory on the hierarchical organization of visual processing was formed (Felleman & Van Essen, 1991). Around that time Mesulam proposed that brain function consisted of parallel distributed

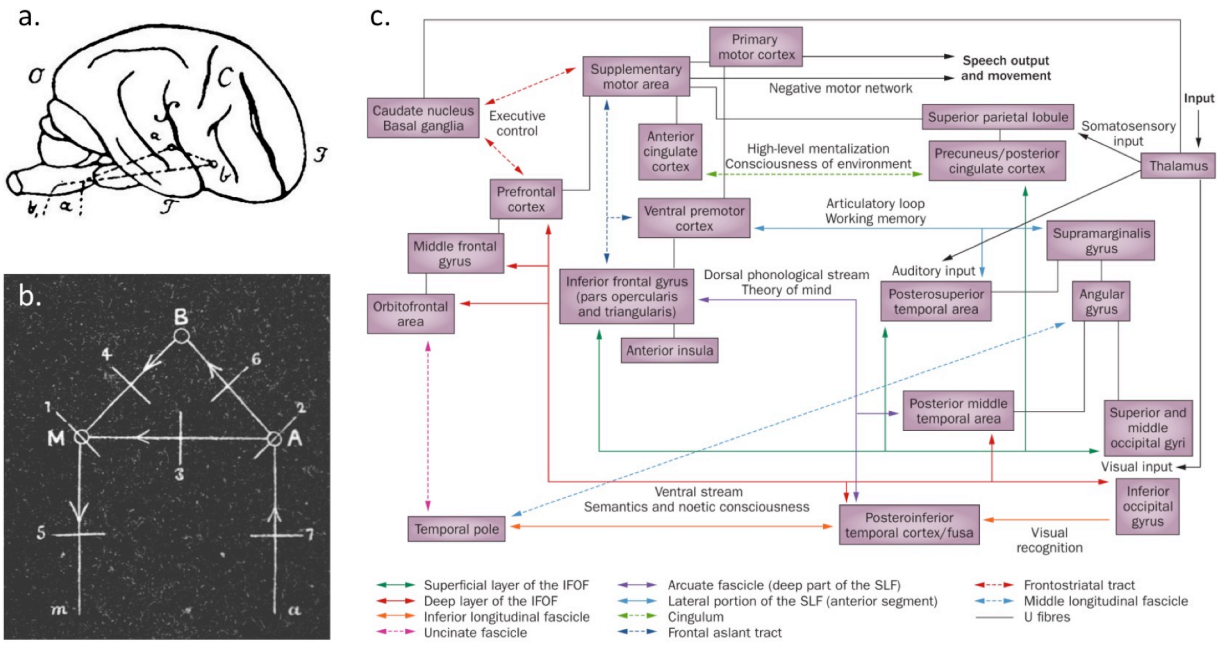

Figure 3. Wernicke (a) and Lichteim's (b) original models of aphasia and a modern model of language function incorporating the anatomical substrate (fibre pathways) (c) (with permission from Duffau, 2015). Such models are important for guiding experiments and formulating hypotheses in order to disentangle language processing in the brain by considering both its cortical areas and pathways.

processing arranged in large-scale networks (Mesulam, 1990). In 1998, Mesulam formalized a general theory of hierarchical processing of brain function proposing that the flow of information proceeds in a hierarchical way from primary areas to associative areas that are tuned to process increasingly more complex stimuli. He also proposed that, based on the macaque cortex, the cortex could be divided into five principal zones: primary sensory-motor, unimodal, heteromodal, paralimbic and limbic that are connected in a predictable way (Mesulam, 1998). Mesulam's theory, like those of Ungerleider and Mishkin and Goodale and Milner, remains highly influential. Given the complexity of the brain, there is a need for detailed maps to define the structural substrate of integrated cerebral activity. They provide an anatomical basis, which constrains models of function providing the bedrock for new hypotheses on how brain areas work together to produce these functions.

Models hypothesizing the functional roles of processing streams have continued to form. More recently a dual-stream model for language processing has been proposed (Hickok & Poeppel, 2004, 2007). This proposal, however, was a purely cognitive model based upon an accumulation of functional imaging studies and lacked an anatomical basis. A number of studies have since tried to illuminate the underlying connections supported by the white matter pathways in order to create a biologically-plausible model (Frey et al., 2008; Glasser & Rilling, 2008; Saur et al., 2008; Turken & Dronkers, 2011; Axer et al., 2013; Dick et al., 2014; Bajada et al., 2015). In fact it would appear that language function involves multiple pathways both direct and indirect making up a language circuitry (see Figure 3c). As a result increasing attention has been drawn towards understanding the functional roles of the fibre pathways involved in the language circuitry (Parker et al., 2005; Duffau, 2005, 2008, 2015; Catani et al., 2007, 2013; Mandonnet et al., 2007; Saur et al., 2008; Duffau et al., 2009; Rolheiser et al., 2011; Papagno, 2011; Griffiths et al., 2013; Almairac et al., 2014). Our increased knowledge in brain function and specialized cortical areas makes it possible to speculate on the functional roles of the pathways. Clearly, there is an interest in studying the fibre pathways and they may be the missing ingredient for understanding not only higher cognitive functions such as language but also clinical disorders such as autism, schizophrenia and depression among others. An advantage today is that we can potentially identify the functional role of a specific pathway by correlating it with function or an interruption of function through techniques that were not available a century ago (diffusion imaging, direct electrical stimulation). This information can be modelled computationally to investigate their effects on the system (Ueno et al., 2011). In sum, to understand the brain you need to have both an understanding of the cortical sites and their connections, in particular connections are important for understanding how the cortical sites function computationally and dynamically.

2.3.3 A brief note on scales

The study of brain connections is vast. Connections can be studied at the microscopic, mesoscopic and macroscopic scales. In this thesis we focus on the macroscopic scale, connections between anatomically (generally surface, e.g., gyri, sulci) -defined brain regions. They can also be studied at the whole-brain network level (see, for example, Bullmore et al., 2009) or at a smaller scale in terms of individual fibre pathways as mentioned in the previous section. This work focuses on the fibre pathways.

3 Background on the anatomy of fibre pathways

What's in a name?
William Shakespeare, Romeo and Juliette, 1597

The study of white matter fibre pathways began in the Renaissance and culminated in the 19th century with the work of Dejerine, Sachs and others, describing in great detail the white matter tracts that were known at the time. Since then little has been added to their body of work in terms of the human anatomy of fibre pathways. While axonal tracing has made it possible to create detailed structural maps in animals, there are no equivalent maps in humans. Today we are seeing a renewed interest in fibre pathway anatomy with dMRI tractography, capable of studying the pathways *in vivo*, with exciting clinical applications. It has also come to light that, despite the monumental work that was produced in the last two centuries, there remain many outstanding questions concerning the anatomy of these fibre pathways.

We begin with a historical overview of the study of white matter anatomy that highlights important developments, followed by the confusion and controversy surrounding several of the tracts and how our understanding of white matter tract is evolving based on recent work. Finally, we present the anatomy of both external and extreme capsules, an anatomical area of fibre passage that has remained elusive.

3.1 Historical perspective

3.1.1 The beginnings of the study of nerves and human dissection

There has always been an interest in describing the intricate white matter anatomy. In Greek antiquity (~4th and 5th centuries BC) the concept of nerves was already introduced. The brain was considered to be the "*organ of the mind, the origin of the nerves and the seat of the soul*" (Schmahmann & Pandya, 2006). During Greek antiquity, systematic brain dissections were carried out (Anaxagoras of Klazomenai, 500 BC, Schmahmann & Pandya, 2006). Unfortunately, little regarding the study of the brain is conserved from this time period (Swanson, 2014). After this productive period of study, human dissection was banned covering most of the Medieval period. During this period of proscription, most of what we learned in terms of the anatomy of the brain depended on the pioneering animal dissections and vivisections of Galen (~2nd century, Roman empire). He described and named many of the structures still in use today: the dura mater, pia mater, corpus callosum, the four ventricles, fornix, pineal and pituitary glands (Schmahmann & Pandya, 2006). Galen's work was so highly influential that it dominated the next 1300 years.

Figure 4. The frontispiece to Andreas Vesalius' anatomical text *De Humani Corpus Fabrica* (The Fabric of the Human Body) *Book VII* (1543) depicting one of his public dissections that often drew large crowds. Vesalius is shown (centre left) with one of his students (above Vesalius holding a manuscript) and an older figure that may symbolically represent Galen reacting with displeasure to Vesalius' work (lower right) (Scatliff & Johnston, 2014). For reference, images of Vesalius and Galen are respectively shown in the top left and right. This version for Charles V is reportedly the only one to be hand coloured (New York Public Library).

Human dissection was reintroduced at the end of the Middle Ages (13th century), but many still based their observations on the work of Galen, which was based on various different animals and also potentially erroneous. Realism was starting to appear in Da Vinci's (1452-1519) drawings of the anatomy, but it wasn't until the 16th century that the scientific investigation of human neuroanatomy began. Andreas Vesalius (1514-1564) led the way, encouraging his students to challenge the work of Galen and to use direct observation to draw conclusions about the anatomy (Empiricism). Vesalius held public dissections that often drew crowds of over 500 people. The frontispiece of his acclaimed anatomy text *De Humani Corporis Fabrica* (1543), reportedly drawn by a student of Titian, depicts the scene of one of his public dissections showing Vesalius, one of his students that may be either documenting the dissection or comparing it with Galen's work and an older figure that may symbolically represent Galen reacting to Vesalius' work (Figure 4).

Early on, dissections were performed *in situ* (in Latin, "on site") in other words with the brain still sitting inside the head. This can be seen in the illustration from Vesalius' brain dissections in *Fabrica*. In the cross-sectional view several structures are labelled, representing one of the first modern atlases. In 1573, Costanzo Varolio published a method to perform dissection by removing the brain from the skull and slicing it horizontally from the base up (as opposed to top down). This revolutionized the way dissection was performed allowing better visibility by viewing the brain structures on serial slices, especially for the lower structures that were previously more difficult to access. This was how Varolio discovered the pons, that was later named after him – pons Varolii or "bridge of Varolius" (Varolio, 1573).

3.1.2 Recognition of white matter as an organized structure

It was also during this period (16th century) that white matter was no longer considered an amorphous mass but an intricately organized system of fibres. Galen distinguished the corpus callosum earlier, but there was yet to be a clear distinction between the grey and white matter. Vesalius was the first to remark the "*softer and yellowish cerebrum from the harder and whiter deeper substance below it*" (Schmahmann & Pandya, 2006). He also elaborated on Galen's corpus callosum describing its fibres that appear to connect the two cerebral hemispheres. In 1586 Piccolhomini introduced the terms cerebrum for the cerebral cortex and medulla for the white matter (Clarke & O'Malley, 1996). This development, although a simple observation, was an important one as it brought more interest to the study of the white matter or medulla oblongata, as it was known.

It also became understood that the white matter consisted of fibres that terminated in the cortex. Using one of the first microscopes, Marcello Malpighi (1628-1694) observed the white matter fibres by following them and remarked that they all joined with the cortex (1664). Although, he later confirmed this with no need of a microscope, explaining that the white matter fibres that end in the cortex was apparent in the fish brain seen through the fish by simply holding it up to the light of day (from Diemerbroeck, 1695).

3.1.3 Beginnings of gross dissection

The practice of gross dissection (see Chapter 4) began a century later. Thomas Willis and Nicolas Steno were important pioneers. Steno intuited the relevance of white matter and was way ahead of his time, providing insights not only about how to study the white matter, but how it is arranged and that it may differ between individuals. Willis was one of the first to perform gross dissections of the white matter and published *Cerebri Anatome*, a detailed description of brain anatomy, in 1664. During this period, several notable white matter structures were identified including the centrum oviale (schematically shown in Vieussens, 1684), anterior and posterior commissure and some of the thalamocortical fibres Vicq d'Azyr, 1786).

3.1.4 Gross dissection flourishes (19th century)

It took over another century for gross dissection to be practiced widely, which was aided by new fixing techniques to preserve the brain. During this period, many new fibre pathways were identified, whose names (and in large part their definitions) would remain in use up to the present day. Johann Christian Reil introduced the term corona radiata to refer to the fibres radiating out of Vieussens' centrum ovale and described some of the first association fibre bundles that he named in German (Reil, 1809). Burdach published a 3-volume work (Burdach, 1819) that expanded on Reil's work describing the association pathways in more detail and identifying new ones. He also gave Latin names to the pathways for the first time including the tapetum, cingulum, uncinate fasciculus, arcuate fasciculus and inferior longitudinal fasciculus

among others (Burdach, 1819). Other notable anatomists who practiced gross dissection and contributed to the study of the fibre pathways were Gall and Spurzheim (1810), Mayo (1827) and Arnold (1838).

3.1.5 Gross histology (and the return to gross dissection)

During the second half of the 19th century, the focus shifted from gross dissection to brain sections as a result of new techniques. The discovery of the compound achromatic microscope in the 1830s rapidly advanced staining methods applied to brain sections, enabling better visibility and discrimination of certain cellular structures. The Weigert stain, for example, was used to visualize myelinated axons, which Paul Fleischig used to study myelogenesis in fetuses and young infants. It did not, however, improve the ability to discriminate between fibre pathways. Additionally, Augustus Waller's classic discovery that nerve fibres degenerate distal to the site of injury (anterograde degeneration) (Waller, 1850) led to the beginnings of contemporary tract tracing methods, however these could only be performed in experimental animals. The developments of staining methods together with the microtome evolved into histology (microscopic study of the anatomy). However, those who were interested in the anatomy of fibre pathways continued to use histology-prepared brain sections to study its macroscopic anatomy (Meynert, Sachs, Dejerine, Forel, Wernicke, von Monakow). Gross dissection continued to be used although there was a clear preference towards sectional anatomy. This led to the seminal work of the Dejerines that described both microscopic and macroscopic anatomy in their comprehensive two-volume publication *Anatomie des Centres Nerveux* (Dejerine & Dejerine-Klumpe, 1895). Other important developments during this time included the classification system of fibre pathways that Meynert established through his histology studies in the bat (Meynert, 1872). Meynert proposed that the white matter consisted of commissural pathways that connect the two hemispheres, projection pathways that connect the cortex with the subcortical nuclei and short and long association pathways that connect the cortex within a hemisphere, the short fibres being U-shaped connecting adjacent gyri. Heinrich Sachs described the connections of the occipital lobe in meticulous detail (Sachs, 1892).

However, the motivation to study the fibre pathways on serial slices was not well received by all. In 1909, Jamieson wrote:

> *Dissections of the brain to show the internal structure, as contrasted with slicing, is not a new method, but the practice has fallen into disuse, and apparently even into dishonour. Illustrations of the internal structure of the brain in the current text-books of anatomy and of physiology are almost all drawings of sections, or they are merely schemata. A few dissections are still reproduced from the old text-books* (p.226, Jamieson, 1909*).*

The criticism arose because of the difficulty in following the course, trajectory and terminations of the fibre pathways on serial sections. It was also difficult to visually compare fibre trajectories in brain sections with those obtained from gross dissection. Nicolas Steno condemned the use of brain sections for studying the white matter two centuries earlier, stating albeit extremely that "it [the method of brain sections] does not provide any anatomical elucidation [of the white matter]" (Steno, 1665). Being cautious, Sachs emphasized the importance of validation to use at least two complementary methods to determine the existence of brain connections (Forkel et al., 2015), perhaps as a result of the difficulty of the technique in following the fibre trajectories. Brain sections may have made considerable contributions to describing the detailed sectional organization of structures in the brain, however, it would appear that they are not optimal for seeing the complex relationships between tracts. It would appear that gross dissection enables better visualization of the fibre pathways, the mechanical separation of the fibres being necessary to discriminate between the intermingling or crossing tracts.

This resulted in a return to gross dissection as the primary method for studying the fibre pathways in humans. Despite an important development in technique that emerged (Klingler, 1935), gross dissection was performed only sparsely in the 20th century. Still, the value of gross

dissection was indisputable. Ludwig and Klingler, recognizing that « the old method of preparation [gross dissection] has been widely superseded by the modern methods of sectioning as an introduction to the study of nuclei and fibre tracts », set out to create an atlas of the fibre pathways with "*three-dimensional presentations*" (Ludwig & Klingler, 1956). Their earlier work, published before the interruption of the war, was highly appreciated and sold out (Ludwig & Klingler, 1936). The use of gross dissection continues to the present day. In fact, there has been a recent revival of studies using gross dissection (now referred to as fibre dissection) to revisit or rediscover the fibre pathways described by the earlier dissectionists and to build upon their work (Türe et al., 1997, 2000; Peuskens & Loon, 2004; Fernández-Miranda et al., 2008; Martino et al., 2010, 2011; Martino et al., 2013; Sarubbo et al., 2013; Vergani et al., 2014; Goga & Türe, 2015; Meola et al., 2015).

3.2 Confusion and controversy in the literature

For centuries neuroanatomists have tried to elucidate the complex relational anatomy of the white matter tracts but, despite their accomplished body of work, they have only done so partially (see next section) and with considerable debate ensuing. By the end of the 19th century, there were many points that remained unclear. In fact, this was one of the motivations behind Jules and Augusta Dejerines' seminal work. Jules Dejerine writes in his preface, rather paradoxically:

> *…despite the sophisticated means of investigation available to us today, there is still, as regards especially the brain, more than one obscure point to elucidate*[1] (Dejerine & Dejerine-Klumpe, 1895).

Over a century later, Schmahmann and Pandya, in their influential work on the fibre pathways in the monkey (2006), also remarked on the controversy surrounding some of the tracts aiming to resolve these debates. Despite their efforts and the advancements in technology (axonal tracing, staining techniques), the lack of consensus on many fibre tracts persists and has only become more apparent with the growing interest in white matter. Note however that some of the debate has arisen from recent work, particularly studies in monkeys.

For example, some of the biggest controversies concern the existence of certain pathways including the inferior fronto-occipital fasciculus (IFOF) (Curran, 1909; Schmahmann & Pandya, 2006; Forkel et al., 2012), superior fronto-occipital fasciculus (Onufrowicz, 1887; Türe et al., 1997; Nikos Makris, 2007; Schmahmann & Pandya, 2007; Forkel et al., 2012; Meola et al., 2015), inferior longitudinal fasciculus (Davis, 1921; Tusa & Ungerleider, 1985; Catani et al., 2003) and vertical occipital fasciculus (Wernicke, 1881; Yeatman et al., 2014).

There have also been inconsistencies in the descriptions of tracts which appear to arise from unclear boundaries between intermingling or adjacent tracts, for example, Meyer's loop which consists of projection fibres as well as the optic radiations (Goga & Türe, 2015) and the external and extreme capsules which consist of the uncinate fasciculus and IFOF closely lying adjacent to one another (see Section 3.4 and Chapter 7).

There is also a tendency towards oversimplification. For example, the tract known as the IFOF is not strictly fronto-occipital but consists of fronto-temporal and fronto-parietal connections (Curran, 1909; Catani & Thiebaut de Schotten, 2008; Martino et al., 2010; Caverzasi et al., 2014). Similarly, the uncinate fasciculus may not consist only of "hook-shaped" fibres but also ones that have a straighter horizontal trajectory (Dejerine & Dejerine-Klumpe, 1895; Gordinier, 1899; Testut, 1900). While names are given to reflect their appearance or their dominant connections, it will likely be the case that fibre tracts are more complex than their names imply (Dick & Tremblay, 2012).

[1] Original text: "*…malgré les moyens d'investigation perfectionnées dont nous disposons aujourd'hui, il reste encore, pour ce qui concerne le cerveau surtout, plus d'un point obscur à élucider.*"

3.2.1 Causes of the confusion and controversy

Nomenclature

One major contribution to the confusion from the last century has been the lack of a *lingua franca* (or common language) for the white matter. This remains a prevalent issue in the current literature. For example it is not clear whether the middle longitudinal fasciculus and the superior longitudinal fasciculus temporo-parietal component (SLF-TP), both referring to temporo-parietal connections, are in fact the same pathway (Catani et al., 2005; Nikos Makris et al., 2012; Kamali et al., 2014). There are also multiple names given to the same pathway. For example the names arcuate fasciculus (AF) and superior longitudinal fasciculus (SLF) were given to the long arching fronto-temporal pathway around the Sylvian fissure in humans. However, it was identified in the monkey along with three additional components and named them SLF I, II, and III (with SLF IV referring to the AF/SLF) and recently a fifth one has been added (SLF-TP) (Petrides & Pandya, 1984; Schmahmann & Pandya, 2006). In parallel, dMRI tractography studies have demonstrated two additional components of the AF (anterior and posterior indirect AF) in humans that may or may not correspond to the SLF components in the monkey (Catani et al., 2005). However, the AF components have fallen out of use, while the AF is now the preferred term for the long arching pathway and the SLF is used primarily to refer to its subcomponents (the existence of a fifth one is still under debate).

Moreover, anatomical white matter "structures" can refer to both topographical areas of white matter, that are identifiable based on their appearance and location and boundaries with other anatomical landmarks (e.g., the internal capsule, sagittal stratum, centrum semiovale, corona radiata), and tracts which are defined based on their mechanical separations from other white matter tracts and have homologous trajectories and terminations (e.g., AF, cingulum, anterior commissure, vertical occipital fasciculus). Thus topographical areas, because they are arbitrarily defined, in almost all cases consist of multiple fibre tracts (Table 1). Due to the differing sense in meanings of terms used to describe the white matter, it is important to understand what they represent.

While there is an international effort to standardize anatomical terms (Terminologia Anatomica, 1998), the recent literature is riddled with inconsistencies. Clearly, there is a need to establish a *lingua franca* for the white matter anatomy as others have already stated (Bajada et al., 2015).

Table 1. List of topographical white matter structures and their corresponding tracts.

Name of structure	Tracts that pass through
Internal capsule	Thalamocortical, corticospinal, corticobulbar, corticopontine
External capsule	IFOF, UF, projection (claustro-cortical, cortico-striatal)
Extreme capsule	IFOF, UF, projection (claustro-cortical, cortico-striatal)
Sagittal stratum	Optic radiations, splenium, thalamocortical, IFOF, ILF, anterior commissure
Cerebral peduncle	Corticospinal, corticobulbar
Meyer's loop	Optic radiations, anterior commissure, projection
Corona radiata	Thalamocortical, corticospinal, corticobulbar, corticopontine

Generalizations from monkey to human

Connections in the human brain are often extrapolated from animal studies as it is the only technique that can show detailed connections between cytoarchitectonically defined areas (Mesulam, 2012). While there appear to be homologous areas between monkeys and humans, at a more fine-grained level there are profound differences (Orban et al., 2004). It would not be surprising if this were also the case for the white matter pathways given the much larger complexity of the human brain. In fact, while there have been some identified homologies in white matter pathways (Croxson et al., 2005; Thiebaut de Schotten et al., 2012), some of the controversy surrounding the existence of tracts has perpetuated by generalizing pathways from monkey studies to humans. These include a ventral fronto-occipital tract (IFOF) that exists in humans but not in monkeys (Curran, 1909; Schmahmann & Pandya, 2006; Forkel et al., 2012) and a dorsal fronto-occipital tract (SFOF) that exists in monkeys but not in humans (Türe et al., 1997; Schmahmann & Pandya, 2006; Meola et al., 2015).

Representation and interindividual variability

In addition to the above, there are likely several other factors that contributed to the confusion. The differences in the representation of the pathways between brain sections and fibre dissection are one source of controversy that may have led to errors in interpretation. In contrast to Mayo's full illustrations of fibre dissection, Dejerine's sections and schemas are very different ways of representing the fibre anatomy (Figure 5). Several anatomists have remarked on the difficulty in interpreting the trajectories of fibre pathways on brain sections (Steno, 1665; Jamieson, 1909). As one of their reasons for creating their three-dimensional atlas, Ludwig and Klingler wrote: "*[t]he macroscopic method also relieves us of the labour of mentally reconstructing structures, after the observation of numerous sections, a task which is only too often unsuccessful*" (Ludwig & Klingler, 1956). Also, given the limited number of subjects and time and labour involved in fibre dissection, interindividual variability may have rendered some tracts easier to distinguish in some subjects than others (compared with the anatomical textbooks which are

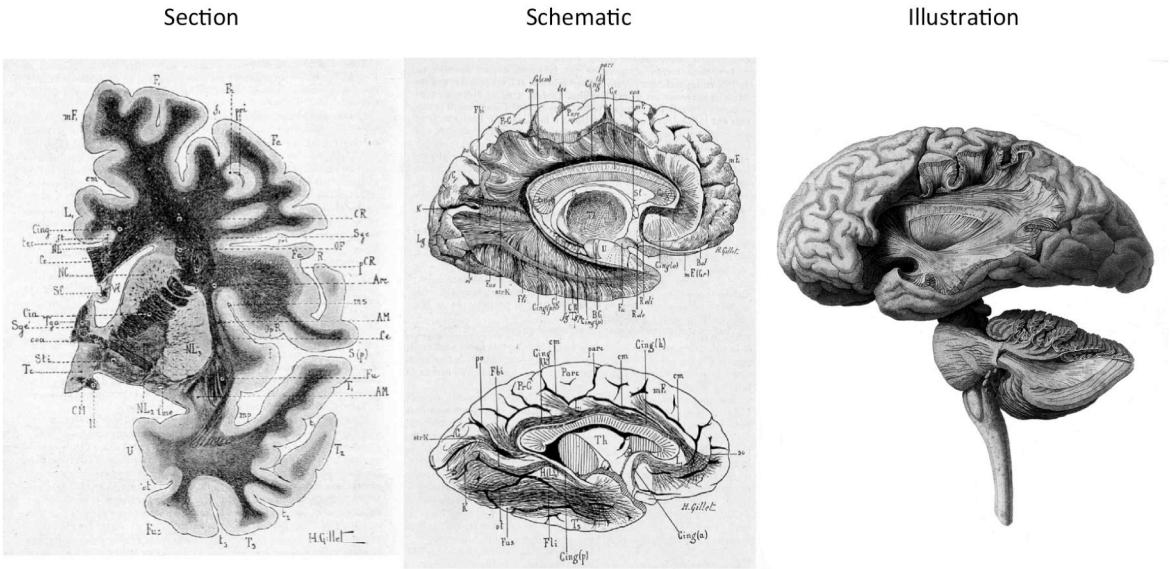

Figure 5. The use of different representations of the fibre pathways was one of the causes that led to some confusion and debate over their location, course and terminations. Left: Brain sections that became widely used in the late 19th century (Dejerine & Dejerine-Klumpke, 1895), Right: three-dimensional depictions of gross dissection studies that were revived in the 20th century and continue today (Mayo, 1827), and Middle: schematic diagrams representing the fibre pathways (Dejerine & Dejerine-Klumpke, 1895).

based on single individuals) and may have led to some misinterpretations or errors. Even performing dissections in different hemispheres (due to the lateralization of pathways) may have resulted in some discrepancies between the descriptions of tracts. Lastly, fibre dissection relies foremost on primary observation with the naked eye, thus combined with the potentially large variability, differences in representing the data and the difficult task of describing the complex relationships between anatomical structures, it is only inevitable that inconsistencies arise.

Much of our present understanding of the fibre pathways in humans rests on the work of the 19th century neuroanatomists. Given the existing controversy over several of the tracts (that have only resurfaced as a result of the renewed interest in white matter), it is necessary to revisit and re-evaluate them with modern techniques. Like Vesalius who challenged Galen's texts, as much as it is important to recognize the trailblazing contributions of the great 19th century dissectionists, we cannot rest on their laurels. What is clear is that the fibre anatomy is highly complex and intricate and much work remains to elucidate their structure.

3.3 Redefining the anatomy of fibre pathways

The development of dMRI tractography has reinvigorated the study of white matter anatomy and opened the field to new discoveries and resolved old debates. dMRI tractography provides us with a virtual image of the white matter structure based on measurements at a voxel resolution in the living human brain. Not only does this enable a unique investigation into the anatomy of fibre pathways (e.g., virtual dissections), the quantitative aspect enables us to characterize the white matter fibre tracts in terms of asymmetries, interindividual variability and to better understand the internal organization of the pathways. It thus has enormous potential for studying the white matter, which is why there has been much effort towards validating this technique (Schmahmann et al., 2007; Thiebaut de Schotten et al., 2011; Jbabdi et al., 2013; Thomas et al., 2014; Azadbakht et al., 2015). In turn this has caused a revival in post-mortem fibre dissection contributing anew to the discussion on fibre pathway anatomy. In this section we focus on the contributions that dMRI tractography has made to the anatomical study of white matter pathways and discuss how it is changing the way we study them.

3.4 Discovering new tracts and resolving debates

Several previously undescribed tracts have been observed in the recent literature coming from dMRI tractography. These include the frontal aslant tract (Lawes et al., 2008; Oishi et al., 2008; Catani et al., 2013), an indirect pathway consisting of two components parallel to the arcuate fasciculus that debunked the long-standing belief that the AF was the only language tract (Catani et al., 2005) and a tract connecting the cuneus with the lingual gyrus that has been named the sledge runner (Vergani et al., 2014). It has also led to the accidental re-discovery of the vertical occipital fasciculus (Yeatman et al., 2014). Additionally, it has been used to investigate, in humans, homologue pathways that were first described in monkeys, for example the SLF I-III have been recently described in humans with dMRI tractography and dissection (Makris et al., 2005; Wang et al., 2015a), as well as the middle longitudinal fasciculus (Lawes et al., 2008; Makris et al., 2009).

The use of filters with dMRI tractography permits new approaches to mapping the white matter. For instance, we can map the connections within a particular lobe which has been recently done for the frontal (Croxson et al., 2005; Catani et al., 2012; Rojkova et al., 2015) and temporal (Binney et al., 2012) lobes, or the superficial U-shaped fibres between adjacent gyri that are difficult to study with the fibre dissection technique (Oishi et al., 2008; Catani et al., 2012). Several of these studies have described novel identifiable tracts demonstrated in a large group (Rojkova et al., 2015) or on an averaged group dataset (Oishi et al., 2008).

Efforts to resolve debates regarding the existence or inexistence of tracts have received complementary evidence from both dissection and dMRI tractography. Fibre dissection provides direct observation and dMRI tractography provides the ability to confirm or disconfirm debated issues in a large number of subjects. This was done in a recent study that used an averaged dataset of 488 subjects and 80 individual subjects (and five brain specimens that were dissected) (Meola et al., 2015). In regards to clarifying the anatomy in difficult areas, it may be necessary to capitalize on the virtual dissection aspect of dMRI tractography. For example, this is the case for Meyer's loop where fibre dissection may not be able to elucidate the anatomy due to the high degree of intermingling (Goga & Türe, 2015). This is also the case for the external and extreme capsules (see Section 3.4).

3.4.1 More extensive connections and subcomponents

The descriptions of tracts given by the early dissectionists were often coarse, relying on general lobar landmarks. Recent studies have revealed a more complex anatomy regarding several of the tracts, including more detailed descriptions of their terminations showing more extensive connections than previously thought. Refinements in dissection technique with an emphasis on investigating tract terminations have led to fuller descriptions of the IFOF, extending to more areas in the cortex (Martino et al., 2010; Sarubbo et al., 2013). This finding has been reproduced with dMRI tractography (Caverzasi et al., 2014, see also Chapter 5). More extensive connections of the AF have also been observed (Frey et al., 2008).

Some studies have recently classified tracts into finer-grained divisions, describing subcomponents of tracts. Pathways are not homogeneous structures but composed of many sub-routes. Such divisions will help to better characterize the functional implications or roles of the larger pathway and enable us to disentangle the different subcomponents that may underlie very different functions. Subcomponents have recently been described in the IFOF, in particular a superficial component between the inferior frontal gyrus and superior and middle occipital gyri and a deep component between the frontal lobe and inferior occipital gyrus and temporo-basal areas (Martino et al., 2010; Sarubbo et al., 2013). dMRI tractography enables the automatic classification of subcomponents from a segmented tract bundle. In Chapter 7 we applied a novel method to segment the uncinate fasciculus into subcomponents showing each with distinct connectivity patterns. Moreover, this may reveal important characteristics regarding the internal structure of the tracts as subcomponents have been shown to have different properties. (Lebel et al., 2010) revealed different maturation patterns in different parts of the corpus callosum. We recently revealed different asymmetries in the subcomponents of the IFOF (see Chapter 5) and the uncinate fasciculus (Chapter 7).

3.4.2 Describing tract properties and connectional anatomy

Additionally, with dMRI tractography, we can now study new aspects of the fibre pathways, addressing questions that were not possible with the available techniques, for example the lateralization of pathways, inter-individual variability, differences between healthy and diseased populations and the functional roles of the pathways.

Quantitative information such as volume, length, the number of streamlines and microstructural properties of the white matter (e.g., fractional anisotropy) as well as the connectivity profiles of tracts can be obtained automatically across a large group of subjects. Based on such information, structural asymmetries can be assessed in terms of the tract volume for example or its microstructural properties. A number of dMRI tractography studies have started to look at the lateralization of pathways (Barrick et al., 2007; Thiebaut de Schotten et al., 2011; Takao et al., 2013). Studying the asymmetry of white matter pathways with dissection is possible through innovative techniques such as stereology, however this was not exploited until recently (Highley et al., 2002). The analysis of asymmetries can further be applied to

subcomponents and even individual site-to-site connections of a tract (see Chapters 5 and 7). Another possibility is to consider the connectivity patterns of tracts. One study found a lateralized pattern in the middle longitudinal fasciculus connecting the temporal lobe with the angular gyrus in the left hemisphere whereas in the right hemisphere it connects the temporal lobe with the superior parietal lobe (Makris et al., 2012).

With dMRI tractography, for the first time we can study the interindividual variability of white matter pathways across large groups, for example with respect to the frequency of connectivity patterns (Makris et al., 2012) as well as the presence of tracts (Wang et al., 2015a).

The recent discovery of previously undescribed tracts shows that our current knowledge in white matter anatomy is incomplete and the work of the previous two centuries is not finished as there remains many aspects that require clarification. Additionally, there remains much to be learned not only in terms of the exact origins and terminations of tracts and their internal organization (arrangement in subcomponents), but also the lateralization of tracts, their distribution within the different brain regions and how these vary are across the population. Finally, dMRI tractography may be able to provide insight regarding areas that are difficult to dissect as a result of complicated and multiple crossings and in cases where boundaries between pathways are not clear (see Chapter 7).

3.5 Background on the external and extreme capsule complex

The external (named by Burdach in 1822, originally *capsula externa*) and extreme (distinguished later on in the late 19th century, Obersteiner 1896, Gordinier 1899, from Schmahmann & Pandya, 2006) capsules are topographical divisions of white matter located between the insula and the putamen. They constitute a bottleneck comprised of multiple fibre tracts that pass through them. These include the anterior commissure, Meyer's loop, projection fibres and several association tracts that have been identified as the inferior fronto-occipital fasciculus (IFOF) and uncinate fasciculus (UF). A thin strip of grey matter called the claustrum separates these two capsules with the external capsule (EC) located medially (between the claustrum and putamen) and extreme capsule (EmC) located laterally (between the claustrum and insula) (Figure 6).

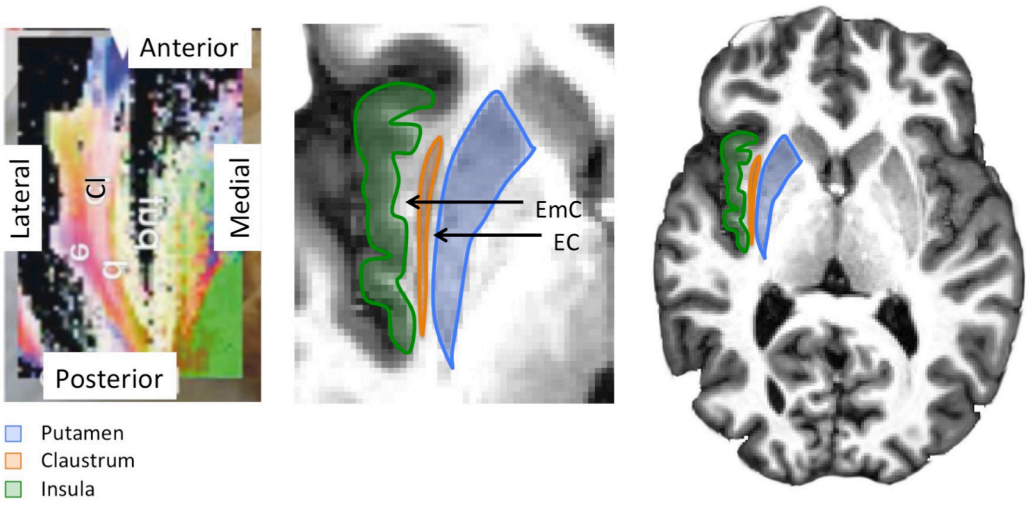

Figure 6. Left: Polarized light image of the external and extreme capsules showing axonal orientations on an axial slice colour-coded for their orientation (Cl = claustrum) (modified from Axer et al., 2011). Middle and right: The external and extreme capsules shown on the axial slice of an anatomical T1 image in a single subject, indicated by the arrows. The external capsule (EC) lies more medially, between the putamen (outlined in blue) and claustrum (outlined in orange) and the extreme capsule (EmC) lies laterally, between the insula (outlined in green) and the claustrum.

In recent years, there has been significant interest in the association pathways of the EC and EmC. In particular, the IFOF, UF and extreme capsule fibre tract have been considered to play a role in the language circuitry, being cited as part of a "ventral language system" (Frey et al., 2008; Saur et al., 2008; Duffau et al., 2009; Makris & Pandya, 2009; Papagno et al., 2011; Weiller et al., 2011; Almairac et al., 2014; Dick et al., 2014; Bajada et al., 2015). Recently, the connectional anatomy of these pathways and their functional roles has come to the forefront.

Here we discuss the consensus and controversy surrounding the external and extreme capsule complex regarding its association pathways, highlighting the questions we aim to address in this thesis.

3.5.1 A complex area of passage

The external and extreme capsules are an especially intricate area. Whereas the division line of these capsules is clear, that being the claustrum, the boundaries between the fibre pathways is less clear. In this area of passage the claustrum has claustro-cortical fibres that emanate from it dorsally (Fernández-Miranda et al., 2008), and ventrally it is flanked by the IFOF and the UF that are adjacent to one another. This can be seen with polarized light imaging visualizing the axonal orientations on a brain section (Figure 7).

A point of debate has been the configuration of these tracts when passing through the external and extreme capsules (i.e., does each tract pass distinctly through either the external or extreme capsule? How are they organized within this bottleneck area?) Attempts to describe the anatomy of each capsule individually have resulted in little clarification (Dejerine & Dejerine-Klumpe, 1895; Makris & Pandya, 2009). Most notably, Dejerine described fibres from the external capsule running into the extreme capsule, intermingling with the fibres of the extreme capsule. There is now a consensus that both the IFOF and UF occupy both the external and extreme capsules (Klingler & Gloor, 1960; Ebeling & Cramon, 1992; Kier et al., 2004; Fernández-Miranda et al., 2008; Martino et al., 2010). It can thus be understood that the external and extreme capsule distinction is based on an arbitrary anatomical landmark and they have no one-to-one correspondence with these fibre tracts.

A second point of debate concerned whether the IFOF and UF should be considered as a single continuous tract or two independent tracts. Both the IFOF and UF fan out to the fronto-orbital areas and there is some merging within the external and extreme capsules (Kier et al., 2004). Several dissectionists, including a few recent studies, have remarked on the difficulty in

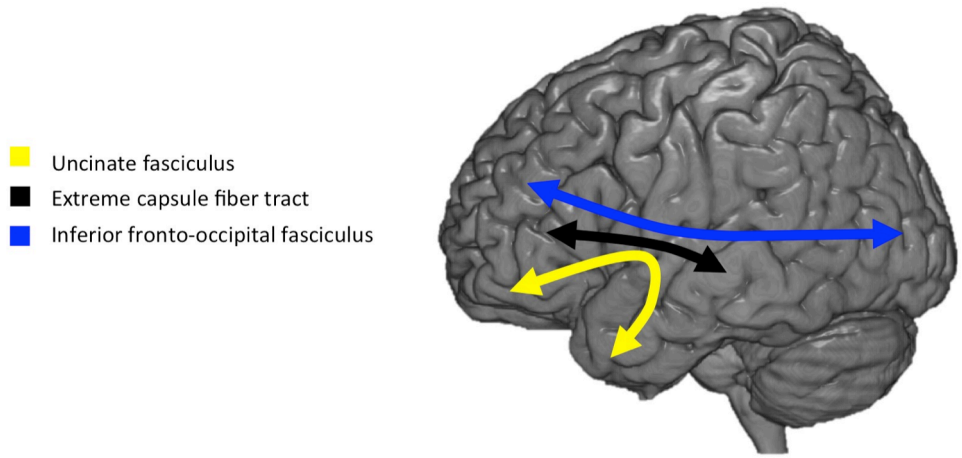

Figure 7. Schematic diagram of the association pathways of the external and extreme capsules. The uncinate fasciculus (yellow) connects the frontal and anterior portion of the temporal lobes and has a characteristic hooked shape. The inferior fronto-occipital fasciculus (blue) is located medial and dorsal to the UF and connects the frontal and posterior occipital, parietal and temporal lobes. The extreme capsule fibre tract (black) is located dorsal and lateral to the UF and connects the frontal and middle portion of the temporal lobes.

dissociating these two fibre pathways (Trolard, 1906; Villiger & Ludwig, 1940; Türe et al., 2000; Travers, 2008). In particular Trolard (1906) writes:

> *On pourrait peut-être réunir l'unciné au faisceau qui vient d'être décrit [IFOF]. Mais il vaut mieux, à notre avis, laisser à chacun d'eux sa personnalité. / Perhaps we could reunite the uncinate with the tract I just described [IFOF]. But it would be best, in our opinion, to let each of them express their own personalities.*

Given the earlier controversy surrounding the existence of the IFOF, it was also often confused with the UF (Sedat & Duvernoy, 1990; Clara 1942; Kopsch, 1914). However, despite this ambiguity, there is a generally accepted definition of these tracts that are drawn from their classical definitions. The IFOF is a tract that passes from the frontal lobe, descends and collects within the external and extreme capsules and continues on a posterior course (Curran, 1909; Martino et al., 2010; Sarubbo et al., 2013), and the UF descends from the frontal lobe through the external and extreme capsules and hooks around to terminate within the anterior temporal lobe (Burdach, 1819; Ebeling & Cramon, 1992). Within the external and extreme capsules, the IFOF has been consistently reported to be located superior and medial to the UF (Ebeling & Cramon, 1992; Kier et al., 2004; Martino et al., 2010).

Recently, a tract connecting the middle portion of the superior and middle temporal gyri with the frontal lobe, laying laterally adjacent to the UF within the external and extreme capsules was described in the monkey (Schmahmann & Pandya, 2006). Since the IFOF does not exist in the monkey and, although adjacent to the UF, its course did not follow that of the UF fibres it was thus named the extreme capsule fibre tract (ECFT). This connection has been recently observed in humans (Parker et al., 2005; Frey et al., 2008; Saur et al., 2008), however there appears to be some confusion regarding this tract. It is not clear whether it should be considered as a distinct tract (ECFT), as part of the UF (Parker et al., 2005) or as part of the IFOF, which exists in humans although it is known to terminate in the temporo-basal regions within the temporal lobe. A recent review article interestingly points out that no study has ever demonstrated the existence of both the IFOF and ECFT in one brain (Gierhan, 2013).

To sum up, these three association tracts (IFOF, UF and ECFT) lie adjacent to one another within the external and extreme capsules. The reported difficulty in dissociating between the IFOF and UF may be due in part to the ECFT that terminates within the middle portion of the temporal lobe, filling in the gap between the IFOF and the UF fibres that terminate within the temporal lobe (the UF fibres terminating in the anterior temporal lobe and IFOF fibres terminating in the posterior temporo-basal regions) (Figure 7).

One of the aims of this thesis is to reconciliate the definitions of these tracts. The outstanding questions are thus as follows: Are the IFOF and UF indeed two separate pathways? How should the connections of the ECFT be classified (as part of the IFOF, UF or as a separate tract?)

4 Techniques for studying the anatomy of fibre pathways

Where the telescope ends, the microscope begins.
Which of the two has the grander view?
Victor Hugo, Les Misérables, 1862

In 1665, Nicolas Steno wrote that to study the white matter, one would need to "*follow the nerve threads through the substance of the brain in order to see where they go and where they end*" (Steno, 1665). This encapsulated the idea that the relevance of connections lies in where they originate and where they terminate. While he was referring to the method of dissection and there now exists several techniques for studying the white matter structure, this notion still holds true.

The challenge of studying white matter connections in the human brain is that they exist on multiple nested spatial scales (from the level of single neurons or synapses to neuronal populations and their interconnecting circuitries to long-range regional connections) (Sporns, 2011). While mapping its complete connections is not currently realizable at the microscopic scale due to the sheer number of connections, it is conceivable at the macroscopic scale, that is between anatomically defined regions. Even at the macroscopic scale, the resolution of techniques can range from tracing connections in a population of single axons to gross fibre bundles (Figure 8). The use of multiple techniques may thus be necessary to acquire a complete picture of the anatomy of the fibre pathways.

Dependent on the technologies of the time, different techniques have been used to study the macroscopic white matter structure. It began with classical (sectional and gross) dissection that was the first method used dating from antiquity, followed by a period of gross histology (visualizing fibre tracts on stained brain sections) in the late 19th century, followed by axonal

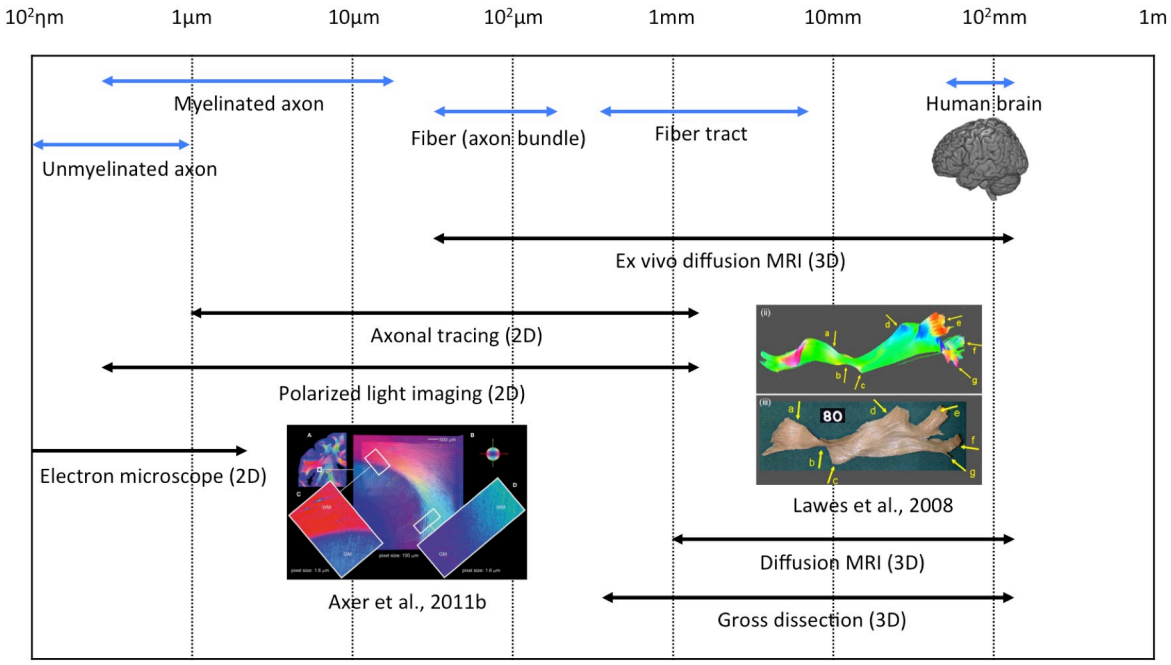

Figure 8. The multiple scales of white matter study. The sizes of various anatomical structures (indicated by blue arrows) and resolutions of different techniques for studying the white matter (indicated by black arrows) (adapted from Axer, 2011).

tracing appearing in the 20th century which led to greater precision in identifying the terminations but was limited to study in animals. Following this period, no new radical developments were made. Then in 1993, Crick and Jones published an open letter urgently calling for new techniques, identifying the gap in our knowledge in human neuroanatomy in contrast to the many developments made in non-human primates, appropriately titled "the backwardness of human neuroanatomy". Shortly after, developments in imaging methods including polarized light imaging (2000s) and in particular dMRI tractography (1990s), which enables the in vivo study of the white matter structure were proposed as techniques for the new study of white matter structure.

In this chapter we review the different techniques for studying the white matter structure at the macroscopic level. We cover dissection, axonal tracing and polarized light imaging highlighting their advantages and disadvantages. Finally we devote the remaining part of the chapter to diffusion MRI tractography reviewing the methodological aspects of the technique in greater detail and focus on how we can apply it to the study of fibre pathways.

4.1 Gross dissection

Gross dissection consists of using a variety of blunt tools, in particular watchmakers' forceps and wooden spoons, to gradually remove tissue in the brain (by scraping it away) in a step-wise manner to reveal the organization and arrangement of the internal structures. Through such a gradual progression from superficial to deep, peeling back the different layers of white matter, the complex relationships between anatomical structures can be observed. Since the use of fresh brain tissue is not only too soft to dissect but rapidly decayed, it is necessary to preserve or fix the brain. Early attempts at fixing included boiling the brain in water or oil (Malpighi, Vieussens) and later submerging it in a substance mixture. Some of the substances that were used include alcohol, potash, ammonia and, more recently, formaldehyde (introduced in 1893), which is still used today. Fibre tracts are distinguished based on observable cleavage lines or stems, through which applied pressure to these areas could separate them (Curran, 1909). The dissectionist can then follow the fibres from this stem to their respective terminations. In the early 20th century, new methods were devised to facilitate the separation of the fibre tracts. For example, Rosett (1933) proposed a method of immersing the fixed brain in a hermetic container filled with liquid $C0_2$, then quickly releaving the valve resulting in an « internal explosion » of the tissue to reveal the natural lines of cleavage. Along the same lines, Klingler (1935) proposed an alternative method that consists of freezing the brain to mechanically separate the fibres caused by the expansion of water passing from liquid to solid. The Klingler technique remains the most widely used method today.

Although gross dissection requires a high level of anatomical expertise, skill and precision, as well as a fair amount of time, it enables the direct observation of fibre pathways and their relationships with one another and allows for generally good discrimination between the fibre pathways. Nevertheless, this technique is limited by the fact that the fibres are susceptible to breakage and the removal of tissue is definitive making it difficult to precisely localize and follow all of the fibres to their terminations in the cortex. It is important to note that the distinction between fibre tracts is not always clear, for example when there are no apparent cleavage lines separating adjacent fibre tracts or in diffuse areas where there are multiple intersecting/interweaving tracts making it impossible to dissociate them as has been described by (Curran, 1909; Klingler & Gloor, 1960; Türe et al., 2000). Another limitation is that post-mortem brain specimens may not be readily available and thus the number of subjects that can be studied will be limited. Finally, this technique remains qualitative therefore the extent to which a tract connects two regions cannot be reported (although this is technically possible through stereological methods, see Highley et al., 2002), nor can the direction of connections (efferent or afferent) be determined.

4.2 Axonal tracing

Currently the most precise way of identifying the structural connections on a macroscopic level is with axonal tracing, long considered the gold standard but can produce false negatives (Azadbakht et al., 2015). In axonal tracing, a substance such as horseradish peroxidase (Kristensson & Olsson, 1971) or radiolabeled amino acids (Cowan et al., 1972) is injected into a cortical site and is transported along the axons through active transport in a live specimen. After a certain delay (ranging from a few days to several weeks), the origin, termination and course of the tracers can be seen on brain slices revealed post-mortem. Because the transport mechanism is specific to the direction of transport (anterograde transport which is directed from the cell body to the synapse and retrograde transport which is directed from the synapse to the cell body), the direction of information transfer can be distinguished (afferent or efferent connection). Axonal tracing has been attempted on the post-mortem human brain. For example lipophile substances can be injected into formalin-fixed brains and passively transported along the axons. However, the transport time is rather long and as a result it has only been successfully applied for short distances (Galuske et al., 2000). Traditionally, this technique has been applied to studying connections in terms of origins and terminations as opposed to their trajectories. When applying this technique to study the fibre pathways as in (Schmahmann & Pandya, 2006) the axonal trajectories can be followed from slice to slice and schematically represented in three-dimensions. The connections are attributed to pathways based on their local patterns of axonal orientation and packing density that can be distinguished (i.e., identifying stems) on a Nissl-stained brain section viewed under a microscope (Schmahmann & Pandya, 2006, p. 44).

While this technique has a high resolution and can provide very detailed and precise information on the origins, terminations and courses of neural pathways as well as directional information on the connections, it suffers from several limitations. Its major limitation is that its application is limited to animals therefore its utility in understanding human fibre pathways relies on inference that may or may not be valid. It requires prior anatomical knowledge since the cortical sites of injection must be carefully chosen and the number of injections is limited to a small number and as a result there is a potential for undersampling. Although it enables a very fine and detailed discrimination between the fibre pathways, it is more difficult to appreciate the relationships between the fibre pathways since it requires following the fibres on serial slices (losing perspective of their overall trajectories).

4.3 Polarized light imaging

Polarized light imaging (PLI) is an optical imaging method that takes advantage of the birefringent properties of the myelin sheath covering the axons. It requires assessing light transmission through serial histological brain sections with a polarization filter shone at different angles to estimate the underlying neural structure (Larsen et al., 2007). First the ex-vivo brain is fixed and sliced into 60-100 μm thick sections using a specialized cryostat microtome in order to avoid dissolutioning the myelin sheaths. The sections are then repeatedly imaged with different angles of polarized light to acquire multiple measurements of the reflected light and estimate the orientation of the axons at every voxel in the image. The stack of imaged sections can then be assembled into a 3D volume and the white matter fibres computationally reconstructed by following the fibre orientations.

The main advantages of PLI are its very high spatial resolution (submillimeter) and its direct measurement of neuronal fibres (based on the myelin sheath). Therefore it has the potential to reveal the fibre pathways in humans at an unprecedented level of detail and at the mesoscopic scale bridging both micro and macroscopic information. However, it is currently limited by the available technology requiring terabytes of storage for a single brain, thus due to these computational requirements the three-dimensional reconstruction of fibres can only be achieved for very small areas at a time (millimeters). As such whole-brain PLI tractography

remains a distant goal and in its current form the applications for studying the fibre pathways is rather limited (Axer et al., 2011). PLI also does not provide any information on the direction of connections.

4.4 Diffusion MRI Tractography

Diffusion MRI tractography combines the imaging technology of diffusion MRI with an image processing technique, tractography, that enables the *in vivo* three-dimensional reconstruction of the underlying neural fibre structure. It achieves this by mapping the diffusion processes occurring at a microscopic level contained in each ~1-2mm cubic volume of the image. Since diffusion processes are constrained by the geometrical structure of the environment, it can be used to probe biological structures. The central assumption of this technique is that in tissue with fibrous structures such as white matter (i.e., groups of axons), water molecules diffuse more freely along the constrained structure than across it. From these measurements, mathematical models and algorithms are used to estimate and reconstruct the white matter structure.

The early version of this technique, called diffusion tensor imaging, had a major modelling limitation but was still able to reliably visualize the location and course of the major pathways. Over the last twenty years significant advancements have been made with increasingly sophisticated models and algorithms and new image acquisition schemes. In this work, from the original diffusion-weighted images that were acquired for the BIL&GIN cohort (Mazoyer et al., 2016), we improved on our tractography data by applying advanced methods. In the section on tractography, we focus specifically on the improvements that were made in our processing pipeline.

Although this is an indirect measure and thus is susceptible to some inaccuracies in the reconstruction, it is currently the only non-invasive technique for studying the white matter structure, enabling its in vivo study in humans. This technique has opened up new possibilities for investigating the structural organization of the different fibre pathways.

4.4.1 Diffusion MRI

We begin with a brief introduction on the principles of diffusion MRI before moving onto tractography methods.

Diffusion coefficient

In 1827, while studying pollen grains under a microscope, botanist Robert Brown described the seemingly random motion of the pollen grains suspended in water. He reported that they would move with no apparent cause (Brown, 1828). He was in fact observing the kinetic energy of the particles colliding with one another causing the perpetual and random motion of the grains (i.e., the process of diffusion).

In 1855, Adolf Fick introduced the diffusion coefficient, D. Fick's first law describes the phenomenon of diffusion between substances with different concentrations, given by:

$$J = -D\nabla \mathrm{C},$$

relating the flux of particles J, with different concentrations, by a constant of proportionality: the diffusion coefficient D. He thus observed that during the process of diffusion, the flux is proportional to the variation of concentration with the constant of proportionality reflecting the substance. Although Fick's first law refers to the diffusion of substances with different concentrations, his diffusion coefficient still applies for a single substance, called self-diffusion.

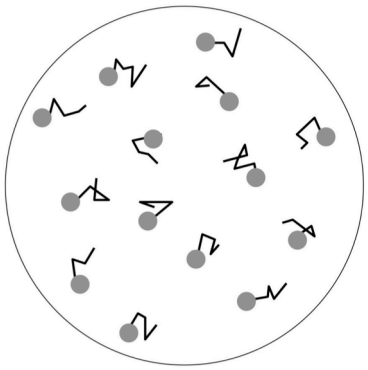

Figure 9. The process of diffusion involves the kinetic energy of particles causing their motion. Robert Brown viewed pollen grains under a microscope and remarked on their perpetual and random motion, which turned out to be caused by the collision of water molecules with the pollen. Inspired from Johansen-Berg & Behrens (2013).

Einstein (1905) was able to derive a relationship between the mean squared displacement of the particles, characterized by Brownian motion, and Fick's diffusion coefficient:

$$\langle r^2 \rangle = 6Dt,$$

where t is the elapsed time, r is the net displacement of the particles and D is the diffusion coefficient. This relationship between the mean displacement of the particles and diffusion coefficient was important because the degree of diffusion could be directly derived from the displacement of the particles. For example, any discrepancy of this relation with the actual displacement is an indicator that the particles do not lie in free space but constrained space. As a result, because the degree of diffusion changes depending on its surroundings (the degree of hindrance against diffusion), it could be used as an indicator of hindrance, giving rise to the term apparent diffusion coefficient (ADC) (Le Bihan et al., 1986).

Diffusion applied to medical imaging

Building on the important developments of nuclear magnetic resonance imaging that relies on the spin echo to capture the dephasing of proton spins (Hahn, 1950), Carr and Purcell (1954) proposed a framework for sensitizing the echo magnitude to directly measure molecular diffusion, by applying a magnetic field gradient. A decade later, improvements by Stejskal and Tanner (1965) made it possible to acquire diffusion-weighted images with MRI.

Although the technological developments were already in place in the mid-1960s, it wasn't until 1985 that diffusion imaging was developed and applied for the first time (Bihan & Breton, 1985). Le Bihan saw the potential of the diffusion coefficient, which he called ADC (to differentiate its application to MRI), for medical imaging. He applied diffusion-weighted imaging to patients with brain tumours. On the acquired images the tumours, which had restricted diffusion and thus a low ADC, would show up as bright spots due to less signal attenuation resulting in high intensity whereas areas of relatively unrestricted diffusion (thus high ADC) would appear dark as a result of signal attenuation (due to the dispersion of molecules). Thus diffusion imaging introduced a useful new contrast for imaging the brain that was not possible with previously available scans (T1-weighted, T2-weighted) (Figure 10).

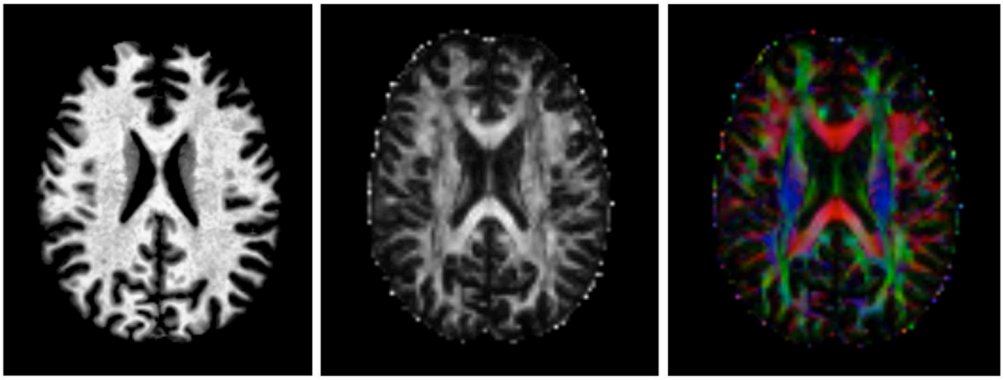

Figure 10. New contrast acquired from diffusion-weighted images. From left to right: anatomical T1 image, fractional anisotropy (FA) map and colour-coded FA map shown on an axial slice in a single subject. (Red=left-right, blue=superior-inferior, green=anterior-posterior orientations).

Anisotropic diffusion

The ability of diffusion imaging to measure anisotropic structure was recognized and cleverly demonstrated by Moseley (1990). Diffusion is sensitive to its environment such that water molecules diffuse along or around structures or barriers limiting their movement. When diffusion is anisotropic the movement of water molecules is fastest along a single direction (orientation-dependent), in contrast to isotropic diffusion in which the water molecules move equally in all directions (orientation-independent). In the brain, given its fibrous structure, the diffusion in white matter is highly anisotropic whereas the gray matter, made up of corpuscular forms is isotropic (Figure 11).

The signal of a diffusion-weighted image is dependent on the direction of the applied field gradient. When applying a magnetic field gradient in orthogonal directions, the signal for anisotropic tissue will be highly variable whereas in isotropic tissue it will be invariant. This can be seen in Figure 12 where the largest changes in the signal between the three images correspond to areas that have a highly ordered structure. For example, notice (in the images from left to right) the dark spots of the commissural tracts that run in the left-right direction, association tracts that run in the anterior-posterior direction and projection tracts that run in the superior-inferior direction. By acquiring multiple images, each with a different direction of the field gradient, and comparing them with a baseline image (with no applied gradient), it is possible to measure the degree of anisotropy (called fractional anisotropy or FA) and obtain information regarding the directional orientation(s) of the underlying structure. For instance, see the FA and color-coded FA maps in Figure 10.

It needs to be noted that the diffusion processes do not depend solely on the orientation of the axonal membranes but on a number of factors – myelination, axon density, axon diameter, extra-axonal cells and intra-axonal cells, although it has been shown that the main contributor to diffusion anisotropy in tissue is cellular membranes (Beaulieu, 2002). There is now concentrated effort towards compartmentalizing these diffusion processes (Assaf & Basser, 2005; Zhang et al., 2012; Girard et al., 2015). It should also be noted that diffusion imaging which has a relatively low spatial resolution represents a voxel-averaged measure of diffusion, which is likely to contain several populations of axons (axon diameter is on the scale of μm).

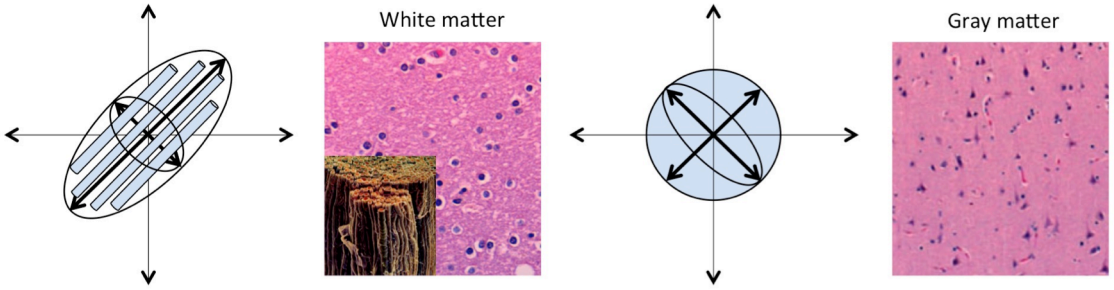

Figure 11. Diffusion is anisotropic (left) and isotropic (right) in white and grey matter, respectively. Diffusion processes can be modelled by a tensor and is ellipsoidal (left) when anisotropic and spherical (right) when isotropic. Microscopic stains of cross-sectional white and grey matter tissue are shown.

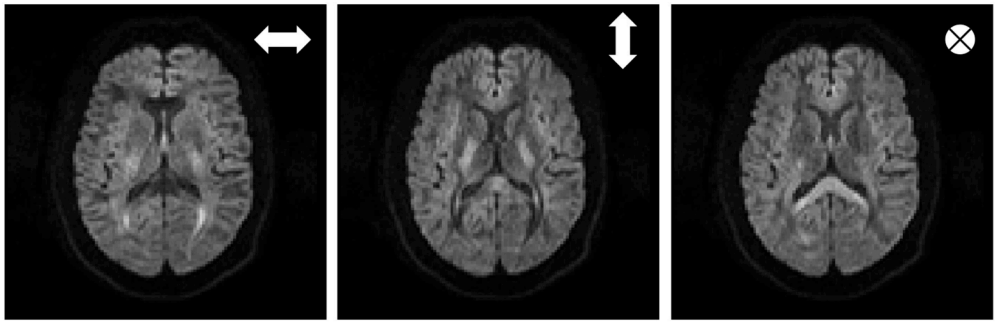

Figure 12. Effect of changing the orientation of the applied diffusion gradient on a diffusion-weighted image. From left to right, gradient direction applied in the left-right, anterior-posterior and superior-inferior orientations, respectively, resulting in signal attenuation (dark spots) in the callosal, association and projection tracts, respectively.

4.4.2 Tractography

The goal of tractography is to reconstruct as accurately and reliably as possible the anatomical structure of the white matter based on the information from the diffusion measurement. Tractography reconstructions are called tractograms and can consist of the whole-brain fibre structure or pre-defined areas (defined by seed regions). Tractograms are made of streamlines that represent a sampling of the diffusion processes measured over several voxels. Streamlines should therefore not be confused with individual axons. Tractography generally involves two steps: the first is to model the local diffusion processes within the voxel and the second is to track the streamlines across the brain volume. Significant advances have been made in terms of both local modelling and tracking algorithms to produce reconstructions that are more faithful to the underlying anatomy. We review both basic and more advanced methods of tractography that were used in this thesis work.

Local modelling

In order to infer the fibre structure from the measured diffusion processes, it requires modelling the diffusion signal. While both global and local modelling methods exist, global tractography is outside the scope of this review. Local modelling refers to the mathematical model used to represent the diffusion processes with respect to the fibre structure within a

single voxel. Here we review the basic diffusion tensor (DTI) and more advanced constrained spherical deconvolution (CSD) models.

The diffusion tensor model assumes that the underlying fibre structure can be represented as a unimodal Gaussian distribution of orientations and provides an estimate of the principle direction of the diffusion (Basser et al., 1994). In order to characterize Gaussian diffusion, a 3 x 3 symmetric matrix called the diffusion tensor is used to describe the displacements in three-dimensional space,

$$\boldsymbol{D} = \begin{bmatrix} D_{xx} & D_{xy} & D_{xz} \\ D_{xy} & D_{yy} & D_{yz} \\ D_{xz} & D_{yz} & D_{zz} \end{bmatrix}.$$

This describes the degree of variance along (diagonal elements) and covariance across (off-diagonal elements) the three orthogonal axes. The diffusion tensor can be represented in three-dimensional space as an ellipsoid. The shape of this ellipsoid encodes the degree of diffusion in each direction. When diffusion is anisotropic the ellipsoid has a principle direction much larger along one direction, whereas when diffusion is isotropic the directions are approximately equal in all directions and is modelled as a sphere (Figure 11).

The problem with DTI is that it cannot resolve areas of multiple fibre populations with different orientations (Figure 13). For example, if there is a dominant tract and a smaller tract passing through, only the dominant tract will be represented. Along the same lines, within a voxel a fibre crossing involving two equal-sized tracts could appear isotropic. Thus this can result in entirely inaccurate estimations of the underlying fibre structure. A number of studies have shown that compared with DTI, higher-order models which accommodate more than one fibre population within the voxel can significantly improve this problem (Descoteaux et al., 2009; Tournier et al., 2012; Farquharson et al., 2013; Chamberland et al., 2014).

Constrained spherical deconvolution (CSD) is one of several higher-order models for representing the diffusion signal as multiple fibre populations (Tournier et al., 2004; Descoteaux et al., 2009). In higher-order models, the diffusion signal is represented as a distribution of fibre populations thus capturing the possibility of expressing more complex fibre configurations. Three-dimensionally, this can be modelled by the fibre orientation distribution function (fODF). Spherical deconvolution uses sophisticated mathematics to recover multiple fibre populations from the diffusion signal. It assumes that the signal is a sum of measurements that you would get from a fibre population with each orientation weighted by the fraction of fibres with that

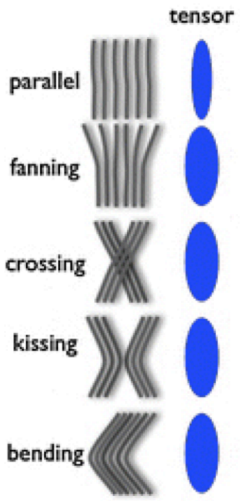

Figure 13. The limitation of the tensor model as being too simple is well-known. Shown here are different examples of fiber configurations within a voxel and their estimated tensors. It is effective at modelling the parallel fibres but is unable to capture the more complex ones such as crossings (from Saad Jbabdi & Johansen-Berg, 2011).

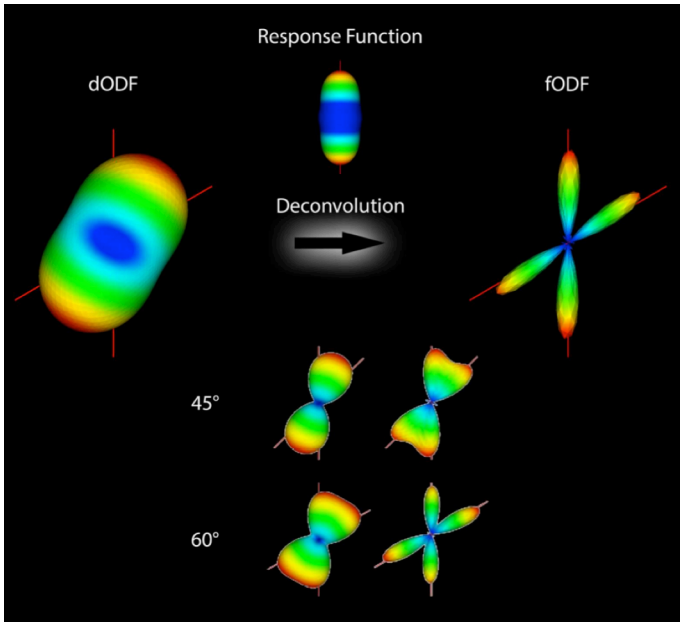

Figure 14. Spherical deconvolution is used to recover the fibre orientation distribution function (fODF). Based on a given response function, the diffusion signal (dODF) can be devolved or sharpened. This enables the representation of more complex fibre configurations beyond the basic tensor model (from Descoteaux, book chapter, in press).

orientation. In order to do this, it must first estimate the fibre orientation distribution, which can be done by calculating the average signal from the most anisotropic voxels. It then uses the response function to devolve or sharpen the diffusion signal (dODF) recovering fODFs with better angular resolution (Figure 14). Different regularization processes can be applied to reduce noise and help provide sharper fODFs. When these are applied it is referred to as constrained spherical deconvolution.

While higher-order models can overcome the crossing fibres problem, there nevertheless remain certain fibre configurations that are impossible to resolve (e.g., with CSD, kissing and crossing fibres produce the same fODF). These require further modelling solutions.

Fiber tracking

Once the fibre structure has been estimated locally, streamline tracking can be performed. Based on the local fibre orientation estimates, we can sample the fibre structure by following the local orientations through the entire volume using a tracking algorithm. Fibre tracking essentially consists of three steps: 1) seeding, 2) track propagation and 3) criteria to stop tracking.

Seeding

Fibre tracking is initiated by selecting seed points from which the streamlines will commence their paths and determining the number of seeds. The seeding strategy could involve seeding from the entire image (referred to as the brute-force approach), from a region of interest (such as a specific anatomical region), or from a select area (such as the white matter or gray-white matter interface). The number of seeds can be specified in terms of the total or per voxel.

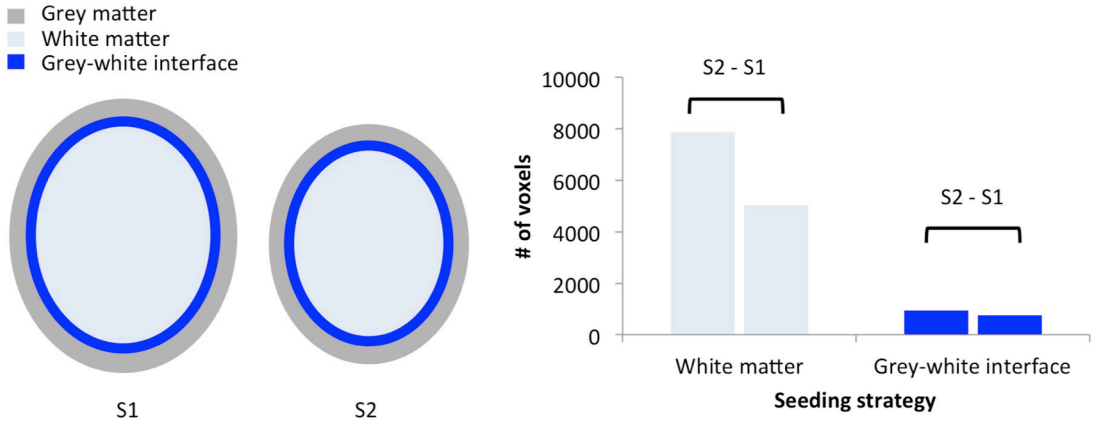

Figure 15. Bias in seeding strategy. Brain variability can influence seeding, for example if seeding from the white matter volume (light blue area), significantly larger brains will have significantly more seeds, whereas seeding from the interface between the gray and white matter (blue area) will reduce this bias.

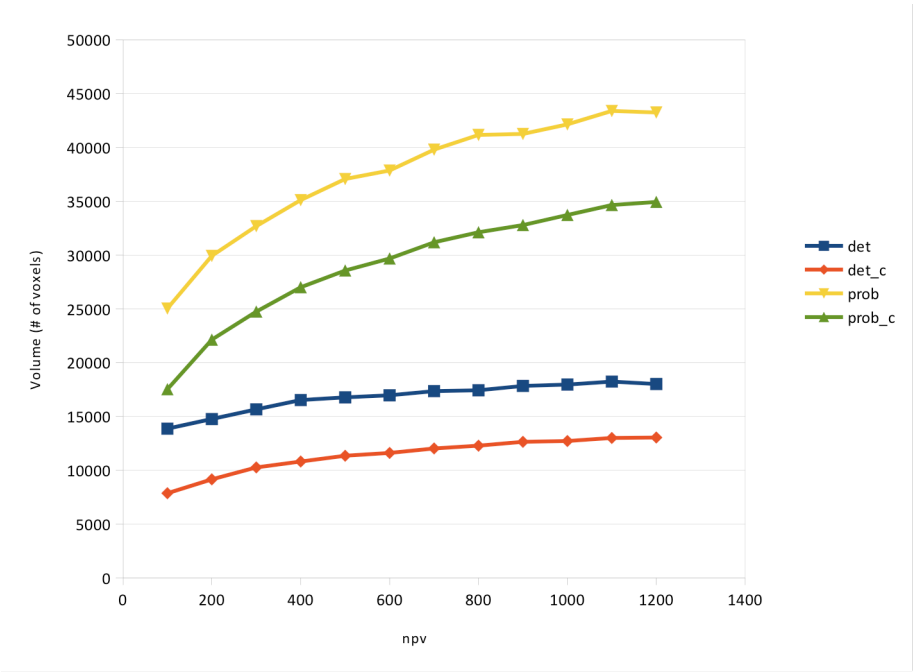

Figure 16. The number of seeds versus tract volume seeding from the stem of the IFOF with deterministic and probabilistic tracking, with a backtracking (PFT) implementation ('_c') and without it.

The seeding strategy is important as the number of streamlines produced is dependent on these parameters and the selected seeding area may vary significantly between subjects. Many studies seed from the white matter volume, but brain volume can vary considerably between subjects. Thus seeding from the entire brain volume would introduce bias into the number of streamlines produced, with larger brains having more streamlines given the larger volume to seed from. One solution is to seed from the ribbon between the grey and white matter (grey-white matter interface). This will help reduce this bias in the number of seeds (Figure 15).

Additionally, determining the number of seeds is also an important factor to consider. Too few seeds will lead to undersampling and more seeds require more computation time. The optimal number of seeds thus is not clear. Information that may help to determine the number of seeds may be to evaluate the relationship between the number of seeds and tract volume. We

could consider the optimal number to be when the tract volume begins to stabilize. In Figure 16 we plotted the number of seeds against tract volume, seeding from the IFOF stem using deterministic and probabilistic tracking, with and without PFT implementation (see below for more details). Deterministic tracking has a more stable relationship and plateaus earlier (around 600) compared with deterministic tracking, which plateaus later (around 1000). The backtracking implementation appears to increase the tract volume by a constant shifting the curve upwards.

Track propagation

Track propagation involves propagating the streamline by following the orientation estimate from voxel to voxel. The most basic tracking algorithm is Fibre Assignment By Continuous Tracking (FACT) which follows the principal diffusion direction of each voxel across the voxel in a straight line and continues in such a way (Mori et al., 1999). More sophisticated interpolation methods have been developed that allow for smoother or more flexible propagation such as the tensor deflection algorithm (Lazar et al., 2003) that can also be tuned, for example to specify the step size. In the case of multiple fibre populations, generally the orientation closest to its preceding orientation will be used, however this may not be the best strategy in all cases and might lead to false reconstructions.

There are two main classes of tracking algorithms: deterministic and probabilistic. Deterministic algorithms assume that the orientation estimate is a strict representation of the fibre structure and thus tracking always continues along the orientation of maximum amplitude. In contrast, probabilistic algorithms account for some uncertainty in the representation of the orientation estimate and are more flexible. In probabilistic tracking, the path of the streamline is determined by sampling from the distribution of possible directions. In general, probabilistic tracking is generally preferred as it is able to characterize the uncertainty in the track direction and is better at tracking branching and dispersion (see Figure 17) (Tournier et al., 2011). One of the problems is that tracking can stop prematurely when passing through areas of low anisotropy, for example near the subcortical grey matter. In cases where tracks need to pass through such difficult areas, one proposed solution called particle filtering tractography (PFT) is to backtrack its course and find alternative paths when the tracking is unable to continue

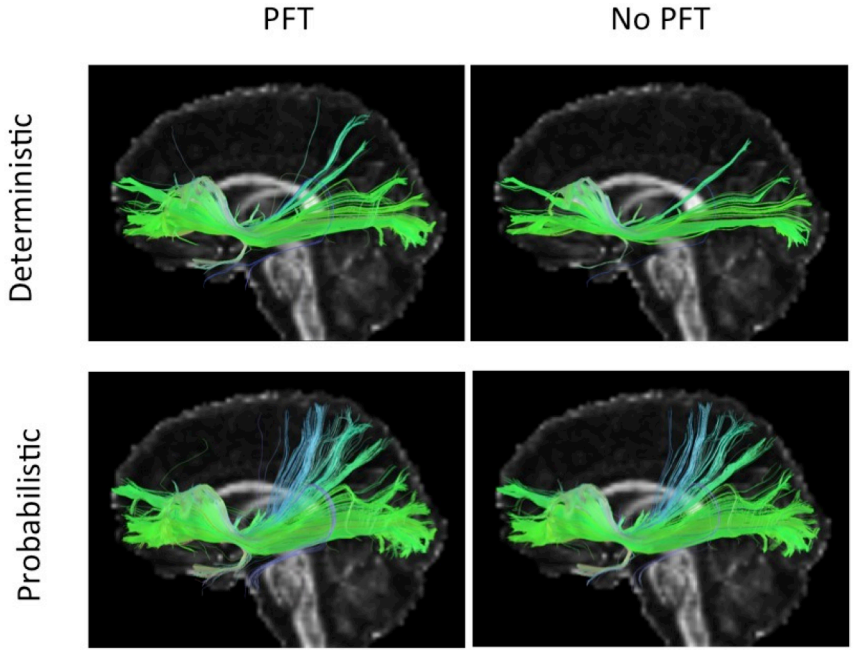

Figure 17. Example of deterministic and probabilistic tracking of the IFOF seeding from the stem both with and without particle filtering tractography (PFT).

(Girard et al., 2014). An example of PFT applied to deterministic and probabilistic tracking for the IFOF seeding from the stem is shown in Figure 17.

In this work deterministic tracking is used, as it was not feasible to perform virtual dissections using the stem-based approach on the probabilistic reconstructions because the visibility and boundary of the stems were severely reduced. As a result, the tracking results may be more limited and conservative than what we would expect with probabilistic tracking. Nevertheless deterministic tracking has been shown to produce better connectivity results than probabilistic tracking (Côté et al., 2013).

Stopping criteria

The last step of fibre tracking is when to stop propagating. This is defined by the stopping criteria, which usually involves specifying a threshold, for example when the fractional anisotropy drops below a certain value (indicating that it is no longer in white matter) or when the curvature falls below a certain angle threshold reducing improbable fibre trajectories.

In recent years, approaches to reduce implausible streamlines (e.g., streamlines stopping prematurely in the white matter) have been proposed that employ anatomical priors (Smith et al., 2012; Girard et al., 2014). These constrain the tracking to preferentially include streamlines that represent valid connections (cortico-cortical or cortico-subcortical) and probabilistically discard those that are implausible. Anatomically constrained tracking can significantly improve tracking results for connectivity analysis (see Section 6.2).

The choice of the tractography method can drastically impact the results of the reconstructed tractogram (Bastiani et al., 2012). Moreover, different tracking parameters are optimal for different tracts (Chamberland et al., 2014). It is thus important to interpret the tractography results keeping in mind the many parameters and factors involved in tractography processing. In Chapter 6, we perform a comparison of our original and improved tractography processing pipelines and assess their impact within the findings of our first study.

4.4.3 Tract segmentation

From whole-brain tractograms, the fibre structure can be segmented into smaller datasets, fibre tracts for example. This step, called tract segmentation, is the same problem that the early dissectionists were confronted with, in other words how to define a fascicle or white matter structure. One of the main advantages with dMRI tractography is that it can be used in an exploratory manner to perform 'virtual' dissections (Catani et al., 2002). The filtering capabilities and powerful visualization (e.g., colour-coding the mean orientation of the streamlines based on their endpoints or applying a solid colour for specific fibre groups to visualize the relationships between them in addition to the subject's anatomical T1 image) enable a new way to approach the study of the anatomy of the fibre pathways. The problem of tract segmentation remains an open question.

Early uses of the technique focused on reproducing our knowledge of the white matter anatomy (Catani et al., 2002; Mori & van Zijl, 2002; Wakana et al., 2003; Jellison et al., 2004; Lawes et al., 2008). Tract segmentation methods were thus aimed at reproducibility and reliability rather than precision (Wakana et al., 2007; Catani & Thiebaut de Schotten, 2008). The regions of interest (ROI)-based approach is the most widely used method for extracting individual fibre tracts (Conturo et al., 1999). Essentially, ROIs are defined (as exclusion or inclusion and passage or ending zones) to selectively filter the streamlines in order to isolate a known tract of interest. The ROIs can be manually defined or automatically defined using a template. Current approaches generally define a tract based on its regions of termination (or main passage areas) and therefore rely heavily on prior anatomical information (Catani & Thiebaut de Schotten, 2008; Zhang et al., 2010). However the definitions of many tracts are restricted to the consensus on their known anatomy consisting of only the most dominant

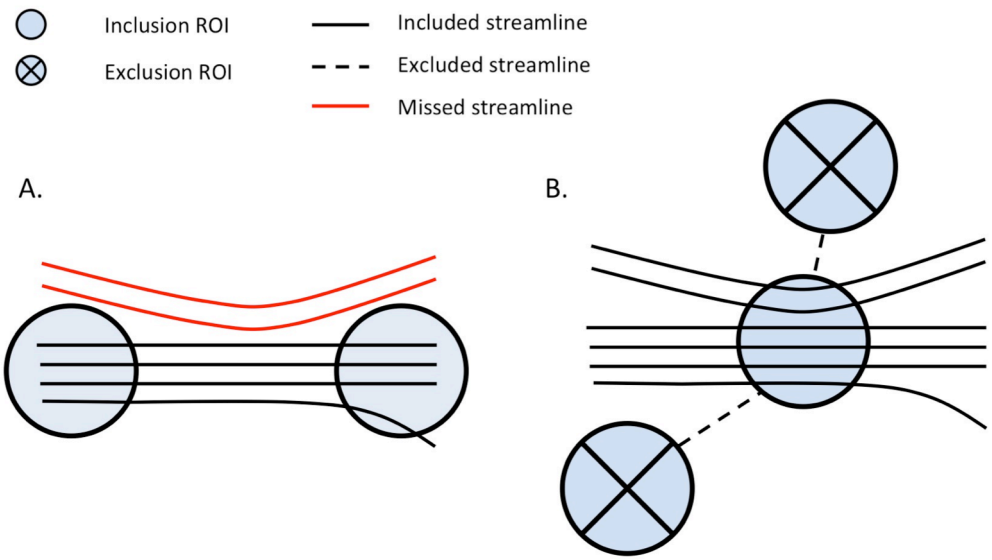

Figure 18. ROI-based approaches to tract segmentation. A) The classic multi-ROI strategy that extracts streamlines according to their areas of termination (based on prior knowledge) and B) the stem-based approach that extracts streamlines passing through their bottleneck or stem (minimizing a priori on the tract's terminations). While both strategies extract the dominant tract connections (black lines) only the stem-based approach captures the minor tract branches that are missed with the classic multi-ROI strategy (red lines).

components of the tracts. Thus limited insight regarding the anatomy of fibre tracts can be gained from these studies (Gierhan, 2013, Hau et al., under review). Computational methods based on clustering algorithms have also been proposed, however their aim has also been to extract tracts that correspond to their expected anatomy (O'Donnell et al., 2006; Guevara et al., 2012). Another method that has recently been proposed is based on the registration of streamlines, called Streamline-based Linear Registration, (SLR) using a model tract bundle to extract similar streamlines in other subjects within the same reference space (Garyfallidis et al., 2015). This has been tested for the UF on the BIL&GIN database processed with the CSD-based pipeline in thirty subjects and the preliminary results are promising (see Chapter 8).

In contrast to these approaches, we utilized a stem-based approach, which aims to reproduce the method introduced by the early neuroanatomists, to define fibre tracts based on their stem (Figure 18). This is done through an interactive virtual dissection of the tractogram, manually delineating an ROI around the bundle of fibres. Such an approach minimizes a priori on the terminal projections of a pathway enabling an exploratory approach in which the complete fibre tract can be identified (including its minor, less-studied components or branches). A few studies have used the stem to segment tracts but these were based on selecting voxels on FA maps rather than an interactive tractography dissection (Makris et al., 2005, 2009).

Tract segmentation is often combined with quantitative maps (see section below on microstructural properties) using the segmented tracts as regions of interest to provide tract-specific measurements, a practice referred to as 'tractometry' (Jbabdi & Johansen-Berg, 2011). Another potential application is to study the connectional anatomy of tracts.

4.4.4 Mapping the connectional anatomy of fibre pathways

A major advantage of dMRI tractography is that the analysis of cortical terminations and connections can be done automatically and systematically. Early work with dMRI tractography focussed on reproducing dissection studies but despite its potential little focus has gone towards describing the structural connections, in particular the fibre pathways.

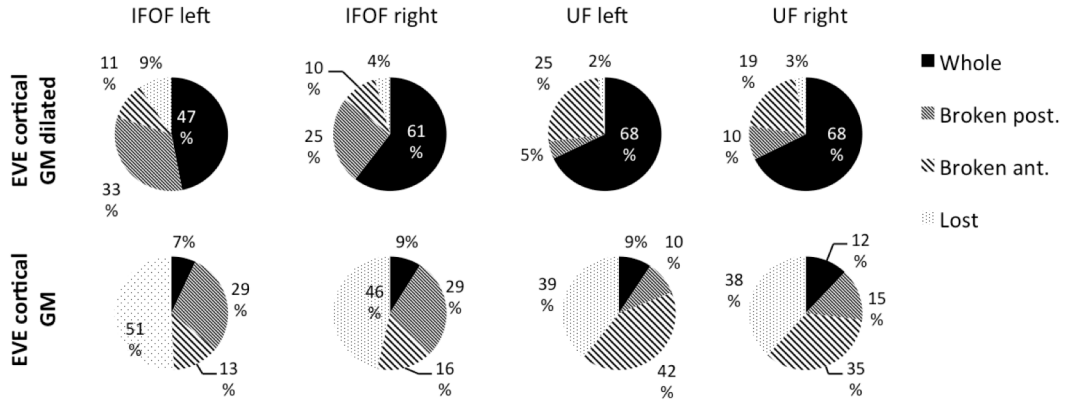

Figure 19. Proportion of whole, anteriorly broken, posteriorly broken and lost streamlines for the IFOF and UF (DTI) obtained with the Eve atlas and Eve atlas dilated once.

To map the connections of streamlines, it is necessary to parcellate the brain into regions in order to identify the terminations of streamlines. Most commonly, an anatomical template or atlas in a standard space is used containing pre-segmented areas. The template can then be registered to the subject's space. Templates such as the Desikan-Killiany (Desikan et al., 2006) and John's Hopkins University (JHU) (Oishi et al., 2009) templates are freely available online. Since tracking stops in or more often near the grey matter (low areas of FA) it is then necessary to extend or dilate the template so that it covers the grey-white matter interface Figure 19. If anatomically constrained fibre tracking methods are used, the template should be adapted to the anatomical constraints employed. A map of connections based on the termination regions of streamlines can be obtained in this way, indicating the structural connections reconstructed with dMRI tractography.

Alternatively, what is more often done is creating a probabilistic map of fibre tracts across a group of subjects. The fibre tracts of each subject are registered to a standard space and their overlap is computed thus revealing the most common areas where the fibre tract is present and the more variable areas. In general, there is considerable overlap within the main portion of the tract and greater variability as the fibres reach their terminations in the cortex. Although this is a useful indication of the variability in the overall location of the tract, it does not provide precise information in terms of where the tracts terminate.

The proportion of whole, posteriorly and anteriorly broken and lost streamlines for the tracts from our first study (see Section 6.2) are presented in Figure 19. First, note that using the dilated EVE cortical template to register the streamline terminations dramatically increases the proportion of whole streamlines and decreases the proportion of lost streamlines compared to the original EVE cortical template. Also, note the biases resulting from differences in the distance that must be travelled by the streamline to reach its destination. Given that the IFOF is a longer tract compared with the UF, it has a longer distance to follow making it more difficult to track. As a result, the mean percentage of whole streamlines is higher for the shorter UF (68%, bilaterally) compared with the IFOF (47 and 61% in the left and right hemispheres, respectively). Similarly, the percentage of posteriorly broken streamlines for the IFOF (33-25%) is higher relative to its percentage of anteriorly broken streamlines (11-10%) which travel a shorter distance from the stem to the frontal lobe. Likewise, this explains the higher percentage of UF streamlines broken anteriorly (25-19%) that must travel further to the frontal lobe relative to its percentage of streamlines broken posteriorly (5-10%).

4.4.5 Measuring microstructural properties

Another main advantage of dMRI tractography is that it enables the extraction of quantitative measures. Such measures can give an indication of the microstructural properties of

white matter, and have enormous potential for studying clinical disorders, aging and brain development.

The classic measures are derived from the diffusion tensor model and include fractional anisotropy (FA), mean diffusivity (MD), axial diffusivity (AD) and radial diffusivity (RD). FA is this most widely used measure, representing the degree of anisotropy, which may be an indication of white matter integrity (i.e., changes in FA would suggest changes in axon density, axon diameter, degree of myelination, etc.). Given its lack of specificity, the other components of the diffusion signal are also often reported. MD (also called ADC, mentioned earlier) refers to the degree of diffusion and measures the degree of hindrance potentially indicating membrane density. AD and RD refer to the principal and secondary diffusion direction respectively and may help disentangle changes in FA, with changes in RD potentially indicating changes in myelination, axonal density and/or diameter (Feldman et al., 2010). Additionally, the number of streamlines (or streamline count) has often been used as a « surrogate » measure of connectivity or connection probability. Its use has been actively advocated against (Jones & Cercignani, 2010; Jones et al., 2013) due to the number of confounding variables involved arising from tractography (biases include length, curvature, local fibre geometry). Nonetheless, the number of streamlines does represent the probability of least hindrance, and if the proper precautions are taken to control for tractography biases, it can be a meaningful measure of connectivity. In fact, a recent study using cortico-cortical evoked potentials showed that track count was correlated with conductivity (Conner et al., 2012).

The interpretation of DTI-derived quantitative measures is difficult as they are affected by many factors including noise, artifacts, partial volume effects (between white matter and the cerebrospinal fluid), and in particular fibre geometry (i.e., crossings or fanning configurations which will reduce FA as a result of their arrangement within the voxel), which can significantly alter the measures (Alexander et al., 2007). Recently, there has been much effort towards developing orientation-specific quantitative measures that use the information from higher-order tractography approaches (Raffelt et al., 2012, 2015; Dell'Acqua et al., 2013).

4.4.6 Limitations of diffusion tractography

Diffusion MRI tractography is still undergoing its development phase and will only continue to be improved with better methods. The main limitation of diffusion tractography is that it is an indirect technique and thus results obtained with it require careful interpretation with respect to the tractography methods used. Some of the drawbacks of diffusion tractography are its low spatial resolution making it susceptible to partial volume effects, the difficulty involved in both resolving complex fibre configurations within the voxel and developing a tracking algorithm that can accurately reconstruct the fibre architecture. Another disadvantage is that, unlike axonal tracing, it does not provide directional information and therefore cannot distinguish afferent from efferent connections.

4.5 Summary and concluding remarks

In this chapter we reviewed the advantages and disadvantages of the main techniques for studying macroscopic white matter connections, summarized in Table 2. Today we are still faced with the problem of no single best technique for studying the macroscopic connections precisely and comprehensively. The techniques range in their application (in animals/humans, in vivo/ex vivo) and abilities to discriminate between fibre tracts, comprehensively describe them and precisely locate their origins and terminations, making it necessary to use multiple techniques. One advantage for us is that the white matter structure is relatively stable: "anatomical connections either exist, or they don't, and different ways of measuring anatomy should ultimately converge and render a consistent map of their architecture" (Sporns, 2013).

Axonal tracing may provide the most precise information on tract connections, however it can only be applied to animals. Dissection has been the main source of our knowledge on human fibre pathway anatomy, however it has major weaknesses including the finality of the dissection process (tissue or fibre tracts cannot be put back once they are dissected), the difficulty in following fibres from end to end and the limited number of subjects that can be studied. dMRI tractography enables the comprehensive representation of the fibre anatomy (virtual tractogram) and the potential to systematically study the connectional anatomy and characteristics of fibre pathways in large populations. Using PLI to refine and constrain tractography methods may be an important step for validating dMRI tractography. New findings observed with dMRI tractography will require converging evidence from both axonal tracing in animals (homologue connections) and dissection in humans.

Table 2. Techniques for studying the macroscopic fibre connections in the brain.

Technique	**Performed**	**Species**	**Advantages**	**Disadvantages**
Gross dissection	Ex vivo	Humans, animals	Direct observation Good ability to discriminate between tracts Observe complex relationships between tracts	Less precise, dependent on expertise, qualitative Time consuming Limited subjects
Axonal tracing	Ex vivo (requires in vivo during injection)	Animals	Direct observation High level of detail Dissociate efferent/afferent	Not possible in humans Limited to a few cortical injections at a time (potential undersampling)
Polarized light imaging	Ex vivo	Humans, animals	Direct observation High level of detail Enables computational study	Ex-vivo only Require specimens Limited by current technology
dMRI tractography	In vivo, ex vivo	Humans, animals	Clinical applications Quantitative measures Large group studies Enables computational study Observe complex relationships between tracts	Indirect observation, thus susceptible to inaccuracies, artifacts, noise Lower spatial resolution

5 Cortical terminations of the IFOF and UF: Anatomical stem-based virtual dissection

Summary

In this first study, we combined the neuroanatomists' approach of defining a fascicle as all fibers passing through its compact stem with dMRI tractography to investigate the cortical terminations of two association tracts, the inferior fronto-occipital fasciculus (IFOF) and the uncinate fasciculus (UF), which have recently been implicated in the ventral language circuitry. The aim was to provide a detailed and quantitative description of their terminations in 60 healthy subjects and to do so to apply an anatomical stem-based virtual dissection, mimicking classical post-mortem dissection, to extract with minimal a priori the IFOF and UF from tractography datasets. In both tracts, we consistently observed more extensive termination territories than their conventional definitions, within the middle and superior frontal, superior parietal and angular gyri for the IFOF and the middle frontal gyrus and superior, middle and inferior temporal gyri beyond the temporal pole for the UF. We revealed new insights regarding the internal organization of these tracts by investigating for the first time the frequency, distribution and hemispheric asymmetry of their terminations. Interestingly, we observed a dissociation between the lateral right-lateralized and medial left-lateralized fronto-occipital branches of the IFOF. In the UF, we observed a rightward lateralization of the orbito-frontal and temporal branches. We revealed a more detailed map of the terminations of these fiber pathways that will enable greater specificity for correlating with diseased populations and other behavioral measures. We conclude that anatomical stem-based virtual dissection with diffusion tractography is a fruitful method for studying the structural anatomy of the human white matter pathways.

5.1 Introduction

Both inferior fronto-occipital (IFOF) and uncinate (UF) fasciculi are crucial for the ventral intra-hemispheric transfer of information between the frontal cortex and the occipital, temporal and parietal cortices, and knowing their cortical terminations is fundamental for understanding their role in mediating language semantics (Turken and Dronkers, 2011; Duffau, 2015). The earliest description of the IFOF dates back to Burdach (1819-1826) who described direct fronto-occipital connections although he misattributed them to the inferior longitudinal fasciculus. The UF was described even earlier by Reil (1809), characterized as the hooked-shape fibers behind the insula. While the anatomical description of the UF has remained stable (connecting fronto-orbital cortices with the temporo-polar cortex), there have been some inconsistencies surrounding the IFOF's anatomical course and terminations (Dejerine & Dejerine-Klumpe, 1895; Trolard, 1906; Curran, 1909; Crosby, 1962) due to its complex anatomy.

Only recently have *post-mortem* dissection studies begun to investigate the precise terminations of white matter pathways, developing updated techniques to improve precision in locating and identifying their cortical fiber terminations (Martino et al., 2011). A clearer picture of the IFOF's precise cortical terminations is starting to emerge. In particular, two recent dissection studies have provided in-depth descriptions of its anterior (Sarubbo et al., 2013) and posterior (Martino et al., 2009) terminations. Although less recent, Ebeling and Cramon's (1992) meticulous dissection study on the anatomy of the uncinate fasciculus provides a detailed description of its anatomical projections within the frontal and temporo-mesial areas that elaborates on earlier descriptions. While these dissection studies confirmed the conventional definition of the respective tracts, they also revealed termination territories in more detail and beyond those previously described, suggesting more expansive definitions are needed. Previous dissection work indicates that there is some inter-individual variability in the tract projections (Martino et al., 2010). This no doubt contributes to the inconsistencies in the cortical terminations observed in the IFOF and to a limited extent the UF. Dissection studies are limited in the number of subjects they can study and thus are not able to address inter-individual variability. Tractography with dMRI enables the *in vivo* anatomical study of fiber pathways in large samples. To our knowledge, since the seminal single-subject tractography study of Catani (2002), only one tractography study has examined the cortical terminations of the IFOF in a group (twenty subjects) confirming some of the more extensive projections described inconsistently thus far in the literature, in particular within the parietal lobe (Caverzasi et al., 2014). There has been no detailed study of the UF terminations using tractography (Von Der Heide et al., 2013).

Figure 20 summarizes the consensus coming from both *post-mortem* dissection and *in vivo* tractography studies, that the IFOF connects the ventral occipital cortex with the inferior frontal and fronto-orbital cortices (Dejerine & Dejerine-Klumpe, 1895; Trolard, 1906; Curran, 1909; Crosby, 1962; Catani & Thiebaut de Schotten, 2008; Martino et al., 2010; Zhang et al., 2010; Forkel et al., 2012; Sarubbo et al., 2013; Caverzasi et al., 2014). But, IFOF projections to the superior and middle frontal (Sarubbo et al., 2013; Caverzasi et al., 2014), medial occipital (i.e., the lingual gyrus and cuneus) (Lawes et al., 2008; Martino et al., 2011; Caverzasi et al., 2014; Forkel et al., 2014), temporo-basal (Crosby et al., 1962; Catani and Thiebaut de Schotten, 2008; Lawes et al., 2008; Martino et al., 2011; Caverzasi et al., 2014) and parietal (Curran, 1909; Martino et al., 2009; Sarubbo et al., 2013; Caverzasi et al., 2014; Forkel et al., 2014) regions are inconsistently observed and their inclusion in its definition is debated. The consensus on the UF is that it connects, along with the fronto-orbital and temporo-polar cortices, ventral temporal areas (Ebeling and von Cramon, 1992; Catani and Thiebaut de Schotten, 2008). Questions also remain concerning the UF terminations, in particular concerning its projections to the amygdala (Klinger and Gloor, 1960; Ebeling and von Cramon, 1992; Croxson et al., 2005; Thiebaut de Schotten et al., 2012) and cingulate gyrus (Ebeling and von Cramon, 1992; Thiebaut de Schotten et al., 2012) posteriorly and to the superior and middle frontal gyri, anteriorly (Dejerine &

Dejerine-Klumpe, 1895; Kier et al., 2004; Thiebaut de Schotten et al., 2012). A common understanding of the anatomy of these tracts is needed.

In order to study these open questions of whether a particular cortical region belongs to the IFOF or UF, we adopted the approach of neuroanatomists who first locate the stem (i.e., the point of passage where all fibers pass through) and use it as an anatomical reference to identify the tract. We therefore performed an anatomical stem-based virtual dissection to extract these two bundles from whole-brain tractography datasets in a large cohort of 60 healthy subjects. Starting from widely accepted anatomical evidence regarding the locations of the IFOF and UF stems, we exposed their respective stems and manually delineated a single region of interest (ROI) around each of them. This approach enables us to minimize a priori on their terminations and provide the complete set of cortical terminations of IFOF and UF, as well as their variability and their asymmetries.

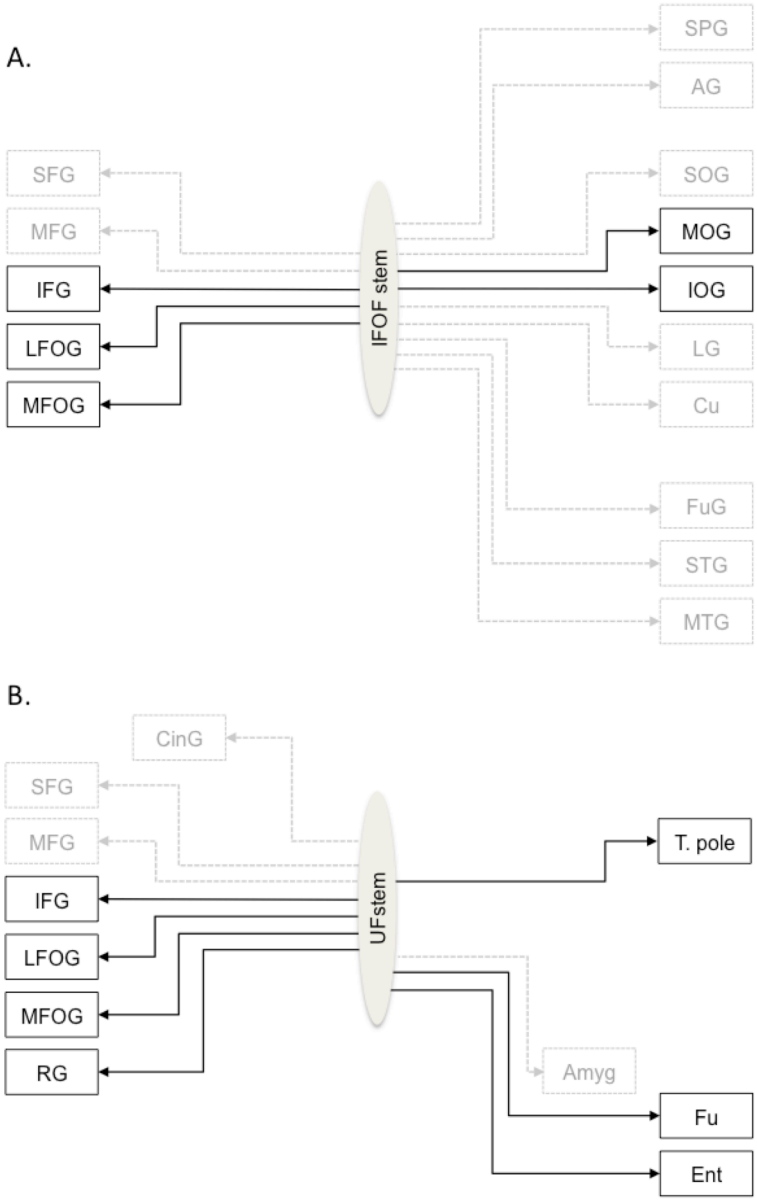

Figure 20. Schemas summarizing the cortical termination territories of the IFOF (A) and UF (B) in the literature. The cortical territories corresponding to their conventional definitions are shown by solid black arrows and the debated cortical territories are shown by dashed grey arrows. Abbreviations: SFG, MFG, IFG: superior, middle and inferior frontal gyri; LFOG, MFOG: lateral and medial fronto-orbital gyri; RG: rectus gyrus; SOG, MOG, IOG: superior, middle and inferior occipital gyri; Cu: cuneus; LG; lingual gyrus; T. pole: temporal pole; STG, MTG, ITG: superior, middle and inferior temporal gyri; Fu: fusiform gyrus; SPG: superior parietal gyrus; AG: angular gyrus; Ent: entorhinal gyrus.

5.2 Methods

Image acquisition

Diffusion-weighted images were previously acquired for 60 healthy right-handed (30 female, mean age = 30.1, age range = 20-53) belonging to the BIL&GIN database (Brain Imaging of Lateralization by the Groupe d'Imagerie Fonctionnelle (Mazoyer et al., 2015). All the subjects gave written informed consent to participate in the study, which was approved by the local ethics committee (*CCPRB Basse-Normandie*). Imaging was performed on a Philips Achieva 3 Tesla MRI scanner using a single-shot spin-echo echo-planar sequence with 21 non-collinear diffusion gradient directions (b=1000 s/mm^2). Seventy axial slices parallel to the AC-PC plane were acquired from the bottom of the cerebellum to the vertex. Imaging parameters were as follows: TR = 8500 ms, TE = 81 ms, angle = 90°, SENSE reduction factor = 2.5, FOV 224 mm, acquisition matrix 112 x 112, 2x2x2 mm^3 isotropic voxel. The series of 21 directions was acquired twice by reversing the gradients' polarity, for a total of 42 diffusion-weighted volumes. To improve the signal-to-noise ratio, a second series of 42 volumes was acquired leading to a total acquisition time of 15 min 30 sec.

Whole-brain tractography

The raw diffusion images were corrected for eddy current distortion using the FMRIB Software Library (Smith et al., 2004) and processed with the Diffusion Toolkit software package to obtain the local tensor orientation estimates and fractional anisotropy maps and perform fiber tracking (Figure 21, top row). Deterministic whole-brain fiber tracking was performed in the native space of each subject using the Fiber Assignment by Continuous Tracking algorithm (Mori et al., 1999) with stopping criteria of 0.2 fractional anisotropy and a 45° angle threshold. Tracking was initiated by seeding from all voxels in the volume to generate the streamlines. This produced a 3D reconstruction of streamlines in the whole brain, namely a tractogram, which can then be segmented into anatomically defined bundles.

Template and regions of interest

The Johns Hopkins University (JHU) template (Oishi et al., 2009), containing 176 pre-segmented regions, was modified to create an additional temporal pole region in the standard space of the template. The superior, middle and inferior temporal regions (gyri and superficial white matter) were split in two: the temporal pole (anterior to the anterior commissure) and their respective superior, middle and inferior temporal regions (posterior to the anterior commissure) for the left and right hemispheres. In addition, we created three large divisions (Figure 21) representing the cortical grey matter (CGM), comprising all cortical areas of the template, deep white matter (DWM), comprising all deep white matter areas of the template and superficial white matter (SWM), comprising all superficial white matter areas related to the gyral regions (*i.e.*, situated between the cortex and the deep white matter). The modified JHU template and tissue division ROIs were warped to the native space of each subject using ANTS (Avants et al., 2011) linear and non-linear registration. For the cortical terminations analysis, the modified template was modally dilated once to include the interface between the grey and white matter.

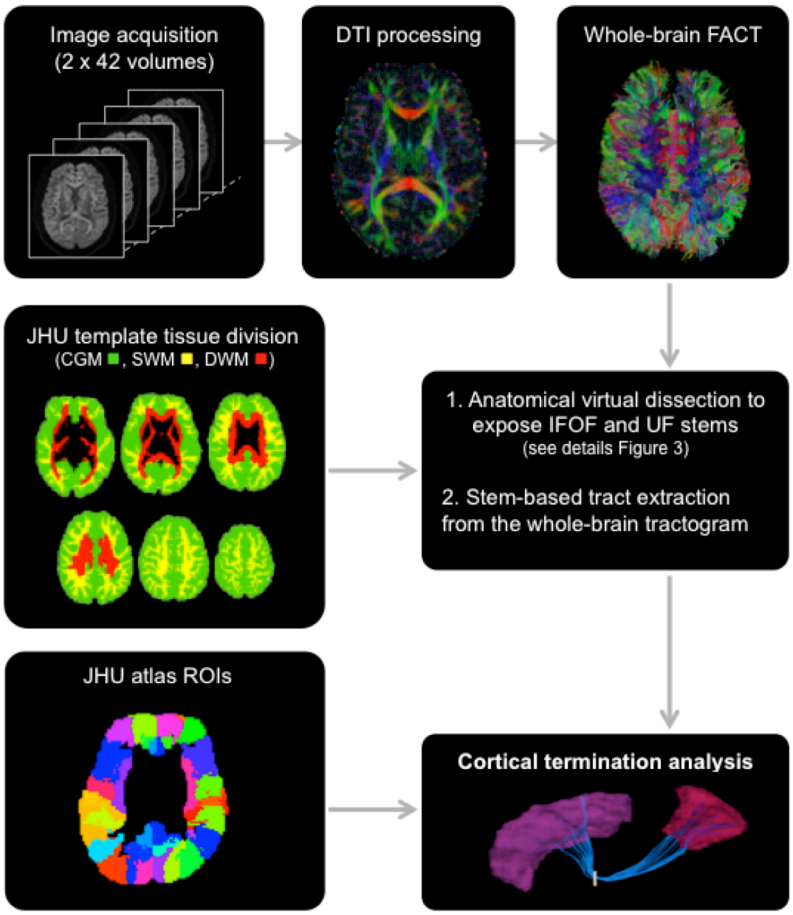

Figure 21. General scheme of the different steps involved in the study from data acquisition to the extraction of the tracts using the stem-based approach to tract connectivity analysis. a. The temporal lobe from the EVE atlas was split to create its grey and superficial white matter pole (shown) and corresponding superior, middle and inferior divisions. The three large divisions, cortical grey matter (green), superficial white matter (yellow) and deep white matter (red), were created by combining regions of the EVE atlas, and used to select the different sub-types of streamlines.

Stem-based anatomical virtual dissection of IFOF and UF

Both IFOF and UF were extracted by performing a virtual dissection in each hemisphere of the 60 whole-brain tractograms. To do so, we mimicked the post-mortem cortex-sparing fiber dissection method recently reported (Martino et al., 2009; Martino et al., 2011; Sarubbo et al., 2013), which exposes the IFOF and UF stems, collecting all the fibers belonging respectively to the IFOF and UF, after meticulous removal of the cortical and U-shaped fibers. Once these two stems were isolated, we were able to perform a quantitative analysis of their cortical terminations with minimal anatomical *a priori*. The software TrackVis (Wang et al., 2007) was used to perform the virtual dissection using the streamline filtering tools to select streamline groups and to display simultaneously the streamlines and FA maps. A combination of in-house Matlab and TrackVis command line tools were used to prepare the tractograms and extract the tracts.

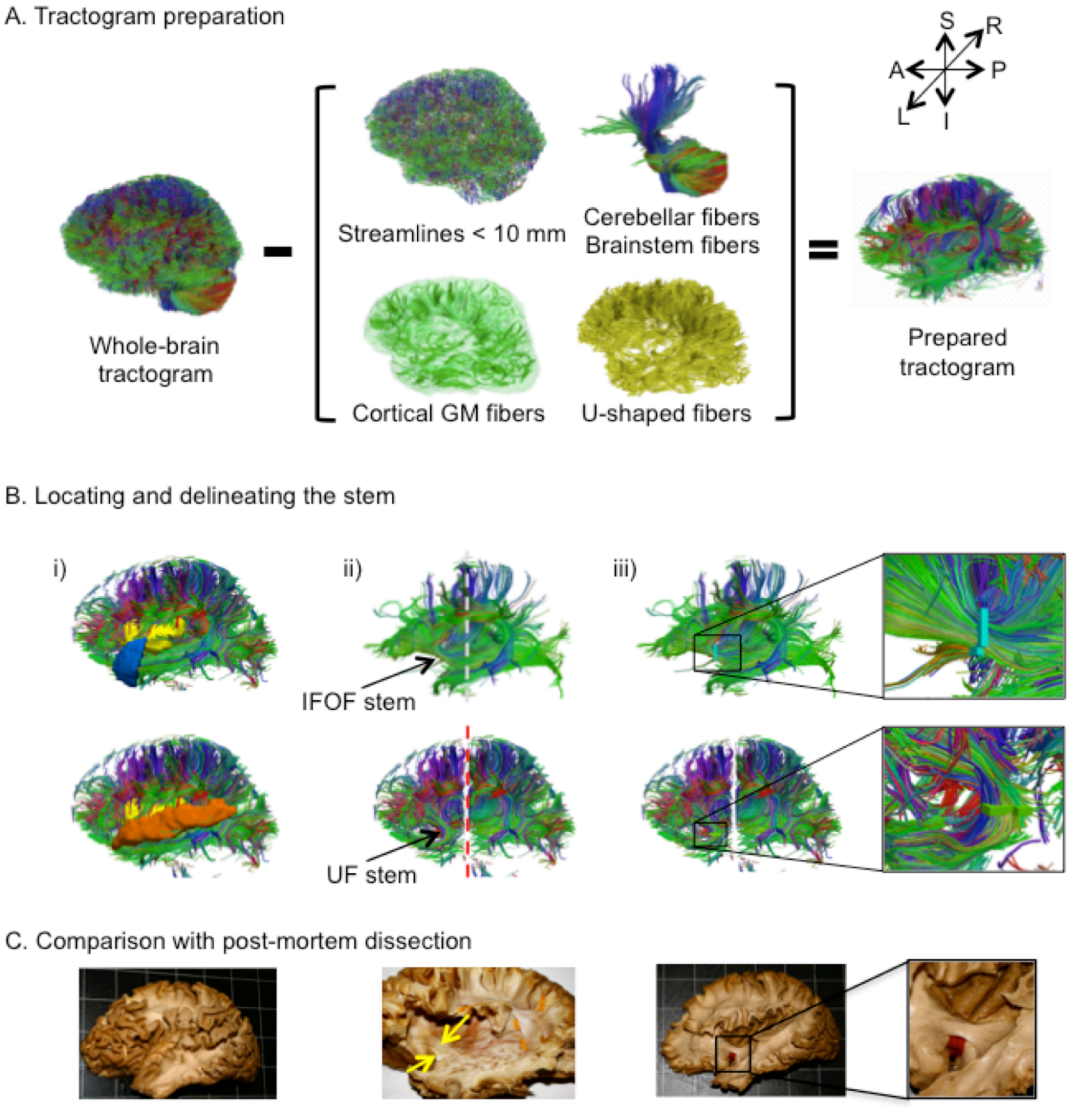

Figure 22. (A, B). The stem-based method. A) The preparation of the tractogram, inspired from the postmortem dissection technique to selectively remove streamline groups not belonging to the long association pathways and B) the procedure to delineate the stems of the IFOF and UF are shown on a single subject. Steps of the virtual dissection for the IFOF (B, first row) and UF (B, second row) with analogous images from a post-mortem dissection of the IFOF (B, third row): i) Template regions used to remove select groups of cortical streamlines, ii) window revealing the stem of the tract (dashed lines represent the coronal inclusion (grey) and exclusion (red) filtering slices, iii) ROI drawn to encompass the stem of the tract, while in post-mortem dissection a red tag separates the IFOF stem from the dorsal claustrum and putamen.

An overview of the complete virtual dissection is shown in Figure 22. In the first step, we removed from the whole-brain tractogram (Figure 22A): the extraneous streamlines shorter than 10 mm, the superficial streamlines restricted to the cortical GM region and the U-shaped streamlines passing through the SWM region. We also removed the streamlines passing through the cerebellum and the brainstem as well as the callosal streamlines passing through the inter-hemispheric fissure as they do not belong to the association pathways. In the next step, the removal of the U-shaped streamlines with terminations within the insula and the temporal pole exposed the IFOF stem (Figure 22B, top), while the removal of the streamlines terminating within the insula and the superior temporal gyrus exposed the UF stem (Figure 22B, bottom). Note that all these steps were performed automatically using TrackVis command line tools and the ROIs of the modified JHU template. Once the stem was exposed, a ROI was manually drawn

that strictly encompassed it in the same manner a paper tag is inserted under a narrow stem during post-mortem dissection (Figure 22C). The criteria for the inclusion of streamlines within the ROI were judged with respect to: 1) their location and proximity to the central bundle and 2) the cohesiveness of the shape of the streamlines to those within the core of the stem bundle. Therefore streamlines that created a gap in the stem and deviated significantly from the shape of the streamlines in the core of the bundle were not included. The IFOF stem was drawn on a single coronal slice where the streamlines converged into a compact bundle and the width of the bundle is the smallest before projecting to the cortex. The UF stem was drawn on a single axial slice at the point where the streamlines curve downwards and gather into a compact bundle, before descending to the temporal cortex. Of note, a small group of streamlines following a different course than the IFOF bundle, coming rather vertically from the parietal regions, passing the lateral aspect of the IFOF stem and terminating within the external capsule, was observed in the majority of the subjects. These streamlines belonging the claustro-cortical system (Fernandez-Miranda et al., 2008; Milardi et al., 2015) were not included in the IFOF and UF tracts.

The final step was the extraction of the IFOF and UF. This was done by specifying all streamlines that pass through their respective stems from the original whole-brain tractogram. This is a key advantage of tractography while in post-mortem dissection the removal of brain tissue is definitive. We aimed to apply the least constraints possible on the analysis of the cortical termination of the two tracts. Nevertheless, exclusion regions were used to prevent including streamlines that pass through one stem and belong to the other tract. At the level of the anterior temporal cortex, the streamlines of the IFOF are directed posteriorly whereas the streamlines of the UF curve in an anterior direction to reach the temporal pole (Ebeling and von Cramon, 1992; Martino et al., 2009). Therefore, the IFOF was extracted by including all streamlines passing through the IFOF stem while excluding those that pass through the temporal pole. The UF was extracted by including all streamlines passing through the UF stem

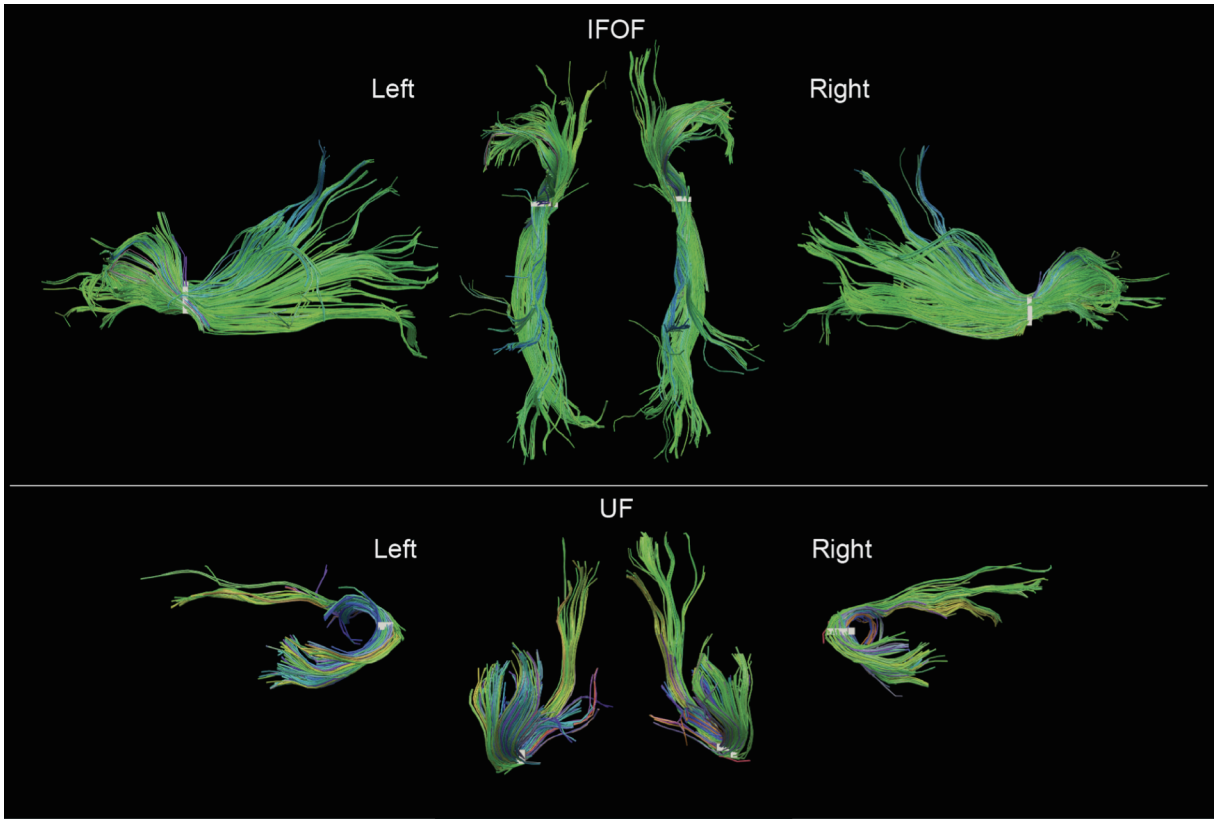

Figure 23. Examples of both left and right IFOF and UF of a typical subject extracted using the stem-based anatomical virtual dissection and shown with their stems (white). Middle top row, dorsal view of the two IFOF; middle bottom row, ventral view of the two UF.

and a coronal slice posterior to the external capsule was specified to exclude the streamlines oriented too posteriorly and belonging to the IFOF. Figure 23 shows an example of both left and right IFOF and UF virtually dissected in one of the 60 subjects.

Since our focus was on the cortical terminations of these association streamlines, the projection streamlines passing through the IFOF and/or UF stems but terminating within the subcortical nuclei were not taken into account nor were those terminating within the insula whose the nearby position along these stems requires a separate study. Note also that to be considered as belonging to the final IFOF or UF, a streamline must terminate at least in one cortical region either anterior or posterior to the stem. This led us to discard the streamlines passing through a stem but stopping short of the cortical ROIs.

Analysis of the IFOF and UF stems

Both IFOF and UF stems were normalized to the standard Montreal Neurological Institute (MNI) space using the inverse linear and non-linear registration process. The Euclidean distance between the IFOF and UF stem center of mass coordinates was also calculated within each hemisphere as well as their respective volumes.

In order to evaluate the reliability of the stem delineation, both IFOF and UF stems were manually drawn by two different operators (GP, JH) in the 60 subjects. Their spatial matching were examined by comparing the stem volumes and the Euclidean distance between the center of mass coordinates of the stems drawn by the two operators.

Analysis of the IFOF and UF cortical terminations

Once the IFOF and UF streamlines were extracted, we can describe within each subject their cortical termination territories based on macro-anatomical landmarks. Each streamline ending in one of 28 cortical regions of the JHU template was tallied to produce a measure of tract termination density for this region. The tallies were obtained using the UCLA Multimodal Connectivity Software Package (Brown et al., 2012). A normalized termination density score (NTDS) was obtained for each region by dividing the total number of tract streamlines ending in it by the total number of tract streamlines for each tract respectively, extracted in the left and right hemispheres. A first assessment was done to consider a cortical region as a termination territory of a given tract. We applied a threshold on the NTDS for each cortical region by choosing a region where there are known false positives. The precentral and superior parietal gyri were chosen as the regions containing false positives (FP_REG) for the IFOF and UF, respectively. The threshold for each tract was calculated based on the population, as follows:

$$\text{Threshold}_{\text{TRACT}} = \text{Mean NTDS}_{\text{FP\_REG}} + (2 \times \text{Standard deviation}_{\text{FP\_REG}}).$$

An individual adjusted score was therefore calculated for the regions with a NTDS superior to the $\text{Threshold}_{\text{FP\_REG}}$ by the following:

$$\text{Adjusted NTDS}_{\text{REG}} = \text{NTDS}_{\text{REG}} - \text{Threshold}_{\text{FP\_REG}}.$$

The adjusted normalized density score for each region underwent the Wilcoxon Signed-Rank test, since the distributions for almost all regions were non-normal, with the null hypothesis set at ≤ 0. Only those surviving a Bonferroni correction ($p < 0.018$) were considered termination territories of the tract. For each tract, the percentage of subjects with tract terminations in each of these territories was calculated.

To assess laterality effects, asymmetry indexes were calculated on the normalized density scores for each termination region using the following formula: $\frac{(\text{Right}-\text{left})}{(\text{Right}+\text{left})}$. Two-tailed ANOVAs using the Bonferroni correction were performed to test for significant asymmetries.

5.3 Results

Description of the IFOF and UF stems

In the following, the results of the IFOF and UF stems drawn by one operator (GP) are presented (see inter-operator reliability below). The mean stem volumes (in mm^3) of the left and right IFOFs were 82.5 ± 35.5 and 100.3 ± 47.0, respectively (Table 3). The mean stem volumes of the left and right UFs were 74.0 ± 33.0 and 93.9 ± 33.1, respectively. The ANOVA with Tract (IFOF, UF), Hemisphere (Left, Right) and their interaction (Tract x Hemisphere) as within-subject factors and Sex as a between-subjects factor only revealed an Hemisphere effect with both IFOF and UF stems significantly larger in the right hemisphere ($F = 40.9$, $p < 0.0001$).

Figure 24 shows the individual and mean center of mass locations of the IFOF and UF stems as points projected on a single-subject MNI T1 brain. The locations of the stems were highly consistent across subjects for both tracts and their relative positions within the ventral part of the external capsule are clearly distinct (Figure 24, coronal section). On average, the delineated IFOF stem was located between the posterior part of the putamen and the claustrum (Figure 24, axial section) while the delineated UF stem tended to be situated more ventrally within the external capsule. The mean center of mass coordinates of the IFOF and UF stems are presented in Table 1. The mean Euclidean distances between the left IFOF and UF stem centers of mass were 9.4 ± 2.7 mm and for the right IFOF and UF stems was 10.5 ± 2.1 mm, both being significantly different from 0 (Student's t-test, $p < 0.0001$). The mean center of mass coordinates of the left and right UF stems were situated significantly more ventral than the respective IFOF stems in each hemisphere (mean ± standard deviation, left: 8.2 ± 2.3 mm and right: 9.7 ± 1.9 mm, $p < 0.0001$). They were also slightly but significantly more posterior (left: 2.0 ± 2.9 mm and right: 1.7 ± 2.4 mm, $p < 0.0001$) and more lateral (left: 2.7 ± 1.9 mm; right: 1.9 ± 1.6 mm, $p < 0.0001$).

Inter-operator reliability to delineate the IFOF and UF stems

The delineation of the stems was consistent between operators both in terms of volumes and mean centers of mass (Table 3). The mean differences of volume between operators were between 6 and 9 mm^3 for left and right IFOF stems and between 7 and 8 mm^3 for left and right UF stems, which corresponds approximately to a difference of one voxel (8 mm^3) and was not significant between operators (all Student's t-tests, $p > 0.05$). The mean Euclidean distances between the stems drawn by the two operators was 1.7 ± 0.8 mm and 1.9 ± 0.8 mm for the left and right IFOF stems and was 1.4 ± 1.1 mm and 1.4 ± 0.9 for the left and right UF stems, distances below the 2-mm voxel resolution at which our stems were drawn.

Table 3. Summary of mean volume (in mm^3) and mean centre of mass in MNI space, for the IFOF and UF stems drawn by the two operators (JH, GP) across the 60 subjects.

		Volume	X	Y	Z
IFOF	Left (GP)	82.5 ± 35.5	-30.6 ± 1.5	+0.5 ± 2.9	-8.0 ± 1.5
	Left (JH)	88.7 ± 20.4	-31.0 ± 1.5	-1.0 ± 2.8	-9.0 ± 1.5
	Right (GP)	100.3 ± 47.0	+31.7 ± 1.5	+0.6 ± 2.5	-7.4 ± 1.7
	Right (JH)	91.2 ± 20.1	+31.1 ± 1.5	-0.1 ± 2.5	-8.6 ± 1.6
UF	Left (GP)	74.0 ± 33.0	-33.3 ± 1.7	-2.4 ± 2.7	-16.2 ± 2.4
	Left (JH)	66.7 ± 21.8	-33.8 ± 1.9	-2.7 ± 2.6	-16.8 ± 2.6
	Right (GP)	93.9 ± 33.1	+33.6 ± 1.5	-1.2 ± 2.2	-17.2 ± 2.1
	Right (JH)	86.1 ± 29.0	+33.1 ± 1.8	-1.7 ± 2.3	-17.6 ± 2.1

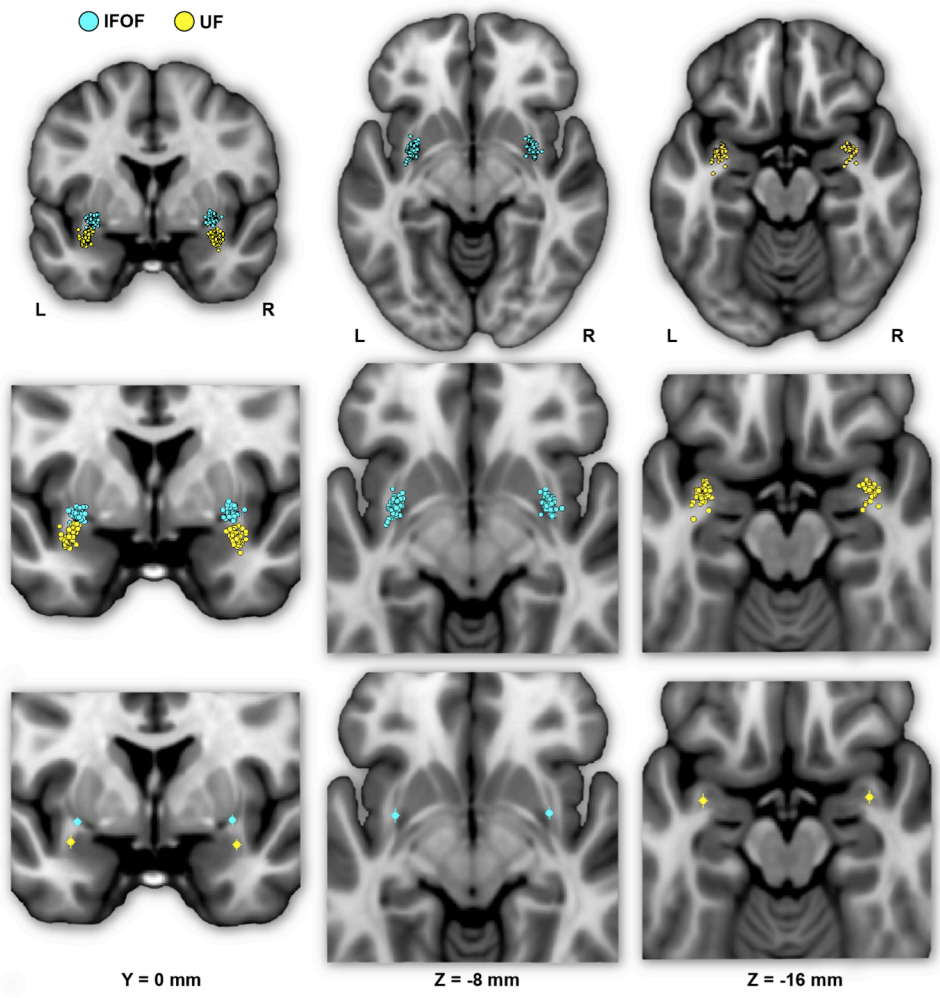

Figure 24. The individual (first row) and mean (second row) locations of the IFOF and UF stem centers of mass are shown in MNI space projected on a single-subject T1 image from the on their mean coronal section (left) and axial sections (middle and right). The IFOF stem centers of mass are located dorsally, anteriorly and medially with respect to the UF stems.

Description of the tracts

We present the frequency and distribution of each tract's terminations below.

Frequency of tract terminations in cortical regions among 60 subjects

For the IFOF, Table 4A shows the percentage of subjects with tract terminations in each of the 14 cortical regions that showed an adjusted normalized density score above 0. Anteriorly, the IFOF always projected to the inferior frontal gyrus (present in all subjects, bilaterally), almost always projected to the lateral fronto-orbital gyrus (87 and 90% for the left and right hemispheres, respectively henceforth) and less frequently projected to the medial fronto-orbital gyrus (63 and 32%) and middle frontal gyrus (60 and 55%). Projections to the superior frontal gyrus were observed in the minority of subjects (35 and 20%). Posterior IFOF termination frequencies were lower, never reaching 100%, which is related to long streamlines passing through the stem but stopping before reaching the termination territory (see methodological limitations in discussion section). The most frequent posterior termination regions were the middle occipital gyrus (65 and 95%) and lingual gyrus (80 and 78%). The IFOF also terminated in the inferior occipital gyrus (30 and 77%), in the temporal lobe in the superior (73 and 45%) and middle (33 and 52%) temporal gyri, and in the parietal lobe in the superior parietal gyrus (35 and 57%). Projection to the cuneus (38 and 15%), fusiform gyrus (12 and 32%) and angular gyrus (10 and 33%) were observed in the minority of subjects.

For the UF, Table 4B shows the percentage of subjects with tract terminations in each of the 11 cortical regions that showed an adjusted normalized density score above 0. Anteriorly, the UF always terminated in the medial fronto-orbital gyrus (present in all subjects, bilaterally), almost always projected to the lateral fronto-orbital (88 and 98%) and rectus (83 and 93%) gyri. Projections to the middle (12 and 60%) and inferior (37 and 35%) frontal gyri were also observed but with less frequency. Posteriorly, the UF always terminated in the temporal pole (present in all subjects, bilaterally) and superior temporal gyrus (present in all subjects, bilaterally) and almost always in the middle temporal gyrus (98 and 97%). The UF also frequently projected to the inferior temporal gyrus (88 and 92%) and entorhinal gyrus (77 and 78%). Projections to the fusiform gyrus were observed in the minority of subjects (37 and 43%).

Distribution of tract terminations

A description of the distribution of the tract terminations can be given based on the quantity of streamlines from the reconstructed streamlines terminating within each cortical region. Figure 25 shows the normalized termination densities of each region as box plots for the IFOF and UF tracts.

Anteriorly, the IFOF terminates predominantly in the inferior frontal gyrus (NTDS: 0.19 and 0.26 for the left and right, respectively henceforth) with minor branches projecting to the lateral (0.08 and 0.10) and medial fronto-orbital (0.09 and 0.06) and superior (0.05 and 0.04) and middle frontal gyri (0.07 and 0.06). Note that these NTDS do not account for 100% of the tract streamlines as a result of the streamlines stopping prematurely anteriorly and posteriorly. Given the larger proportion of posteriorly broken streamlines, posterior densities are likely to be underestimated. Posteriorly the largest proportions of IFOF projections are in the middle occipital (0.06 and 0.08) and lingual (0.08 and 0.07) gyri, followed by the superior temporal gyrus (0.07 and 0.06) with widely distributed minor branches in the occipital lobe in the inferior occipital gyrus (0.04 and 0.06) and cuneus (0.05 and 0.03), in the temporal lobe in the middle temporal (0.05 and 0.04) and fusiform (0.05 and 0.03) gyri, and in the parietal lobe in the superior parietal (0.05 and 0.07) and angular (0.06 and 0.03,) gyri.

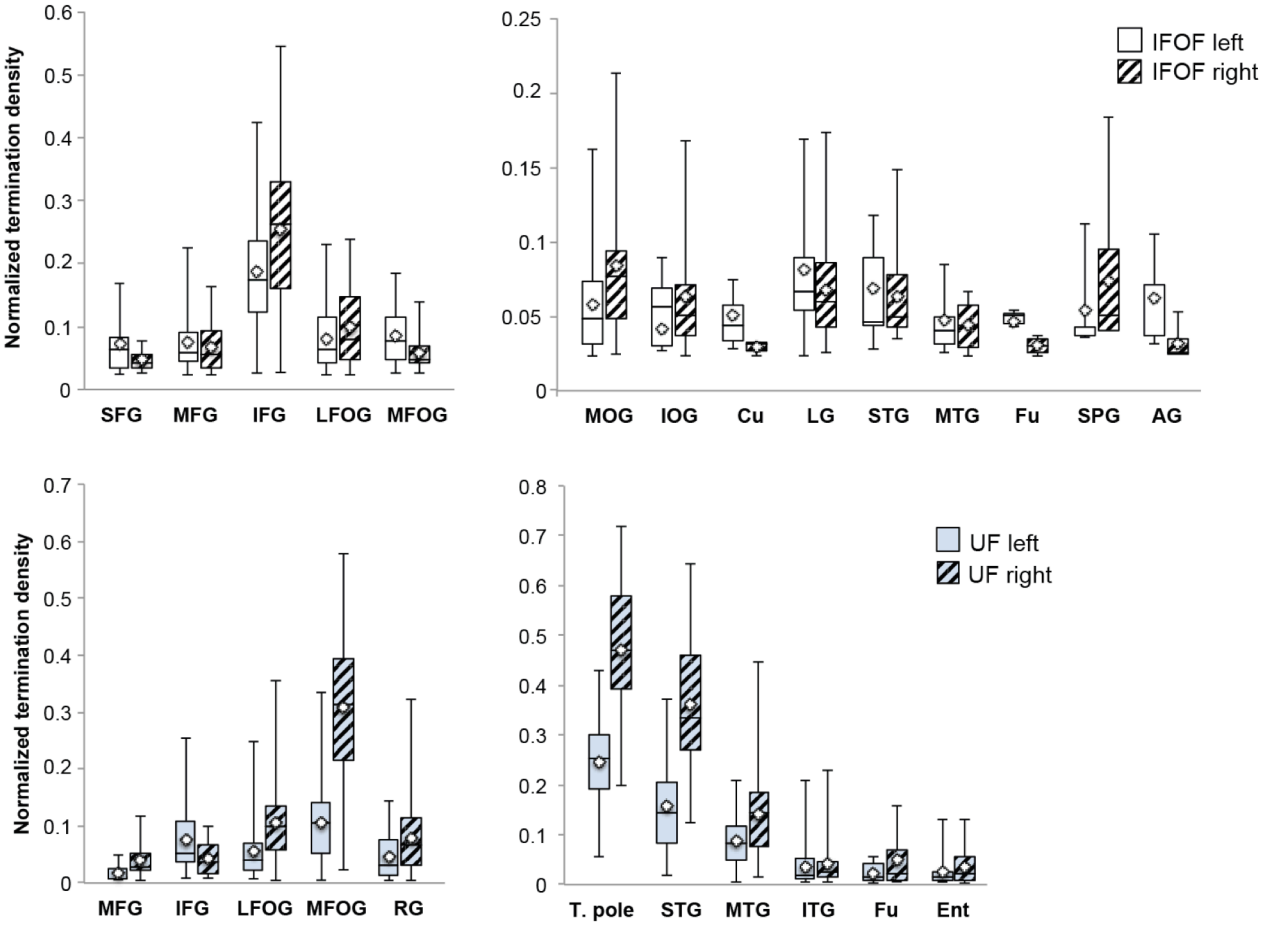

Figure 25. The normalized termination density scores of each anterior and posterior cortical region for the IFOF and UF are shown as box plots with their means (diamonds). Abbreviations (see Figure 20).

For the UF, the anterior projections are most predominant in the medial fronto-orbital gyrus (0.10 and 0.31) and distributed across the lateral fronto-orbital (0.05 and 0.11), rectus (0.05 and 0.08) and inferior frontal (0.08 and 0.04) gyri with the fewest projections in the middle frontal gyrus (0.02 and 0.04). Posteriorly, the UF projects in a graded manner with the largest portion in the temporal pole (0.25 and 0.47), followed by the superior temporal (0.16 and 0.36) and middle temporal (0.09 and 0.14) gyri and with minor branches in the inferior temporal (0.04 bilaterally), fusiform (0.03 and 0.05) and entorhinal (0.03 and 0.05) gyri.

Table 4. Percentage of subjects with terminations present in each region for the IFOF (A) and UF (B). A connection to a region was considered present for a subject if the termination density score for the region was above the threshold determined using the false positive region for each tract.

A. IFOF	**Frontal**					**Occipital**				**Temporal**			**Parietal**		
	SFG	MFG	IFG	LFOG	MFOG	MOG	IOG	Cu	LG	STG	MTG	Fu	SPG	AG	SMG
Left	35%	60%	100%	87%	63%	65%	30%	38%	80%	73%	33%	12%	35%	10%	7%
Right	20%	55%	100%	90%	32%	95%	77%	15%	78%	45%	52%	32%	57%	33%	28%

B. UF	**Frontal**					**Temporal**					**Limbic**
	MFG	IFG	LFOG	MFOG	RG	T. pole	STG	MTG	ITG	Fu	Ent
Left	12%	37%	88%	100%	83%	100%	100%	98%	88%	37%	77%
Right	60%	35%	98%	100%	93%	100%	100%	97%	92%	43%	78%

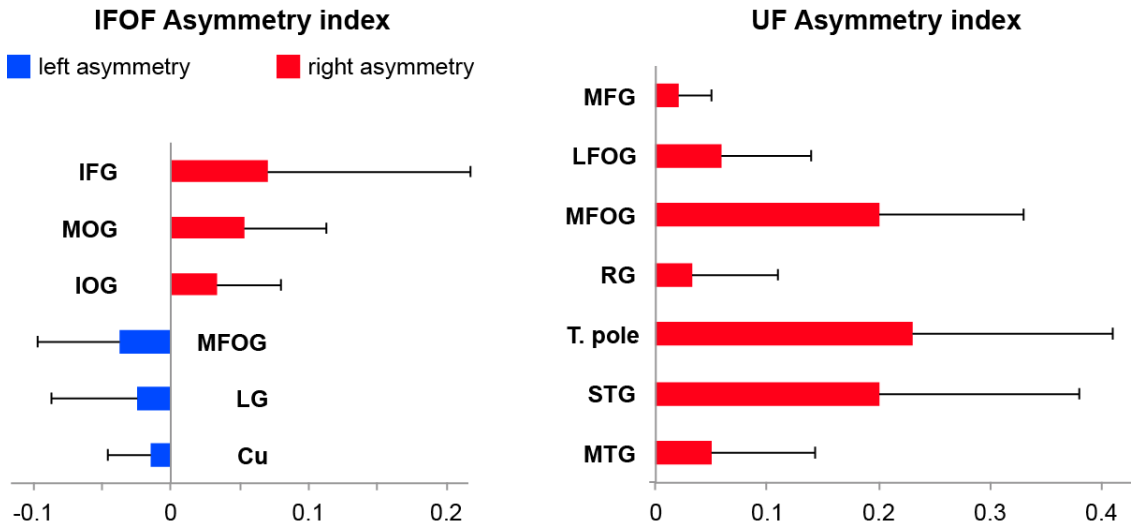

Figure 26. Mean tract termination density asymmetry indexes of the IFOF and UF showing significant lateralization for the number of streamlines.

Asymmetry of tract terminations in individual regions

Among the 14 IFOF terminal regions, significant lateralization patterns were observed differently for its anterior and posterior projections (all Bonferroni-corrected p values < 0.004). A rightward lateralization of the inferior frontal projections and leftward lateralization of medial fronto-orbital projections were observed for anterior IFOF terminations (Figure 26). Among its posterior projections, significant rightward lateralization of middle occipital, inferior occipital projections were observed. Significant leftward lateralization was observed in the medial occipital areas in the cuneus and lingual gyrus (Figure 26).

Among the 11 UF terminal regions (all Bonferroni-corrected p values < 0.005), significant rightward lateralization was observed in lateral and medial fronto-orbital gyri, in the middle frontal gyrus and rectus gyrus (Figure 26). Posterior UF terminations were significantly rightward lateralized in the temporal pole, superior and middle temporal gyri.

5.4 Discussion

The present anatomical stem-based virtual dissection allowed us to efficiently isolate and extract both IFOF and UF, two distinct bundles that pass through the external and extreme capsules. To dissociate these two adjacent bundles, the IFOF stem was delineated on the coronal section as it continues straight posteriorly to the occipital cortex using the temporal pole to exclude UF streamlines, and the UF stem was delineated on the axial section as it descends to reach the anterior temporal lobe using a coronal slice to exclude IFOF streamlines. Previous dissection studies have noted that the distinction between these two tracts is difficult to make due to the intermingling of their fibers (Ebeling and von Cramon, 1992; Kier et al., 2004). In fact, in some cases clinically important features of the IFOF such as the spread of tumor growth may be misattributed to the UF (Kier et al., 2004). However they are clearly distinct at the level of the stem and can be separated by a notable cleavage line (Curran, 1909; Kier et al., 2004; Martino et al., 2009; Sarubbo et al., 2013). This was confirmed by the clearly distinct IFOF and UF stem locations in this study, with the UF stem situated significantly ventral, posterior and lateral to the IFOF stem (Figure 24). Such a difference in their locations is consistent with two studies on the relative topographies of tracts in this area, known as the temporal stem (Ebeling and von Cramon, 1992; Kier et al., 2004).

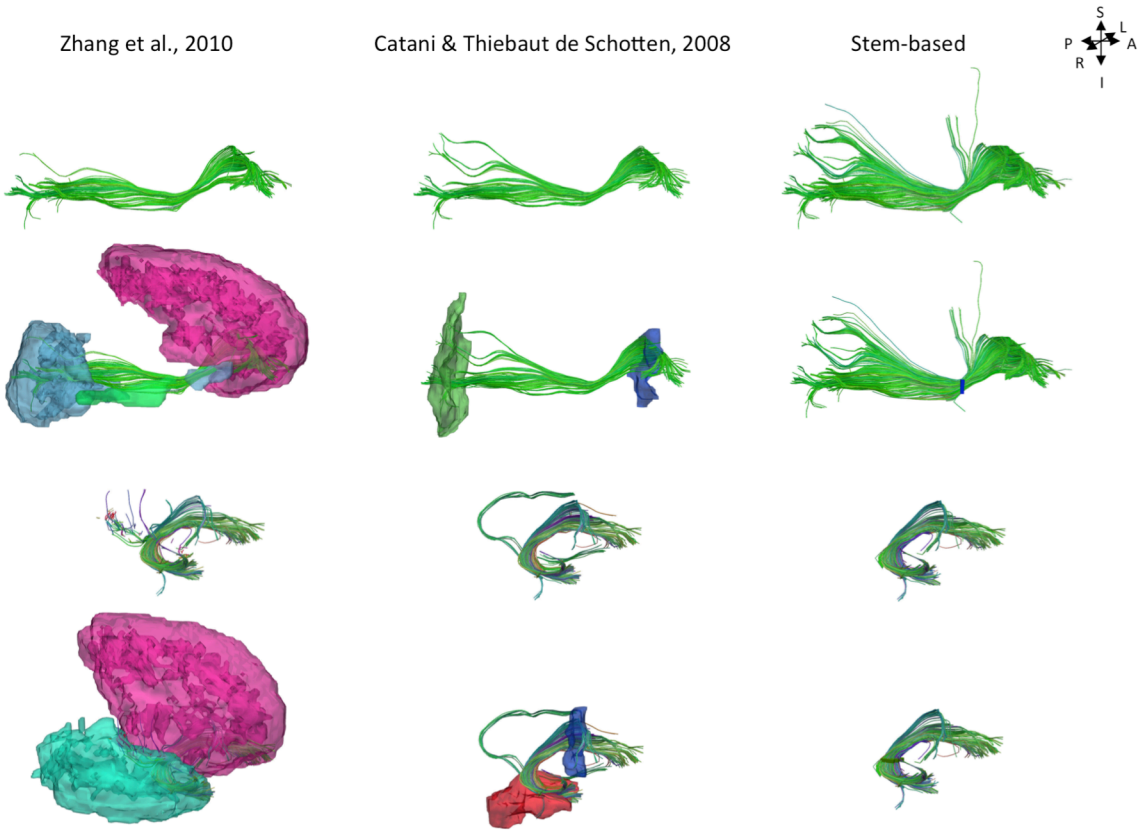

Figure 27. Examples of the IFOF and UF tracts in a single subject segmented using different ROI-based methods: automatic template ROI sets (left; Zhang et al., 2010), obligatory passages method (middle; Catani & Thiebaut de Schotten, 2008) and the stem-based method (right, only whole anterior-to-posterior cortical streamlines are shown). The ROIs are shown in the second and fourth rows (exclusion ROIs are not shown).

Compared with current set-of-ROIs tractography segmentation approaches for these two association tracts (Catani and Thiebaut de Schotten, 2008; Zhang et al., 2010), our stem-based virtual dissection results in more extensive IFOFs and UFs. Figure 27 compares the different IFOFs and UFs of a single subject obtained by applying current set-of-ROIs methods and the present stem-based virtual dissection. Note the parietal and superior frontal projections of the IFOF present in the stem-based extraction that are absent in the other IFOFs.

Before discussing the results of both IFOF and UF terminations, we address some noticeable limitations that are due to the tractography method used to obtain the whole-brain tractograms. We used the diffusion tensor model (FACT, Mori et al., 1999), which is well known for its limited ability to resolve crossing fiber configurations within a voxel. Thus areas of intersecting/overlapping/bordering pathways will greatly affect the tracking process and cause it to stop, producing broken streamlines. In our case, the streamlines start within a cortical region, pass through the stem, but stop before reaching their final cortical destination. This is especially noticeable for the IFOF, which presents the longest streamlines with the highest chance to cross other tracts. This is likely to account for the lack of IFOF projections to the superior frontal gyrus and relatively low occurrence of posterior projections for example in the middle and superior occipital gyri. Post-mortem dissection studies have noted considerable overlap between the infero-superior course of the IFOF and antero-posterior course of the arcuate fasciculus near the inferior and middle frontal regions (Martino et al., 2009; Sarubbo et al., 2013). Similarly the posterior projections of the IFOF need to pass 400 through the inferior longitudinal fasciculus within the temporal lobe in order to reach the middle occipital gyrus. Moreover the large variability observed in the frequency of projections 402 among subjects in these areas are likely to be due to such limitations and thus their densities 403 may also be

underrepresented. Note that, in future studies, using more advanced 404 tractography methods such as higher-order modeling (Descoteaux et al., 2009; Tournier et al., 2012) and anatomically constrained tracking (Girard et al., 2014) will help to prevent 406 broken streamlines and enable the study of their whole connectional anatomies. Nonetheless, thanks to the stem-based virtual dissection our approach allowed us to: 1) reproduce the consensus findings regarding IFOF and UF tract projections, and 2) provide clear evidence for more extensive projections beyond their conventional definitions that are in line with the more recent literature using improved fiber dissection techniques (Martino et al., 2009; Sarubbo et al., 2013). Note that almost all of the debated termination territories were consistently observed for both IFOF and UF and, the cortical regions in the conventional definitions corresponded to the most prominent termination regions observed (see Figure 28 for a revised definition of both tracts).

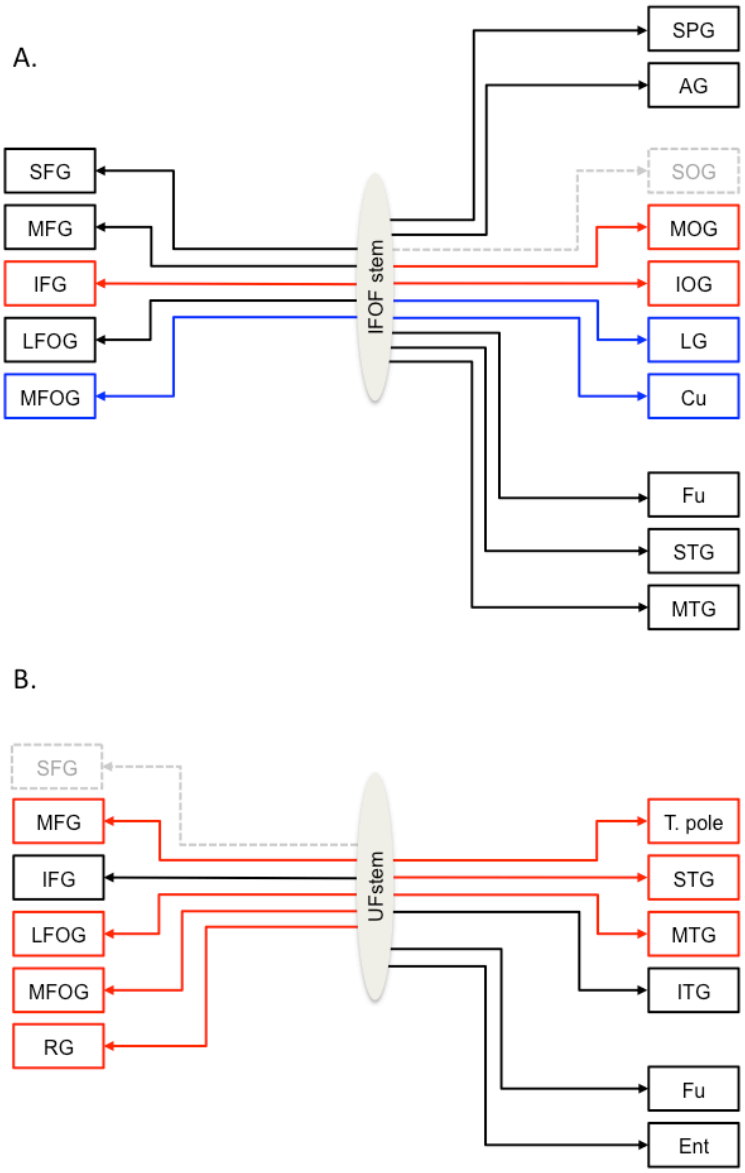

Figure 28. Schemas representing the cortical termination territories of the IFOF (A) and UF (B) based on our stem-based tractography study. The confirmed cortical territories are represented by solid lines and the regions that remain questionable are represented by dashed lines. The significant left lateralized projections are shown in blue and the right lateralized projections in red. Abbreviations (see Figure 20).

Cortical terminations of the stem-based IFOF

Our study confirmed frontal IFOF terminations within the inferior frontal and lateral and medial fronto-orbital gyri corresponding to the conventional IFOF definition. We also found frontal terminations beyond these areas in the superior and middle frontal gyri in line with previous studies (Sarubbo et al., 2013; Caverzasi et al., 2014). We showed that the IFOF's primary branch is clearly the inferior frontal/superficial subcomponent followed by the orbito-frontal subcomponent, with about equal density across the superior frontal and middle frontal subcomponents. These are consistent with the proportions reported in (Croxson et al., 2005) that used probabilistic tractography. The prominence of the inferior frontal and orbito-frontal terminations may explain why these regions are consistently observed in the literature. It could also be that the fanning of the superior frontal projections (clearly observed in a probabilistic tractography study, (Caverzasi et al., 2014) are more difficult to follow in dissection as well as in DTI-related tractography as the arcuate fasciculus intersects perpendicularly with the IFOF fibers on its infero-superior course (Martino et al., 2010; Sarubbo et al., 2013). Thus, in line with the fact that the superior frontal projections were only present in a minority of subjects (35-20%), the most superior frontal streamlines densities may be underrepresented given the limitations of the tractography method in the present study.

Posteriorly, we observed occipital projections to the middle and inferior occipital gyri also consistent with the conventional definition of the IFOF, as well as additional terminations in the occipital (cuneus and lingual gyrus), temporal (superior and middle temporal gyri, fusiform gyrus) and parietal (superior parietal and angular gyri) cortices. This corresponds to one of the earliest descriptions of the IFOF by Curran (1909) who described it as *"... a large associating bundle of fibers uniting, as it name indicates, the occipital with the frontal lobe. It also contains fibers, which join the frontal lobe with the posterior part of the temporal and parietal lobes*". In terms of posterior density distribution, we showed that the IFOF projects mainly to the occipital lobe (especially the middle occipital and lingual gyri, with minor projections to the inferior occipital gyrus and cuneus), with minor projections to the temporal lobe (superior and middle temporal and fusiform gyri) as well as to the parietal lobe (superior parietal and angular gyri), consistent with Curran's description of the distribution of projection. The dominance of the occipital projections likely accounts for these terminations being the consensus, while the temporal and parietal projections have been debated due to their being minor branches.

In the occipital lobe, the medial occipital cortex (cuneus and lingual gyrus) are not often cited as a termination territory of the IFOF and may be due to a lack of anatomical specificity in some of the earlier descriptions of the tract, with its first mention appearing late (Crosby et al., 1962). Projections to the lingual gyrus were observed in almost all subjects consistent with Caverzasi et al. (2014) however Martino et al. (2009) reported no projections to the lingual gyrus and instead considered them as part of the optic radiations. Projections to the cuneus were infrequent in the right hemisphere (present in 15% vs. 38% in the left hemisphere) showing the opposite pattern of Caverzasi et al. who reported more subjects in the left than in the right hemispheres. These differences may be due in part to the difference in templates used to register the terminations (they used the Freesurfer Desikan-Kyliany atlas whereas we used the JHU atlas). Projections to the inferior occipital gyrus were not frequently observed in the left hemisphere, twice less than in the right hemisphere, though it was reported in all subjects in a dissection study (Martino et al., 2009). This may be due possible crossings with other prominent tracts (inferior longitudinal, vertical occipital fasciculi) in the occipital lobe, especially for the left hemisphere. In contrast, the superior occipital gyrus was not significant as a termination territory (Martino et al., 2009) and. This may also be due to technical limitations arising from the tractography method since it is further and may require tracking through areas of crossings.

In the temporal lobe, the IFOF projects to the superior and temporal gyri and to a lesser extent to the fusiform gyrus, confirming dissection studies (Crosby et al., 1962; Martino et al., 2009). Neither the superior temporal nor middle temporal gyri were reported previously (Caverzasi et al., 2014).

We were able to observe parietal projections by using the present stem-based virtual dissection and were specifically found in the superior parietal gyrus and to a lesser extent in the angular gyrus. As shown in Figure 27, projections to the parietal lobe are systematically excluded using the method of (Zhang et al., 2010) and are likely to be missed using the method of (Catani and Thiebaut de Schotten, 2008) that use ROIs delineated around the frontal and occipital lobes, as was the case in (Sarubbo et al., 2013). There is converging evidence for the existence of fronto-parietal connections for the IFOF from post-mortem (Curran, 1909; Martino et al., 2009) and tractography studies (Mori et al., 2005; Caverzasi et al., 2014). In the present DTI study, we observed IFOF terminations in the superior parietal gyrus in the majority of the subjects consistent with dissection (Martino et al. reported parietal connections in 9 out of 14 hemispheres), and less frequently in the angular gyrus in contrast to Caverzasi and colleagues who reported it in 100% of subjects.

Asymmetry of cortical IFOF terminations

In this study we described, for the first time, asymmetries with respect to IFOF terminations within specific cortical regions. Interestingly, we observed a rightward lateralization of projections to the infero-frontal/superficial subcomponent, and a leftward lateralization of projections to the superior frontal and medial fronto-orbital gyri corresponding to the deep subcomponents (Figure 28). These lateralization patterns correspond to the different anterior subcomponents of the IFOF defined by Sarubbo et al. (2013).

Mirroring these results, posteriorly, we found a rightward lateralization of the projections to the lateral occipital areas (middle and inferior occipital gyri) and leftward lateralization of the projections to the medial occipital areas (lingual gyrus and cuneus) (Figure 28). These do not correspond to the posterior deep and superficial subcomponents identified in the literature (Martino et al., 2009; Sarubbo et al., 2013), however they do provide strong evidence for a medio-lateral dissociation of the posterior IFOF projections. Although our results do not permit us to draw conclusions on the connectivity of the tract, they suggest distinct anatomo-functional roles for a right lateralized component connecting the superficial component (inferior frontal gyrus) with the lateral occipital areas and a left lateralized component connecting the deep subcomponent (fronto-orbital, middle and superior frontal gyri) with the medial occipital areas (Figure 28).

These different lateralization patterns within the IFOF subcomponents may partly explain the conflicting reports regarding the asymmetry of the IFOF (Thiebaut de Schotten et al., 2011; Forkel et al., 2012).

Cortical terminations of the stem-based UF

We first confirmed anterior UF terminations mainly within the medial and lateral orbito-frontal areas, and minor branches in the middle and inferior frontal and rectus gyri consistent with dissection and tractography studies (Klinger and Gloor, 1960; Ebeling and von Cramon, 1992; Thiebaut de Schotten et al., 2012; Von Der Heide et al., 2013). The present results are also consistent with the proportions reported in Croxson et al. (2005). Projections to the frontal territories described above are consistently observed across subjects with the exception of the middle and inferior frontal gyri (Table 4B).

We observed posterior UF terminations predominantly within the temporal pole consistent with Ebeling and Cramon (1992), followed by the superior and middle temporal gyri, and then by fusiform and entorhinal gyri. We did not observe projections to the cingulate gyrus, neither to the amygdala in contrast to (Klinger and Gloor, 1960; Croxson et al., 2005; Thiebaut de Schotten et al., 2012) but in agreement with (Dejerine & Dejerine-Klumpe, 1895; Ebeling & Cramon, 1992). These discrepancies may be due to the existence of adjacent tracts, such as the amygdalo-temporo or amygdala-prefrontal pathways (Klinger and Gloor, 1960; Kim & Whalen,

2009) which may have been sometimes misattributed to the UF. Importantly, projections to the nuclei of the amygdala reported in Ebeling and Cramon refers to the entorhinal cortex and should not be mistaken for the amygdala proper as is often done (Schmahmann & Pandya, 2006; Kim & Whalen, 2009).

We showed evidence of terminations in the superior, middle and inferior temporal gyri beyond the temporal pole, posterior to the vertical plane passing through the anterior commissure. These terminations were highly consistent across the 60 subjects. Note that the hook-shaped pattern of these streamlines looks more like UF than IFOF streamlines, which led us to consider them as belonging to the UF. This was in line with our goal to follow as close as possible the neurodissectionist gesture. As such, we consistently observed a cleavage zone within the ventral portion of the external and extreme capsules between the UF fibers turning anteriorly and inferiorly to the temporal lobe (including the superior, middle and inferior temporal gyri posterior to the temporal pole) and the IFOF fibers going deeply and dorsally (Martino et al., 2009; Sarubbo et al., 2013).

Asymmetry of cortical UF terminations

The UF projections were mainly right lateralized. Hemispheric asymmetry in the UF has been observed for both volume and diffusion metrics but there are inconsistencies in the directionality of this asymmetry. Previous diffusion studies reported a rightward lateralized UF (Highley et al., 2002; Park et al., 2004; Thomas et al., 2015) however asymmetry in the opposite direction has also been shown (Kubicki et al., 2002; Hasan et al., 2009) and some did not find any asymmetry in the UF (Thiebaut de Schotten et al., 2011). Such inconsistencies underline the need for further investigation, possibly with more advanced tractography methods (see below).

5.5 Conclusion

In this study, we applied a sophisticated anatomical ROI-based tractography method to virtually dissect two association tracts, IFOF and UF, in a large group of subjects. By delineating anatomically both IFOF and UF stems, we minimized the constraints on the tract terminations and observed far more extensive projections than their conventional definitions. These previously unconsidered projections of the IFOF and UF need to be integrated into their structural definitions and considered in future studies when interpreting the multi-functional roles of these tracts. In addition, the quantitative information available through diffusion imaging provides not only tract-specific but branch-specific measures of the tracts providing better specificity that can be correlated with behavioral measures or patient populations. Such studies paired with complementary techniques such as direct electrical brain stimulation studies (Duffau, 2015), will be an important step in understanding their functional roles that will be relevant in the clinical setting.

The work in this chapter is currently under review in the journal Frontiers in Neuroanatomy.

6 Methodological considerations

In this chapter we take a deeper look at some of the methodological aspects of the work presented in the previous chapter. In particular, we discuss: 1) some of the inherent problems related to segmenting virtual fibres (i.e., streamlines) using a single stem and explore the idea of whether stem delineation could be automatized and 2) some of the drawbacks of using DTI to study tract anatomy and the advantages gained through the use of advanced tractography techniques by comparing tractography pipelines (basic vs. advanced) and studying their impact on the tractography results. This chapter is presented in the form of informal experiments.

6.1 A further analysis on stems

The notion of stems, the compact portion of fibre bundles, was demonstrated in one of the earliest DTI studies (Makris et al., 1997). They showed that the locations of tracts could be identified by their stems viewed on a brain section. This was done to map the fibre tracts during the era of gross histology and can be seen throughout Jules and Augusta Dejerine's atlas (Dejerine & Dejerine-Klumpe, 1895). Fig. 2 in Makris et al.'s study represents one of the first attempts to map the fibre tracts based on brain sections acquired from diffusion imaging, labelling the tracts as Dejerine had done (Figure 29A). They created Tensor Orientation Maps (TOM) that displayed the principal orientation in each voxel, indicated by the colour (red = left-right, green = anterior-posterior, blue = superior-inferior). Today modern atlases use a combination of fractional anisotropy maps coloured with the principal orientation to show both the degree of anisotropy and the orientation (Figure 29B).

We performed additional analyses on the stems of the IFOF and UF from the first study (n = 30). Our aim was to test the stem hypothesis, in particular: 1) What would happen with successive dilations of the stem and 2) If we looked more closely at the stem would we find pure single fibre populations or multiple fibre populations and would it be possible to segment a tract based solely on its stem.

We dilated the IFOF and UF stems within the plane in which they were drawn (in all directions) iteratively and calculated the density of streamlines at the stem at each iteration as follows: # of streamlines / # of (stem) voxels. If the stem was the densest part of the bundle we would expect the density to decrease as the stem dilates. Indeed, for both tracts the streamline

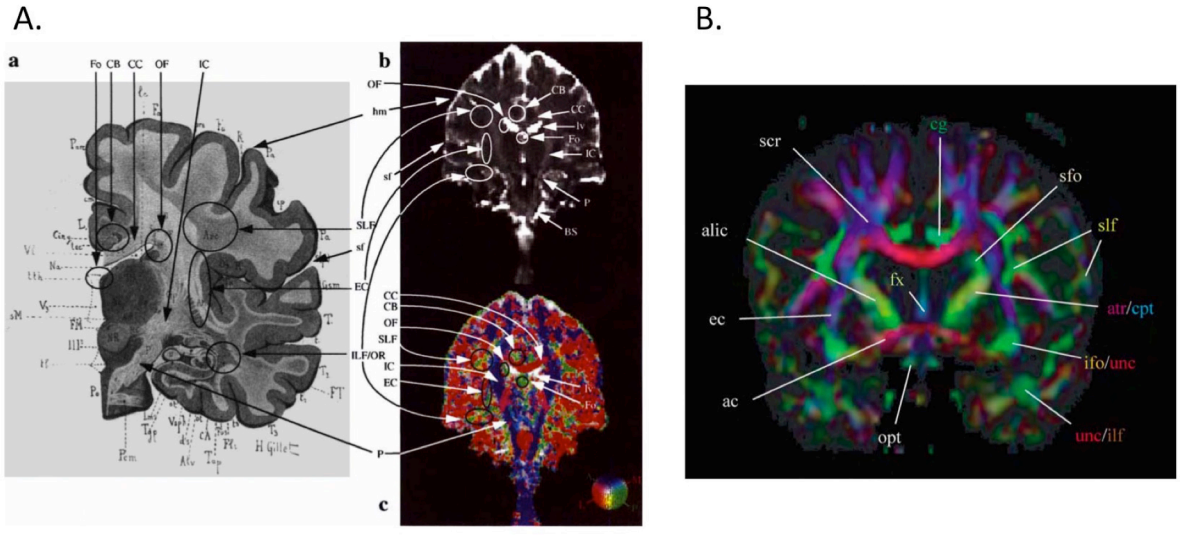

Figure 29. Fibre tracts labelled on coronal sections from (A) Dejerine's atlas (left) and on an early processed *in vivo* diffusion image (right), and (B) a modern diffusion imaging atlas. (A from Fig. 2 in Makris et al., 1997; B from Mori et al., 2005).

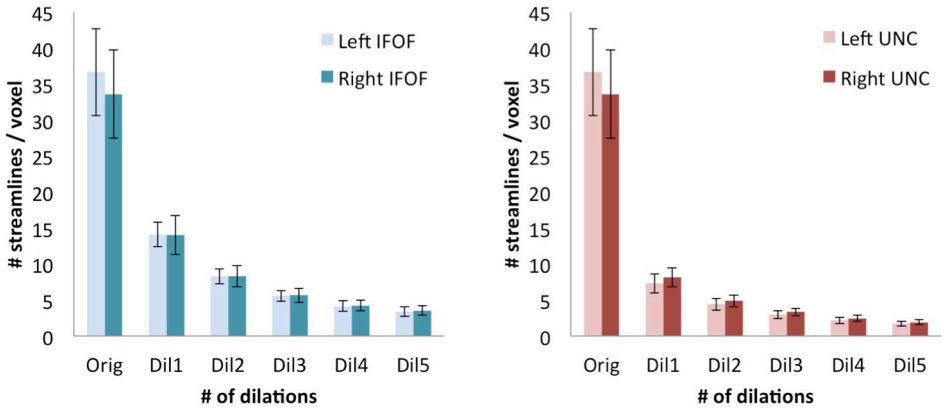

Figure 30. Density of streamlines with successive dilations of the stem for the IFOF (left) and UF (right) on DTI processed data (n = 30).

density decreased by more than 50% from the first dilation with less drastic decreases up to the fifth dilation (Figure 30). This supports the hypothesis of a stem as a dense bundle of streamlines.

We can generally identify the locations of tracts based on their stems with diffusion imaging, but can we segment the tracts based solely on their stems? We looked at the number of fibre orientation populations in the stem. If the stem hypothesis held, we would expect only single fibre orientations within the stem. While we observed this to be the case for many of the voxels in the stem, there were several voxels that had multiple fibre orientations. Figure 31 shows the left IFOF stem with the fODFs overlaid on a FA colour map in a typical subject. At the supero-medial part of the stem there are crossings with other tracts, which explains the voxels with multiple fibre orientation. But notice that inferiorly there are single orientation fODFs that appear very similar to those within the stem but belong to other tracts, most likely the UF that runs, in some of its segments, in a superior-inferior direction (purple coloured voxels). There appears thus to be no clear distinguishable boundary of the IFOF stem based on the fODFs. At the voxel resolution, it may be too coarse to dissociate the stem. But even if we could visualize every individual axon, defining a fibre tract may require more than knowing the orientation information contained within a single brain section. In other words, it may require knowing both the orientation at the stem and the trajectory of the fibres.

Finally, we were interested in how the streamlines extracted from the 1-fiber orientation, 2-fiber orientation etc. voxels within the stem differ. An example in a typical subject seeding from only the voxels in the stem that contained 1-4 fibre orientations is shown in Figure 32. As somewhat expected, the single fibre orientation streamlines are densely packed together (even at their terminations) and appear to resemble the core of the bundle. As it progresses in the number of fibre orientations the tracking results are more dispersed with more fanning (2-orientation) and are located at the peripheral limits of the bundle (3 and 4-orientations).

6.2 Comparison of tractography pipelines

The limitations of the DTI model were clearly apparent in our first attempts at mapping the structural connections of the fibre pathways. There were many streamlines that stopped prematurely within the deep white matter[2] (see Figure 19). These were implausible streamlines that do not exist on a real specimen. Qualitatively these streamlines resembled the valid (i.e., anatomically plausible) streamlines following a similar course from the stem however because

[2] We divided the streamlines into 3 categories: *whole* (streamlines connecting cortical regions anterior and posterior to the stem), *broken* (streamlines with only one end terminating in either of the frontal or posterior regions) and *lost* (streamlines that do not terminate in the cortical areas). The *broken* streamlines were also subdivided into anteriorly broken and posteriorly broken groups (see Figure 33).

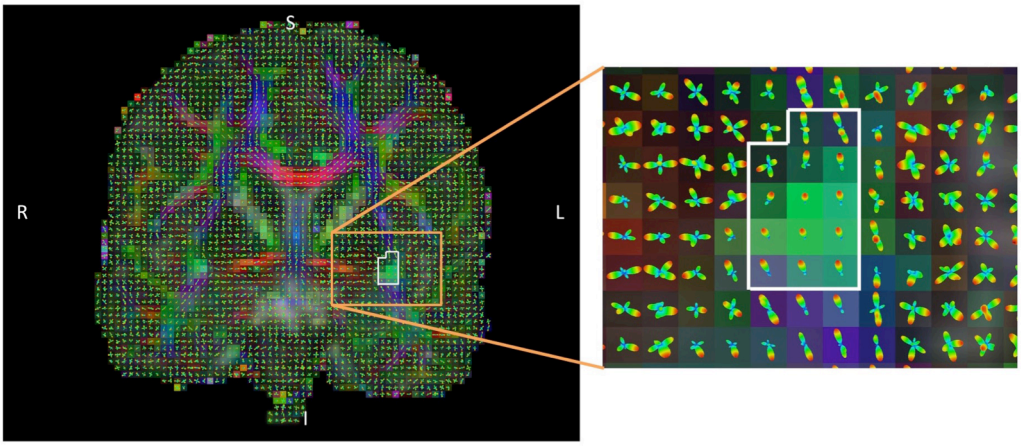

Figure 31. The IFOF stem (white outline) of a typical subject shown on a FA colour map (higher intensity indicates higher anisotropy) with the fODFs overlaid.

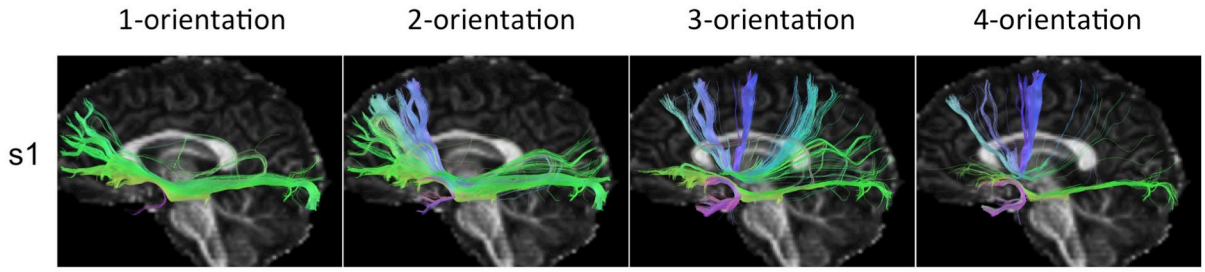

Figure 32. Results of tracking from seeding in voxels with 1-fiber up to 4-fiber orientations in the IFOF stem in a typical subject.

they fell short of the cortical region masks, they could not be considered in the analysis (see Figure 33). We thus concluded that DTI was not sufficient for performing analyses on tract connectivity, especially for region-to-region connections.

A few studies have addressed the problem of "broken" and "lost" streamlines. For example, Tractometer (Côté et al., 2013) is a tool that evaluates the performance of different tractography algorithms and processing pipelines using a ground truth phantom that mimics features of the white matter anatomy (e.g., short U-shaped fibres, commissural fibres, fanning and crossing fibre arrangements). They are evaluated based on a set of criteria including the percentage of true positives, false positives and average coverage of the "ground truth" bundles. The focus on improving tractography methods has been a hot topic in recent years and there are now many alternatives to the basic tensor and tracking methods (see reviews of Jbabdi & Johansen-Berg, 2011; Tournier et al., 2011). We sought to improve the quality of the tractography data using more advanced processing methods.

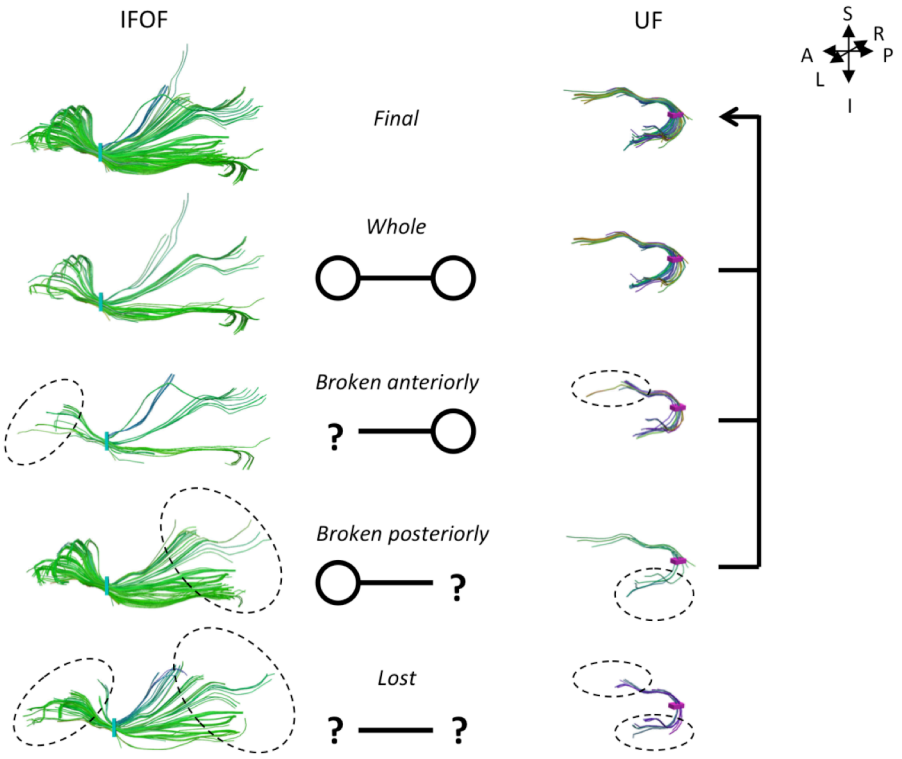

Figure 33. An example of the left IFOF and UF of a typical subject obtained using the stem-based method from the first study shown with their stems (first row). These final tracts do not include lost streamlines (that do not end in the cortex) and can be divided into whole (second row), broken (third and fourth rows) and lost (fifth row) streamlines. The dotted ovals indicate streamlines stopping prematurely before reaching the cortical template (see footnote 2 for definitions of whole, lost and broken).

6.2.1 Technical improvements in our tractography data

Our originally acquired BIL&GIN diffusion images were processed with a new pipeline using advanced tractography methods that enabled us to significantly improve the tractography data and build upon the results of the first study. The following key improvements were made:

- The use of a higher-order model (vs. the diffusion tensor) to estimate the local fibre orientations from the diffusion signal, such as constrained spherical deconvolution (CSD) (Descoteaux et al., 2009).
- A more sophisticated tractography algorithm than the FACT algorithm that incorporates anatomical constraints and backtracking into the tracking process (CMC+PFT) (Girard et al., 2014).
- Upsampling of the diffusion data from $2mm^3$ native resolution to $1mm^3$.
- Better seeding strategies that reduce biases in the tractography reconstruction (i.e., increasing the number of seeds and seeding from the grey-white matter ribbon)

These are summarized in Table 5. For more detail see Chapter 4.

We were interested in understanding how the differences in the tractography pipelines would influence the results on tract anatomy. Below we performed a brief comparison of the anatomical results for the IFOF and UF between the DTI- and new CSD-based pipelines.

Table 5. Summary of the improvements made in the tractography pipeline between the first and second studies.

	DTI	CSD
Local model	Tensor	fODF
Tracking algorithm	FACT deterministic	CMC and PFT deterministic
Image resolution	2x2x2 mm	1x1x1 mm
Seeding strategy	Brute-force seeding (1 per voxel)	Seeding in interface (10 per voxel)

6.2.2 Method

The comparison was based on 30 right-handed subjects (15 female, mean age = 26.3, age range = 22-34) sampled from the 60 subjects in the study. The IFOF and UF stems traced on the DTI tractograms of the 30 subjects were used to extract a second set of tracts from the CSD tractograms of the same subjects (see Chapter 4 for CSD processing methods). For both datasets we performed analyses on the tract terminations (i.e., their frequency and distribution) and tract properties (number of streamlines, volume and length) (Figure 34).

Since the CSD datasets were resampled to 1mm^3 resolution, the stems had to be resampled to match the resolution. As well, given that we used a more sophisticated tracking algorithm employing anatomical constraints (Girard et al., 2014), the Eve template was adapted to reflect these tracking constraints (see Chapter 4 for more on the adapted template). The adapted template, created in 1mm^3 diffusion space, was resampled to match the resolution of the DTI datasets. Except for the template, we followed the same method for the analysis of tract terminations as in the first study. We divided the streamlines into whole and broken categories and analyzed their terminations independently to see how they contribute to the termination results. Additionally, we calculated the difference in the frequency results between the final (i.e., whole and broken) and whole streamlines to better understand the contribution of broken tracts, as well as the difference between CSD and DTI tracts. In other words, how would the results look if we only considered whole streamlines. For simplicity, we compared only the regions found to be significant in the first study.

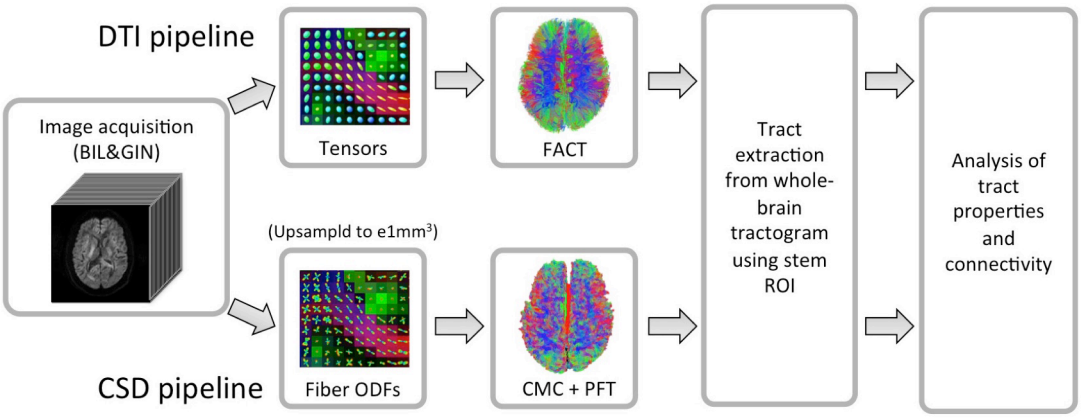

Figure 34. The comparison study involved processing the BIL&GIN data (left) with a DTI (upper row) and CSD (lower row) –based pipeline (see Chapter 4 for details), followed by a common protocol for tract extraction and tract analysis.

6.2.3 Results

Percentage of whole, broken and lost

We first evaluated each of the pipelines for their performance in studying tract connectivity (i.e., the percentage of whole cortico-cortical streamlines). The percentage of whole streamlines was considerably higher for the CSD pipieline (~80%) vs. DTI (<50%) for both tracts bilaterally (Figure 35). Note also that for the CSD pipeline these percentages are relatively stable across tracts whereas for the DTI pipeline the percentages are very different between tracts (reflecting length bias, see Chapter 4, Tractography). These results show that the CSD pipeline greatly improved the tracking results for tract connectivity analysis.

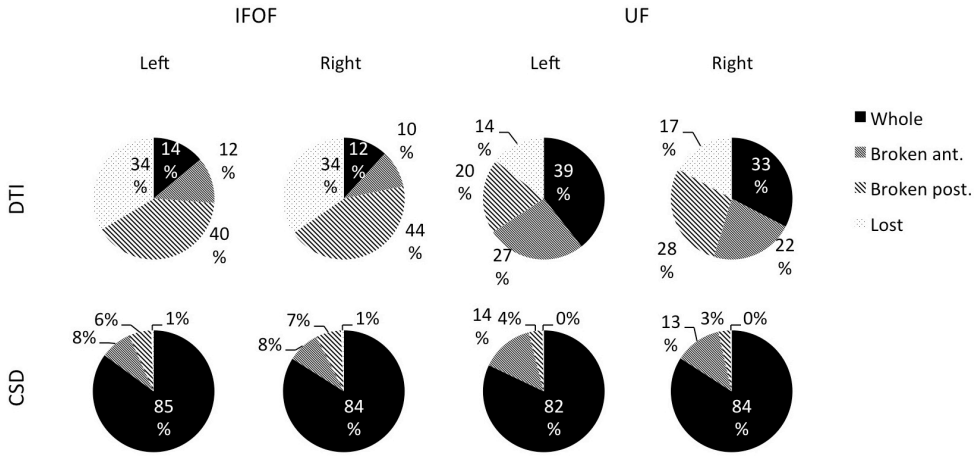

Figure 35. Percentage of valid (whole) and invalid (broken, lost) streamlines for the IFOF and UF obtained with DTI and CSD pipelines. Valid streamlines are defined as cortico-cortical streamlines while invalid streamlines have at least one end terminating in a non-cortical area (i.e., deep white matter).

General description of tracts

Figure 36 shows an example of the IFOF and UF in a single subject obtained with the DTI and CSD pipelines. Qualitatively, the CSD tracts appear denser, fuller and have a more extensive overage of the cortex than the DTI tracts. Quantitatively, the CSD tracts had a larger quantity of streamlines (14-19 times more for the both tracts bilaterally, $p < .0001$) and covered a larger area given by their much larger volume (2-3 times larger for both tracts bilaterally, $p < .0001$; see Table 6). The CSD tracts had a longer mean streamline length for the IFOF (mean difference = 27 and 24 mm for the left and right respectively, $p < .0001$) but was shorter for the UF (mean difference = -6 and -8 mm for the left and right respectively, $p < .0001$).

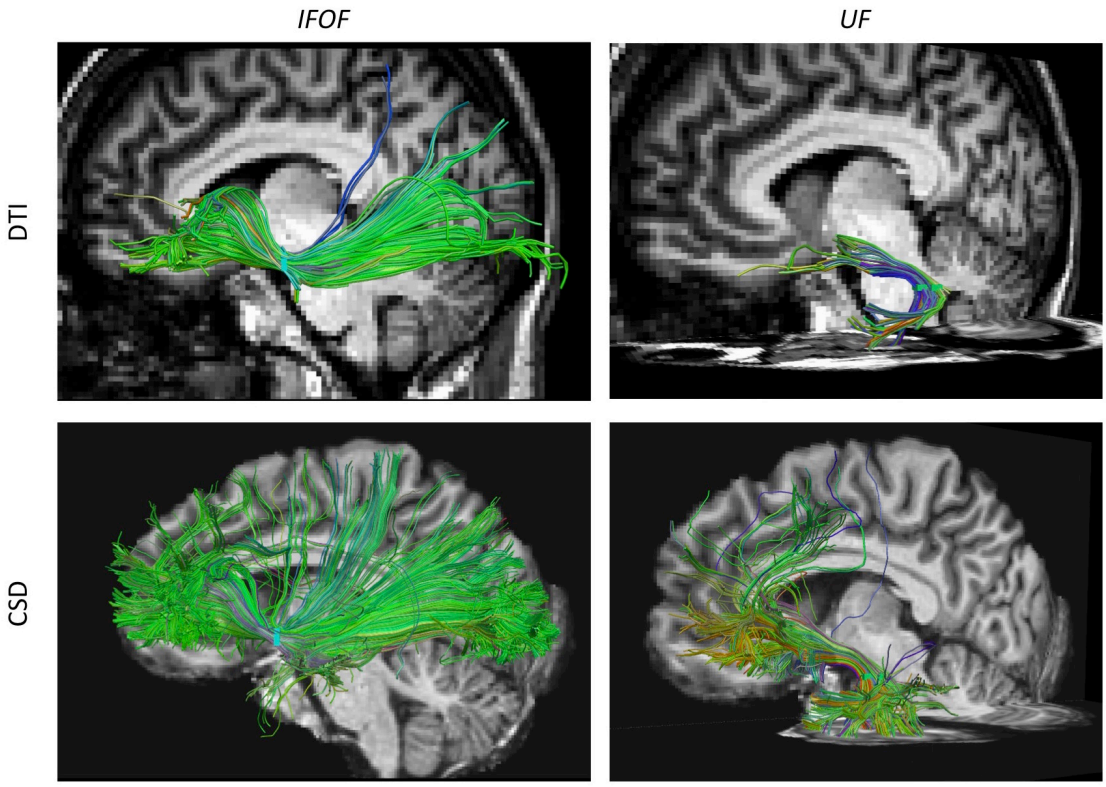

Figure 36. Example of the IFOF and UF obtained with the same stems extracted from the DTI and CSD-based pipelines in a single subject. The CSD tracts show only whole streamlines.

Table 6. Summary of mean tract properties for the IFOF and UF based on the DTI and CSD processing pipelines across 30 subjects.

	IFOF		UF	
	Left	Right	Left	Right
DTI				
# of streamlines	224 ± 70	285 ± 68	55 ± 25	129 ± 49
tract volume (mm^3)	13055 ± 3056	15093 ± 2595	2828 ± 1063	4550 ± 1488
mean length (mm)	113 ± 12	109 ± 14	61 ± 12	63 ± 9
CSD				
# of streamlines	3645 ± 1322	3877 ± 1225	1037 ± 493	2278 ± 841
tract volume (mm^3)	42997 ± 10772	42800 ± 7519	6967 ± 3480	9155 ± 3270
mean length (mm)	140 ± 9	133 ± 11	55 ± 13	55 ± 10

Frequency of tract terminations

The frequencies of tract terminations for the IFOF and UF for both pipelines are presented in Table 7. The contributions of the broken streamlines to the frequency results have a much larger impact on the DTI tracts than CSD with many regions showing higher frequencies (>10) than if we had only considered the whole streamlines (Table 7, in red). This is true for both tracts, but especially noticeable for the IFOF (in particular the superior and middle frontal and orbitofrontal regions). For the UF the right side is more affected by broken streamlines than the right.

We also assessed the differences in frequencies between the DTI and CSD tracts (Table 7, in red). There were many regions with much lower frequency in DTI compared with CSD for both tracts (Table 7, negative numbers in red). In particular, the superior frontal and fusiform gyri were less frequent in DTI compared with CSD for the IFOF, and the frequency across all of the temporal regions with the exception of the temporal pole was much lower in DTI vs. CSD for the UF. This is likely due to the more dominant inferior longitudinal fasciculus, which crosses the UF posteriorly limiting the DTI results.

Distribution of tract terminations

The distributions of terminations for the IFOF and UF are presented in Figure 37 and Figure 38, respectively. The distribution is relatively unchanged for the UF between DTI and CSD pipelines when taking into account the broken streamlines of DTI (Figure 38). For the IFOF, there were several changes including the distribution in the anterior regions being more evenly spread out across frontal areas for CSD, whereas DTI showed predominant terminations in IFG and LFOG relative to the other frontal areas (Figure 37). The posterior distribution was similar between CSD and DTI, but note that the normalized number of streamlines is generally much lower for DTI due it having more streamlines broken posteriorly. Posteriorly, there is likely some undersampling for DTI for the IFOF (note the asymmetry pattern of the cuneus and inferior occipital gyrus which are contradictory to both the CSD distributions and the findings from our first study, Figure 37).

6.2.4 Conclusion

We have performed a brief comparison of the anatomical results of the IFOF and UF obtained with DTI and CSD-based tractography pipelines processed from the same original diffusion images. The new CSD pipeline improves our ability to perform connectivity analysis on the tracts. It produced denser and more extensive tracts reaching more areas of the cortex, which is reflected in the frequencies of terminations for both tracts. There was less of an impact of pipelines on the termination distribution of the UF but there were clear differences for the IFOF between pipelines especially in the posterior regions, which can be explained by undersampling. These results show the limitations of DTI and highlight the advantages of our new tractography pipeline.

Table 7. Frequencies of IFOF (A) and UF (B) tract termination presence in cortical regions among the 30 subjects shown for DTI and CSD pipelines. The results for the whole and broken streamlines combined, the contribution of the broken streamlines (w+b)-w (in red) and the difference between DTI and CSD frequencies (in blue). A connection to a region was considered present if the normalized number of streamlines was >.01. The largest differences termination regions (>|10| for the IFOF and >|5| for the UF) are in bold and negative differences are shown in red.

A.		**Frontal**					**Occipital**				**Temporal**			**Parietal**	
		SFG	MFG	IFG	LFOG	MFOG	MOG	IOG	Cu	LG	STG	MTG	Fu	SPG	AG
DTI	IFOF left	14	26	30	29	25	24	16	13	18	27	21	8	16	7
	IFOF right	13	27	29	30	26	26	15	17	19	19	9	13	19	11
CSD	IFOF left	29	29	30	30	29	30	23	29	30	27	30	27	20	6
	IFOF right	30	30	28	30	30	30	30	23	30	25	29	29	25	10
DTI	IFOF(w+b)-IFOF(w) left	**13**	**13**	4	**15**	**15**	**12**	**10**	6	5	6	**11**	3	**10**	5
	IFOF(w+b)-IFOF(w) right	**10**	**10**	2	**10**	**20**	7	7	4	**10**	**11**	5	7	9	9
CSD	IFOF(w+b)-IFOF(w) left	0	3	2	0	0	0	4	2	1	**10**	2	**10**	**14**	4
	IFOF(w+b)-IFOF(w) right	1	4	2	0	1	0	3	8	0	**12**	1	4	6	8
	IFOF(DTI)-IFOF(CSD) left	**-15**	-3	0	-1	-4	-6	-7	**-16**	**-12**	0	-9	**-19**	-4	1
	IFOF(DTI)-IFOF(CSD) right	**-17**	-3	1	0	-4	-4	**-15**	-6	**-11**	-6	**-20**	**-16**	-6	1

B.		**Frontal**						**Temporal**				**Limbic**
		MFG	IFG	LFOG	MFOG	RG	T. pole	STG	MTG	ITG	Fu	ENT
DTI	UF left	5	12	25	27	7	30	10	1	2	2	0
	UF right	12	7	30	30	24	30	3	1	2	4	2
CSD	UF left	6	9	30	30	16	30	14	21	27	14	13
	UF right	4	2	29	30	30	30	16	21	30	21	26
DTI	UF(w+b)-UF(w) left	1	3	2	1	0	0	**5**	1	0	0	0
	UF(w+b)-UF(w) right	**7**	**6**	3	1	**8**	0	2	1	2	3	1
CSD	UF(w+b)-UF(w) left	0	1	0	0	0	0	3	2	3	2	2
	UF(w+b)-UF(w) right	0	0	0	0	0	0	2	1	1	0	1
	UF(DTI)-UF(CSD) left	-1	3	**-5**	-3	**-9**	0	-4	**-20**	**-25**	**-12**	**-13**
	UF(DTI)-UF(CSD) right	**8**	**5**	1	0	**-6**	0	**-13**	**-20**	**-28**	**-17**	**-24**

7 Revisiting the uncinate fasciculus, its subcomponents and asymmetries with stem-based tractography and microdissection validation

Summary

In this second study, we focussed on characterizing the connectional anatomy of the uncinate fasciculus (UF) and its subcomponents using the stem-based approach on constrained spherical deconvolution (CSD) and anatomically constrained particle-filtering (CMC-PFT) tractography in a group of 30 subjects. Surprisingly, we obtained striking results with the stem-based approach, observing consistently a UF that consists of not only its classic hook-shaped fibres but also straight horizontally oriented fibres. These have brought to the surface a century old debate regarding the posterior limit of the UF and its boundary with the IFOF (briefly discussed in Chapter 3). We discuss these results with respect to the current and classic literature. We also applied an automatic clustering method to subdivide the UF bundle. We revealed five subcomponents with distinctive connectivity profiles. These were validated with post-mortem fibre dissection. We also assessed their asymmetries and observed opposing lateralized patterns among the subcomponents. A leftward lateralized dorsal subcomponent corresponding to the recently described "extreme capsule fiber tract" and a rightward lateralized ventro-medial subcomponent corresponding to a subset of the classic hook-shaped fibres were observed. These findings reconcile the recent controversy surrounding the asymmetry of the UF and provide a resolution to the debate about the anatomical identity of the tract formerly known as the extreme capsule fiber tract. We discuss the importance of considering the UF as a multicomponent pathway.

7.1 Introduction

The recent literature has revealed that the definitions of many of the fibre pathways based on 19th century dissection studies are steeped in controversy and confusion (Türe et al., 1997; Schmahmann & Pandya, 2007; Forkel et al., 2012; Yeatman et al., 2014; Meola et al., 2015). Some of the debates are starting to resurface including the area of white matter passage known as the external and extreme capsules, which may have important implications for understanding language function (Axer et al., 2013; Bajada et al., 2015; Mars et al., 2015). In this study, we re-evaluate the uncinate fasciculus, one of the association pathways that passes through this area, whose anatomy has received little attention but has been of significant interest in clinical disorders such as psychopathy, Alzheimer's disease, schizophrenia and major depression (Price et al., 2008; Yasmin et al., 2008; Craig et al., 2009; Phan et al., 2009; Steffens et al., 2011; Hernando et al., 2015; Wong et al., 2015) and various brain functions/states including language processing, empathy and associative learning (Parker et al., 2005; Duffau et al., 2009; Papagno et al., 2011; Von Der Heide et al., 2013; Oishi et al., 2015; Thomas et al., 2015).

The definition of the UF has remained relatively uncontroversial. It was first described by J.C. Reil who named it ('Häkenbundel' in the original text), describing a pathway that:

> *... encircles the gap by which the frontal lobe is separated from the temporal lobe, and is constituted by the fan-like expansions of the central fibres of the gyri of the frontal and temporal lobes that aggregate from both sides in one stem* (p. 200, Reil, 1809, translation from Schmahmann & Pandya, 2006).

Karl Burdach expanded on Reil's description, observing fibres that curve laterally from the external capsule to the frontal lobe "*into its lateral areas as well as into the lateral portions of the basal areas*" (p.152, Burdach, 1822, translation from Schmahmann & Pandya, 2006), and gave it its current Latin name. Over the next two centuries most studies confirmed their descriptions, however, sporadic dissection studies on the UF, including recent ones, have noted significant difficulty (even impossibility) in dissociating the UF from its adjacent inferior fronto-occipital fasciculus (IFOF), both of which pass within the external and extreme capsules (Trolard, 1906; Villiger & Ludwig, 1940; Türe et al., 2000; Travers, 2008). Elucidation of this area is needed as the stems of both tracts lie adjacent here and there have been reports of some "merging" of the two bundles (Ebeling & Cramon, 1992; Kier et al., 2004). From their stems both tracts exhibit a double fan shape and their courses within the frontal lobe have been reported as highly intermingled with no distinct separation between them (Kier et al., 2004). Posteriorly, they are said to be distinguishable with the UF hooking around to the anterior part of the temporal lobe while the IFOF continues on a straight posterior course towards the posterior temporal and occipital areas (Kier et al., 2004; Martino et al., 2010). Indeed the question of whether the UF and IFOF should be considered as one continuous pathway or two discrete pathways was posed even a century ago (Trolard, 1906). The dissociation between the UF and IFOF remains to be clarified.

Additionally, there have been some descriptions that have contrasted with the UF's classic hook-like shape. Dejerine, who referenced Burdach's work 80 years later, described the UF as having not only the characteristic hook-shaped fibres but fibres that become straight and may even curve in the inverse direction (Dejerine & Dejerine-Klumpe, 1895). In the same vein, Gordinier (1899) described the UF as being composed of fibers originating from the anterior part of the superior and middle temporal gyri and projecting to the frontal lobe with external hook-shaped fibers owing to the proximity of the inferior frontal cortex and temporal pole, while the most internal fibers present a more horizontal course and radiate to the orbital part of the superior and inferior frontal gyri (Gordinier, 1999). Testut (1900) described an anterior part that forms a sharp curve into the temporal pole and a smaller posterior part that reaches the middle to posterior part of the temporal lobe (Testut, 1900). Both Gordinier and Testut proposed specific subcomponents of the UF whereas Dejerine did not make the differentiation. One relatively recent study (Ebeling & Cramon, 1992) proposed a ventral and dorsal subcomponent for the UF however the basis for its anatomical divisions is unclear as they

appear to be concluded from a survey of the literature. A division of the UF into subcomponents thus remains to be defined.

Diffusion imaging tractography has been applied to the anatomical study of white matter and has not only been able to resolve some of the debates surrounding fibre tract anatomy, such as the existence or inexistence of tracts and their termination territories (Catani et al., 2003; Forkel et al., 2012; Yeatman et al., 2014; Meola et al., 2015) but reveal previously undescribed tracts in humans (Catani et al., 2005; Makris et al., 2005; Oishi et al., 2008; Catani, Dell'acqua, et al., 2012). Today the UF is widely considered as an exclusively hook-shaped fascicle connecting the inferior, orbital and mesial frontal regions with the temporal pole despite the reported deviations from this description.

In the present study we aim to address the above questions by re-evaluating the anatomy of the UF in 30 subjects using diffusion imaging tractography with constrained spherical deconvolution (CSD) and tracking with particle-filtering and anatomical priors (CMC-PFT). CMC-PFT has shown to be able to address many of the current tractography biases of length/size/curvature by including knowledge of the anatomy from the T1-weighted image and tracking seeds placed at the WM/GM interface (Girard et al., 2014). Hence, streamlines produced by CMC-PFT tracking must end in the GM, cannot stop in WM or CSF, thus overcoming many limitations of current tractography algorithms. It has been able to reproduce to a good degree the detailed connections from tract tracing studies in monkeys (Schmahmann et al., 2007; Azadbakht et al., 2015).

The whole UF was extracted by applying an approach that minimizes *a priori* on the tract's course, based on the interactive delineation of the stem of the bundle from the whole-brain tractogram (Hau et al., under review). This approach is aimed to reproduce the definition of the fascicle introduced by the early dissectionists, who consequently delineated fiber tracts by identifying them at their stem before following the fibers to see where they terminate. We also for the first time applied a clustering approach to divide the UF bundle into subcomponents without any *a priori* on the number of subcomponents. Moreover studies on UF asymmetry have so far been inconclusive (Highley et al., 2002; Park et al., 2004; Rodrigo et al., 2007). We assessed the connectional anatomy and asymmetry of each subcomponent.

In order to validate the anatomical findings observed from tractography, we additionally performed post-mortem dissection of the UF in 4 specimens. A lateral to medial layer-by-layer approach was taken to reveal the specific connections in relation to their topographical organization (i.e., we present the connections first observed in the most superficial layer progressing to the deepest layer).

7.2 Methods

Image acquisition and tractography

The present study uses diffusion-weighted images of 30 healthy right-handed subjects left-lateralized for language (15 female, mean age = 26.3 years, age range = 22-34 years, years of education ≥ 15) that were previously acquired for the BIL&GIN database (details in Mazoyer et al., 2015). All subjects gave written consent to participate in the study, which was approved by the local ethics committee (CCPRB Basse-Normandie).

The diffusion-weighted images were processed using the MRtrix software package (http://www.brain.org.au/software/). First the diffusion tensor and fractional anisotropy (FA) maps were created. A single fibre response function was estimated from FA values above 0.7. The response function was used as input for constrained spherical deconvolution (CSD) (Tournier et al., 2007; Descoteaux et al., 2009) to compute the fibre orientation distribution functions (fODF), with a spherical harmonic order of 6. The processed datasets (fODF, FA, RGB maps) were upsampled to 1mm^3 spatial resolution using trilinear interpolation (Girard et al., 2014; Tournier et al., 2012). Fibre tracking was performed on the upsampled fODF maps using

an implementation of MRtrix's deterministic tractography algorithm developed by (Girard et al., 2014), creating a whole-brain tractogram (three-dimensional reconstruction of the white matter structure) for each subject. Girard et al.'s tracking algorithm is based on a continuous map criterion (CMC) to keep only the streamlines that terminate in the grey matter, based on the tissue partial volume estimation maps processed from the subject's T1 image. To create the tissue partial volume estimation maps, the T1 was first warped to the diffusion space using ANTS linear and non-linear registration (http://stnava.github.io/ANTs/, see Avants et al., 2011). The T1 was segmented into regions of grey matter, white matter and cerebrospinal fluid using FSL's (http://www.fmrib.ox.ac.uk/fsl/index.html) fast tool (Smith, 2002) and the partial volume (include and exclude, see Girard et al., 2014) maps were created based on these segmentations. In addition to optimizing the stopping criteria this method uses particle filtering (PFT), which applies a backtracking step to find alternative valid pathways to continue the tracking in order to reduce premature stopping in areas of low anisotropy. Seeding was initiated from the white/grey-matter interface with 10 seeds per voxel. A length threshold was set at a minimum of 10 and maximum of 250 mm. If not otherwise specified the default parameters were used.

Anatomical template and regions of interest

A modified version of the Johns Hopkins University Type I Eve template (Oishi et al., 2009) that includes the division of the temporal pole within the temporal lobe regions was used to automatically parcellate the brain into cortical regions (see Hau et al., under review). This template was adapted to the anatomical constraints used in the CMC-PFT tracking algorithm. This was done in order to increase the correspondence between streamline terminations and the template improving the track filtering results, and additionally optimizes the results for the connectivity analysis. The template was first warped from the standard space to the native diffusion space of each subject through linear and non-linear registration with ANTS. A subset of the template was created that included all of the grey matter regions (i.e., cortical and subcortical, including superficial white matter regions which were merged with their corresponding gyral region). The maps defining the anatomical constraints for tracking (interface, exclude map and include map, see Girard et al., 2014) were added together and binarized to create a termination hit mask. Finally, the values from the template subset (modally dilated three times) were attributed to the termination hit mask to create the adapted template. The steps for creating the adapted template are summarized in Figure 39. The parcellations from this adapted template were used as regions of interest (ROIs) to filter the streamlines and determine their termination regions for the connectivity analysis.

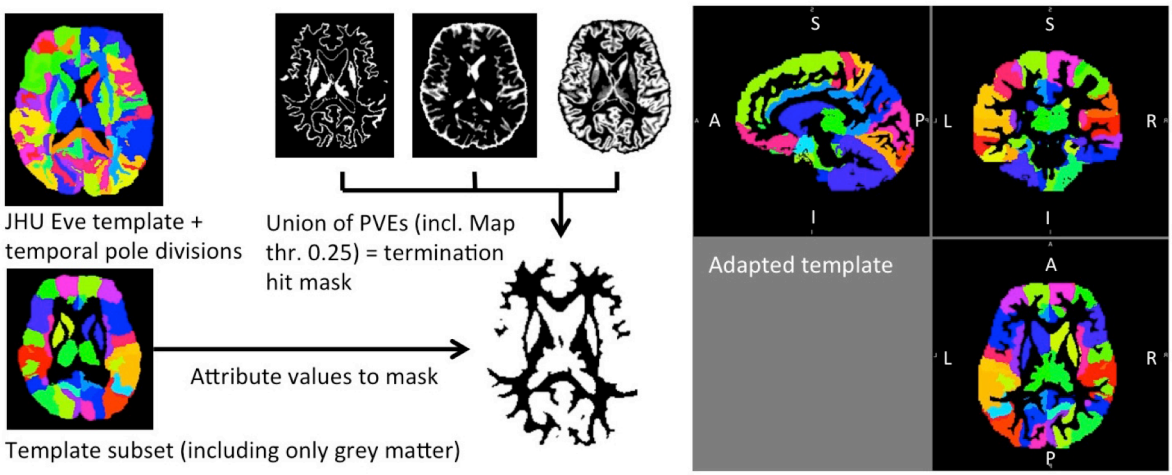

Figure 39. Steps to create the adapted template.

Stem-based anatomical virtual dissection of the UF

The UF was extracted by performing a stem-based anatomical virtual dissection in each hemisphere of the 30 whole-brain tractograms in the subject's diffusion space (Figure 40A). We first took into account only streamlines with one cortical termination in the frontal lobe and the other in the temporal, parietal, and occipital lobes, all lobes constituted with the modified JHU template (Figure 40B). The UF was easily identifiable as the compact bundle of streamlines with a characteristic hook-shaped trajectory connecting the frontal and temporal lobes (Figure 40C). A rectangular ROI was drawn on a single coronal section covering the entire stem with a margin of a few voxels and used to extract a set of candidate UF streamlines (Figure 40C, zoom). Note that only a small percentage of the streamlines were first visualized (10%) to reduce computational demands given the large size of the whole-brain tractograms. Once the ROI filter was applied all the streamlines were visualized to check that the UF stem included the entire bundle, or otherwise it was modified interactively (Figure 40D). We removed adjacent IFOF streamlines still passing through the UF stem by adjusting for each subject and hemisphere a coronal slice filter in a break separating UF from IFOF in their posterior temporal courses (Figure 40E). All remaining streamlines passing through the UF stem and connecting the frontal lobe with the temporal (or limbic) cortical areas were therefore considered as UF streamlines (Figure 40F). We finally applied an outlier removal algorithm (Côté et al., 2015) that used hierarchical QuickBundles clustering (Garyfallidis et al., 2012) to prune anatomical outlier streamlines (cut-off at 20%), namely streamlines 'flitting around' a direct UF projection with multiple curves and loops between their frontal and temporal terminations (Figure 40G). Visualization, streamline filtering and the manual delineation of the stem ROIs were performed with the software Trackvis (http://www.trackvis.org/).

To differentiate the stem-based UF from nearby tracts, we also delineated several tracts that project to the temporal lobe including the inferior longitudinal fasciculus (ILF), inferior fronto-occipital fasciculus (IFOF), middle longitudinal fasciculus (MdLF), anterior commissure (AC) and arcuate fasciculus (AF) (see Figure 41). The ILF and IFOF were segmented following the protocols from a well-known atlas (Catani & Thiebaut de Schotten, 2008). The AF, AC and MdLF were segmented using a two-ROI approach based on their recent descriptions (Catani & Thiebaut de Schotten, 2008; Maldonado et al., 2013; Goga & Türe, 2015).

Each UF stem was registered to MNI space using the inverse warp and affine matrices that were used to register the anatomical template to the diffusion space in order to report their mean stem volume and center of mass coordinates in each hemisphere.

Automatic segmentation of subcomponents

We used a clustering method to automatically classify the UF bundles into subcomponents. A twelve-dimensional Gaussian mixture model was trained to encode the joint distribution of the locations and orientations of the pairs of streamline endpoints (two locations + two directions in three-dimensional space) with the expectation maximization algorithm (Dempster et al., 1976). Each ending orientation was measured between the endpoint and the point located at 10% from it with respect to the total length. Each Gaussian of the model represents the distribution of endpoints in one cluster that can be visualized with a pair of ellipses (see Figure 42). The number of clusters was automatically selected based on the Bayesian Information Criterion (Schwarz, 1978). Clusters with less than 25 streamlines were discarded and the streamlines in these groups were reassigned to the remaining clusters. All streamlines were classed and a streamline could only be assigned to one cluster.

Clustering was performed on the entire set of UF streamlines across all subjects and hemispheres. The UFs were transformed to MNI space using tract registration tools in tract_math (Wassermann et al., 2013) and merged in their respective hemispheres. The right UF dataset was flipped on the x-axis and combined with the left UF dataset to create the full UF dataset. Once the clusters were finalized on the full dataset, they were applied to the merged

datasets of each hemisphere, re-flipping on the x-axis for the right hemisphere. The subcomponents were attributed to each subject in their native diffusion space.

As the solution of such clustering depends on the choice of an initialization, we ran the

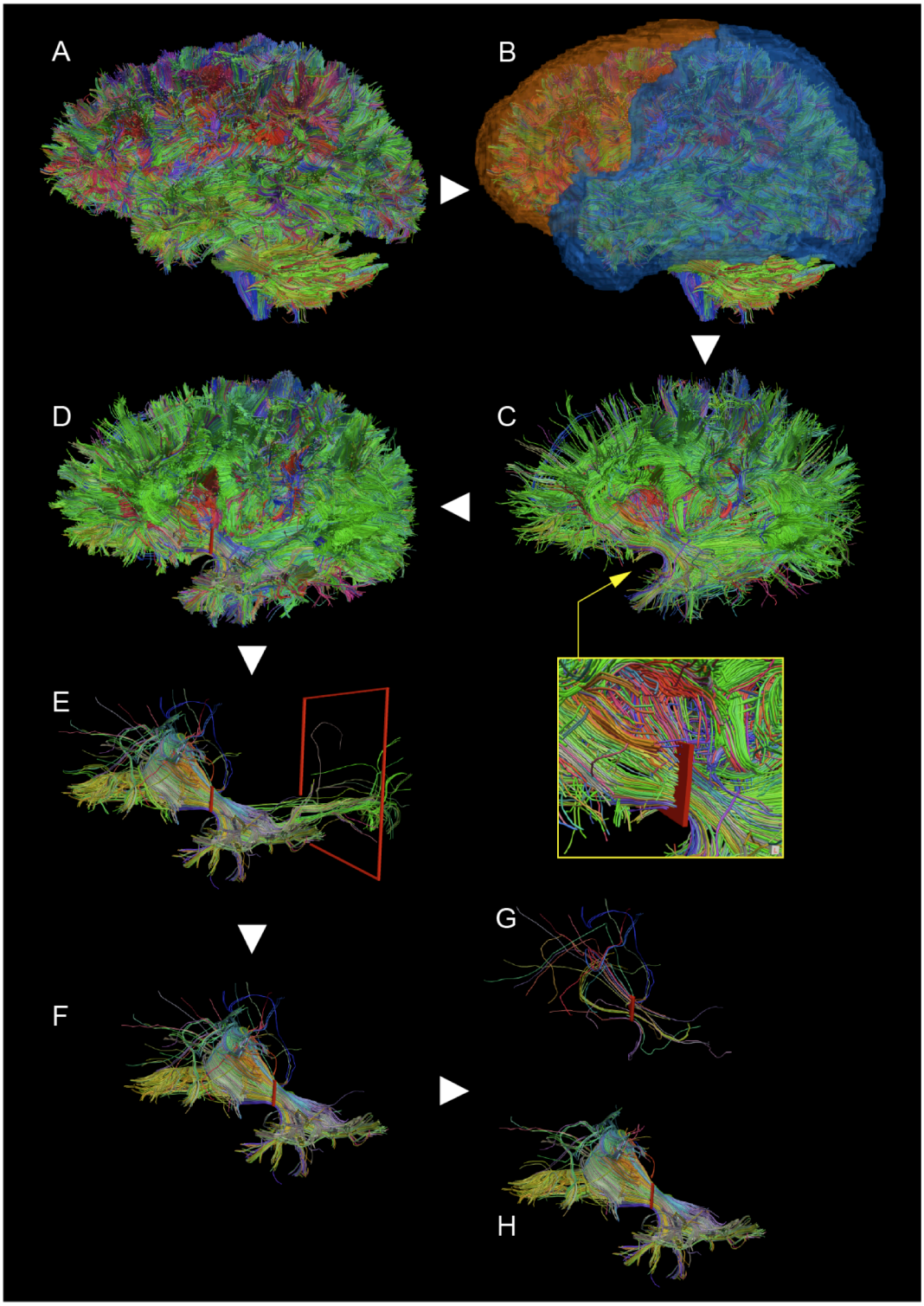

Figure 40. Anatomical stem-based virtual dissection of UF. **A.** View of 10% of the left intra-hemispheric streamlines of a single whole-brain tractogram; **B to C.** View of 10% of the streamlines with one termination in the frontal lobe (in orange) and the other either in the temporal, cingulate, parietal or occipital lobes (in blue); **C (zoom in).** Initial rectangular ROI (in red) drawn at the level of the hook-shaped streamlines (yellow arrow); **D.** View of 100% of the streamlines once the UF stem size adjusted (in red); **E.** All the streamlines passing through the UF stem are exposed. An additional coronal slice filter (red frame) was used to remove the remaining IFOF streamlines. **F.** Application of the outlier removal algorithm to prune outlier streamlines (**G**) and provide the final UF bundle (**H**).

clustering three additional times with random initialization. To assess the reliability of the clusters between runs, we calculated Jaccard indexes to determine the degree of overlap between the subcomponents obtained in the first run and those in the additional runs. The Jaccard index measures similarity between finite sample sets, and is defined as the size of the intersection divided by the size of the union of the sample sets.

Analysis of subcomponents

We first assessed the frequency of presence of each subcomponent across the group. A subcomponent was considered to be present in a subject's hemisphere if it passed a threshold of 2% of the total number of UF streamlines extracted in this hemisphere. We therefore computed the number of streamlines, voxel-based volume and mean streamlines length to assess these properties for each subcomponent.

A key advantage of tractography is the ability to automatically and systematically identify the terminations of the virtually reconstructed fibres. This was done in the subject's diffusion space. Using the adapted anatomical template to register the streamline terminations, the number of streamlines connecting each pair of regions can be tallied to provide a measure of tract density (also called "connection probability"). A streamline score, that normalized the number of streamlines by the left and right hemispheres and was adjusted to account for biases in the tracking distance, was calculated as follows:

$$\text{Streamline score} = \frac{\text{\# of streamlines}}{\text{\# of left and right tract streamlines}} \text{x Mean streamline length.}$$

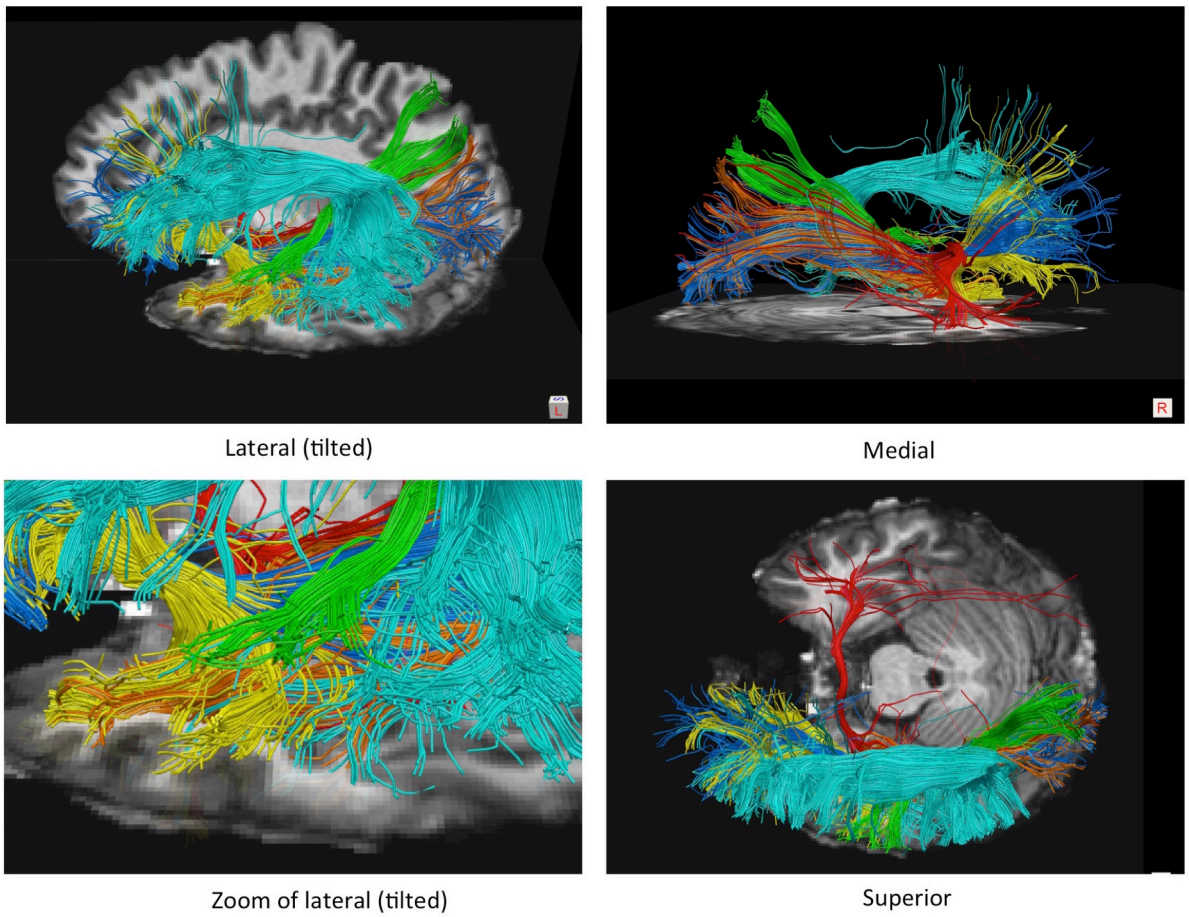

Figure 41. The UF bundle (yellow) is shown with neighbouring tracts that terminate in the temporal lobe including the ILF (orange), IFOF (blue), AF (cyan), MdLF (green) and AC (red) from different views in a typical subject. Note the intermingling of the posterior part of the UF with the ILF.

The tallies were obtained using the UCLA Multimodal Connectivity Software Package (http://ccn.ucla.edu/wiki/index.php, Brown et al., 2012).

First we determined if a connection between a pair of regions was significant across the group for the UF bundle. We tested the normalized number of streamlines for each pair of regions using the Wilcoxon Signed-Rank test with the null hypothesis of 0 (Bonferroni-corrected, $p < 0.05$). Only the connections that were significant in the UF bundle were retained. The distribution of paired connections in each subcomponent was investigated by calculating a mean streamline score only on the subjects in whom the subcomponent was present.

To assess laterality effects for the number of streamlines and volume, asymmetry indexes were calculated on each measure using the following formula: $\frac{\text{Right}-\text{Left}}{\text{Right}+\text{Left}}$. Two-tailed t-tests were used to test for asymmetry with a null hypothesis of 0 using the Bonferroni correction ($p < 0.05$). Least squares effects of age, gender and head circumference were also tested.

To understand the relative organization of the subcomponents, we obtained the mean and individual center of mass coordinates of each subcomponent at the stem. We binarized the subcomponents to create a volume and then extracted the intersection between the stem and the subcomponent in the subject's diffusion space. The intersections were registered to MNI space using the same registration process was done for the stems and their centers of mass were calculated. Repeated measures ANOVA tests were used to assess global differences in the center of mass locations across subcomponents. If significant, these were followed by two-tailed t-tests to assess differences in the x, y and z coordinates of each subcomponent with respect to their closest subcomponent.

Post-mortem dissection of UF

Four left hemispheres were treated with 10% formalin, according to a modified preparation of Klingler's technique, as previously described (Sarubbo et al., 2015). Blunt microdissection (x 5) was performed with wooden spatulas, according to Klingler's cortex sparing techniques, as previously described (Sarubbo et al., 2013; Sarubbo et al., 2015). In the first step we removed the cortices of the frontal lobe and of the anterior two-thirds of the temporal lobe. In the second step the short U-fibers of the frontal and temporal regions were removed. Then we proceeded to remove the gray matter of the long and short gyri of the insula. Finally, after localization of the frontal and temporal opercula we removed the WM of the extreme capsule and claustrum, demonstrating the stem of UF within the most ventral third of the external capsule (EC), at the level of limen insulae.

In all the specimens the dissection and data collection started at the *limen insulae* where we followed the arching fibers of UF (layer by layer) up to the terminal sites, collecting the reciprocal connectivity between frontal and temporal cortices. Distinction between UF and IFOF stems were performed considering the hook-shaped and posterior course of the fibers composing these.

7.2.1 Results

The stem-based uncinate fasciculus (UF)

The UF streamlines were observed in all 30 subjects bilaterally, represented as a dense, compact and coherent bundle connecting the frontal and temporal lobes. The dissociation between the UF and IFOF based on their posterior courses in the temporal lobe was clearly observed in 57 out of 60 hemispheres. In the 3 exceptional cases the posterior terminations of the two tracts within the temporal lobe appeared to be continuous and the coronal filter was placed based on a best guess. In all cases the coronal slice filter was effective in isolating the UF streamlines from the adjacent IFOF streamlines which were present at the supero-medial edge

Table 8. **A**. Mean ± standard deviation of the center of mass of the drawn UF stems in MNI space. **B.** Mean ± standard deviation of the location of each subcomponent within the UF stem.

A.	**Left hemisphere**			**Right hemisphere**		
	x	**y**	**z**	**x**	**y**	**z**
UF stem	-30 ± 2	2 ± 3	-10 ± 1	29 ± 2	5 ± 3	-10 ± 1
B.						
Dorso-lateral UF	-31 ± 1	2 ± 3	-9 ± 1	30 ± 1	5 ± 3	-9 ± 2
Ventro-lateral UF	-29 ± 2	2 ± 3	-11 ± 1	29 ± 1	5 ± 3	-10 ± 1
Ventro-medial UF	-30 ± 2	2 ± 3	-12 ± 1	29 ± 1	5 ± 3	-11 ± 1
Postero-medial UF	-29 ± 2	1 ± 3	-13 ± 1	29 ± 2	5 ± 3	-12 ± 1
Antero-medial UF	-28 ± 2	2 ± 3	-12 ± 1	28 ± 3	5 ± 3	-10 ± 1

of the UF stem (Figure 40E). The mean coronal filter in MNI space was located at -43 ± 12 mm and -40 ± 13 mm from the vertical plane passing through the anterior commissure in the left and right hemispheres, respectively.

The mean UF stem volumes (in mm^3) in the left and right hemispheres were 57 ± 14 and 63 ± 26, respectively. The mean center of mass coordinates of the left and right UF stems were symmetrically situated between the posterior part of the putamen and the claustrum (Table 8A).

The stem-based UF bundle could be differentiated from other fibre tracts that project to the temporal lobe including the IFOF, ILF, AF, MdLF and AC. This was confirmed in three subjects and shown in a typical subject in Figure 41. The IFOF runs medially and superiorly adjacent to the UF at the stem and follows a straight posterior course in the temporal lobe. The AF is located much more laterally to the UF with its posterior course overlapping minimally with the most posterior UF streamlines. The AC lies medial to the UF and does not interfere with the UF course. The MdLF terminations occupy the space slightly superior to the UF within the middle portion of the temporal lobe. The ILF runs within the white matter of the temporal lobe and intersects considerably with the middle and posterior UF streamlines at the middle portion of the temporal lobe.

Subcomponents of the UF

Five subcomponents were consistently identified across four runs of the automatic clustering method. The relative difference in the Gaussin mixture model parameters from run to run did not impact the clustering results. Indeed, the mean Jaccard index for the initial run with respect to the three additional runs was 1 for all subcomponents indicating that the clustering produced identical segmentation results across the four runs. The pairs of terminations obtained for each cluster on the full dataset are represented as ellipses in Figure 42, encoding the distinct locations of the paired termination groupings. In order to get a better interpretation of all such clusters in terms of trajectory we also computed the average and covariance of streamlines in each cluster and represented both statistics as a three-dimensional tube, see Figure 42. Each of the five subcomponents had a distinctive structural pattern of their trajectory and connections (Figure 43). Figure 43 also shows an example of each subcomponent in the left and right hemispheres for the group, subsampled to show 5% of the streamlines from all subjects. The frequency of presence across the group for each subcomponent was generally high (ranging from 19-30 out of 30 subjects bilaterally). The frequencies and mean number of streamlines, volume and mean length of each subcomponent are summarized in Table 9. Significant asymmetries were observed in the individual subcomponents, although not always in the same direction (Table 10). Below, we describe the region-to-region connections, frequencies and asymmetries of each subcomponent. They have been named on the basis of their anatomical definition and location within the UF stem.

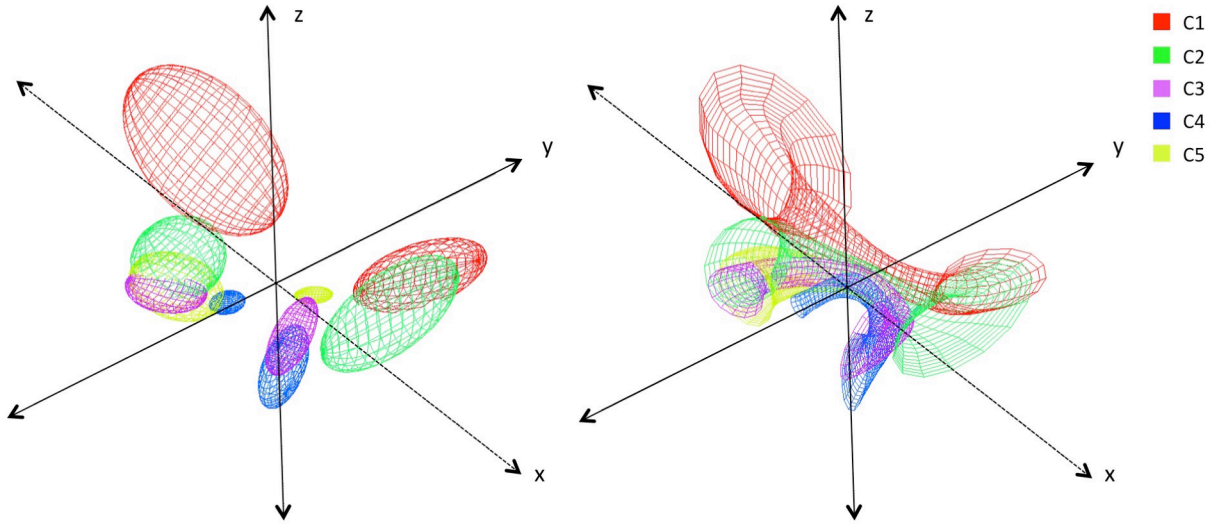

Figure 42. Visualization of the clusters in three-dimensional space obtained from the entire dataset (n=30). On the left, each pair of ellipses (with matching colours) corresponds to a cluster, representing the locations of their termination groupings. On the right, the clusters are represented as tube renderings showing the course and terminations of each cluster group.

Class 1 grouped large fan-shaped streamlines in a *dorso-lateral UF subcomponent* connecting the superior (SFG), middle (MFG) and inferior (IFG) frontal areas with the superior (STG), middle (MTG) and inferior (ITG) temporal gyri and in a less extent the temporal pole (Figure 3-C1 and 4-C1). Both SFG and IFG to MTG connections appear to be the most predominant. It was more frequently present in the left (27 subjects) than right hemisphere (19 subjects). Its volume was left lateralized ($p < 0.01$), due to more frequent streamlines terminating in the dorsal part of the SFG (Figure 3-C1) and, although there was a left lateralized trend for the number of streamlines (AI=-0.24), this did not reach the Bonferroni-corrected level of significance ($p = 0.03$), controlling for age, gender and brain volume.

Class 2 grouped horizontal fan-shaped streamlines in a *ventro-lateral UF subcomponent* mainly connecting the orbito-frontal regions with the MTG and ITG and temporal pole (Figure 3-C2 and 4-C2). It was present in all subjects bilaterally, with no significant asymmetry.

Class 3 grouped hook-shaped streamlines in a *ventro-medial UF subcomponent* connecting the orbito-frontal regions with the temporal pole (Figure 3-C3 and 4-C3). The medial orbito-frontal to temporal pole connections are the most predominant. It was present in 26 subjects in the left hemisphere and in all subjects in the right hemisphere, and a right lateralized asymmetry for the number of streamlines ($p < 0.001$) and volume ($p < 0.001$), controlling for age, gender and brain volume.

Class 4 grouped short hook-shaped streamlines in a *short postero-medial UF subcomponent* that connects the posterior part of the orbito-frontal and rectus gyri with the temporal pole and fusiform gyrus (Figure 3-C4 and 4-C4). The medial fronto-orbital to temporal pole connections are the most predominant. It was present in almost all subjects bilaterally (29 and 28 in the left and right hemispheres, respectively) with no significant asymmetry.

Class 5 grouped short straight streamlines in a *short antero-medial UF subcomponent* that connects the orbito-frontal and rectus gyri with the most antero-medial part of the STG and ITG temporal gyri (Figure 3-C5 and 4-C5). The most predominant connections are between the medial orbito-frontal and inferior temporal gyri. It was present in all subjects in the left hemisphere and in 24 subjects in the right hemisphere, and showed a right lateralized asymmetry for volume ($p=0.004$) only, controlling for age, gender and brain volume.

Table 9. UF subcomponents properties. Frequency is determined as the number of subjects with a number of subcomponent streamlines exceeding the threshold of 2% of the UF streamlines. Number, volume (cm3) and length (mm) of streamlines are expressed as the mean ± standard deviation with this number of subjects.

	C1		C2		C3		C4		C5	
	L	R	L	R	L	R	L	R	L	R
Freq.	27 (90%)	19 (63%)	30 (100%)	30 (100%)	26 (87%)	30 (100%)	29 (97%)	28 (93%)	30 (100%)	24 (80%)
Number	276 ± 200	122 ± 147	593 ± 296	729 ± 453	256 ± 231	575 ± 362	273 ± 169	358 ± 285	191 ± 111	205 ± 201
Volume	6.6 ± 3.7	3.6 ± 2.8	7.3 ± 2.1	8.4 ± 2.6	2.4 ± 1.3	3.8 ± 1.4	1.4 ± 0.6	1.6 ± 0.7	1.3 ± 0.7	1.8 ± 1.2
Length	100.8 ± 8.5	96.4 ± 12.6	81.6 ± 8.5	81.1 ± 8.4	70.1 ± 16.0	72.6 ± 6.5	47.7 ± 5.5	40.1 ± 9.2	31.2 ±10.6	46.1 ± 10.2

Table 10. Mean asymmetry indexes of the number of streamlines and volume for the UF subcomponents.
Significant asymmetries are notated with an asterisk.

n=30	C1	C2	C3	C4	C5
# streamlines AI	-0.24	0.06	0.32*	0.10	0.00
Tract volume AI	-0.19*	0.07	0.19*	0.04	0.17*

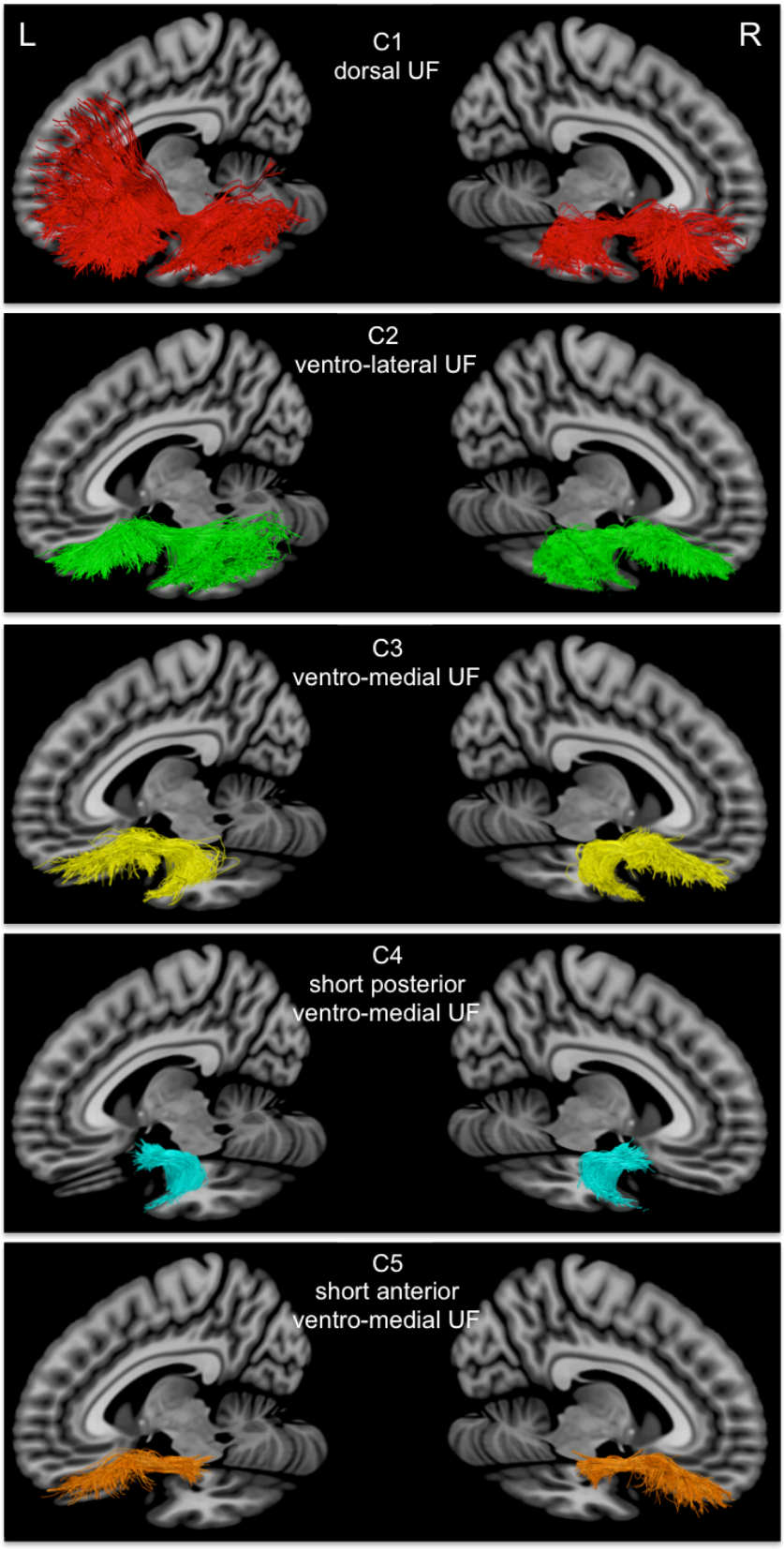

Figure 43. The five UF subcomponents, subsampled at 20% of the total of streamlines for each cluster on the group data for visual display.

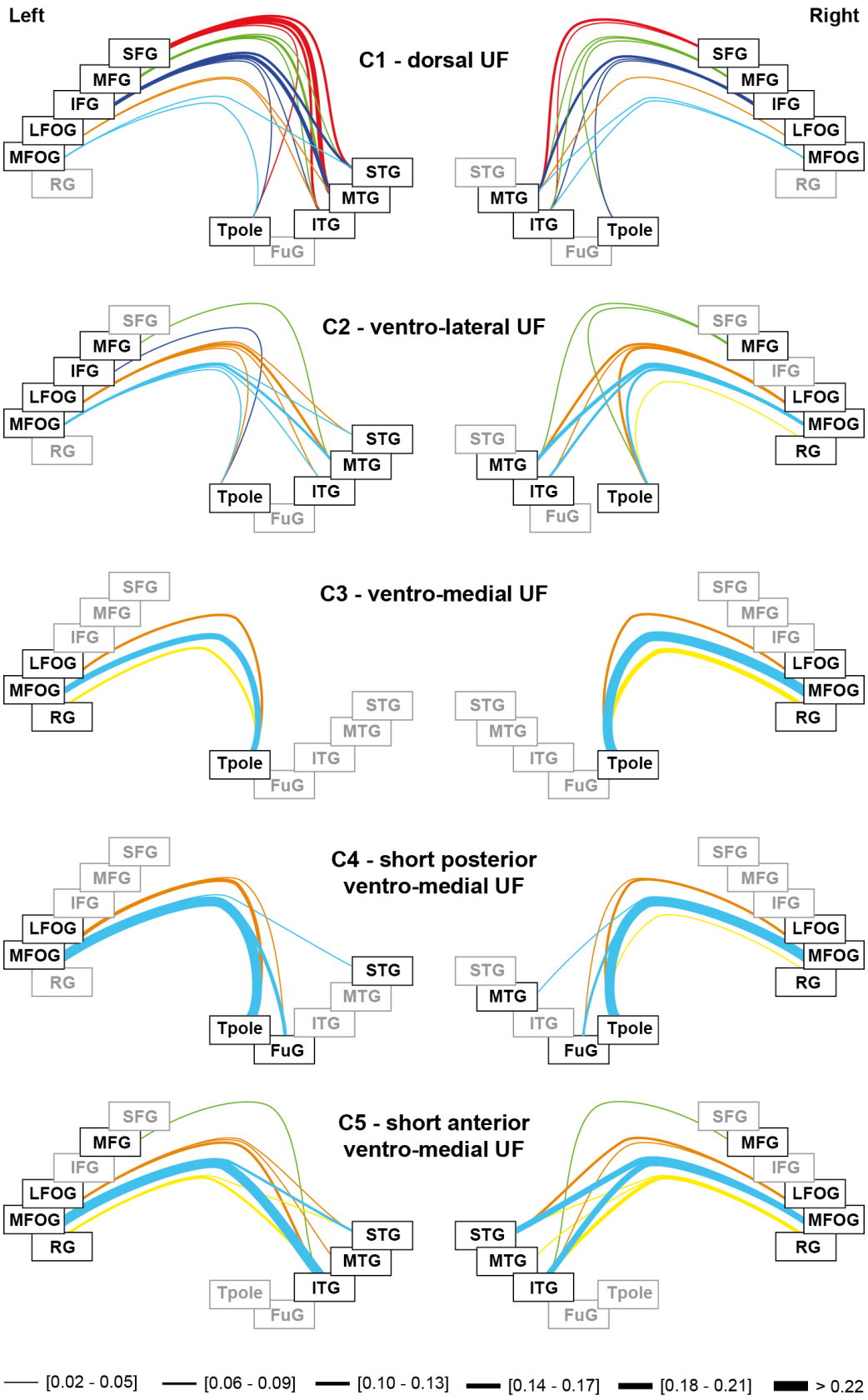

Figure 44. Mean connectional anatomies of each subcomponent. The lines thickness is proportional to the mean normalized number of streamlines connecting a pair of regions. The lines color helps to distinguish the lines from the different frontal regions. SFG (red), MFG (green), IFG (blue): superior, middle and inferior frontal gyri; LFOG (orange), MFOG (light blue): lateral and medial fronto-orbital gyri; RG (yellow): rectus gyrus; STG, MTG, ITG: superior, middle and inferior temporal gyri; Tpole: temporal pole; FuG: fusiform gyrus.

Cortex-sparing UF fiber dissection

Note first that all the sites of UF terminations reported were systematically observed in the 4 specimens dissected. Each UF dissection started from its classical anatomical definition by exposing fibers arching around the anterior and ventral third of the external and extreme capsules and connecting the temporal and frontal lobe. After the removal of the insula and claustro-opercular fibers, we proceeded from the most superficial to the deepest layers of fibers passing through the UF stem (Figure 45).

We first exposed the most superficial and lateral layer of UF fibers that closely arch around the frontal and temporal opercula. They connect the *pars opercularis* and *triangularis* of IFG with the middle third of STG and the anterior third of MTG, respectively, and the *pars orbitalis* of IFG and the basal fronto-orbital cortex with the antero-lateral portion of the temporal pole (Figure 45A).

A second deeper layer of fibers with a larger fan-shaped course was demonstrated to connect a large portion of the fronto-lateral cortices with the lateral convexity of the temporal cortex and the temporal pole (Figure 45B). We found reciprocal connectivity between: the middle third of STG and middle/anterior third of MTG with, respectively, the posterior third of SFG and MFG and the anterior third of the MFG; the antero-lateral portion of the temporal pole with the dorsal portion of the anterior third of IFG. Fibers of this subcomponent cover the most superficial portion of the IFOF stem (Figure 45B).

At this level, the orientation and the location of fibers within the UF stem changed. The fibers of a third layer of the UF all appeared to be positioned antero-medially with respect to the IFOF stem. These fibers have a shorter, more anterior and arched course. We found a common pattern of connectivity between the lateral temporal pole and the lateral fronto-orbital cortices and between the anterior portion of the temporal pole and the frontal pole (Figure 45C-45D). The deepest UF fibers have the shortest and the most medial trajectory. Considering their different course, orientation and terminations they can be divided in a fourth and fifth layer connecting respectively (Figure 45D), the antero-medial cortices of the temporal pole with the basal fronto-orbital cortices and the medial portion of the temporal pole with the medial orbito-frontal cortex and gyrus rectus.

Note that given the considerable overlap between the different UF subcomponents, one could not expect to dissect each UF subcomponent separately. But, as illustrated in Figure 46, extracting the streamlines of the different UF subcomponents from their most superficial to deepest positions allows us to relate them to the dissection results. The most superficial streamlines terminating in IFG and belonging to the dorso-lateral UF subcomponent (Figure 46A) correspond to the most superficial lateral dissected fibers (Figure 45A). Once removed, it exposed the large fan-shaped streamlines belonging to the dorso-lateral UF subcomponent (Figure 46B) and the horizontal fan-shaped streamlines of the ventro-lateral UF subcomponent (Figure 46C), also observed in dissection in Figure 45B. Continuing deeper after removing both dorso-lateral and ventro-lateral UF streamlines (Figure 46D) revealed the hook-shaped streamlines corresponding to the change in the orientation and the location of fibers observed during dissection. The most medial UF streamlines of the short antero-medial and postero-medial UF subcomponents corresponded to the deepest and shortest dissected UF fibers (Figure 46E to 46G).

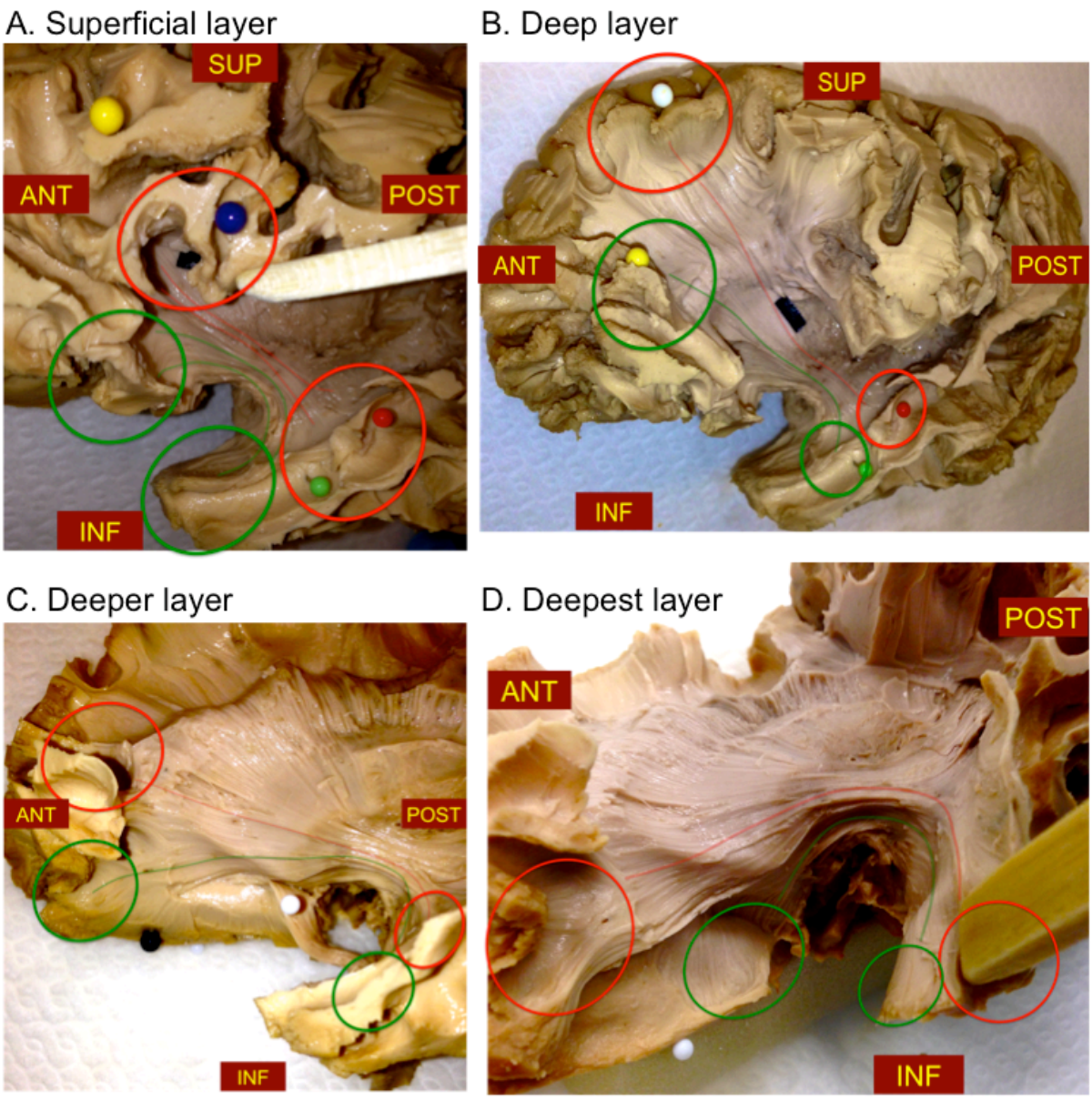

Figure 45. **A.** View of the fronto-temporal opercular region with the exposed UF stem exposing the fibers (red lines) connecting the middle third STG and anterior third of MTG (inferior red circle) with the pars opercularis and triangularis of IFG (superior red circle); the fibers (green lines) connecting pars orbitalis and basal fronto-orbital cortex (inferior green circle) with the basal fronto-orbital cortex (superior green circle). **B.** Complete view of a left hemisphere with the fibers of the second layer. The posterior portion (red line) connect the middle third of STG and middle/anterior third of MTG (inferior red circle) with the posterior third of SFG and MFG (superior red circle). The anterior portion (green line) connects the antero-lateral portion of the temporal pole (inferior green circle) with the dorsal portion of the anterior third of IFG (superior green circle). **C.** Detail of the anterior temporal and frontal cortices to demonstrate the fibers connecting: the lateral temporal pole (inferior red circle) with the lateral fronto-orbital cortices (superior red circle); the anterior temporal pole (inferior green circle) with the latero-fronto orbital cortices (superior green circle). **D.** Detail of the anterior portion of the frontal and temporal poles showing the deepest layers. The red line follows the course of the most lateral fibers connecting the antero-medial temporal pole (inferior red circle) with the basal fronto-orbital cortices (superior red circle). The green line highlights the course of the deepest short UF fibers connecting the medial temporal pole (inferior green circle) with the medial orbito-frontal cortex and gyrus rectus (superior green circle).

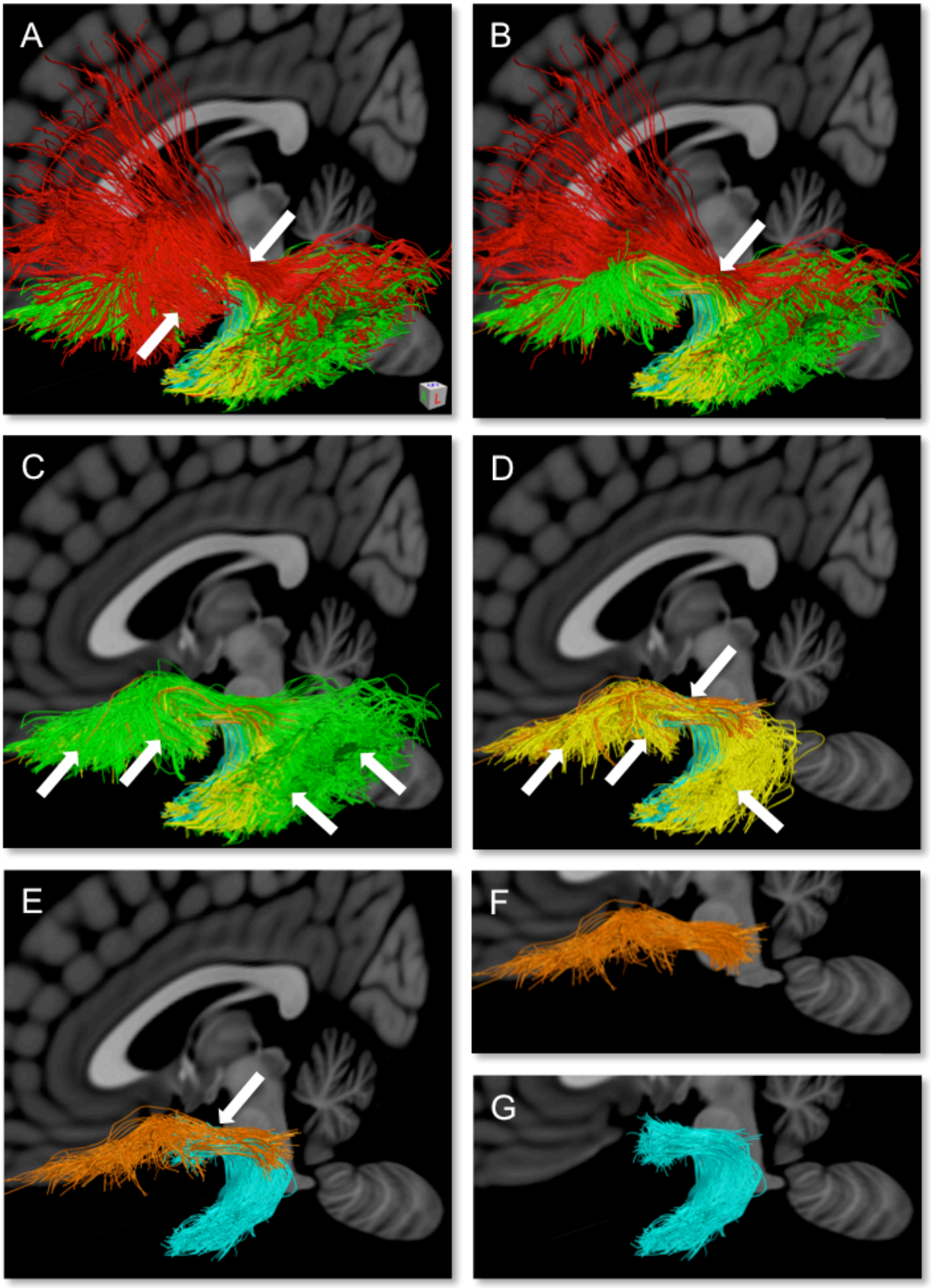

Figure 46. Latero-medial organization of the five UF subcomponents for the left hemisphere, subsampled at 20% of the total of streamlines for each cluster on the group data (see text for details).

Location of subcomponents within the UF stem

The mean and individual center of mass coordinates of the subcomponents within the stem are shown in MNI space (Figure 47). They are situated at the ventral portion of the external and extreme capsule complex. Even with the large overlap between the subcomponents when looking at individuals, there is a clear topological organization of the subcomponents. Within the stem, the dorso-lateral UF subcomponent is located the most superiorly and laterally (C1 vs. C2 x-coordinate: $p < 0.0001$ and $p = 0.027$ in the left and right hemispheres, respectively, and z-coordinate: $p < 0.0001$ bilaterally). The ventro-lateral, ventro-medial and short postero-medial UF subcomponents are arranged in a supero-inferior manner (see coronal slice, C2 vs. C3 z-coordinate: $p < 0.0001$ bilaterally, C3 vs. C4 z-coordinate: $p < 0.0001$ bilaterally) and the short antero-medial UF subcomponent is situated the most medially (C5 vs. C4 x-coordinate: $p = 0.0017$ and 0.0002 in the left and right hemispheres, respectively). The mean coordinates of each UF subcomponent within the UF stem are given in Table 8B.

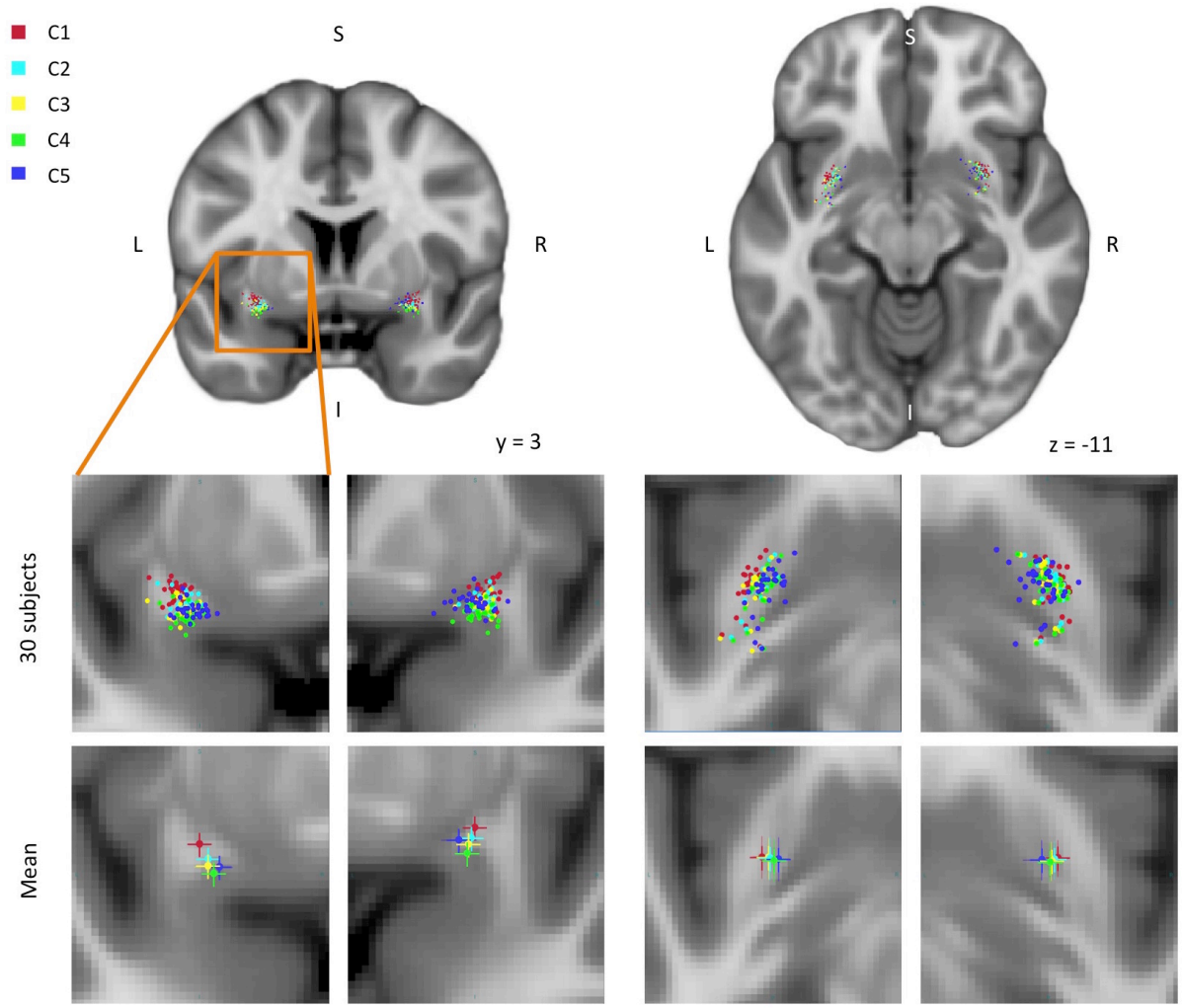

Figure 47. Topological organization of the subcomponents within the UF stem. Mean and individual subject centre of mass locations of each subcomponent at the intersection with the delineated stem in MNI space projected on the mean coronal and axial slice. Colors correspond to each class (C1=deep red, C2=cyan, C3=yellow, C4=green, C5=blue).

7.2.2 Discussion

In this study, we combined an *in vivo* stem-based segmentation approach applied to advanced T1-weighted anatomically constrained tractography data with a layer-by-layer blunt microdissection of post-mortem brains to re-evaluate the structural organization and terminations of the UF. We first observed an UF pattern that consists of not only the classic hook-shaped UF fibers, but progressing posteriorly, fibers that fan out and appear more horizontally-oriented. The use of spherical deconvolution enabled us to better resolve crossing/kissing configurations that would be problematic for example with the posterior part of the UF intersecting the incoming inferior longitudinal fasciculus. Furthermore, the anatomically constrained particle filtering tractography algorithm allowed improved tracking results by reducing premature stopping through areas of low anisotropy (Girard et al., 2014).

A clustering method based on the location and orientation of UF streamline endpoints revealed that the UF can be considered as a multi-component bundle with five types of UF streamlines that were consistently observed with post-mortem dissection. Interestingly, the UF subcomponents showed different (opposing) lateralized patterns.

Converging on a more expansive definition of the UF

We observed a more extensive UF fanning pattern closely similar to the one Dejerine and others described (Dejerine & Dejerine-Klumpe, 1895; Gordinier, 1899; Testut, 1900), namely, with fibres that exhibit the classic hook shape connecting the frontal and anterior temporal lobes and, progressing posteriorly along the tract as they fan out, fibres that follow a straight horizontal trajectory and even curve somewhat in the inverse direction of the hook. Dejerine's description of the UF trajectory stated:

> *Because the orbital aspect of the frontal lobe is very close to the temporal pole, the most medially situated fibres in this fascicle are as curved as the U fibres that cover the bottom of the sulci. This pronounced curvature gives rise to the name fasciculus uncinatus, but only the most medial fibres exhibit this accentuated curved shape. As one moves away from the anterior perforated substance the more laterally situated fibres of the fascicle become straighter with a less accentuated curvature so that these fibres not only become straight, but they appear to have an inverse curvature in the other direction* ([see Figure 48, first row]) (p. 753, Dejerine & Dejerine-Klumpe, 1895).[3]

These horizontal streamlines that we consistently observed in our study were continuous with the classic UF streamlines and could be dissociated from the IFOF lying adjacent to it at the stem but separated by a gap in their posterior temporal course (Figure 40E). They could also be dissociated from other nearby fibre tracts connecting the temporal lobe including the ILF, MdLF, AF and AC (Figure 41). The progressive posterior fanning of the UF transitioning into a horizontally-oriented trajectory can also be clearly seen in other dissection studies (Fig. 2 in Kier et al., 2004; Fig. 19, p. 43 in Meynert, 1885), in particular Curran's dissection of the IFOF which demonstrated a relatively clear boundary between the IFOF and UF at the stem level (Figure 48) (Curran, 1909).

[3] Original text: «Comme la face orbitaire du lobe frontal est très rapprochée du pôle temporal, les fibres les plus internes de ce faisceau sont aussi arquées que les fibres en U qui tapissent le fond des sillons; c'est cette incurvation si prononcée qui a valu à ce faisceau son nom de *fasciculus uncinatus*. Mais les fibres les plus internes possèdent seules une incurvation aussi accentué; plus on s'éloigne de l'espace perforé antérieur et par conséquent plus on considère les fibres plus externes du faisceau, plus la courbure se redresse, de telle sorte que les dernières fibres devienne non seulement rectilignes, mais affectent même une courbure en sens inverse. »

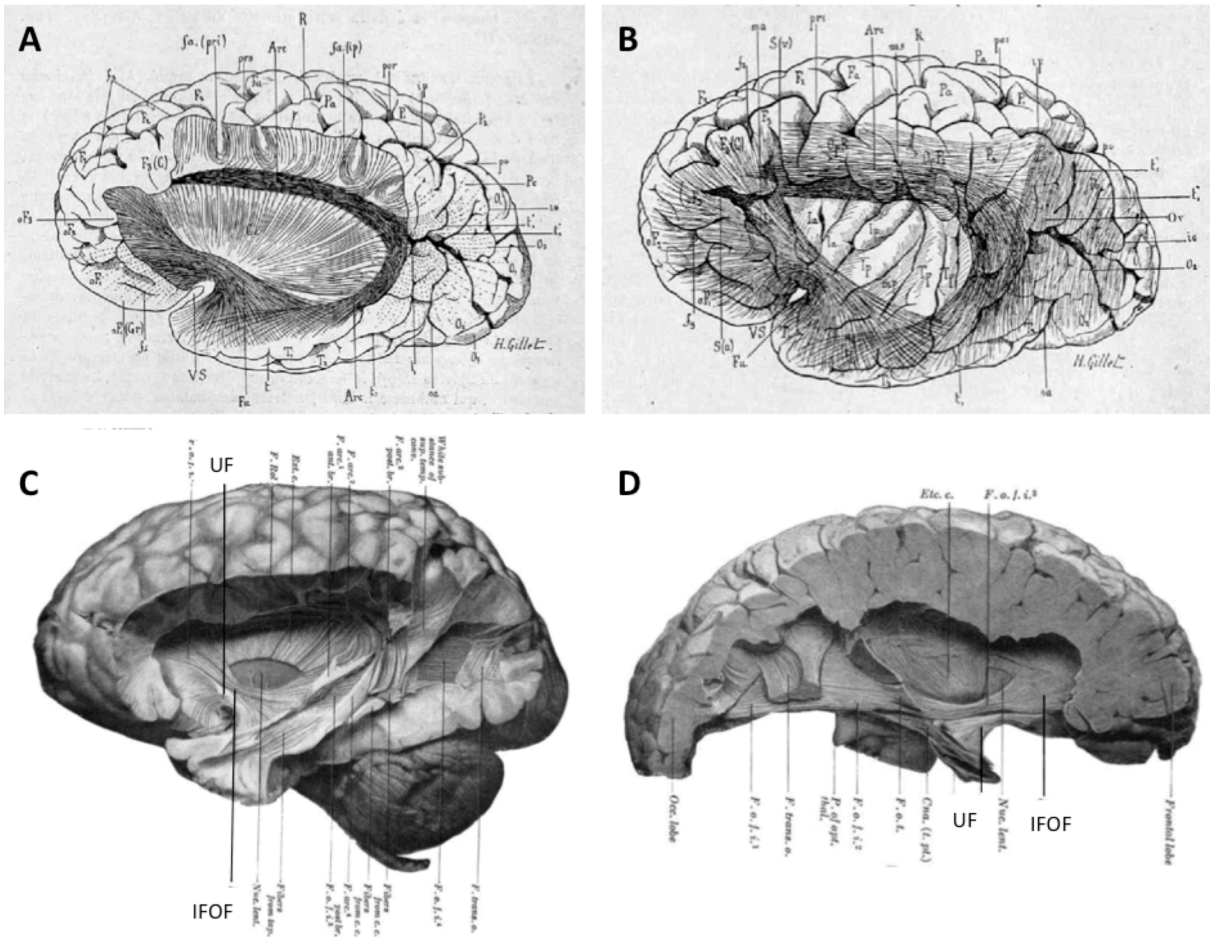

Figure 48. Dejerine's schematic representation of the UF at medial (A) and lateral (B) stages of dissection (Figs. 366-367 in Dejerine & Dejerine-Klumpke, 1895). Curran's dissection of the left (C) and right (D) IFOF where the dorsal horizontal subcomponent of the UF can clearly be seen (Plate I, Curran, 1909).

The UF definition has long been established as a hook-shaped bundle connecting the frontal and anterior temporal lobes. The anatomy that this name implies, however, is an oversimplification of the pathway. As anatomists widely considered only the hook-shaped fibres, the horizontally oriented segment of the UF, which crosses with the ILF also likely contributed to its neglect. It could be argued that the hook-shaped definition refers to only specific subcomponents of the larger bundle, such as the ventro-medial subcomponents. However, it can clearly be seen that the ventro-lateral subcomponent also contains hook-shaped fibres as well as more horizontally, and even inverse curving, oriented ones in a continuum (Figure 43 and 45). In fact, it would seem that the very idea of a hook-shaped bundle is unclear as "hook-shapedness" is subjective and therefore corresponds to a rather arbitrary boundary. Note that the inverse curving streamlines that we observed connect not only the middle portions of the superior and middle temporal gyri but have also more extensive frontal terminations than its classic description, fanning out dorsally beyond the fronto-orbital regions.

Subcomponents of the 'new' UF bundle

The evidence for a multicomponent UF has been accumulating. Some early (Gordinier, 1899; Testut, 1900) and more recent (Ebeling & Cramon, 1992) descriptions of the UF included subcomponent divisions of the bundle but no study has proposed a comprehensive and detailed

account of its subcomponents. In the present study, we further investigated the UF bundles by subdividing them using an automatic clustering method. We revealed five localized sub-groups of streamlines that were consistently observed across subjects and each revealed a distinct pattern of anatomical connections (Figure 44). The dorsal subcomponent corresponds to that observed by Gordinier, Testut and what Dejerine described as the horizontal fibres, although he did not make the distinction between subcomponents. Ebeling and Cramon's (1992, see their Figure 1) ventral and dorsal UF subcomponents may partially correspond to our findings but they consider only the hook-shaped segments. Their ventral subcomponent consists of connections between the rectus gyrus and fronto-subcallosal areas with temporal mesial areas and may correspond to the present short medial ventral subcomponent (Figure 43-C5) passing the most medially through the UF stem (Figure 47). But their dorsal subcomponent consists of orbito-frontal and inferior frontal terminations with the superior and middle temporal gyri, whereas our dorsal component consists of uniquely superior, middle and inferior frontal terminations with the superior and middle temporal gyri.

A frontal to middle temporal tract, namely the extreme capsule tract (also known as the extreme capsule fiber tract) which lies dorso-laterally adjacent to the UF stem has been identified in the macaque monkey with axonal tracing (Schmahmann & Pandya, 2006). The existence of such a tract has been discussed in humans (Parker et al., 2005; Saur et al., 2008; Weiller et al., 2011). There is however some ambiguity regarding its anatomical identity. It has been considered as an independent tract (Schmahmann and Pandya, 2006; Saur et al., 2008; Makris and Pandya, 2009), as the temporal part of the IFOF (Binney et al., 2012; Thiebaut de Schotten et al., 2012; Gierhan, 2013) and as part of the UF (Dejerine and Dejerine-Klumpke, 1895; Wernicke, 1908; Parker et al., 2005). In 1908, Wernicke already reported that "*some portions of [the UF] certainly extend to the third convolution, including Broca's convolution and the speech region of the first temporal convolution*" (Wernicke, 1908, p. 314-315). Based on the present results we propose that the tract known as the extreme capsule fascicle is in fact the most dorsal subcomponent of the UF. This ventral frontal to middle temporal lobe connection provides an alternative pathway to the dorsal arcuate fasciculus between the frontal and temporal lobes (Weiller et al., 2011) and needs to be considered in the anatomical definition of the UF.

Topography of subcomponents at the stem

There was also a topographical organization of the subcomponents that was observed at the stem (Figure 47). The dorsal UF subcomponent was systematically located superiorly and laterally with respect to the other subcomponents within the stem and the lateral and medial ventral UF subcomponents were organized in a supero-inferior manner along the central portion of the stem. The short anterior ventro-medial subcomponent passed through the stem at its most medial part. This clustered organization as opposed to dispersed intermingling at the stem lends further support for the subcomponents as distinct sub-groups of the UF bundle. The observed topographical organization of the subcomponents is consistent with the appearance of the subcomponents revealed in the layer-by-layer dissection that progresses laterally to medially.

UF blunt dissection

The microdissection of the white matter of the ventral third of the EC confirmed a wide distribution of the UF fibers connecting the whole frontal lobe with the anterior temporal lobe. Starting from the original definition of Dejerine we performed a layer-by-layer dissection demonstrating five layers of fibers belonging to UF stem. These layers were progressively segregated according to their depth, course orientation and territories of terminations. Considering the different anatomical background and principles on which diffusion imaging

clusterization (i.e. five subcomponents) and blunt dissection layers are based, some differences emerged in the fibres distribution. Nonetheless, dissections systematically confirmed all the territories of terminations identified by spherical deconvolution tractography. Moreover, we demonstrated a wider distribution of UF terminations in the SFG, MFG, IFG and fronto-orbital and basal cortices and STG, MTG and temporal pole with respect to the recent DTI and dissection descriptions. Superficial layers (i.e. first and second) provide a wide and fan-shaped connection between lateral frontal and temporal convexity and these fibres occupy the dorsal portion of the stem adjacent to the IFOF fibres. The deeper layers (i.e. third to fifth) provide a shorter connection between fronto-polar and basal cortices and temporal pole. It is worth noting that these fibres occupy the most ventral portion of the stem, anteriorly and medially in respect to the IFOF fibres. These terminations have a progressively increasing anterior and medial direction corresponding to the progressively deeper location of the respective fibres within the stem (Figure 45). As a consequence of this wide and differently oriented distribution of terminations we demonstrated a progressive (i.e. from first to fifth layer) latero-medial and anterior torsion of the fibres of UF stem.

Regarding the controversial asymmetry of the UF

We observed asymmetries in opposite directions in two subcomponents. It is left lateralized in the dorsal UF for volume and right lateralized in the ventro-medial UF for volume and the number of streamlines, and we observed no lateralization in the ventro-lateral and posterior ventro-medial subcomponents. A rightward asymmetry was also observed in anterior ventro-medial UF for volume but interestingly not for the number of streamlines, which reflects a longer reach in the right versus left hemisphere (Figure 43) that may be due to gross anatomical asymmetries, specifically the Yakovlevian torque pushing the right frontal cortex anteriorly (Toga and Thompson, 2003). These opposing asymmetries elucidate the controversy surrounding the asymmetry of the UF. Studies on the asymmetry of the UF have only been conducted on the entire bundle and they have been inconclusive with some revealing leftward (Kubicki et al., 2002; Hasan et al., 2009; Thomas et al., 2015), rightward (Highley et al., 2002; Rodrigo et al., 2007) and no lateralization (Thiebaut de Schotten et al., 2011; Lebel et al., 2012). Interestingly, a previous DTI study observed a leftward asymmetry in voxels located at the superior portion and a rightward asymmetry in the inferior portion of the UF stem (Park et al., 2004) consistent with the present asymmetries of the UF subcomponents with the left lateralized dorsal UF located dorsally and right lateralized ventro-medial UF located inferiorly within the stem. Tract quantitative measures (such as FA, number of streamlines, volume) depend on how the tract is segmented and therefore are contingent on its definition. Whether the dorsal subcomponent of the UF is considered or if only the "hook-shaped" portion is considered will affect the results on its asymmetry. The inconsistency in the accurate identification and localization of tracts has already been raised as an issue for comparing quantitative measures across groups and across studies (Jones, 2008). The quality of the data and the tractography results will also influence it. For example, the posterior part of the UF will be more difficult to obtain in DTI studies due to the crossing with the dominant ILF. Thus, given the opposite asymmetries observed in our present findings regarding two of the UF subcomponents and no observed asymmetries in two of its subcomponents, and the above reasons regarding its inconsistent definitions, studies on the asymmetry of the UF have remained inconclusive. This underlines the need to study the UF in terms of its subcomponents instead of considering it as a homogeneous bundle whose definition has some ambiguities. We have reported asymmetry results in healthy subjects that will be of interest for clinicians investigating patients with disorders that have been linked with the UF such as schizophrenia (Park et al., 2004; Price et al., 2008), clinical depression (Steffens et al., 2011; Zhang et al., 2012), Alzheimer's disease (Yasmin et al., 2008; Taoka et al., 2009) and psychopathy (Craig et al., 2009; Sobhani et al., 2015).

Multifunctional roles for a multicomponent bundle

Indeed due to the UF being a multicomponent bundle, its functional role has been difficult to disentangle. For instance, there have been conflicting results regarding whether or not lesions to the UF disrupt language function (Duffau et al., 2009; Papagno et al., 2011). Over a century ago Wernicke described the UF as one of "*two important association bundles which must be considered in the anatomy of the speech regions*" (Wernicke, 1908, p. 314-315). More recently, the dorsal UF subcomponent has been postulated as a ventral language pathway responsible for semantic processing (Duffau et al., 2005; Saur et al., 2008). It has also been linked to associative learning (Von Der Heide et al., 2013; Thomas et al., 2015). The ventral subcomponents may have an important role in mnemonic associations and value judgments (Von Der Heide et al., 2013). A recent study investigating the circuitry of the temporal lobe suggested that the medial and lateral branches of the ventral UF may have distinct functions (Binney et al., 2012). They hypothesized that a ventro-lateral prefrontal branch might be related to social cognition and an orbital and medial frontal branch related to emotional valence.

Contrary to previous diffusion tractography studies, to segment the tract we used an interactive stem-based approach with minimal a priori on the tract's terminations. We have shown that this approach is a fruitful way to investigate the precise anatomy of fibre pathways and is faithful to their definition as fibre bundles, which is a general property of white matter tracts (though there are exceptions including those with diffuse sheet-like structures such as the thalamo-cortical tract).

These novel results on the UF anatomy obtained from constrained spherical deconvolution tractography are supported by post-mortem fibre dissection. Diffusion tractography is an important complementary tool for investigating the anatomy of the fibre pathways, capable of systematically identifying and quantifying tract connections, assessing asymmetries and inter-individual variability *in vivo*. As we have seen in this study the UF is a highly heterogeneous bundle. It is thus imperative to consider the UF with respect to its anatomically distinct subcomponents. Several other white matter pathways have recently been identified as multicomponent bundles including the IFOF (Martino et al., 2010; Sarubbo et al., 2013; Hau et al., under review), the SLF/AF (Catani et al., 2005; Makris et al., 2005; Wang et al., 2015b) suggesting that our knowledge has much to gain regarding the detailed anatomy of the fibre pathways. Studies on subcomponents have been performed with diffusion tractography and fibre dissection. To our knowledge, no axonal tracing study has demonstrated a division of a fibre pathway into defined subcomponents. Shifting our understanding of the UF to a multicomponent bundle will improve the specificity of studies relating it to function and disorders and will be helpful for surgical interventions.

The work in this chapter was recently submitted to the journal Brain, Structure and Function.

8 General discussion

Our modern understanding of the brain relies on how the primary sites work together to create integrated function. This communication between brain areas passes via the white matter axons that are organized into fibre pathways. Fibre pathways form the bedrock of this communication but are not well established in the human brain. When Crick and Jones (1993) commented on the gap in knowledge of human neuroanatomy they were mainly referring to the micro and mesoscopic scales. In this thesis we would like to emphasize the lack of knowledge of the white matter structure at the macroscopic scale, which has been plagued by centuries of controversy from gross dissection and histology, and more recently tract tracing in non-human primates. Axonal tracing and dissection allow us to observe first-hand the white matter structure and are important techniques for anatomical validation however their ability to map the fiber pathways suffers from some important limitations (reviewed in Chapter 4).

In this thesis we used diffusion imaging tractography to study the detailed anatomy of fibre pathways in humans. Diffusion imaging tractography currently provides the only way to study the white matter structure in the living human brain quantitatively and across large populations. We focussed on elucidating the external and extreme capsule complex (E2C2), which has remained a controversial area of fibre passage. Our goal was to map precisely and comprehensively the connections of the association pathways of this area, namely the IFOF and UF, which are of interest for their putative roles in language processing. Importantly, we used a novel interactive stem-based approach to extract the two tracts from tractography datasets, which minimizes *a priori* on tract terminations. This approach allows for the comprehensive extraction of the fibre bundles.

8.1 Contributions of the thesis

In a first study (Chapter 5), we put in place a way to quantitatively investigate the terminations of the IFOF and UF and provided their detailed description. We also revealed asymmetries within the specific branches of the tracts, which brought new insight regarding the medial and lateral subcomponents of the IFOF. This first study was based on a basic diffusion tensor imaging (DTI)-based pipeline that made us aware of its technical limitations.

We made significant improvements to the tractography pipeline by applying advanced methods through a collaboration with Maxime Descoteaux (Université de Sherbrooke, Canada). It drastically improved both the quality of our data and our ability to perform connectivity analysis on fibre pathways (Chapter 6).

Building on our first study, we performed an in-depth investigation focussing on the UF with the constrained spherical deconvolution (CSD)-based tractography pipeline. We resolved a centuries old debate regarding the dissociation between the IFOF and UF. We also revealed a novel anatomy of the UF as a multicomponent bundle, by dividing it into subcomponents using a clustering method. The division of the UF subcomponents also resolved recent controversy surrounding its asymmetry that has remained inconclusive. We provided results that reconcile the contradictory findings observed in the previous studies on UF asymmetry. We also showed that the tract known previously as the extreme capsule fascicle, whose anatomical identity was unclear, is in fact the dorsal UF subcomponent. These results were supported with post-mortem dissection through a collaboration with Silvio Sarubbo (Santa Chiara Hospital, Italy).

We have thus provided some elucidation to the association fibre pathways of the E2C2 (Figure 49).

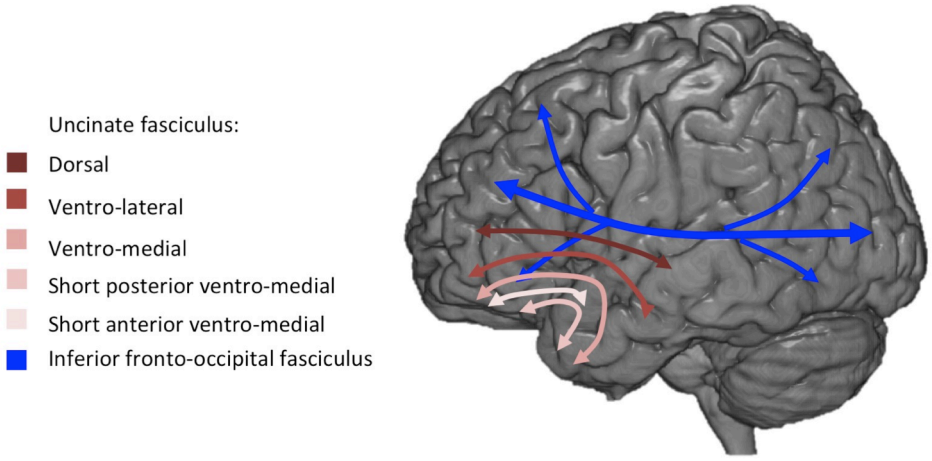

Figure 49. Schematic diagram showing the connectional anatomy of the human association pathways of the extreme and external capsules.

Perspectives:

The interactive stem-based approach that we used to segment the IFOF and UF enabled the full characterization of their connectional anatomies. As mentioned already in this thesis, current approaches for segmenting fibre tracts impose anatomical constraints based on *a priori* knowledge to obtain reproducible results at the cost of accuracy (their full representation as defined by a stem). In both studies, our minimal *a priori* approach revealed more extensive terminations in the cortex than studies revealed with these *a priori* segmentation methods. Since our knowledge of the anatomy of fibre pathways is incomplete, these approaches will not be able to provide insights regarding their anatomy. Our interactive stem-based approach applied to diffusion imaging tractography enables a new way to study them. Its application to the anatomical study of other fibre pathways may bring new insights into their anatomo-functional organization.

A critical part of assessing fibre pathways is tract segmentation. This can greatly impact the results of a study because tract-based measurements depend on the segmentation, as we have seen with the controversy over the UF asymmetry. Our division of the UF into subcomponents provides a framework to study its more fine-grained anatomy with respect to function and behaviour. Subcomponents (based on fibre dissection) of the IFOF have also recently been proposed (Martino et al., 2010; Sarubbo et al., 2013). Thus tracts should be studied in the context of being heterogeneous rather than homogeneous structures. It would be fruitful to extend our present findings of the IFOF, a known multicomponent bundle, by fully characterizing its subcomponents using the clustering method we applied to the UF.

Scientists have recently started to explore the link between white matter pathways and different clinical disorders which may bring insight into the causes of these disorders. As a result of its anatomical connections connecting the frontal and temporal lobes, the UF has been linked to a number of clinical disorders including schizophrenia (Park et al., 2004; Price et al., 2008), depression (Steffens et al., 2011; Zhang et al., 2012) and psychopathy (Sobhani et al., 2015). Exactly how the UF relates to these different disorders will require detailed anatomical knowledge of this pathway. For example, testing different symptoms or features of the disorders with respect to specific subcomponents rather than the averaged bundle will increase specificity in the findings. Finding anatomical correlates of these disorders with respect to features of the white matter may provide some insights into their causes, which today remain unknown.

A note on template usage:

The template that we used in this thesis is based on a single subject. We recognize the limitations of a template derived from the anatomy of a single subject, which may introduce some additional variability in the template regions. However, we chose this atlas because it included parcellations of the white matter (including both deep and superficial white matter regions corresponding to the gyri, see Mori et al., 2005) that were used in the virtual dissection of the tractogram in the first study. To remain consistent in this thesis work, we continued using the template for the second study. Future studies (for determining the tract terminations) will employ the more widely used Desikan-Killiany template, which is based on an averaged dataset of 40 subjects.

8.2 Perspectives for the BIL&GIN and UF

To extend the findings of the UF study, we can investigate the UF in the large cohort of 411 subjects with diffusion imaging data from the BIL&GIN database. This unique cohort is balanced for gender and handedness with 50% left-handers, functional language lateralization evaluated in 71% of the 411 subjects among other measures including performance on spatial processing, number processing and language skills as well as functional MRI data.

The aim would be to describe its normative connectional anatomy, microstructural properties and asymmetries of the UF subcomponents within the healthy population with respect to factors such as age, gender, handedness and language lateralization. A first goal would be to look at the inter-individual variability of the UF anatomy and its microstructural properties across the subjects evaluated for language lateralization, as the UF has been implicated in language processing.

Preliminary results based on the DTI pipeline have shown that handedness has a significant effect on the degree of asymmetry exhibited in the UF for the number of streamlines, with left-handers (n = 30) showing stronger asymmetry than right-handers (n = 60). Why there is an influence of handedness on the UF, a fronto-temporal pathway is not clear. We will try to reproduce these results in the data processed with the CSD pipeline in a larger cohort within the BIL&GIN.

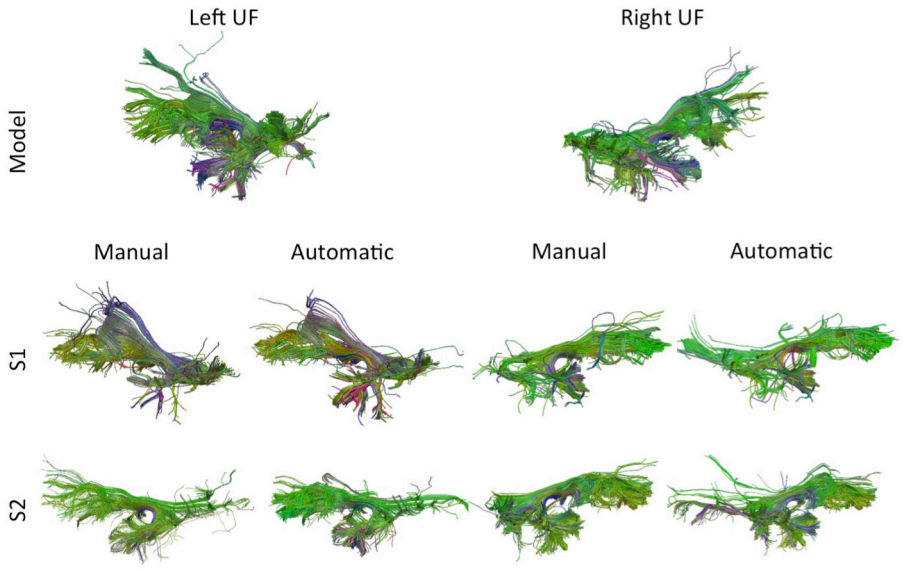

Figure 50. Preliminary results of the automatic SLR-based extraction of the UF bundle with a manually delineated stem-based model bundle for the left and right hemispheres are shown for two subjects.

Since the stem-based approach requires manual delineation of the stems and thus requires considerable time, an automatic method will need to be used to segment the UF in such a large group. There is currently no automatic method to delineate the stems as we have done from the whole-brain tractogram. As an alternative solution, we have collaborated with Maxime Descoteaux's team in Sherbrooke to use streamline-based linear registration (SLR) to extract the UF based on a model fibre bundle (one of we delineated manually). Preliminary results with SLR-based tract segmentation on CSD-processed data are shown for two subjects in Figure 50. Future work may involve developing an automatic stem-based segmentation method.

8.1 Final remarks

We conclude that diffusion imaging paired with tractography is a complementary technique for the anatomical study of human white matter pathways. It brings the unique capacity to perform virtual dissections of the white matter and obtain quantitative measures on a living population. Nevertheless it remains an indirect measure of the white matter structure and therefore validation with primary techniques is essential. By combining diffusion imaging with the primary techniques of blunt dissection and axonal tracing to validate and converge on the anatomy of the fiber pathways, we will be able to understand more precisely the functions and behaviours that they support.

BIBLIOGRAPHY

Alexander, A. L., Lee, J. E., Lazar, M., & Field, A. S. (2007). Diffusion tensor imaging of the brain. *Neurotherapeutics : The Journal of the American Society for Experimental NeuroTherapeutics*, *4*(3), 316–329.

Almairac, F., Herbet, G., Moritz-Gasser, S., de Champfleur, N. M., & Duffau, H. (2014). The left inferior fronto-occipital fasciculus subserves language semantics: a multilevel lesion study. *Brain Structure & Function*, (APRIL 2014).

Arnold, F. (1838). Tabulae anatomicae.

Assaf, Y., & Basser, P. J. (2005). Composite hindered and restricted model of diffusion (CHARMED) MR imaging of the human brain. *NeuroImage*, *27*(1), 48–58.

Avants, B. B., Tustison, N., & Song, G. (2011). Advanced Normalization Tools (ANTS), 1–35.

Axer, H., Beck, S., Axer, M., Schuchardt, F., Heepe, J., Flucken, A., … Witte, O. (2011). Microstructural analysis of human white matter architecture using polarized light imaging: views from neuroanatomy. *Frontiers in Neuroinformatics*, *5*(November), 1–12.

Axer, H., Klingner, C. M., & Prescher, A. (2013). Fiber anatomy of dorsal and ventral language streams. *Brain and Language*, *127*(2), 192–204.

Axer, M., Amunts, K., Grässel, D., Palm, C., Dammers, J., Axer, H., … Zilles, K. (2011). A novel approach to the human connectome: Ultra-high resolution mapping of fiber tracts in the brain. *NeuroImage*, *54*(2), 1091–1101.

Azadbakht, H., Parkes, L. M., Haroon, H. a., Augath, M., Logothetis, N. K., de Crespigny, a., … Parker, G. J. M. (2015). Validation of High-Resolution Tractography Against In Vivo Tracing in the Macaque Visual Cortex. *Cerebral Cortex*, 1–11.

Bajada, C. J., Lambon Ralph, M. a., & Cloutman, L. L. (2015). Transport for Language South of the Sylvian Fissure: The routes and history of the main tracts and stations in the ventral language network. *Cortex*, *69*, 141–151.

Barrick, T. R., Lawes, I. N., Mackay, C. E., & Clark, C. a. (2007). White matter pathway asymmetry underlies functional lateralization. *Cerebral Cortex*, *17*(3), 591–598.

Basser, P., Mattiello, J., & LeBihan, D. (1994). Estimation of the effective self-diffusion tensor from the NMR spin echo. *Journal of Magnetic Resonance. Series B*.

Bastiani, M., Shah, N. J., Goebel, R., & Roebroeck, A. (2012). Human cortical connectome reconstruction from diffusion weighted MRI: the effect of tractography algorithm. *NeuroImage*, *62*(3), 1732–49.

Beaulieu, C. (2002). The basis of anisotropic water diffusion in the nervous system - a technical review. *NMR in Biomedicine*, *15*(7-8), 435–455.

Bihan, D. Le, & Breton, E. (1985). Imagerie de diffusion in-vivo par résonance magnétique nucléaire. *Comptes-Rendus de l'Académie.*

Binney, R. J., Parker, G. J. M., & Lambon Ralph, M. A. (2012). Convergent connectivity and graded specialization in the rostral human temporal lobe as revealed by diffusion-weighted imaging probabilistic tractography. *Journal of Cognitive Neuroscience*, *24*(10), 1998–2014.

Brown, J. a., Rudie, J. D., Bandrowski, A., Van Horn, J. D., & Bookheimer, S. Y. (2012). The UCLA multimodal connectivity database: a web-based platform for brain connectivity matrix sharing and analysis. *Frontiers in Neuroinformatics*, *6*(November), 1–17.

Brown, R. (1828). A brief account of microscopical observations made in the months of June, July and August 1827, on the particles contained in the pollen of plants; and on the general existence of active molecules in organic and inorganic bodies. *Philosophical Magazine Series 2*, *4*(21), 161–173.

Bullmore, E., Bullmore, E., Sporns, O., & Sporns, O. (2009). Complex brain networks: graph theoretical analysis of structural and functional systems. *Nat Rev Neurosci*, *10*(3), 186–198.

Burdach, K. (1819). *Vom bau und leben des gehirns und rückenmarks*. *der Dyk'schen Buchhandlung, Leipzig*.

Catani, M. (2007). From hodology to function. *Brain*, *130*(3), 602–605.

Catani, M., Allin, M. P. G., Husain, M., Pugliese, L., Mesulam, M. M., Murray, R. M., & Jones, D. K. (2007). Symmetries in human brain language pathways correlate with verbal recall. *Proceedings of the National Academy of Sciences of the United States of America*, *104*(43), 17163–8.

Catani, M., Bodi, I., & Dell'Acqua, F. (2012). Comment on "The geometric structure of the brain fiber pathways". *Science (New York, N.Y.)*, *337*(6102), 1605.

Catani, M., Dell'acqua, F., Vergani, F., Malik, F., Hodge, H., Roy, P., … Thiebaut de Schotten, M. (2012). Short frontal lobe connections of the human brain. *Cortex; a Journal Devoted to the Study of the Nervous System and Behavior*, *48*(2), 273–91.

Catani, M., Howard, R. J., Pajevic, S., & Jones, D. K. (2002). Virtual in Vivo Interactive Dissection of White Matter Fasciculi in the Human Brain. *NeuroImage*, *17*(1), 77–94.

Catani, M., Jones, D. K., Donato, R., & Ffytche, D. H. (2003). Occipito-temporal connections in the human brain. *Brain : A Journal of Neurology*, *126*(Pt 9), 2093–107.

Catani, M., Jones, D. K., & Ffytche, D. H. (2005). Perisylvian language networks of the human brain. *Annals of Neurology*, *57*(1), 8–16.

Catani, M., Mesulam, M. M., Jakobsen, E., Malik, F., Martersteck, A., Wieneke, C., … Rogalski, E. (2013). A novel frontal pathway underlies verbal fluency in primary progressive aphasia. *Brain*, *136*(8), 2619–2628.

Catani, M., & Thiebaut de Schotten, M. (2008). A diffusion tensor imaging tractography atlas for virtual in vivo dissections. *Cortex*, *44*(8), 1105–32.

Catani, M., & Thiebaut De Schotten, M. (2012). *Atlas of human brain connections*.

Caverzasi, E., Papinutto, N., Amirbekian, B., Berger, M. S., & Henry, R. G. (2014). Q-ball of inferior fronto-occipital fasciculus and beyond. *PloS One*, *9*(6), e100274.

Chamberland, M., Whittingstall, K., Fortin, D., Mathieu, D., & Descoteaux, M. (2014). Real-time multi-peak tractography for instantaneous connectivity display. *Frontiers in Neuroinformatics*, *8*(May), 59.

Clarke, E., & O'Malley, C. (1996). *The human brain and spinal cord: a historical study illustrated by writings from antiquity to the twentieth century* (2nd rev.). San Francisco: Norman Publishing.

Conner, C. R., Ellmore, T., Disano, M., Pieters, T., Potter, A., & Tandon, N. (2012). Anatomic and electro-physiologic connectivity of the language system : a combined DTI-CCEP study, *41*(12), 1100–1109.

Conturo, T. E., Lori, N. F., Cull, T. S., Akbudak, E., Snyder, a Z., Shimony, J. S., … Raichle, M. E. (1999). Tracking neuronal fiber pathways in the living human brain. *Proceedings of the National Academy of Sciences of the United States of America*, *96*(18), 10422–10427.

Côté, M., Girard, G., Boré, A., Garyfallidis, E., Houde, J., & Descoteaux, M. (2013). Tractometer : Towards validation of tractography pipelines, *17*, 844–857.

Craig, M. C., Catani, M., Deeley, Q., Latham, R., Daly, E., Kanaan, R., … Murphy, D. G. M. (2009). Altered connections on the road to psychopathy. *Molecular Psychiatry*, *14*(10), 946–953, 907.

Crick, F., & Jones, E. (1993). Backwardness of human neuroanatomy. *Nature*, *361*(6408), 109–110.

Crosby, E. (1962). Correlative anatomy of the nervous system.

Croxson, P. L., Johansen-Berg, H., Behrens, T. E. J., Robson, M. D., Pinsk, M. a, Gross, C. G., … Rushworth, M. F. S. (2005). Quantitative investigation of connections of the prefrontal cortex in the human and macaque using probabilistic diffusion tractography. *The Journal of Neuroscience : The Official Journal of the Society for Neuroscience*, *25*(39), 8854–8866.

Curran, J. (1909). A new association fiber tract in the cerebrum. *Journal of Comparative Neurology and Psychology*, *19*(6), 645–656.

Davis, L. (1921). An anatomic study of the inferior longitudinal fasciculus. *Archives of Neurology & Psychiatry*.

Dejerine, J., & Dejerine-Klumpe, A. (1895). *Anatomie des Centres Nerveux*. Paris: Rueff et Cie.

Dell'Acqua, F., Simmons, A., Williams, S. C. R., & Catani, M. (2013). Can spherical deconvolution provide more information than fiber orientations? Hindrance modulated orientational anisotropy, a true-tract specific index to characterize white matter diffusion. *Human Brain Mapping*, *34*(10), 2464–83.

Dempster, A. P., Laird, N. M., & Rubin, D. B. (1976). *Maximum Likelihood from Incomplete Data via the EM Algorithm*. *Journal of the Royal Statistical Society. Series B (Methodological)* (Vol. 39).

Descoteaux, M., Deriche, R., Knösche, T., & Anwander, A. (2009). Deterministic and Probabilistic Tractography Based on Complex Fiber Orientation Distributions. *IEEE Transactions on Medical Imaging*, *28*(2), 269–286.

Desikan, R. S., Ségonne, F., Fischl, B., Quinn, B. T., Dickerson, B. C., Blacker, D., … Killiany, R. J. (2006). An automated labeling system for subdividing the human cerebral cortex on MRI scans into gyral based regions of interest. *NeuroImage*, *31*(3), 968–980.

Dick, A. S., Bernal, B., & Tremblay, P. (2014). The Language Connectome: New Pathways, New Concepts. *The Neuroscientist*, *20*(5), 453–467.

Dick, A. S., & Tremblay, P. (2012). Beyond the arcuate fasciculus: consensus and controversy in the connectional anatomy of language. *Brain*.

Diemerbroeck, I. de. (1695). *L'Anatomie du corps humain, Tome 2*. Lyon: Anisson & Posuel.

Duffau, H. (2005). New insights into the anatomo-functional connectivity of the semantic system: a study using cortico-subcortical electrostimulations. *Brain*, *128*(4), 797–810.

Duffau, H. (2008). The anatomo-functional connectivity of language revisited. New insights provided by electrostimulation and tractography. *Neuropsychologia*, *46*(4), 927–934.

Duffau, H. (2015). Stimulation mapping of white matter tracts to study brain functional connectivity. *Nature Reviews Neurology*.

Duffau, H., Gatignol, P., Moritz-Gasser, S., & Mandonnet, E. (2009). Is the left uncinate fasciculus essential for language? : A cerebral stimulation study. *Journal of Neurology*, *256*(3), 382–389.

Ebeling, U., & Cramon, D. (1992). Topography of the Uncinate Fascicle and Adjacent Temporal Fiber Tracts. *Acta Neurochirurgica*, *115*, 143–148.

Einstein, A. (1905). The theory of the brownian movement. *Ann. Der Physik*.

Farquharson, S., Tournier, J.-D., Calamante, F., Fabinyi, G., Schneider-Kolsky, M., Jackson, G. D., & Connelly, A. (2013). White matter fiber tractography: why we need to move beyond DTI. *Journal of Neurosurgery*, *118*(6), 1367–77.

Feldman, H. M., Yeatman, J. D., Eliana, L., Barde, L., & Gaman-Bean, S. (2010). Diffusion Tensor Imaging: A review for pediatric reearchers and clinicians. *J Dev Behav Pediatr.*, *31*(4), 346–356.

Felleman, D. J., & Van Essen, D. C. (1991). Distributed hierarchical processing in the primate cerebral cortex. *Cerebral Cortex (New York, N.Y. : 1991)*, *1*(1), 1–47.

Fernández-Miranda, J. C., Rhoton, A. L., Álvarez-Linera, J., Kakizawa, Y., Choi, C., & de Oliveira, E. P. (2008). Three-Dimensional Microsurgical and Tractographic Anatomy of the White Matter of the Human Brain. *Neurosurgery*, *62*(Supplement 3).

Fernández-Miranda, J. C., Rhoton, A. L., Kakizawa, Y., Choi, C., & Alvarez-Linera, J. (2008). The claustrum and its projection system in the human brain: a microsurgical and tractographic anatomical study. *Journal of Neurosurgery*, *108*(4), 764–774.

Forkel, S. J., Mahmood, S., Vergani, F., & Catani, M. (2015). The white matter of the human cerebrum: Part I The occipital lobe by Heinrich Sachs. *Cortex*, *62*, 182–202.

Forkel, S. J., Thiebaut de Schotten, M., Kawadler, J. M., Dell'acqua, F., Danek, A., & Catani, M. (2012). The anatomy of fronto-occipital connections from early blunt dissections to contemporary tractography. *Cortex; a Journal Devoted to the Study of the Nervous System and Behavior*, 1–12.

Frey, S., Campbell, J. S. W., Pike, G. B., & Petrides, M. (2008). Dissociating the human language pathways with high angular resolution diffusion fiber tractography. *The Journal of Neuroscience : The Official Journal of the Society for Neuroscience*, *28*(45), 11435–44.

Gall, F., & Spurzheim, J. (1810). Anatomie et physiologie du système nerveux en général et du cerveau en particulier... Atlas.

Galuske, R., Schlote, W., Bratzke, H., & Singer, W. (2000). Interhemispheric asymmetries of the modular structure in human temporal cortex. *Science*.

Garyfallidis, E., Ocegueda, O., Wassermann, D., & Descoteaux, M. (2015). Robust and efficient linear registration of white-matter fascicles in the space of streamlines. *NeuroImage*.

Gierhan, S. M. E. (2013). Connections for auditory language in the human brain. *Brain and Language*, *127*(2), 205–221.

Girard, G., Fick, R., Descoteaux, M., Deriche, R., Girard, G., Fick, R., … Ax-, D. W. (2015). AxTract : microstructure-driven tractography based on the ensemble average propagator.

Girard, G., Whittingstall, K., Deriche, R., & Descoteaux, M. (2014). Towards quantitative connectivity analysis: reducing tractography biases. *NeuroImage*, *98*, 266–78.

Glasser, M. F., & Rilling, J. K. (2008). DTI tractography of the human brain's language pathways. *Cerebral Cortex (New York, N.Y. : 1991)*, *18*(11), 2471–82.

Goga, C., & Türe, U. (2015). The anatomy of Meyer's loop revisited: changing the anatomical paradigm of the temporal loop based on evidence from fiber microdissection. *Journal of Neurosurgery*, *122*(June), 1–10.

Goodale, M. a., & Milner, a. D. (1992). Separate visual pathways for perception and action. *Trends in Neurosciences*, *15*(1), 20–25.

Gordinier, H. (1899). The gross and minute anatomy of the central nervous system.

Griffiths, J. D., Marslen-Wilson, W. D., Stamatakis, E. a., & Tyler, L. K. (2013). Functional organization of the neural language system: Dorsal and ventral pathways are critical for syntax. *Cerebral Cortex*, *23*(1), 139–147.

Guevara, P., Duclap, D., Poupon, C., Marrakchi-Kacem, L., Fillard, P., Le Bihan, D., … Mangin, J.-F. (2012). Automatic fiber bundle segmentation in massive tractography datasets using a multi-subject bundle atlas. *NeuroImage*, *61*(4), 1083–99.

Hasan, K. M., Iftikhar, A., Kamali, A., Kramer, L. a, Ashtari, M., Cirino, P. T., … Ewing-Cobbs, L. (2009). Development and aging of the healthy human brain uncinate fasciculus across the lifespan using diffusion tensor tractography. *Brain Research*, *1276*, 67–76.

Hentschel, H. G. E., & Ooyen, A. Van. (1999). Models of axon guidance and bundling during development, (June).

Hernando, K. a., Szaflarski, J. P., Ver Hoef, L. W., Lee, S., & Allendorfer, J. B. (2015). Uncinate fasciculus connectivity in patients with psychogenic nonepileptic seizures: A preliminary diffusion tensor tractography study. *Epilepsy & Behavior*, *45*, 68–73.

Hickok, G., & Poeppel, D. (2004). Dorsal and ventral streams: a framework for understanding aspects of the functional anatomy of language. *Cognition*, *92*(1-2), 67–99.

Hickok, G., & Poeppel, D. (2007). The cortical organization of speech processing. *Nature Reviews. Neuroscience*, *8*(5), 393–402.

Highley, J. R., Walker, M. a, Esiri, M. M., Crow, T. J., & Harrison, P. J. (2002). Asymmetry of the uncinate fasciculus: a post-mortem study of normal subjects and patients with schizophrenia. *Cerebral Cortex (New York, N.Y. : 1991)*, *12*(11), 1218–1224.

Jamieson, E. B. (1909). The means of displaying, by ordinary dissection, the larger tracts of white matter of the brain in their continuity. *Journal of Anatomy and Physiology*.

Jbabdi, S., & Johansen-Berg, H. (2011). Tractography: where do we go from here? *Brain Connectivity*, *1*(3), 169–83.

Jbabdi, S., Lehman, J. F., Haber, S. N., & Behrens, T. E. (2013). Human and Monkey Ventral Prefrontal Fibers Use the Same Organizational Principles to Reach Their Targets: Tracing versus Tractography. *Journal of Neuroscience*, *33*(7), 3190–3201.

Jellison, B. J., Field, A. S., Medow, J., Lazar, M., Salamat, M. S., & Alexander, A. L. (2004). Diffusion tensor imaging of cerebral white matter: a pictorial review of physics, fiber tract anatomy, and tumor imaging patterns. *AJNR. American Journal of Neuroradiology*, *25*(3), 356–69. Retrieved from http://www.ncbi.nlm.nih.gov/pubmed/15037456

Johansen-Berg, H., & Behrens, T. (2014). *Diffusion MRI: from quantitative measurement to in vivo neuroanatomy* (2nd ed.). Academic Press.

Jones, D. K., & Cercignani, M. (2010). Twenty-five pitfalls in the analysis of diffusion MRI data. *NMR in Biomedicine*, *23*(7), 803–20.

Jones, D. K., Knösche, T. R., & Turner, R. (2013). White matter integrity, fiber count, and other fallacies: the do's and don'ts of diffusion MRI. *NeuroImage*, *73*, 239–54.

Kamali, A., Flanders, A., Brody, J., Hunter, J., & Khader, H. (2014). Tracing Superior Longitudinal Fasciculus Connectivity in the Human Brain using High Resolution Diffusion Tensor Tractography. *Brain Structure and Function*, *219*(1).

Kandel, E., Schwartz, J., & Jessell, T. (2014). Principles of neural science.

Kier, E. L., Staib, L. H., Davis, L. M., & Bronen, R. a. (2004). MR imaging of the temporal stem: Anatomic dissection tractography of the uncinate fasciculus, inferior occipitofrontal fasciculus, and Meyer's loop of the optic radiation. *American Journal of Neuroradiology*, *25*(5), 677–691.

Klingler, J. (1935). Erleichterung der makrokopischen Präparation des Gehirns durch den Gefrierprozess. *Schweiz. Arch. Neurol. Psychiatr.*, *36*, 247–256.

Klingler, J., & Gloor, P. (1960). The connections of the amygdala and of the anterior temporal cortex in the human brain. *The Journal of Comparative Neurology*, *115*(669), 333–369.

Krestel, H., Annoni, J. M., & Jagella, C. (2013). White matter in aphasia: A historical review of the Dejerines' studies. *Brain and Language*, *127*(3), 526–532.

Kubicki, M., Westin, C.-F., Maier, S. E., Frumin, M., Nestor, P. G., Salisbury, D. F., … Shenton, M. E. (2002). Uncinate fasciculus findingsin schizophrenia: a magnetic resonance diffusion tensor imaging study. *American Journal of Psychiatry*, *159*(18), 813–820.

Lawes, I. N. C., Barrick, T. R., Murugam, V., Spierings, N., Evans, D. R., Song, M., & Clark, C. a. (2008). Atlas-based segmentation of white matter tracts of the human brain using diffusion tensor tractography and comparison with classical dissection. *NeuroImage*, *39*(1), 62–79.

Lazar, M., Weinstein, D. M., Tsuruda, J. S., Hasan, K. M., Arfanakis, K., Meyerand, M. E., … Alexander, A. L. (2003). White matter tractography using diffusion tensor deflection. *Human Brain Mapping*, *18*(4), 306–321.

Le Bihan, D., Breton, E., Lallemand, D., Grenier, P., Cabanis, E., & Laval-Jeantet, M. (1986). MR imaging of intravoxel incoherent motions: application to diffusion and perfusion in neurologic disorders. *Radiology*, *161*, 401–407.

Lebel, C., Caverhill-Godkewitsch, S., & Beaulieu, C. (2010). Age-related regional variations of the corpus callosum identified by diffusion tensor tractography. *Neuroimage*.

Lehman, J. F., Greenberg, B. D., McIntyre, C. C., Rasmussen, S. A., & Haber, S. N. (2011). Rules Ventral Prefrontal Cortical Axons Use to Reach Their Targets: Implications for Diffusion Tensor Imaging Tractography and Deep Brain Stimulation for Psychiatric Illness. *Journal of Neuroscience*, *31*(28), 10392–10402.

Lichtheim, L. (1885). Sur l'aphasie.

Ludwig, E., & Klingler, J. (1936). Photographs of macroscopic preparations of the encephalon. In *International Congress of Anatomy*. Milan.

Ludwig, E., & Klingler, J. (1956). *Atlas Cerebri Humani (The Inner Structure of the Brain Demonstrated on the Basis of Macroscopical Preparations)*. Basel: Little, Brown and Company.

Makris, N. (2007). Makris_occipitofrontal_fasicicle_in_humans.pdf, 1100–1111.

Makris, N., Kennedy, D. N., McInerney, S., Sorensen, a G., Wang, R., Caviness, V. S., & Pandya, D. N. (2005). Segmentation of subcomponents within the superior longitudinal fascicle in humans: a quantitative, in vivo, DT-MRI study. *Cerebral Cortex (New York, N.Y. : 1991)*, *15*(6), 854–69

Makris, N., & Pandya, D. N. (2009). The extreme capsule in humans and rethinking of the language circuitry. *Brain Structure & Function*, *213*(3), 343–58.

Makris, N., Papadimitriou, G. M., Kaiser, J. R., Sorg, S., Kennedy, D. N., & Pandya, D. N. (2009). Delineation of the middle longitudinal fascicle in humans: a quantitative, in vivo, DT-MRI study. *Cerebral Cortex (New York, N.Y. : 1991)*, *19*(4), 777–85.

Makris, N., Preti, M. G., Asami, T., Pelavin, P., Campbell, B., Papadimitriou, G. M., … Kubicki, M. (2012). Human middle longitudinal fascicle: variations in patterns of anatomical connections. *Brain Structure & Function*.

Makris, N., Worth, A. J., Sorensen, A. G., Papadimitriou, G. M., Wu, O., Reese, T. G., … Kennedy, D. N. (1997). Morphometry of in vivo human white matter association pathways with diffusion-weighted magnetic resonance imaging. *Annals of Neurology*, *42*(6), 951–62.

Maldonado, I. L., De Champfleur, N. M., Velut, S., Destrieux, C., Zemmoura, I., & Duffau, H. (2013). Evidence of a middle longitudinal fasciculus in the human brain from fiber dissection. *Journal of Anatomy*, *223*(1), 38–45.

Mandonnet, E., Nouet, A., Gatignol, P., Capelle, L., & Duffau, H. (2007). Does the left inferior longitudinal fasciculus play a role in language? A brain stimulation study. *Brain : A Journal of Neurology*, *130*(Pt 3), 623–9.

Markov, N. T., Ercsey-Ravasz, M. M., Ribeiro Gomes, a. R., Lamy, C., Magrou, L., Vezoli, J., … Kennedy, H. (2014). A Weighted and Directed Interareal Connectivity Matrix for Macaque Cerebral Cortex. *Cerebral Cortex*, *24*(1), 17–36.

Markov, N. T., Misery, P., Falchier, a., Lamy, C., Vezoli, J., Quilodran, R., … Knoblauch, K. (2011). Weight consistency specifies regularities of macaque cortical networks. *Cerebral Cortex*, *21*(6), 1254–1272.

Mars, R. B., Foxley, S., Verhagen, L., Jbabdi, S., Sallet, J., Noonan, M. P., … Rushworth, M. F. S. (2015). The extreme capsule fiber complex in humans and macaque monkeys: a comparative diffusion MRI tractography study. *Brain Structure and Function*, 1–13.

Martino, J., Brogna, C., Robles, S. G., Vergani, F., & Duffau, H. (2010). Anatomic dissection of the inferior fronto-occipital fasciculus revisited in the lights of brain stimulation data. *Cortex; a Journal Devoted to the Study of the Nervous System and Behavior*, *46*(5), 691–9.

Martino, J., da Silva-Freitas, R., Caballero, H., Marco de Lucas, E., García-Porrero, J. a, & Vázquez-Barquero, A. (2013). Fiber dissection and diffusion tensor imaging tractography study of the temporoparietal fiber intersection area. *Neurosurgery*, *72*(1 Suppl Operative), 87–97; discussion 97–8.

Martino, J., De Witt Hamer, P. C., Berger, M. S., Lawton, M. T., Arnold, C. M., de Lucas, E. M., & Duffau, H. (2013). Analysis of the subcomponents and cortical terminations of the perisylvian superior longitudinal fasciculus: a fiber dissection and DTI tractography study. *Brain Structure & Function*, *218*(1), 105–21.

Martino, J., De Witt Hamer, P. C., Vergani, F., Brogna, C., de Lucas, E. M., Vázquez-Barquero, A., … Duffau, H. (2011). Cortex-sparing fiber dissection: an improved method for the study of white matter anatomy in the human brain. *Journal of Anatomy*, *219*(4), 531–41.

Mayo, H., Finden, E., & Taylor, R. (1827). A series of engravings intended to illustrate the structure of the brain and spinal chord in man.

Mazoyer, B., Mellet, E., Perchey, G., Zago, L., Crivello, F., Jobard, G., … Tzourio-Mazoyer, N. (2016). BIL&GIN: A neuroimaging, cognitive, behavioral, and genetic database for the study of human brain lateralization. *NeuroImage*, *124*, 1225–1231.

Meola, A., Comert, A., Yeh, F.-C., Stefaneanu, L., & Fernandez-Miranda, J. C. (2015). The controversial existence of the human superior fronto-occipital fasciculus: Connectome-based tractographic study with microdissection validation. *Human Brain Mapping*.

Mesulam, M. M. (1990). Large-scale neurocognitive networks and distributed processing for attention, language, and memory. *Annals of Neurology*.

Mesulam, M. M. (1998). From sensation to cognition. *Brain*, *121*, 1013–1052.

Mesulam, M. M. (2006). Foreword. In *Fiber pathways of the brain, Schmahmann J D, Pandya, D N*. New York: Oxford University Press.

Mesulam, M. M. (2012). The Evolving Landscape of Human Cortical Connectivity: Facts and Inferences. *Neuroimage*, *62*(4), 2182–2189.

Meynert, T. (1872). In Handbuch der Lehre von den Geweben des Menschen und der Tiere. *Stricker S, Leipzig*.

Meynert, T. (1885). Psychiatry: Clinical Treatise on the Diseases of the Fore-Brain, trans. *B. Sachs. New York & London: GP Putnam*.

Mikula, S., Binding, J., & Denk, W. (2012). Staining and embedding the whole mouse brain for electron microscopy. *Nature Methods*, *9*(12), 1198–1201.

Milner, a. D., & Goodale, M. a. (2008). Two visual systems re-viewed. *Neuropsychologia*, *46*(3), 774–785. http://doi.org/10.1016/j.neuropsychologia.2007.10.005

Mishkin, M., Ungerleider, L. G., & Macko, K. a. (1983). Object vision and spatial vision: two cortical pathways. *Trends in Neurosciences*, *6*, 414–417.

Mori, S., & van Zijl, P. C. M. (2002). Fiber tracking: principles and strategies - a technical review. *NMR in Biomedicine*, *15*(7-8), 468–80.

Mori, S., Wakana, S., Zijl, P. Van, & Nagae-Poetscher, L. (2005). *MRI atlas of human white matter*. Amsterdam: Elsevier.

Mori, S., Xue, R., Crain, B., & Solaiyappan, M. (1999). 3D reconstruction of axonal fibers from diffusion tensor imaging using fiber assignment by continuous tracking (FACT). *8th Annual Meeting of the ISMRM*.

Moseley, M., & Cohen, Y. (1990). Early detection of regional cerebral ischemia in cats: comparison of diffusion-and T2-weighted MRI and spectroscopy. *Magnetic Resonance.*

Nornes, H. O., & Das, G. D. (1972). Temporal pattern of neurogenesis in spinal cord: cytoarchitecture and directed growth of axons. *Proceedings of the National Academy of Sciences of the United States of America*, *69*(7), 1962–1966.

O'Donnell, L. J., Kubicki, M., Shenton, M. E., Dreusicke, M. H., Grimson, W. E. L., & Westin, C. F. (2006). A method for clustering white matter fiber tracts. *AJNR. American Journal of Neuroradiology*, *27*(5), 1032–6.

Oishi, K., Faria, A., Jiang, H., Li, X., Akhter, K., Zhang, J., … Mori, S. (2009). Atlas-based whole brain white matter analysis using large deformation diffeomorphic metric mapping: Application to normal elderly and Alzheimer's disease participants. *NeuroImage*, *46*(2), 486–499.

Oishi, K., Faria, A., van Zijl, P. C. M., Mori, S., Wakana, S., Zijl, P. Van, & Nagae-Poetscher, L. (2005). *MRI atlas of human white matter* (2nd ed.). Amsterdam: Elsevier.

Oishi, K., Faria, A. V., Hsu, J., Tippett, D., Mori, S., & Hillis, A. E. (2015). Critical role of the right uncinate fasciculus in emotional empathy. *Annals of Neurology*, *77*(1), 68–74.

Oishi, K., Zilles, K., Amunts, K., Faria, A., Jiang, H., Li, X., … Mori, S. (2008). Human brain white matter atlas: identification and assignment of common anatomical structures in superficial white matter. *NeuroImage*, *43*(3), 447–57.

Onufrowicz, W. (1887). Das balkenlose Mikrocephalengehirn Hofmann. *European Archives of Psychiatry and Clinical.*

Orban, G. a., Van Essen, D., & Vanduffel, W. (2004). Comparative mapping of higher visual areas in monkeys and humans. *Trends in Cognitive Sciences*, *8*(7), 315–324.

Papagno, C. (2011). Naming and the role of the uncinate fasciculus in language function. *Current Neurology and Neuroscience Reports*, *11*(6), 553–559.

Papagno, C., Miracapillo, C., Casarotti, A., Romero Lauro, L. J., Castellano, A., Falini, A., … Bello, L. (2011). What is the role of the uncinate fasciculus? Surgical removal and proper name retrieval. *Brain*, *134*(2), 405–414.

Park, H. J., Westin, C. F., Kubicki, M., Maier, S. E., Niznikiewicz, M., Baer, A., … Shenton, M. E. (2004). White matter hemisphere asymmetries in healthy subjects and in schizophrenia: A diffusion tensor MRI study. *NeuroImage*, *23*(1), 213–223.

Parker, G. J. M., Luzzi, S., Alexander, D. C., Wheeler-Kingshott, C. a M., Ciccarelli, O., & Lambon Ralph, M. a. (2005). Lateralization of ventral and dorsal auditory-language pathways in the human brain. *NeuroImage*, *24*(3), 656–666.

Petrides, M., & Pandya, D. (1984). Projections to the frontal cortex from the posterior parietal region in the rhesus monkey. *Journal of Comparative Neurology*.

Petrides, M., & Pandya, D. (1988). Association fiber pathways to the frontal cortex from the superior temporal region in the rhesus monkey. *Journal of Comparative Neurology*.

Peuskens, D., & Loon, J. van. (2004). Anatomy of the anterior temporal lobe and the frontotemporal region demonstrated by fiber dissection.

Phan, K. L., Orlichenko, A., Boyd, E., Angstadt, M., Coccaro, E. F., Liberzon, I., & Arfanakis, K. (2009). Preliminary Evidence of White Matter Abnormality in the Uncinate Fasciculus in Generalized Social Anxiety Disorder. *Biological Psychiatry*, *66*(7), 691–694.

Price, G., Cercignani, M., Parker, G. J. M., Altmann, D. R., Barnes, T. R. E., Barker, G. J., … Ron, M. a. (2008). White matter tracts in first-episode psychosis: A DTI tractography study of the uncinate fasciculus. *NeuroImage*, *39*(3), 949–955.

Raffelt, D. a., Smith, R. E., Ridgway, G. R., Tournier, J.-D., Vaughan, D. N., Rose, S., … Connelly, A. (2015). Connectivity-Based Fixel Enhancement: Whole-Brain Statistical Analysis of Diffusion MRI Measures in the Presence of Crossing Fibres. *NeuroImage*, *117*, 40–55.

Raffelt, D., Tournier, J.-D., Rose, S., Ridgway, G. R., Henderson, R., Crozier, S., … Connelly, A. (2012). Apparent Fibre Density: a novel measure for the analysis of diffusion-weighted magnetic resonance images. *NeuroImage*, *59*(4), 3976–94.

Rauschecker, J. P., & Tian, B. (2000). Mechanisms and streams for processing of "what" and "where" in auditory cortex. *Proceedings of the National Academy of Sciences of the United States of America*, *97*(22), 11800–6.

Reil, J. (1809). Die sylvische grube oder das thal, das gestreifte grobe hirnganglium, dessen kapsel und die seitentheile des grobn gehirns. *Archiv Fur Die Physiologie*, *9*, 195–208.

Rodrigo, S., Oppenheim, C., Chassoux, F., Golestani, N., Cointepas, Y., Poupon, C., … Meder, J. F. (2007). Uncinate fasciculus fiber tracking in mesial temporal lobe epilepsy. Initial findings. *European Radiology*, *17*(7), 1663–1668. http://doi.org/10.1007/s00330-006-0558-x

Rojkova, K., Volle, E., Urbanski, M., Humbert, F., Dell'Acqua, F., & Thiebaut de Schotten, M. (2015). Atlasing the frontal lobe connections and their variability due to age and education: a spherical deconvolution tractography study. *Brain Structure and Function*, (FEBRUARY). http://doi.org/10.1007/s00429-015-1001-3

Rolheiser, T., Stamatakis, E. a., & Tyler, L. K. (2011). Dynamic Processing in the Human Language System: Synergy between the Arcuate Fascicle and Extreme Capsule. *Journal of Neuroscience*, *31*(47), 16949–16957. http://doi.org/10.1523/JNEUROSCI.2725-11.2011

Sachs, H. (1892). Das hemisphärenmark des menschlichen grosshirns. *DMW-Deutsche Medizinische.*

Sarubbo, S., De Benedictis, A., Maldonado, I. L., Basso, G., & Duffau, H. (2013). Frontal terminations for the inferior fronto-occipital fascicle: Anatomical dissection, DTI study and functional considerations on a multi-component bundle. *Brain Structure and Function*, *218*(1), 21–37.

Sarubbo, S., De Benedictis, A., Milani, P., Paradiso, B., Barbareschi, M., Rozzanigo, U., … Chioffi, F. (2015). The course and the anatomo-functional relationships of the optic radiation: A combined study with "post mortem" dissections and "in vivo" direct electrical mapping. *Journal of Anatomy*, *226*(1), 47–59.

Saur, D., Kreher, B. W., Schnell, S., Kümmerer, D., Kellmeyer, P., Vry, M.-S., … Weiller, C. (2008). Ventral and dorsal pathways for language. *Proceedings of the National Academy of Sciences of the United States of America*, *105*(46), 18035–40.

Scatliff, J. H., & Johnston, S. (2014). Andreas vesalius and Thomas willis: their anatomic brain illustrations and illustrators. *AJNR. American Journal of Neuroradiology*, *35*(1), 19–22.

Schmahmann, J. D., & Pandya, D. N. (2006). *Fiber pathways of the brain*. New York: Oxford University Press.

Schmahmann, J. D., & Pandya, D. N. (2007). The complex history of the fronto-occipital fasciculus. *Journal of the History of the Neurosciences*, *16*(4), 362–77.

Schmahmann, J. D., Pandya, D. N., Wang, R., Dai, G., D'Arceuil, H. E., De Crespigny, A. J., & Wedeen, V. J. (2007). Association fibre pathways of the brain: Parallel observations from diffusion spectrum imaging and autoradiography. *Brain*, *130*(3), 630–653.

Schwarz, G. (1978). Estimating the dimension of a model. *The Annals of Statistics*, *6*(2), 461–464.

Smith, R. E., Tournier, J.-D., Calamante, F., & Connelly, A. (2012). Anatomically-constrained tractography: Improved diffusion MRI streamlines tractography through effective use of anatomical information. *NeuroImage*, *62*(3), 1924–1938.

Smith, S. M. (2002). Fast robust automated brain extraction. *Human Brain Mapping*, *17*(3), 143–155.

Sobhani, M., Baker, L., Martins, B., Tuvblad, C., & Aziz-zadeh, L. (2015). NeuroImage : Clinical Psychopathic traits modulate microstructural integrity of right uncinate fasciculus in a community population, *8*, 32–38.

Sperry, R. W. (1943). Effect of 180 degree rotation of the retinal field on visuomotor coordination. *The Journal of Experimental Zoology*, *92*(3), 263–279.

Sporns, O. (2011). The human connectome: a complex network. *Annals of the New York Academy of Sciences*, *1224*, 109–25.

Sporns, O. (2013). The human connectome: origins and challenges. *NeuroImage*, *80*, 53–61.

Steffens, D. C., Taylor, W. D., Denny, K. L., Bergman, S. R., & Wang, L. (2011). Structural integrity of the uncinate fasciculus and resting state functional connectivity of the ventral prefrontal cortex in late life depression. *PLoS ONE*, *6*(7).

Steno, N. (1665). Discours de Monsieur Stenon sur l'anatomie du cerveau. In *de Ninville*. Paris.

Swanson, L. (2014). *Neuroanatomical terminology: a lexicon of classical origins and historical foundations*.

Takao, H., Hayashi, N., & Ohtomo, K. (2013). White matter microstructure asymmetry: effects of volume asymmetry on fractional anisotropy asymmetry. *Neuroscience*, *231*, 1–12.

Terminology, F. C. on A. (1998). Terminologia Anatomica.

Testut, L. (1900). *Traité d'anatomie humaine: Tome 2* (4th ed.). Paris: Octave Doin.

Thiebaut de Schotten, M., Dell'Acqua, F., Valabregue, R., & Catani, M. (2012). Monkey to human comparative anatomy of the frontal lobe association tracts. *Cortex*, *48*(1), 82–96.

Thiebaut de Schotten, M., Ffytche, D. H., Bizzi, A., Dell'acqua, F., Allin, M., Walshe, M., … Catani, M. (2011). Atlasing location, asymmetry and inter-subject variability of white matter tracts in the human brain with MR diffusion tractography. *NeuroImage*.

Thomas, C., Avram, A., Pierpaoli, C., & Baker, C. (2015). Diffusion MRI properties of the human uncinate fasciculus correlate with the ability to learn visual associations. *Cortex*, *72*(2015), 1–14.

Thomas, C., Ye, F. Q., Irfanoglu, M. O., Modi, P., Saleem, K. S., Leopold, D. a., & Pierpaoli, C. (2014). Anatomical accuracy of brain connections derived from diffusion MRI tractography is inherently limited. *Proceedings of the National Academy of Sciences*, *111*(46), 16574–16579.

Tournier, J. D., Calamante, F., & Connelly, A. (2007). Robust determination of the fibre orientation distribution in diffusion MRI: Non-negativity constrained super-resolved spherical deconvolution. *NeuroImage*, *35*(4), 1459–1472.

Tournier, J. D., Calamante, F., Gadian, D. G., & Connelly, A. (2004). Direct estimation of the fiber orientation density function from diffusion-weighted MRI data using spherical deconvolution. *NeuroImage*, *23*(3), 1176–1185.

Tournier, J. J.-D., Mori, S., & Leemans, A. (2011). Diffusion tensor imaging and beyond. *Magnetic Resonance in Medicine : Official Journal of the Society of Magnetic Resonance in Medicine / Society of Magnetic Resonance in Medicine*, *65*(6), 1532–1556.

Tournier, J.-D., Calamante, F., & Connelly, A. (2012). MRtrix: Diffusion tractography in crossing fiber regions. *International Journal of Imaging Systems and Technology*, *22*(1), 53–66.

Travers, N. (2008). L ' étude micro-anatomique des fibres du faisceau unciné et ses implications dans la chirurgie fronto-temporo-insulaire Microsurgical anatomical study of the uncinate fasciculus, *7*(4), 31–41.

Trolard, P. (1906). Le faisceau longitudinal inférieur du cerveau. *Rev Neurol*.

Türe, U., Yasargil, G. M., Friedman, A. H., & Al-Mefty, O. (2000). Fiber Dissection Technique : Lateral Aspect of the Brain. *Neurosurgery*, *47*(2), 417–427.

Türe, U., Yasargil, G. M., & Pait, G. T. (1997). Is there a superior occipitofrontal fasciculus? A microsurgical anatomic study, *40*(6), 1226–1232.

Turken, A. U., & Dronkers, N. F. (2011). The neural architecture of the language comprehension network: converging evidence from lesion and connectivity analyses. *Frontiers in Systems Neuroscience*, *5*(February), 1.

Tusa, R. J., & Ungerleider, L. G. (1985). The inferior longitudinal fasciculus: a reexamination in humans and monkeys. *Annals of Neurology*, *18*(5), 583–91.

Ueno, T., Saito, S., Rogers, T. T., & Lambon Ralph, M. a. (2011). Lichtheim 2: Synthesizing aphasia and the neural basis of language in a neurocomputational model of the dual dorsal-ventral language pathways. *Neuron*, *72*(2), 385–396. http://doi.org/10.1016/j.neuron.2011.09.013

Van Essen, D. C., Smith, S. M., Barch, D. M., Behrens, T. E. J., Yacoub, E., & Ugurbil, K. (2013). The WU-Minn Human Connectome Project: an overview. *NeuroImage*, *80*, 62–79.

Vergani, F., Mahmood, S., Morris, C. M., Mitchell, P., & Forkel, S. J. (2014). Intralobar fibres of the occipital lobe: A post mortem dissection study. *Cortex*, *56*, 145–156.

Vicq d'Azyr, F. (1786). *Traité d'anatomie et de physiologie*. Paris: Didot.

Vieussens, R. (1684). *Neurographia universalis*. Lyon: J. Certe.

Villiger, E., & Ludwig, E. (1940). Gehirn und Rückenmark, 11.–13. *Aufl. Leipzig*.

Von Der Heide, R. J., Skipper, L. M., Klobusicky, E., & Olson, I. R. (2013). Dissecting the uncinate fasciculus: disorders, controversies and a hypothesis. *Brain : A Journal of Neurology*, *136*(Pt 6), 1692–707.

Wakana, S., Caprihan, A., Panzenboeck, M. M., Fallon, J. H., Perry, M., Gollub, R. L., … Mori, S. (2007). Reproducibility of quantitative tractography methods applied to cerebral white matter. *NeuroImage*, *36*(3), 630–44.

Wakana, S., Jiang, H., & Zijl, P. C. M. Van. (2003). Radiology Fiber Tract – based Atlas of, 21–29.

Waller, A. (1850). Experiments on the Section of the Glossopharyngeal and Hypoglossal Nerves of the Frog, and Observations of the Alterations Produced Thereby in the Structure of Their Primitive Fibres. *Philosophical Transactions of the Royal Society*, *140*, 423–429.

Wang, R., Benner, T., Sorensen, a G., & Wedeen, V. J. (2007). Diffusion Toolkit : A Software Package for Diffusion Imaging Data Processing and Tractography. *Proc. Intl. Soc. Mag. Reson. Med.*, *15*, 3720.

Wang, X., Pathak, S., Stefaneanu, L., Yeh, F.-C., Li, S., & Fernandez-Miranda, J. C. (2015). Subcomponents and connectivity of the superior longitudinal fasciculus in the human brain. *Brain Structure and Function*.

Wassermann, D., Makris, N., Rathi, Y., Shenton, M., Kikinis, R., Kubicki, M., & Westin, C. F. (2013). On describing human white matter anatomy: The white matter query language. *Lecture Notes in Computer Science (including Subseries Lecture Notes in Artificial Intelligence and Lecture Notes in Bioinformatics)*, *8149 LNCS*(PART 1), 647–654.

Wedeen, V. J., Rosene, D. L., Wang, R., Dai, G., Mortazavi, F., Hagmann, P., … Tseng, W. I. (2012a). Response to Comment on " The Geometric Structure of the. *Science*, *337*(September), 2–3.

Wedeen, V. J., Rosene, D. L., Wang, R., Dai, G., Mortazavi, F., Hagmann, P., … Tseng, W.-Y. I. (2012b). The geometric structure of the brain fiber pathways. *Science (New York, N.Y.)*, *335*(6076), 1628–34.

Weiller, C., Bormann, T., Saur, D., Musso, M., & Rijntjes, M. (2011). How the ventral pathway got lost - And what its recovery might mean. *Brain and Language*, *118*(1-2), 29–39.

Wernicke, C. (1874). *Der aphasische Symptomencomplex: eine psychologische Studie auf anatomischer basis*. Breslau, Cohn and Weigert.

Wernicke, C. (1881). Lehrbuch der gehirnkrankheiten für aerzte und studirende.

Wernicke, C. (1908). Diseases of the nervous system. *Modern Clinical Medicine*.

Wong, N. M. L., Cheung, S.-H., Chan, C. C. H., Zeng, H., Liu, Y.-P., So, K.-F., & Lee, T. M. C. (2015). Diffusivity of the uncinate fasciculus in heroin users relates to their levels of anxiety. *Translational Psychiatry*, *5*(4), e554.

Yasmin, H., Nakata, Y., Aoki, S., Abe, O., Sato, N., Nemoto, K., … Ohtomo, K. (2008). Diffusion abnormalities of the uncinate fasciculus in Alzheimer's disease: Diffusion tensor tract-specific analysis using a new method to measure the core of the tract. *Neuroradiology*, *50*(4), 293–299.

Yeatman, J. D., Weiner, K. S., Pestilli, F., Rokem, A., Mezer, A., & Wandell, B. a. (2014). The vertical occipital fasciculus: A century of controversy resolved by in vivo measurements. *Proceedings of the National Academy of Sciences of the United States of America*.

Zhang, A., Leow, A., Ajilore, O., Lamar, M., Yang, S., Joseph, J., … Kumar, A. (2012). Quantitative tract-specific measures of uncinate and cingulum in major depression using diffusion tensor imaging. *Neuropsychopharmacology : Official Publication of the American College of Neuropsychopharmacology*, *37*(4), 959–67.

Zhang, H., Schneider, T., Wheeler-Kingshott, C. a, & Alexander, D. C. (2012). NODDI: practical in vivo neurite orientation dispersion and density imaging of the human brain. *NeuroImage*, *61*(4), 1000–16.

Zhang, Y., Zhang, J., Oishi, K., Faria, A. V, Jiang, H., Li, X., … Mori, S. (2010). Atlas-guided tract reconstruction for automated and comprehensive examination of the white matter anatomy. *NeuroImage*, *52*(4), 1289–301.